# THERMO-CHEMICAL CONVERSION OF INVASIVE SPECIES (PLANTS) BIOMASS FOR BIOFUEL PRODUCTION AND SUBSEQUENT VALUE ADDITION


*By*

**Ms. VAHSHI CHONGLOI**

**Ph.D. Regd. No. Ph.D./FRS/00381 w.e.f. 30/08/2019**


*Submitted to*

**NAGALAND UNIVERSITY**

***In Partial Fulfilment of the Requirements for Award of Degree***

***of***

**DOCTOR OF PHILOSOPHY IN FORESTRY**


**DEPARTMENT OF FORESTRY**

**SCHOOL OF SCIENCES, NAGALAND UNIVERSITY**

**LUMAMI-798627**

**NAGALAND, INDIA**


**AUGUST, 2025**

# THERMO-CHEMICAL CONVERSION OF INVASIVE SPECIES (PLANTS) BIOMASS FOR BIOFUEL PRODUCTION AND SUBSEQUENT VALUE ADDITION

**By**

**Ms. VAHSHI CHONGLOI**

**and**

**Dr. MAYUR MAUSOOM PHUKAN**

**(Supervisor)**

*Submitted*

*In Partial Fulfilment of the Requirements for the Degree*

*Of*

**DOCTOR OF PHILOSOPHY IN FORESTRY**

**Department of Forestry**

**School of Sciences, Nagaland University**

**Lumami-798627**

**Nagaland, India**

**2025**

*"When the race is complete, still my lips shall repeat*

*Yet not I, but through Christ in me."*

*Dedicated to Late. Mr. Paokholam Chongloi (Father),*

*Mrs. Nengkhonei Chongloi (Mother),*

*Ms. Mengshi Chongloi (Aunt)*

*and*

*Missy*

*with love and respect.*

*Vahshi Chongloi*

# नागालैण्ड विश्वविद्यालय
# NAGALAND UNIVERSITY
## भौतिकी विभाग
(संसद द्वारा पारित अधिनियम 1989, क्रमांक 35 के अंतर्गत स्थापित केंद्रीय विश्वविद्यालय)
(A Central University established by an Act of Parliament No.35 of 1989)
मुख्यालय : लुमामी, जिला : जुन्हेबोटो (नागालैण्ड), पिनकोड – 798627
Hqrs: Lumami, Dist. Zunheboto (Nagaland), Pin Code – 798627
वेबसाइट / Website : www.nagalanduniversity.ac.in
**DEPARTMENT OF FORESTRY**


---

## DECLARATION

I, **Ms. Vahshi Chongloi**, bearing Ph.D. Registration No. Ph.D./FRS/00381 (w.e.f. 30th August, 2019), hereby declare that the thesis entitled **"*Thermo-Chemical Conversion of Invasive Species (Plants) Biomass for Biofuel Production and Subsequent Value Addition*"** is a record of original research work carried out by me. All sources of assistance have been assigned due acknowledgement. I also declare that neither this work as a whole nor a part of it has been submitted to any other University/Institute for any other degree, diploma or award.

This is being submitted to Nagaland University for the degree of Doctor of Philosophy in Forestry.

Vahshi

**Date:** 06-08-2025

**Place:** Lumami, Nagaland

**(Vahshi Chongloi)**
Scholar

**(Dr. M. Mathiyazhagan)**
Head
Department of Forestry
Nagaland University, Lumami

Chairman / Head
Department of Forestry
Nagaland University
Lumami - 798 627

**(Dr. Mayur Mausoom Phukan)**
Supervisor

Dr. Mayur Mausoom Phukan (M.Sc., PhD)
Assistant Professor
Department of Forestry
Nagaland University

# नागालैण्ड विश्वविद्यालय
# NAGALAND UNIVERSITY
## भौतिकी विभाग
(संसद द्वारा पारित अधिनियम 1989, क्रमांक 35 के अंतर्गत स्थापित केंद्रीय विश्वविद्यालय)
(A Central University established by an Act of Parliament No.35 of 1989)
मुख्यालय : लुमामी, जिला : जुन्हेबोटो (नागालैण्ड), पिनकोड – 798627
Hqrs: Lumami, Dist. Zunheboto (Nagaland), Pin Code – 798627
वेबसाइट / Website : www.nagalanduniversity.ac.in
**DEPARTMENT OF FORESTRY**

Dr. Mayur Mausoom Phukan (M.Sc., Ph.D.)
Assistant Professor
Dept. of Forestry
School of Sciences
Mobile No: 9954664500, 9365831101
Mail id: mayur_101@yahoo.com
mayur_101@nagalanduniversity.ac.in
Editorial Board (Ex): Journal of Applied Microbiology (Formerly Wiley-Blackwell)
Editorial Board (Ex): Letters in Applied Microbiology (Formerly Wiley-Blackwell)


---

## CERTIFICATE

This is to certify that the thesis entitled **"*Thermo-Chemical Conversion of Invasive Species (Plants) Biomass for Biofuel Production and Subsequent Value Addition*"** is an original and bonafide research work carried out by **Ms. Vahshi Chongloi** under my supervision. This thesis is being submitted to the School of Sciences, Nagaland University, in partial fulfilment of the requirements for the award of degree of Doctor of Philosophy in Forestry. The matter embodied in this thesis have not been previously submitted to any University/Institution for the award of any degree, diploma or similar title.

All assistance and help received during the entire course of doctoral research has been duly acknowledged.

**Date:** 06-08-2025
**Place:** Lumami, Nagaland

**(Dr. Mayur Mausoom Phukan)**
Supervisor
Department of Forestry
Nagaland University, Lumami

Dr. Mayur Mausoom Phukan (M.Sc., PhD)
Assistant Professor
Department of Forestry
Nagaland University

# नागालैण्ड विश्वविद्यालय
# NAGALAND UNIVERSITY
## भौतिकी विभाग
(संसद द्वारा पारित अधिनियम 1989, क्रमांक 35 के अंतर्गत स्थापित केंद्रीय विश्वविद्यालय)
(A Central University established by an Act of Parliament No.35 of 1989)
मुख्यालय : लुमामी, जिला : जुन्हेबोटो (नागालैण्ड), पिनकोड – 798627
Hqrs: Lumami, Dist. Zunheboto (Nagaland), Pin Code – 798627
वेबसाइट / Website : www.nagalanduniversity.ac.in
**DEPARTMENT OF FORESTRY**


## Plagiarism Self Declaration Certificate

| | |
|---|---|
| **Name of Research Scholar** | Vahshi Chongloi |
| **Ph.D. Registration Number** | Ph.D./FRS/00381 |
| **Title of Ph.D. thesis** | Thermo-Chemical Conversion of Invasive Species (Plants) Biomass for Biofuel Production and Subsequent Value Addition |
| **Name & Institutional Address of theSupervisor** | Dr. Mayur Mausoom Phukan,<br>Department of Forestry,<br>Nagaland University, Lumami-798627 |
| **Name of the Department and School** | Department of Forestry,<br>School of Sciences |
| **Date of Submission** | 06-08-2025 |
| **Date of plagiarism check** | 23-07-2025 |
| **Percentage of similarity detected by the Drillbit software** | 4 % |

I hereby declare/certify that the Ph.D. Thesis submitted by me is complete in all respect, as per the guidelines of the UGC/NU for this purpose. I also certify that the Thesis (soft copy and print version)) has been checked for plagiarism using **Drillbit** similarity check software. Copy of the Report generated by the **Drillbit** software is also enclosed.

Vahshi

**Date:** 06-08-2025
**Place:** Lumami, Nagaland

**Vahshi Chongloi**
(Scholar)

**(Dr. Mayur Mausoom Phukan)**
Supervisor

Dr. Mayur Mausoom Phukan (M.Sc., PhD)
Assistant Professor
Department of Forestry
Nagaland University

07.08

**(Dr. M. Mathiyazhagan)**
Head
Department of Forestry

विभागाध्यक्ष / HOD
वानिकी विभाग / Department of Forestry
नागालैण्ड विश्वविद्यालय / Nagaland University
लुमामी / Lumami - 798 627

DrillBit

The Report is Generated by DrillBit Plagiarism Detection Software

***Submission Information***

| | |
|---|---|
| Author Name | Vahshi Chongloi |
| Title | THERMO-CHEMICAL CONVERSION OF INVASIVE SPECIES (PLANTS) BIOMASS FOR BIOFUEL PRODUCTION AND SUBSEQUENT VALUE ADDITION |
| Paper/Submission ID | 4124172 |
| Submitted by | mayur_101@nagalanduniversity.ac.in |
| Submission Date | 2025-07-23 21:52:27 |
| Total Pages, Total Words | 104, 30237 |
| Document type | Thesis |

***Result Information***

Similarity **4 %**

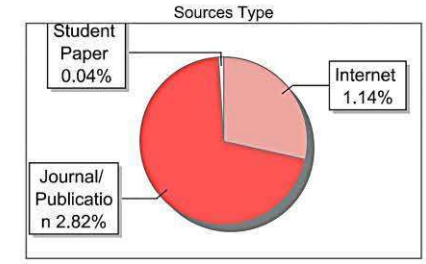


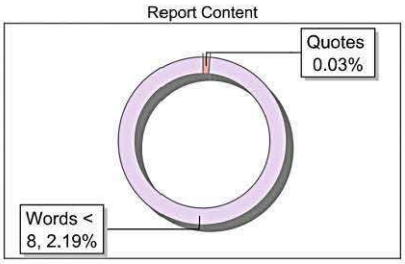


***Exclude Information***

| | |
|---|---|
| Quotes | Not Excluded |
| References/Bibliography | Not Excluded |
| Source: Excluded < 8 Words | Excluded |
| Excluded Source | **0 %** |
| Excluded Phrases | Not Excluded |

***Database Selection***

| | |
|---|---|
| Language | English |
| Student Papers | Yes |
| Journals & publishers | Yes |
| Internet or Web | Yes |
| Institution Repository | Yes |

A Unique QR Code use to View/Download/Share Pdf File

## *Acknowledgement*

I am profoundly aware that no words, however eloquent, can truly capture the depth of gratitude I owe to each individual who supported me throughout this academic journey. Nevertheless, with heartfelt sincerity, I extend the following acknowledgements.

First and foremost, I offer all glory and gratitude to the Architect of the Universe, who in his supreme graciousness has conferred me with the ability to make this humble contribution at the service of the scientific community. His divine grace has been my refuge in weakness and my light in darkness. Without Him, none of this would have been possible.

I extend my heartfelt thanks to my supervisor, Dr. Mayur Mausoom Phukan, for his steadfast support during this research journey. I am grateful to him for his consistent guidance, insightful foresight, constructive feedback, realignment of research strategies, and especially for the meticulous attention he gave to reviewing my manuscripts and thesis. His guidance has played a crucial role in influencing my academic and personal development.

I am deeply indebted to my family, whose unconditional love, unwavering support, and immeasurable sacrifices have been the cornerstone of all that I have achieved. With profound gratitude, I acknowledge that their prayers have sustained me in ways words can never express.

A special note of gratitude is due to Dr. Plaban Bora, Assam Engineering College, for his kind cooperation and constant guidance, which significantly enriched the quality of this study.

I am sincerely thankful to all my friends for their support and companionship throughout this journey. In particular, I would like to acknowledge Mr. Kedukhro Khupfu and Ms. Amenuo Susan Kulnu for being my pillars of strength through thick and thin.

I extend my sincere appreciation to the esteemed faculty members of the Department of Forestry, Dr. G. Bupesh, Dr. Gyati Yam and Dr. Mathiyazhagan, for their time-to-time encouragement and valuable suggestions during my research.

I owe a particular debt of gratitude to my labmate Mr. Samson Rosly Sangma for his invaluable support and companionship which enriched this journey in countless ways. I am equally grateful to the Research scholars of the Department, Mr. Sarabjan Deori, Ms. Nokenketla, Ms. Vieneite-o Koza, Mr. P. Sudharsan, Mr. Longnyu Konyak, and Mr. Joynath Pegu for fostering a positive and intellectually stimulating environment.

I express my sincere sense of obligations and deepest acknowledgement to the Department of Science and Technology (DST), Government of India, for providing financial assistance in the form of the prestigious DST – INSPIRE Fellowship.

My heartfelt gratitude also goes to Mr. Tapanjit Borah, Department of Energy, Tezpur University, for his timely assistance. I am equally indebted to Nagaland GIS and Remote Sensing Centre (NGISRSC), Dr. Moameren Longchar and Mr. Vimha Ritse for providing essential maps that contributed significantly to the study.

**Date:** 06-08-2025

**Place:** Lumami, Nagaland (Vahshi Chongloi)

# ABSTRACT

Invasive species exert tremendous influence on the global ecosystem, altering ecological balance and threatening biodiversity. Characterized by their prolific reproduction, remarkable adaptability and extensive dispersal capabilities, these species pose significant threat to the native flora, soil health, water quality, and overall biodiversity. While conventional management approaches of invasive species (from here on IS for brevity) predominantly focus on eradication, the growing need for ecosystem restoration and bioresource utilization calls for a paradigm shift towards alternative sustainable approaches. These approaches entail sustainable management encompassing rational utilization and leveraging the potential of IS as a valuable resource. Although, complete eradication of IS from native ecosystems is virtually challenging, repurposing these plants as a sustainable, locally accessible, and cost-effective resource for biofuel production and value enhancement warrants consideration. Consequently, IS, typically considered as a waste, are underutilized bioresources that have not been put to their best advantage.

The present study thus delves into the untapped potential of IS, often considered an environmental nuisance and consequently neglected. Integrating the energy and non-energy prospects of IS aids in exploring their suitability for futuristic biorefining potentials in response to the persistent demand for bioenergy. Initially, twenty (20 Nos.) IS were randomly chosen based on prevalence, ecological impact, visual prominence and management challenges. Based on calorific value, three IS viz. *Ageratina adenophora*, *Lantana camara* and *Stachytarpheta jamaicensis* were investigated for biofuel generation and value-enhancement.

Population and distribution assessment of the species was conducted, aimed solely to allocate hotspots for tailored management and targeted biomass harvest. With a contagious distribution pattern across all surveyed sites, *A. adenophora* emerged as the dominant species exhibiting highest frequency (100 %), density (131000 – 622000 Ind./ha.), total basal area (16.83 – 46.32 m sq./ha.) and Importance value index (41.3

– 112.79). The results demonstrated the random distribution pattern of invasive *L. camara* in most sites within the study area. The findings additionally revealed the contagious distribution of *S. jamaicensis*, which despite its restricted range elsewhere displayed high frequency in the sites where it occurred [S – 10: Kohima town (60 %) and S – 16: Thizama (60 %)].

Biomass characterization revealed low moisture and ash content of the three IS. The calorific values in descending order were *S. jamaicensis* (17.06 MJ/Kg) > *A. adenophora* (16.63 MJ/Kg) > *L. camara* (16.49 J/Kg). Ultimate analysis revealed that the IS biomass possessed considerable carbon content [*A. adenophora* (44.47 %), *L. camara* (45.74 %) and *S. jamaicensis* (44.59 %)]. TG-DTG was done from ambient to 700 °C at two heating rates viz. 10 °C and 30 °C/min The degradation profile demonstrated three distinct phases of mass loss up to 700 °C corresponding to active and passive zone of pyrolysis. The brief degradation profile indicated their suitability for thermochemical conversion (pyrolysis).

Biomass of *A. adenophora, L. camara* and *S. jamaicensis* were subjected to pyrolysis at temperatures ranging from ambient to 600 °C at 30°C/min for bio-oil generation. Among the three studied species, *A. adenophora* bio-oil exhibited superior energy yield of 69.87 % followed by *L. camara* (62.58 %) and *S. jamaicensis* (56.25 %). The calorific values of the pyrolytic bio-oil from *A. adenophora*, *L. camara* and *S. jamaicensis* were in the order 33.7 MJ/Kg > 30.99 MJ/Kg > 30.18 MJ/Kg, respectively, demonstrating their potential as energy–dense biofuels. The study employed Fourier transformed infrared spectroscopy (FTIR) analysis, Gas chromatography–mass spectroscopy (GC–MS) analysis and Nuclear magnetic resonance (NMR) as a part of the spectroscopic characterization of the pyrolytic bio–oil. Bio–oil's spectroscopic analyses confirmed the intricate configuration of organic constituents including alcohols, aldehydes, phenols, aromatics, ketones and aliphatics highlighting it as a potential chemical feedstock. The presence of aromatic and aliphatic hydrocarbons is appealing in terms of biofuel perspective while the phenolic contents hold significance from a bioactivity standpoint.

Theoretical economic analysis demonstrated IS biomass–to–biofuel conversion technologies are anticipated to be economically viable compared to petroleum refining. This is contingent upon a reduction in the production cost of *A. adenophora, L. camara* and *S. jamaicensis* biofuel by approximately a factor of ~3 considering the benchmark production cost of biofuel at $ 1000 $ton^{-1}$. Furthermore, the economic analysis of biomass conversion facility with a Payback period of 5.19 years, a Net present value of $ 378,912.829, Internal rate of return of 21 % and Minimum selling price of $ 0.2617/Kg substantiated the project's profitability and commercial feasibility. This aims towards the concept–to–commercialization (trash to cash) aspect of IS as part of resource valorization.

Beyond its biofuel application, the value–addition prospects of IS–derived bio–oils were investigated (antioxidant and antimicrobial assays). Elevated phenolic (96.5 mg GAE/ml in *L. camara* > 71.17 mg GAE/ml in *A. adenophora* > 62.71 mg GAE/ml in *S. jamaicensis*) and moderate flavonoid contents (17.7 mg QE/ml in *L. camara* > 14.75 mg QE/ml in *A. adenophora* > 12.45 mg QE/ml in *S. jamaicensis*) of bio–oil synergistically augment its antioxidant activity. The ferric reducing potential and free radical combating ability of bio–oil further validated its potential as a bioactive resource for pharmaceuticals. Antimicrobial assay revealed that bio–oil derived from *A. adenophora, L. camara* and *S. jamaicensis* exhibited zone of inhibition (ZOI) of 27.7 mm, 31.02 mm and 19.48 mm, respectively, against *Candida albicans. L. camara* bio–oil exhibited enhanced efficacy against *C. albicans* with Minimum Inhibitory Concentration of 3.125 µg/ml. This may be ascribed to the intricate array of bioactive chemicals in the bio–oil demonstrating their potential application in the field of pharmaceuticals, particularly as antimicrobial agents.

Molecular docking studies further reinforced the pharmaceutical significance of bio–oil, identifying significant bioactive ligands that mimicked noteworthy binding preferences to existing breast cancer therapeutics including Anastrozole and Letrozole. Furaltadone in *A. adenophora* bio–oil displayed the strongest binding affinity of – 6.4 kcal/mol, making it the most potent compound and surpassing the standard drugs

Letrozole and Exemestane (− 6.2 kcal/mol), closely followed by Anastrozole (− 5.6 kcal/mol). *In–silico* investigations further revealed that Ala A: 96 in *A. adenophora* and *L. camara* and Arg A:84 in *S. jamaicensis* bio–oil (considering their significant binding) demonstrated critical function in ligand stabilization.

The outcomes of the present study highlight the dual benefits of the prospective management and valorization of IS. This study fosters sustainable development through the integration of bioresource utilization, biofuel production and subsequent value–enhancement, thereby advancing bioenergy generation and therapeutic breakthroughs. The novelty of this doctoral research lies in is its interdisciplinary approach, integrating ecological assessment with bioenergy–bioproduct research to transform environmental nuisance into valuable bioresources. Consequently, by bridging the gap between sustainable IS management, biofuel innovation and biopharmaceutical applications, this study sets the stage for future advancement in renewable energy and zero–waste economy. Additionally, the prospective valorization of IS constitutes a viable environmental strategy that bolsters its management (IS in particular) and aligns with the "Waste to Wealth" concept, reinforcing India's three flagship initiatives such as Swachh Bharat Abhiyan, Aatmanirbhar Bharat Abhiyan and Make in India.

*Keywords*: Biomass, Population assessment, Distribution, Thermochemical conversion, Bio–oil, Economic analysis, Antioxidant, Antimicrobial.

# LIST OF ABBREVIATIONS

| Abbreviation | | Meaning |
|---|---|---|
| $^{1}$H NMR | : | Proton Nuclear Magnetic Resonance |
| $^{13}$C NMR | : | Carbon-13 Nuclear Magnetic Resonance |
| AAE | : | Ascorbic Acid Equivalent |
| Abs | : | Absorbance |
| AC | : | Ash Content |
| Ala | : | Alanine |
| AMR | : | Antimicrobial Resistance |
| Arg | : | Arginine |
| Asp | : | Aspartic Acid |
| ASTM | : | American Society for Testing and Materials |
| BA | : | Binding Affinity |
| BHT | : | Butylated Hydroxytoluene |
| Biovia DS | : | Biovia Discovery Studio |
| BSA | : | Bovine Serum Albumin |
| CAPEX | : | Capital Expenditure |
| CBD | : | Convention on Biological Diversity |
| CE | : | Capillary Electrophoresis |
| COP | : | Conference Of the Parties |
| cSt | : | Centistokes |
| Cys | : | Cysteine |
| DPPH | : | 1, 1-diphenyl-2-picrylhydrazyl |
| DW | : | Distilled Water |
| EPC | : | European Parliament and the Council |

| Abbreviation | | Meaning |
|---|---|---|
| FASTA | : | Fast-All |
| FC | : | Fixed Carbon |
| FCR | : | Folin-Ciocalteu Reagent |
| FCC | : | Fluid Catalytic Cracking |
| FRAP | : | Ferric Reducing Antioxidant Power |
| FTIR | : | Fourier Transformed Infrared Spectroscopy |
| GAE | : | Gallic Acid Equivalent |
| GC-MS | : | Gas Chromatography–Mass Spectroscopy |
| GCV | : | Gross Calorific Value |
| GIS | : | Geographic Information System |
| Gly | : | Glycine |
| GMQE | : | Global Model Quality Estimation |
| GPS | : | Global Positioning System |
| HDO | : | Hydrodeoxygenation |
| HPLC | : | High-Performance Liquid Chromatography |
| $IC_{50}$ | : | Half-Maximal Inhibitory Concentration |
| IEA | : | International Energy Agency |
| Ile | : | Isoleucine |
| IPBES | : | Intergovernmental Science-Policy Platform on Biodiversity and Ecosystem Services |
| IRR | : | Internal Rate of Return |
| IS | : | Invasive Species |
| IUCN | : | International Union for Conservation of Nature |
| IVI | : | Importance Value Index |

| Abbreviation | | Meaning |
|---|---|---|
| IWM | : | Integrated Weed Management |
| LB | : | Lower Bound |
| Leu A | : | Leucine |
| MAE | : | Microwave-Assisted Extraction |
| MaxEnt | : | Maximum Entropy Model |
| MC | : | Moisture Content |
| Met | : | Methionine |
| MFR | : | Mechanically Fluidised Reactor |
| MGNREGA | : | Mahatma Gandhi National Rural Employment Guarantee Act |
| MHA | : | Mueller Hinton Agar |
| MHB | : | Mueller Hinton Broth |
| MIC | : | Minimum Inhibitory Concentration |
| MM2 | : | Merck Molecular Mechanics |
| Mpsi | : | Millisecond Per Sample Increment |
| MSP | : | Minimum Selling Point |
| NCG | : | Non-Condensable Gases |
| NCV | : | Net Calorific Value |
| Ni-Cr-Ni | : | Nickel-Chromium / Nickel-Aluminum |
| NIST | : | National Institute of Standards and Technology |
| NMR | : | Nuclear Magnetic Resonance |
| NPV | : | Net Present Value |
| NUDT5 | : | Nudix Hydrolase 5 |
| OD | : | Optical Density |

| Abbreviation | | Meaning |
|---|---|---|
| OPEC | : | Organization Of Petroleum Export Countries |
| OPEX | : | Operational Expenditure |
| PBP | : | Payback Period |
| PDB | : | Protein Data Bank |
| Phe A | : | L-Phenylalanine |
| Pro A | : | Proline |
| QE | : | Quercetin Equivalent |
| QMEANDisCo | : | Distance Constraints Applied on Model Quality Estimation |
| QSQE | : | Quaternary Structure Quality Estimation |
| RCSB | : | Research Collaboratory for Structural Bioinformatics |
| RD | : | Relative Density |
| RD' | : | Relative Dominance |
| RF | : | Relative Frequency |
| RMSD | : | Root Mean Square Deviation |
| RNS | : | Reactive Nitrogen Species |
| ROS | : | Reactive Oxygen Species |
| RS | : | Remote Sensing |
| RSA | : | Radical Scavenging Activity |
| SCFs | : | Super Critical Fluid |
| SDMs | : | Species Distribution Models |
| SFC | : | Supercritical Fluid Chromatography |
| SGDs | : | Sustainable Development Goals |
| SMILES | : | Simplified Molecular Input Line Entry System |

| Abbreviation | | Meaning |
|---|---|---|
| TFC | : | Total Flavonoid Content |
| TGA | : | Thermogravimetric Analysis |
| TG-DTG | : | Thermogravimetric Analysis - Derivative Thermogravimetric Analysis |
| TIC | : | Total Ion Chromatography |
| TLC | : | Thin-Layer Chromatography |
| TMS | : | Tetramethylsilane |
| TPC | : | Total Phenolic Content |
| TPTZ | : | 2,4,6-Tri(2-Pyridyl)-S-Triazine |
| Tyr A | : | Tyrosine |
| UB | : | Upper Bound |
| UNFCCC | : | United Nations Framework Convention on Climate Change |
| UV-Vis | : | Ultraviolet-Visible |
| Val A | : | Valine |
| VM | : | Volatile Matter |
| WoNS | : | Weeds Of National Significance |
| ZOI | : | Zone Of Inhibition |
| ZSM-5 | : | Zeolite Socony Mobil-5 |

# LIST OF FIGURES

# LIST OF TABLES

# TABLE OF CONTENTS

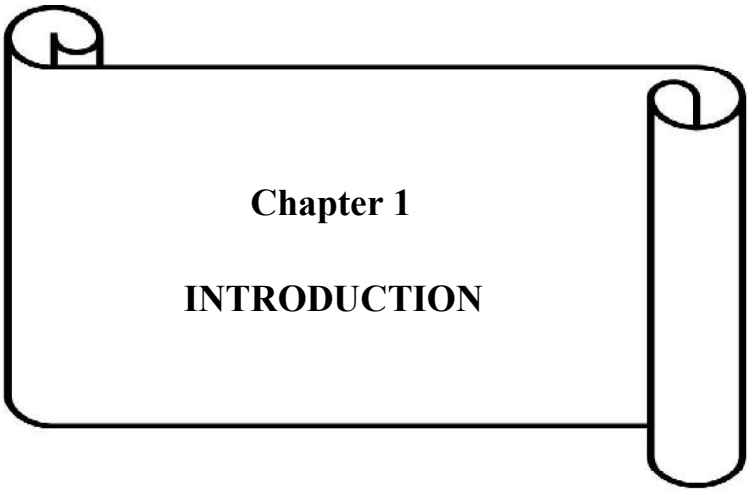

# Chapter 1

# INTRODUCTION

# Chapter 1
# INTRODUCTION

Invasive species (IS) represent one of the most pressing threats to global biodiversity and ecosystem stability. According to the International Union for Conservation of Nature (IUCN), IS are alien species that adversely affect biodiversity, ecosystems, economies and/or human health (IUCN, 2009). Characterized by high adaptability, swift reproduction, and extensive distribution, IS often dominate and outcompete native species for critical resources such as nutrients, light, space and water. This competitive dominance often leads to a decline in native biodiversity, reduce ecosystem functionality, and, in some cases, local extinction of native species. These IS also disrupts the soil microbial communities and indigenous ecosystem topologies including fluctuations in nutrient cycling, organic matter decomposition and energy flow essential for sustaining ecological equilibrium (Wang et al., 2021). Often the first species to colonize in disturbed environments, IS also obstruct the recreational and aesthetic value of the environment. Terms such as alien invasive species, introduced species, exotic species, noxious weeds are commonly used interchangeably for IS in contemporary scientific literature.

Over 1000 IS have established and proliferated threatening the global ecosystem to an alarming extent (Cam et al., 2022). Once established, these species act as a principal catalyst to anthropogenic environmental change and exhibit vigorous biological invasion (Chapple et al., 2022). This invasion typically adheres to a standard sequence: initial introduction (either deliberate or accidental), eventually leading to establishment (wherein the species survives without dispersing), followed by potential spread, often instigated by alterations in environmental conditions (McCormick & Howard, 2013). The rapid expansion of global trade, transportation and climate change have significantly elevated the frequency and geographical scale of IS proliferation (Gulzar et al., 2024). This proliferation is further facilitated by alterations in land–use and ecological disturbances intensified by anthropogenic activities (Jaureguiberry et

al., 2022), creating favourable ecological niches facilitating the survival of IS. Today, approximately one–fifth of the Earth's surface is extremely vulnerable to such invasions (IPBES, 2019; Máximo et al., 2020) with IS ranking as the second leading cause of species endangerment and extinction, following habitat destruction (Pejchar & Mooney, 2009). Given their extensive and far–reaching adverse effects, prompt and coordinated international efforts are essential for impact mitigation and associated IS management strategies.

## 1.1. The global burden of IS

Beyond their ecological ramifications, IS have far–reaching implications on the global environmental health, listing them among the top global environmental concerns (Fang et al., 2020). Native plants which serve as sinks for air pollutants and contribute significantly in carbon sequestration are often displaced by IS (Shackleton et al., 2017). Ultimately, the decline in native diversity may lead to disruption in the environmental quality, indirectly impacting human health. Furthermore, it has been established that specific IS may also function as harbingers of environmental pollution, compounding their harmful effects (Rai, 2016).

One of the pronounced consequences of IS is its adverse impact on the economy. On an economic perspective, the global yearly expense of biological invasions is anticipated to surpass USD $ 423 billion (IPBES, 2023). Diagne et al. (2021) estimated the global economic impact of IS reached approximately $162 billion in 2017 rising from around $ 1.3 trillion incurred before 2017. Brazil allegedly expended around USD 105.53 billion over 35 years, averaging USD 3.02 billion annually due to IS (Adelino et al., 2021). While in India alone, IS has cost the economy between US$ 127.3 billion and US$ 182.6 billion (₹ 8.3 trillion to ₹ 11.9 trillion) from 1960 to 2020, with these expenses continuing to rise over time (Bang et al., 2022). In the agricultural sector, IS function as aggressive weed causing substantial decline in global productivity along with obstruction of forest biodiversity. The resulting economic loss is profound. Global agriculture suffers annual losses of US$ 248 billion due to IS coupled with pests and pathogens rendering agriculture one of the most impacted sector (Fried et al., 2017). IS causes substantial financial consequences

worldwide, with yield decreases estimated around $ 100 million to $ 26 billion (Ahmad et al., 2023). Furthermore, unmanaged IS have led to an estimated 50 % decline in yield, culminating in a projected loss of $ 26.7 billion across Canada and the US alone (Sosnoskie & Duke, 2023). Given the severe ecological and economic consequences of IS, invasive ecology is now being recognized as a trans–disciplinary concept, intersecting with the restoration and conservation biology, health science, economic systems and land–use change (Heshmati et al., 2019). Consequently, addressing the challenges of IS requires integrated management approaches grounded in socio–ecological and socio–economic assessments. Such approaches are essential for biodiversity conservation and public health protection in order to warrant long–term sustainability of ecosystem services.

## 1.2. IS management and challenges

Article 8 (h) of the 1992 UN Convention on Biological Diversity (CBD) (United Nations, 1992) prioritize phases of control as follows:

1. Prevention involving mitigation via proper risk evaluation and execution of quarantine measures
2. Elimination entailing the full eradication of invading species
3. Containment encompassing of halting the proliferation of established IS
4. Management and regeneration of impacted ecosystem

Several tactics including rapid elimination following early diagnosis, mitigating impact and ecosystem restoration have been implemented as means of effective IS management. Among these, prompt detection, usually promoted by community participation and mitigation through conventional strategies including chemical (herbicides), biological (natural enemies) or manual eradication (weeding, mulching, cutting) have gained much recognition (Máximo et al., 2020). These conventional approaches, though labour–intensive incurring significant expenditure, have proven inadequate in controlling and eradicating IS yielding minimal success and may also adversely impact native plants. Consequently, to address the infeasibility of total elimination, it is essential to investigate alternative strategies. These strategies

should aim to optimize the potential benefits of IS while maintaining an ecological equilibrium. This underscores the need for an economically viable approach for effective IS management. IS management is recognised as a primary impediment to ecological restoration (Dong et al., 2019). Biodiversity conservation planners along with international and national governments have prioritized the management of IS. This encompasses formulating numerous policies, rules and mandates to restrict their introduction and limit the geographical proliferation as an attempt to mitigate their adverse impacts on ecosystems and natural resources for sustainable ecosystem management. In Australia, Weeds of National Significance (WoNS) programme emphasized the regulation and management of IS possessing significant threats to biodiversity and ecosystem (Shaik et al., 2022). Likewise, regulation No. 1143/2014 issued by European Parliament and the Council (EPC) aimed for prevention and effective management of IS (European Union, 2014). Despite the endorsement of initiatives including the Intergovernmental Science-Policy Platform on Biodiversity and Ecosystem Services (IPBES) Global Assessment, the Millennium Ecosystem Assessment, the Global Biodiversity Review and the Convention on Biological Diversity, the trajectory regarding ecosystem and biodiversity protection from IS remains increasingly adverse (Peter et al., 2021).

From a management standpoint, IS in agricultural areas are considered undesirable as their existence diminishes crop yields and adversely impact crop quality (Kocira & Staniak, 2021). In forest ecosystems, proactive IS management is crucial to ensure that these ecosystems continue to sequester more carbon than they emit while maintaining sustainable nutrient and water cycles (Miniat et al., 2021). Additionally, increasing cross–border trade has further complicated efforts to contain IS (Hulme, 2021). Integrated weed management (IWM) techniques integrate the formulation and optimization of international and national policies, development of strategic – regulatory tool designing for control and prevention of IS and creation of favourable niche (Tefera et al., 2020). Regrettably, IWM–generated solutions are frequently impeded by substantial labour requirements and capital outlay, yielding minimal to no immediate return. Furthermore, these management approaches may obstruct or alter succession dynamics, adversely impacting the trends in vegetation. Sustainable IS

management requires identifying favourable habitats that support their proliferation and executing appropriate control measures. This includes regulating and managing these IS in accordance with the sustainable biorefinery method under the aegis of "Waste to Wealth" concept. Elucidating the patterns, traits, and determinants of IS establishment and proliferation, along with assessing invasion risk across diverse habitats, can help identify high–risk zones, allowing prompt monitoring, early alerts, prevention, and control strategies (Zhao et al., 2020). To mitigate hazards linked with IS proliferation, such as enacting stringent quarantine measures and devising prompt detection and elimination approaches, comprehensive data on species abundance and distribution under both present and prospective climatic scenarios is crucial (Adhikari et al., 2024).

### 1.3. Bioprospecting of IS

Assessing the distribution and prevalence of IS is crucial for effective management and utilization. While direct field evaluations are often challenging and time–consuming, they remain indispensable for acquiring accurate baseline data. Population studies including parameters such as frequency, density, dominance and Importance value index (IVI) provide detailed understanding on the ecological status and competitive ability of IS relative to native flora. The metrics help identify the species exerting the greatest influence within a community and highlight priority areas for intervention. The initial stage in IS management and intervention warrant the proper identification of their geographical distributions (Dai et al., 2020). Albeit, conventional methods frequently rely on reconnaissance and extensive field surveys, integrating these robust field–derived datasets with advanced tools can efficiently optimize tracking and management efforts. Consequently, in this regards, remote sensing is an increasingly attractive and viable option for detection employing spectral, textural, and/or phenological distinctions between invasive and native species (Bradley, 2013). Among these methods, spectral distinction (utilizing hyperspectral images) is the most effective approach, as it leverages the unique spectral signatures of IS differentiating them from native species (Underwood et al., 2003). Another crucial part of bioprospecting involves evaluating its spread to determine precise sites of its

proliferation. The necessity for precise population distribution of IS and their dispersion emerges due to inadequate data on their presence and spread, hence hindering effective management and utilization strategies (Crall et al., 2015). This data ambiguity is alarming as climate change facilitates the expansion of IS creating conducive environment for their establishment and persistence (Yang et al., 2013). Considering the direct ecological and economic influence of IS, acquiring further insights into their population and distribution dynamics is crucial for addressing critical environmental challenges. In this context, predictive distribution models assist in overcoming the challenges associated with limited distributional data and are essential tools for evaluating species distribution patterns (Yang et al., 2013). Significantly, Geographic Information System (GIS) modelling, particularly through Species Distribution Models (SDMs) like the Maximum Entropy Model (MaxEnt), serves as an essential instrument for predicting IS range and identifying hotspots for targeted management and biomass collection (Elith et al., 2010). These forecasts can subsequently aid in the strategic oversight of IS to enhance their procurement as feedstock for biofuel generation. Certain studies have effectively utilized MaxEnt to forecast the distribution of IS (Verma et al., 2022; Xian et al., 2022). Regions identified as highly conducive to IS may be prioritized for conservation or management interventions, including population eradication, obstruction of invasion routes, and ecosystem restoration in areas vulnerable to invasion (González–Trujillo et al., 2024). The integration of Remote Sensing (RS) and GIS–based modelling enhances the efficiency and data–driven nature of bioprospecting IS. These advances in technology enhance IS detection and monitoring while promoting sustainable management strategies that reconcile ecological conservation with utilization of resources.

## 1.4. IS as a bioenergy feedstock

The 1970 worldwide energy crisis, triggered by petroleum scarcity, drastically altered the previously unbound availability of fossil fuels while largely disregarding emerging global concerns such as climate change (Baloch et al., 2018). The initial major disruption, in 1973, stemmed from the Arab Oil Embargo imposed by Organization of Petroleum Export Countries (OPEC) in retaliation for Western support

of Israel during the Yom Kippur War. This led to severe oil supply disruptions and price escalations. The second crisis followed in 1979, driven by the Iranian Revolution and the subsequent Iran–Iraq War, which interrupted Iranian oil production and resulted in another surge in oil prices (Zhao, 2019). These crises spurred the exploration of alternate sources, particularly biofuels. In response, several nations initiated dedicated research programs focused on biofuel production to enhance energy security and reduce reliance on conventional fossil fuels. Amid escalating oil prices and heightened apprehensions regarding climate change, biofuels garnered significant global attention from leaders and policymakers as a viable substitute for fossil fuel (McCormick & Howard, 2013). Furthermore, India's 2030 decarbonization objective, announced at the 26$^{th}$ Conference of the Parties (COP) to the United Nations Framework Convention on Climate Change (UNFCCC), aims on achieving a 50 % reduction in carbon emissions from energy and increase fossil–free fuel capacity to 500 GW by 2030 (Energy Transitions Commission, 2022). Driven by the ongoing energy crisis and the global pursuit of energy security, biofuel research has gained momentum leading to the investigation of numerous energy crops. However, to enhance efficiency and avoid the conundrum of the Food Vs Fuel debate, a broader array of lignocellulosic feedstocks are being investigated (Tudge et al., 2021). Given the urgency for sustainable energy solutions, IS have been contemplated as a viable feedstock for fulfilling prospective biofuel generation demands. Numerous advantageous traits that render biofuel crops optimal are prevalent in IS including substantial yields, adaptability to marginal environments, prevalence and swift development (Nguyen et al., 2021). Moreover, the potential and economic feasibility of IS as a bioenergy feedstock is robustly supported by its renewable and carbon–neutral characteristics, widespread geographical availability and holocellulose content (Shavyrkina et al., 2023). Furthermore, IS, with its substantial biomass yield and energy density, presents a compelling aspect for exploring new vistas as a prospective feedstock in bioenergy research. Gunaseelan (1997) reported that IS were a potential biomass source for bioenergy generation and their large–scale utilisation constituted one of the promising strategies for their management. According to the International Energy Agency (IEA), IS, when used as a feedstock for biofuel production, fall under the category of second–

generation biofuels. Additionally, IS exhibit the following key biological traits that renders them suitable as feedstock for biomass conversion

- Rapid growth and capacity to surpass indigenous species (Zhang et al., 2020)
- High yields and perennial growth form (Smith et al., 2013)
- Extensive and prolific seed generation (Reuss et al., 2001)
- Tolerance to diverse soil and climatic conditions (Waller et al., 2020)
- Resilience to pests and pathogens (Smith et al., 2013)

Consequently, utilization of IS as feedstock mitigates their adverse environmental impacts while simultaneously contributing to energy security (Bajgai et al., 2021). The IS projects serious threat to the environment in general and agricultural/forestry–based operations in particular. Bio–energy generation may offer a promising avenue to maximise the utility of the otherwise environmentally disfavoured IS and put them to their best advantage. Committed research endeavours in this direction may project IS as sustainable feedstocks for upcoming bio–refineries in the ensuing future. This approach not only leverage an underutilized asset but also offers manifold opportunities for bioenergy production, ecological restoration, environmental management and addressing the Sustainable Development Goals (SDGs), thereby unlocking the untapped potentials of IS in the global transition towards a green economy.

## 1.5. Biofuel production technologies for IS

Various biochemical and thermochemical processes (Fig. 1.1) have been reported to transform IS biomass into valuable bio–based products such as bioethanol, biodiesel, biochar, syngas and biofuels (Debella et al., 2023). This valorization of IS biomass not only contributes towards an alternate energy source but also promotes resource utilization. Biochemical conversion of IS has emerged as a promising pathway offering sustainable means to transform IS biomass into bio–based products through anaerobic digestion and alcoholic fermentation. Anaerobic digestion refers to the microbial decomposition of biomass resulting in the production of biogas (methane) and digestate (fertilizer) (Gautam et al., 2019). Fermentation denotes the

transformation of organic waste into acid or alcohol (such as ethanol or lactic acid) in an anaerobic environment, resulting in a nutrient–dense byproduct (Gautam et al., 2019). Bioproducts derived from IS biomass conversion encompasses of renewable chemical products, renewable gasoline, bioethanol, and other alcohols. Meanwhile, thermochemical conversion methods, such as pyrolysis, gasification, and hydrothermal liquefaction, have been extensively explored for the conversion of biomass into energy–rich biofuels and biochemicals. Among these, pyrolysis has garnered much attention as an economically viable and environmentally suitable approach (Liu & Yu, 2021). These approaches have been rendered suitable for the conversion of IS biomass, which often pose challenges for biochemical conversion due to the complex composition of IS and the limited accessibility of carbohydrate content for bioethanol production (Premjet, 2019). Pyrolysis have demonstrated strong potential for valorization of IS biomass yielding high energy–dense bio–oil revealing its candidature as feedstock for bioenergy generation (Ramesh & Somasundaram, 2020; Pérez et al., 2021). Production of IS–derived biofuel reinforces the viability of thermochemical conversion routes in transforming IS into potential energy sources. Notably, while previous investigations emphasize the substantial energy content and favourable combustion properties of IS–derived biofuel, complementary findings indicate their biodiesel potential for applications in external combustion engines. For instance, Jatropha Biodiesel and *Prosopis juliflora,* as a renewable energy source, finds potential application in compression ignition engines as a substitute to conventional diesel fuel (Mehra et al., 2021; Debella et al., 2023). Bio–oil also projects its candidature as a potential source of valuable chemicals owing to its diverse composition of functional groups. The biochar obtained from pyrolysis reaction is used as a soil amendment which promotes environmental remediation (Fernández et al., 2024). Several other bio–based products derived from IS biomass include high density briquetted pellets (Midhun et al., 2023), biobutanol (Zihare & Blumberga, 2017), succinic acid (Shen et al., 2016), microemulsion based hybrid biofuel (Bora et al., 2015). Syngas ($CO + H_2$), obtained from the thermochemical conversion method of gasification, can be converted to high–value chemicals and hydrocarbon liquid fuel through Fischer–Tropsch synthesis (Mehariya et al., 2020). Furthermore, advanced

catalytic hydrotreatment of IS can yield energy–rich hydrocarbon fuel that closely resembles conventional petroleum products (Ma et al., 2023). The utilization of suitable conversion technologies for biofuel production from IS biomass presents a promising pathway for sustainable energy generation simultaneously alleviating the ecological threats posed by its proliferation. Further advancements in conversion efficiency coupled with cost–effectiveness and large–scale applicability are essential to fully exploit these IS and augment their role in the integrated biorefinery system.

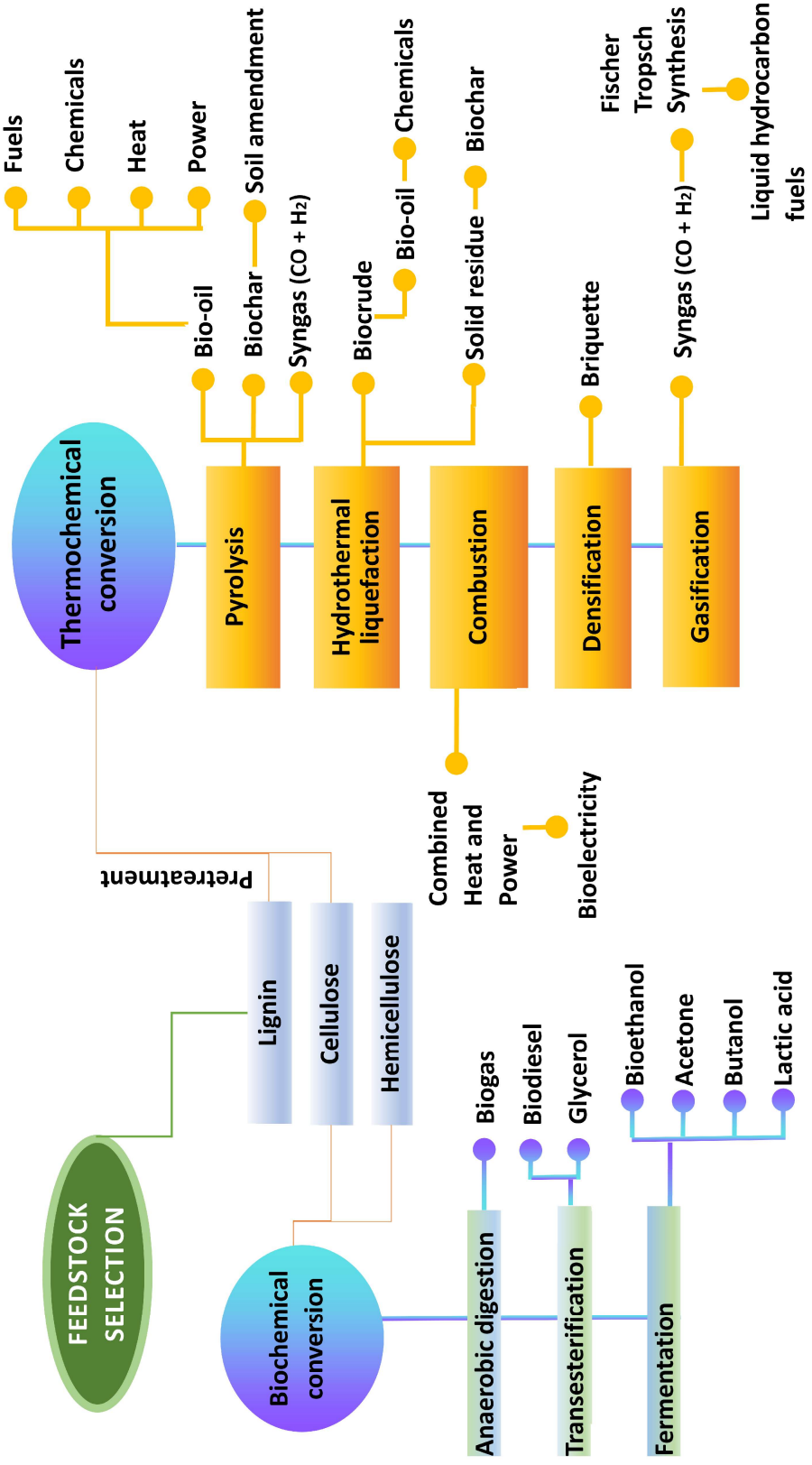


**Fig. 1.1**. Conversion technologies for bioenergy generation (Sikarwar et al., 2017; Khalid & Singh, 2023).

## 1.6. Thermochemical conversion (pyrolysis) of IS biomass

A promising avenue for IS management entails the conversion of its biomass through thermochemical conversion processes (pyrolysis) into sustainable biofuels and value–added products with varying applications. Over the years pyrolysis has been recognised as an efficient waste valorization strategy, leading to an upsurge in investigations in this field. Pyrolysis of IS biomass is regarded as an effective approach, offering both ecological and economic advantages. This process not only manages the proliferation of these undesirable yield reducers, but also facilitates efficient utilization of waste (Du et al., 2018) thereby transitioning towards a circular economy.

Pyrolysis is the process of subjecting biomass to elevated temperatures in an oxygen–deficient environment for the production of three resultant products viz. liquid bio–oil, solid biochar and non–condensable gases (NCG) ($CH_4$, $H_2$, CO and $CO_2$) (Saletnik et al., 2018). Pyrolysis is generally categorized into slow, fast and flash pyrolysis based on its heating rate and residence time (Kan et al., 2016). Fast pyrolysis is presently the favoured method due to its rapid reaction rate and comparatively higher bio–oil yields (Hu & Gholizadeh, 2019). Slow pyrolysis occurs at temperatures ranging from 380 – 500 °C, with 0.1 – 1.0 °C/s heating rate and 5 – 30 min vapor residence time (Bridgwater et al., 2008). This process generates higher yield of biochar in comparison to gaseous and liquid products. Fast pyrolysis, on the other hand, occurs at moderate temperatures (425 – 1000 °C) at a short vapor residence time (2 – 10 s) with an elevated heating rate (10 – 200 °C/s) (Bridgwater, 2003). This process produces high bio–oil yields, depending upon the biomass employed, typically comprising of 10 – 20 wt. % of non–condensable gases, 15 – 25 wt. % of biochar and 60 – 75 wt. % of liquid (Mohan et al., 2006). Flash pyrolysis, also characterized by high yield of bio–oil, occurs at elevated temperatures (> 800 °C), with elevated heating rates (> 1000 °C/s) and residence time of only a few seconds (< 2 s) (Bridgwater, 2003). The pyrolysis process is affected by several factors including biomass composition, operating temperature, heating rate, residence time, particle size and reaction atmosphere. These factors significantly impact the composition and yield of pyrolysis products. Biomass with high holocellulose content is typically associated with

increased bio–oil generation while lignin–rich biomass tends to promote char production (Feng & Lin, 2017). Temperature is another crucial factor that affects the yield and quality of pyrolysis outputs, significantly influencing decomposition reactions and affecting the generation of gases and liquids. Nevertheless, it exerts minimal impact on char development (López et al., 2011). The yields and characteristics of pyrolysis–derived products are considerably influenced by the heating rate and residence durations with higher heating rate and reduced residence period promoting bio–oil generation (Bridgwater, 2012).

### 1.6.1. Mechanism of pyrolysis

A number of processes occur during pyrolysis, including dehydration, depolymerization, isomerization, aromatization, decarboxylation, and charring (Hu & Gholizadeh, 2019). The reactions are listed below

**Primary reactions**: The major reactions consist of char production, depolymerization followed by fragmentation of biomass. Char production occurs due to the conversion or condensation of benzene rings into aromatic polycyclic structures (Kan et al., 2016). Depolymerization includes the cracking of large polymer chains into aromatic monomers, resulting in the generation of gases and volatiles (Collard & Blin, 2014). Fragmentation represents the disruption of covalent bonds linking the unit monomers and polymer. This results in the production of small chain components and non–condensable stable gases (Kan et al., 2016).

**Secondary reactions**: Volatiles generated during primary reactions may lack stability and subsequently undergo secondary reactions. This reaction includes cracking or recombination processes. Furthermore, the obtained char can also act as a catalyst to facilitate the reaction. While cracking of primary compounds yields lighter compounds, recombination leads to the production of heavier components including polycyclic hydrocarbons or deposits on char's surface (Zhang et al., 2018).

### 1.6.2. Stability of pyrolysis–derived bio–oil

The instability of bio–oil can be attributed to various aging reactions, including dimerization, oxidation, acetalization, esterification and polymerization; the oxygen–rich constituents of bio–oil (aldehydes and carboxylic acids) play a substantial role in these aging processes (Meng et al., 2015). The oxygenates in bio–oil has been recognised as the primary factor contributing to its instability, indicating a link between the oxygen level of bio–oil and its stability (Kim et al., 2012). Consequently, a substantial decrease in the oxygen concentration of bio–oil may lead to improved stability. Furthermore, including methanol with an acid catalyst may also enhance the stability of bio–oil, by effectively sealing the reaction sites of carboxyl and carbonyl compounds in the bio–oil, resulting in the formation of rather stable esters and acetals (Moens et al., 2009). This indicates that enhancing bio–oil stability can be accomplished by transforming bio–oil oxygenates into a more stable chemical form, such as alcohol. Therefore, a stable bio–oil could be achieved by modifying its chemical composition to favor more stable oxygenates without extensive deoxygenation. Furthermore, recent studies have also indicated the presence of radicals in bio–oil, which may result in radical–initiated condensation events during the high–temperature processing of bio–oil (Kim et al., 2015).

### 1.6.3. Catalytic upgrading of bio–oil

Pyrolysis–derived bio–oil, however, possess high concentration of oxygen contents, necessitating catalytic upgrading to diminish the oxygen levels prior to utilization. Catalytic pyrolysis integrates pyrolysis with catalytic upgrading processes, wherein the reactor comprises a combination of biomass and catalyst. During this process, the composition of pyrolysis vapours is altered due to the interaction of the thermally converted products with the catalyst (Pham et al., 2022). Various categories of catalysts have been explored for catalytic pyrolysis of biomass, including zeolite catalysts (Beta, ZSM–5 and Y, Mordenite), metal oxide catalysts (silica and alumina), metal catalysts (platinum and nickel) (Cai et al., 2024). These catalysts are often employed to enhance the efficiency of pyrolysis process and elevate the quality of bio–oil obtained (Iliopoulou et al., 2018). Hierarchically zeolite single crystal, exhibiting

fully interconnected and adjustable multimodal porosity across macro–, meso–, and microscales demonstrate enhanced catalytic activity, longevity, and significantly reduce catalyst deactivation due to coke formation (Sun et al., 2020). Bimetallic species doped on HZSM–5 zeolites exhibit enhanced selectivity for aromatics, minimize undesired side reactions, and provide improved resilience to thermal degradation (Salisu et al., 2025). Furthermore, incorporation of a tertiary zeolite such as $ZrO_2$ into dual catalyst system enhances the deoxygenation of bio–oil presenting a promising approach to improve the bio–oil quality, while maintaining its high yield during staged ex–situ catalytic pyrolysis (Jin et al., 2024). In recent years co–pyrolysis involving the amalgamation of two different biomasses, have been employed to enhance product quality and function as fuel (Zhang et al., 2016; Wu et al., 2025).

## 1.7. Value–addition from IS biomass – beyond the biofuel concept

The total eradication of IS from the ecosystem may be a far–fetched attempt, however, employing these under–utilized bioresources for production of biofuels and value–added products is the need of the hour. Complementary to its conventional fuel utilization, bio–oil demonstrates immense potential for diverse bioactive applications due to its intricate composition including oxygenates (alcohols, ketones, esters, ethers, aldehydes, furans), mixed acids, hydrocarbons (aromatics and aliphatics) and phenolic constituents (Alagöz et al., 2023). Consequently, bio–oil have been reported to exhibit antimicrobial, cardio–protective, antiviral, antifungal properties or advantageous impacts against cancer (Simonetti et al., 2020; Montenegro–Landívar et al., 2021; Aqeel et al., 2023; Chen et al., 2023; Maheshwari & Sharma, 2023). The present study thus, in addition to characterizing the target product (bio–oil) for its fuel properties, also aimed to explore its bioactive potential (antioxidant and antimicrobial) and *in–silico* investigations, as a part of value–addition.

A notable aspect of bio–oil is its substantial phenolic constituents, a component well–recognised for mitigating oxidative damage and counteracting free radicals in biological systems (Singh et al., 2024a). These phenolic components are found in a diverse array of compounds, existing as either oligomers or monomers, contingent upon the biomass in use and processing condition (Olcese et al., 2013). Interestingly,

phenolic compounds have garnered increasing interest due to their biological activities. Among several bioactivities exhibited by phenols and its derivatives, their antioxidant capabilities have garnered attention of the scientific community. However, the intricate composition of bio–oils complicate the identification of specific chemicals associated with antioxidant properties, as the presence of other chemical classes may disrupt the reaction of monophenols (Cesari et al., 2019). Subsequently, free phenolic OH groups are mostly attributed to antioxidant effects, whereas aliphatic OH groups are known to exert an opposing influence on radical scavenging capacity (Ugartondo et al., 2008). Furthermore, phenolic compounds possessing a greater quantity of OH groups have been reported to improve Reactive oxygen species (ROS) scavenging activity by protecting cell against diseases associated with oxidative stress (Świętek et al., 2019). Additionally, pyrones isoeugenol, furancarboxaldehydes, vanillins, syringols, catecols, and guaiacols are among the other bioactive compounds present in bio–oil (Matayeva et al., 2019).

Bio–oil has also been well recognised for its notable antimicrobial properties due to its diverse array of chemical composition. Microorganisms including *Trametes versicolor*, *Gloeophyllum trabeum*, *Tyromyces palustris*, *Poria placenta*, *Polyporus sanguineus*, *Fomitopsis palustris*, *Escherichia coli*, *Salmonella* sp., *Listeria* sp., *Yersinia enterocolitica*, *Salmonella enterica*, *Streptomyces scabies*, *Bacillus cereus* and *Xanthomonas campestris* among several others are effectively inhibited due to the antimicrobial property of pyrolysis–derived bio–oil (Hingston et al., 2001; Mohan et al., 2008; Milly et al., 2008; Patra et al., 2015). Key compounds in bio–oil contributing towards its antimicrobial activity includes phenols and its derivatives, organic acids and carbonyl compounds (Mattos et al., 2019). Phenolic compounds (2–methyl, 3–methyl and 4–methylphenol) are responsible for disrupting the function and structure of microbial plasma membrane in microbes. This action results in alterations to cell surface hydrophobicity, leading to the leakage of cytoplasmic contents (Borges et al., 2013). Phenols, including eugenol and catechol modify the composition of the fungal plasma membrane. These compounds, in addition to fungal membrane disruption, can chelate metallic ions, essential for fungal activity involving oxidative attack and the breakdown of hydroxyl radicals (Dias et al., 2023). Organic acids, acetic acid in

particular, contribute towards cytoplasmic acidification, thereby interfering with microbial energy production and enzyme function (Taylor et al., 2012). Compounds including furanic functional groups, 1–hydroxy–2–propanone (acetol), 4–ethyl–2–methoxyphenol (4–ethylguaiacol), 2–methoxy–4– methylphenol, 2–methoxyphenol (guaiacol), 2,6–dimethoxyphenol (syringol), 2–propanone, methanol, 2–furancarboxaldehyde, ketones, and many carboxylic acids are frequently present as major constituents in bio–oil with antimicrobial effects (Mattos et al., 2019; Dias et al., 2023). With advancement in bio–oil research and its prospects in the pharmaceutical industry, there is a growing shift from synthetic antioxidants and antimicrobial agents to plant–based alternatives, driving intensified investigations into their bioactive properties and significantly reduced adverse effects. Ultimately, bio–oil can be explored for its prospective applications in bioactive and therapeutic domains.

**Objectives**

Accordingly, based on the aforementioned background information, the following objectives were formulated for the current research work

1. Assessment of IS distribution in Kohima district, Nagaland
2. Characterization of IS biomass
3. Investigation of the feasibility of thermo–chemical conversion (pyrolysis) of IS biomass as fuel and its subsequent characterization
4. Economic feasibility analysis of the produced biofuel (bio–oil)
5. Investigation of non–energy prospects of bio–oil

This study may aid in facilitating sustainable IS management by converting them into useful biofuels and non–energy products, while evaluating their economic viability.

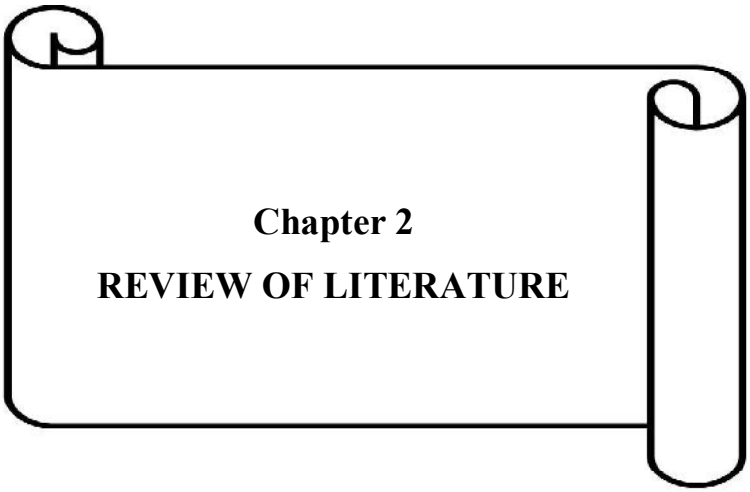

# Chapter 2

# REVIEW OF LITERATURE

# Chapter 2
# REVIEW OF LITERATURE

Diminishing geological reservoirs and increasing environmental concerns has garnered tremendous scientific attention in biomass as a viable alternative to fossil fuels. Owing to their fast growth rate, high biomass yield, resilience and adaptability, invasive species (plants) have become one of the most promising, yet underutilized bioresources among the several biomass feedstocks. IS due to their ubiquitous expansion, frequently outcompete native vegetation and flourish in terrestrial ecosystems, thereby posing serious environmental and economic challenges. However, their prolific biomass production offers lucrative facets for bioresource valorization through thermochemical conversion technologies such as pyrolysis. Thermochemical conversion (pyrolysis) can transform the heterogeneous lignocellulosic biomass of IS into biofuels with added advantage of subsequent value addition. Furthermore, converting IS biomass into biofuels addresses two pressing concerns simultaneously: the need for clean energy and IS management. The distribution of IS is taken into account in the current literature survey. It explores the feasibility of utilizing IS as a feedstock for pyrolytic bio–oil production along with economic analysis. Additionally, the non–energy prospects (antioxidants and antimicrobial studies) are also considered as a part of value addition. The literature review advances the broader goals of sustainable biomass utilization, IS management and circular economy progression.

## 2.1. Work done abroad

### 2.1.1. Population assessment of IS

Wahyuni et al. (2016) examined the distribution, dominance and abundance of IS across various land–use systems in Sumatra, Indonesia. The study employed Importance Value Index (IVI), combining with frequency and coverage, to assess the species dominance. *Clidemia hirta* and *Dicranopteris linearis* emerged as the widely distributed IS across disturbed areas. IS proliferation correlated strongly with canopy openness and air temperature, revealing their shade intolerance characteristics. The

study concluded that intact forest canopy significantly limits the IS proliferation and reforestation of disturbed areas is essential to curb the invasion.

Pérez–Postigo et al. (2021) assessed the distribution and dominance of IS along an elevational gradient in Western Mexico. The study identified *Cynodon dactylon, Eragrostis ciliaris, Melinis repens* and *Urochloa maxima* as the most potentially invasive. The study emphasized that invasion success is species–specific and tied to distinct environmental conditions necessitating targeted management strategies.

Yang et al. (2021) investigated the distribution and establishment of IS in the forested ecosystem of Hainan, China. Surveys across 97 transects revealed that IS were prevalent in human–induced environments but seldom penetrated areas beyond 5 m into intact forests. Experimental analysis revealed IS struggled to establish in shaded region. The findings concluded that IS, due to their shade intolerance and limited seed dispersal, posed minimal threat to closed–canopy forest ecosystems.

Akatov et al. (2022) examined the dominance and frequency of IS versus native species across various regions in Southern Russia. IS made up ~10 % of dominants with slightly higher frequency compared to the native species. The study suggested that the proliferation of IS contributed towards increased vegetation homogeneity highlighting the subtle impact of IS dominants in disturbed areas.

Luo et al. (2022) identified six primary habitats of IS in Pingtan Island, China and surveyed 123 quadrats across 29 locations. A total of 104 IS were documented. The study employed a risk assessment index revealing high–risk (23 Nos.), medium–risk (25 Nos.), and low–risk (44 Nos.) IS, with *Lantana camara* ranking the highest. The research established a scientific basis for IS management offering a transferable risk assessment system to support ecological sustainability and biodiversity preservation.

Salaudeen et al. (2022) investigated the distribution, abundance and composition of IS in maize–based cropping systems in Southern Guinea Savanna, Nigeria using twenty randomly placed 0.25 $m^2$ quadrats per field. The IS in each

quadrat were enumerated and classified. The findings highlighted the need for targeted IS control strategies to mitigate crop losses in affected regions.

Yang et al. (2022) surveyed 373 grassland sites in Guizhou Province and identified 49 IS from 15 families and 41 genera. 90 % of the sites were affected by biological invasion, with 60 % of the sites dominated by high – risk IS. The study emphasized on the need for targeted control efforts, particularly in resource–rich and high accessibility zones, to support grassland sustainability and limit the spread of IS.

dos Santos et al. (2023) conducted sampling in three sunflower fields in Brazil's Parecis region to assess IS density, frequency, abundance, IVI and similarity index. *Bidens pilosa* and *Euphorbia hirta* showed the highest IVI during early and pre–harvest stages. The phytosociological findings provide valuable insights for formulating effective IS management techniques in sunflower cultivation.

Rahmawati & Rosleine (2023**)** explored IS in Bandung, Indonesia, assessing their impact on urban ecosystem health. Using line transect across 22 study sites, they recorded species composition, individual count, frequency, and sample site coordinates to compute the IVI and map the distribution pattern. The study highlighted the dominant invaders and emphasized the need to understand IS' interactions with different land–use types for effective management and biodiversity protection**.**

Yusuf et al. (2024) surveyed sesame fields in Middle Shabelle province, Somalia employing quadrat method and identified 27 IS. The most abundant and harmful IS were *Cynodon dactylon*, *Portulaca oleracea*, and *Cyperus rotundus*. The study addressed concerns to tackle this difficulty and suggested the formulation of region–specific integrated IS management techniques customized for local species and farming systems.

### 2.1.2. Characterization of IS biomass

Aref et al. (2016) investigated the wood and charcoal from *Phragmites australis*, *Rhazya stricta* and *Calotropis procera* to explore their potential for energy generation. TG–DTG analysed the thermal properties of the species. Ultimate analysis

revealed high carbon content of *P. australis* (45.69 %), *R. stricta* (49.91 %) and *C. procera (*45.81 %). Proximate analysis displayed low MC % and high VM % for all three species. Furthermore, *P. australis*, *R. stricta* and *C. procera* exhibited appreciable energy content of 18.52 MJ/Kg, 19.79 MJ/Kg and 18.77 MJ/Kg, respectively. The overall findings revealed *R. stricta* and *P. australis* demonstrated greater suitability for energy generation.

Reza et al. (2019) conducted the proximate, ultimate and thermogravimetric analysis (TGA) of *Acacia holosericea*. The biomass showed low MC % of 9.56 %, AC % of 3.91 %, FC % of 21.21 % and high VM % of 65.12 %. Ultimate analysis indicated that nitrogen, hydrogen and carbon were 0.25 %, 5.67 % and 44.03 %, respectively. TGA showed peak mass loss of biomass at 287 °C (combustion) and 357 °C (pyrolysis). With an HHV of ~18.13 MJ/kg and low MC % (< 10 %), the species displayed strong candidature for bioenergy generation.

Ahmed et al. (2021) investigated the valorization potential of *Acacia mangium* to produce bioenergy. Thermal characterization included FTIR, heating value, proximate analysis and TGA. Proximate analysis revealed ash (1.41–2.69 wt.%), FC % (14.47–18.31 wt.%), VM % (69.82–74.85 wt.%) and MC % (7.88–11.65 wt.%). HHV of sample ranged from 19.51 – 21.58 MJ/kg, with carbon percentage between 45.50–50.65 wt.%. FTIR confirmed the presence of diverse functional groups. TGA revealed short degradation profile. Bio–oil yields of 40 – 58 %, underscored the feasibility of *Acacia mangium* biomass for pyrolysis.

Gonçalves et al. (2021) investigated invasive *Cyperus giganteus's* pruning residue for bioenergy potential through thermal, proximate, chemical and physical assessments. The biomass exhibited calorific value ranging from 14 – 16 MJ/Kg. Its composition, hemicellulose (30.1 – 31.5 wt.%), cellulose (27.8–32.6 wt.%), and lignin (17.3 – 26.8 wt.%), significantly influenced the thermal behaviour. Maximum weight losses varied between 75.91 % – 83.43 %. The findings highlighted its feedstock viability for thermal energy conversion.

Nong et al. (2021) evaluated *Ludwigia Hyssopifolia* as a biofuel feedstock. Ultimate analysis displayed 40.2 % carbon, 5.03 % hydrogen, 22.13 % oxygen, 1.8 % nitrogen and 0.24 % sulphur. Proximate analysis revealed a low MC % of 7.28 % and high VM % of 63.07 %. The study underscored its feedstock potential for biofuel production and recommended further scale–up investigations.

Ayaa et al. (2022) investigated the feedstock potential of *Senna spectabilis, Psidium guajava, Mimosa pigra, Lantana camara, Broussonetia papyrifera* and *Acacia mearnsii* for biofuel generation. Biomass characterization included heating values, ultimate and proximate analysis, chemical characterization, thermal analyses and morphology study. Comprehensive analyses revealed *Senna spectabilis* as the most promising feedstock with the lowest AC %, highest HHV (17.84 MJ/kg) and high cellulose content (48 %), rendering it ideal for both thermochemical conversion and enzyme saccharification.

Karaeva et al. (2023) pyrolyzed *Amaranthus retroflexus* (stems, inflorescences and leaves) at 550 ºC with heating rate of 10 ºC/min. TGA revealed three stages of degradation: dehydration, devolatilization, and carbonation. Inflorescence exhibited the maximum bio–oil yield (55 %) followed by leaves (45 %). GC–MS demonstrated leaf–derived bio–oil was rich in aliphatic hydrocarbon, while bio–oil from stems and inflorescences primarily comprised of oxygenates. The study endorsed *Amaranthus retroflexus* biomass as a viable feedstock for biofuel and chemical production.

Mtshali et al. (2025) evaluated *Solanum mauritianum, Chromolaena odorata* and *Lantana camara* to investigate their suitability for bio–oil generation through ultimate, proximate, HHV and TGA. Proximate analysis showed low MC % and high VM % for all three species indicating good thermal reactivity. Ultimate analysis revealed that the high carbon content and low hydrogen content contributed to the appreciable HHV. TGA displayed three stages including dehydration, active and passive pyrolysis zone. The study demonstrated the feedstock viability of IS for bio–oil production, particularly *L. camara* with an HHV of 19.5 MJ/Kg, though upgrading strategies are needed to improve the fuel quality.

### 2.1.3. Thermochemical conversion (pyrolysis) of IS

Cheng et al. (2019) investigated the pyrolysis of Crofton weed, examining the influence of heating rate, $N_2$ flow rate, pyrolysis duration and temperature on pyrolysis products. Ideal condition for bio–oil production was observed at 600 °C with 200 mL/min $N_2$ flow rate for 50 min and heating rate of 20 °C/min. GC–MS analysis revealed bio–oil was rich in oxygenated compounds including ketones (15.39 %), phenols (13.04 %) and aldehydes (28.09 %), indicating its prospects as a chemical feedstock. The study highlighted the potential of crofton weed for bio–oil production, promoting its utilization in energy and chemical sectors.

Singh et al. (2020) investigated the fast pyrolysis of *Miscanthus* at varying temperatures (400, 450 and 500 °C). Peak bio–oil yield (> 50 wt.%) was achieved at 450 °C with an HHV of 27.6 MJ/Kg, and hydrogen and carbon contents of 9.6 wt. % and 63.2 wt. %, respectively. GC–MS analysis revealed the presence of diverse organic constituents in the bio–oil, signifying prospects for biochemical recovery. The findings endorsed *Miscanthus* as a viable energy crop for sustainable biofuel production and enhanced applications.

Pérez et al. (2021) investigated *Cortaderia selloana* as a prospective energy source through conventional (750 °C at 25 °C/min heating rate) and flash pyrolysis (750 °C and 850 °C at 25 °C/min heating rate). Flash pyrolysis produced bio–oil with a higher heating value (~33 MJ/Kg) in contrast to conventional pyrolysis (~23 MJ/kg). Flash pyrolysis bio–oil predominantly comprised of polycyclic aromatic hydrocarbons while conventional pyrolysis bio–oil contained mostly monoaromatic and nonaromatic hydrocarbons. The study confirmed the potential of transforming *Cortaderia selloana* into biofuels (biogas, bio–oil and bio–char).

Carregosa et al. (2023) explored pyrolysis of *Eichhornia crassipes* at different temperatures (400, 500 and 600 ºC). Peak bio–oil yield (42.11 %) was attained at 500 ºC. Both 400 ºC and 600 ºC favoured the production of pyrolytic gas and biochar. The bio–oil exhibited high concentration of sugar derivatives, phenols, alcohols and acids. Thorough characterization of bio–oil obtained at 500 ºC indicated elevated levels of

nitrogen and oxygen. Pyrolysis of *E. crassipes* was identified as an effective method for controlling its invasive proliferation while generating value–added goods.

Rapoo et al. (2023) investigated the catalytic and thermal fast pyrolysis of *Prosopis juliflora* fractions (leaves, seed pods, wood) at 450, 500 and 550 ºC. Thermal pyrolysis, especially of wood, at 500 ºC demonstrated highest yield of phenolics, aldehydes and ketones (78.67 %). Zeolites–based catalytic pyrolysis revealed enhanced aromatic hydrocarbon production while reducing oxygenates. The incorporation of nickel into the zeolite further boosted aromatics (60.28 %) and hydrocarbons (27.50 %). The present investigation demonstrated *P. juliflora* as a viable feedstock for biofuel and high–value chemical production.

Romero et al. (2023) conducted pyrolysis of *Eichhornia crassipes* achieving optimal bio–oil yield (2.2 %) at 450 ºC with a 30 ºC/min heating rate. GC–MS analysis revealed bio–oil was mainly composed of derivative and linear hydrocarbons (44 %), acids (4 %), phenols and alcohols (6 %) and aromatic hydrocarbons (27 %) while remaining 19 % comprised of nitriles, ethers, ketones and aldehydes. Calorific value attained a peak of 21.641 MJ/Kg. The present study highlighted the potential of improved yield by the utilization of catalysts and varied heating rates, positioning it as a viable option for the advancement of refined chemical products.

Fernández et al. (2024) performed pyrolysis at three distinct temperatures (500, 600 and 700 ºC) on IS *Clusia orthoneura*, *Ruta greveolens*, *Cecropia telenitida*, *Sambucus nigra*, and *Liquidambar styraciflua* to evaluate their efficacy in generating chemical products and fuels. GC–MS revealed bio–oil constituted of levoglucosan (6.7 – 15.4 %), ketones (13.4 – 19.2 %), acids (14.6 – 19.5 %), and phenols (19 – 26.5 %). The study endorsed pyrolysis as a promising strategy for IS management and promoting environmental remediation.

Shezi et al. (2024) conducted pyrolysis of *Arundo donax* biomass at 550 °C across four seasonal variations [late winter (HS–3), late autumn (HS–2), late summer (HS–1), and late spring (HS–4)]. Biomasses calorific values ranged from 18.44 – 19.73 MJ/Kg with HS–2 displaying the highest. Pyrolysis gas, biochar, and bio–oil

were analysed using FTIR, GC–MS and GC–Ms analysis. Bio–oil yield escalated from 5 wt.% in HS–4 to 11 wt.% in HS–3. Calorific value of bio–oil varied from 19.4 – 22.6 MJ/Kg. Furthermore, the obtained bio–oil exhibited high concentration of phenolics.

### 2.1.4. Fuel properties of IS – derived bio–oil

Santos et al. (2017) evaluated *Nymphaea* spp., *Eichhornia azurea*, and *Eichhornia crassipes* as feedstock for pyrolytic–oil production. GC–MS revealed the obtained bio–oils comprised of a range of fuel–relevant compounds including carboxylic acids (oleic and hexadecenoic acid), alcohols, phenols and levoglucosan. Levoglucosan can potentially be utilized for biofuel (butanol and ethanol) production. The study underscored the potential of bio–oil for liquid fuel development highlighting IS as a promising bioenergy source.

Alhumade et al. (2019) assessed the pyrolysis–derived bio–oil from *Phalaris arundinacea* to investigate its suitability as a biofuel. The bio–oil showed an HHV of 22.20 MJ/Kg, low MC % (0.26 wt.%) and density of 1.321 g/ml, indicating good energy potential. FTIR and GC–MS revealed the presence of a complex blend of oxygenates including phenols and ketones. The findings demonstrated the potential of bio–oil as an alternative fuel.

Arias et al. (2019) evaluated the pyrolytic conversion of *Geoffroea decorticans*, *Arundo donax, Panicum prionitis* and *Spartina argentinensis* to assess their potential for biofuel production. Bio–oil, reaching up to 18 wt.% in *Geoffroea decorticans* was rich in ketones, phenols and acids with high molecular weight. The study highlighted the bio–oil's potential as a source of chemical, fuel and energy.

Chukwuneke et al. (2019) investigated the biomass and pyrolysis–derived bio–oil of *Swietenia macrophylla* for bioenergy and commercial applications. Bio–oil characterization revealed HHV (29.52 MJ/kg), LHV (28.08 MJ/kg), viscosity (4.6 $mm^2/s$), AC % (0.15 wt.%), density (0.951 g/ml), MC % (21.4wt.%), sulfur (< 0.06 %), nitrogen (< 0.4 %), hydrogen (6.6 %), oxygen (42.6 %) and carbon (50.2 %). GC–MS analysis identified 24 compounds mainly levoglucosan, hydrogen, phenols,

alkenes, and alkanes. The findings support *Swietenia macrophylla* as a promising fossil fuel alternative with biofuel applications.

Wauton & Ogbeide (2019) evaluated the pyrolysis–derived bio–oil of *Eichhornia crassipes*. Aromatics, aldehydes, alkanes, alkenes, quinones, ketones, carboxylic acids, alcohols and phenols were identified through FTIR, while GC–MS revealed 21 distinct compounds in bio–oil. Fuel properties assessment yielded the following results: pour point at +15 °C, viscosity at 19.8 cSt, pH at 2.93, density at 1004.3 kg/m$^3$, flash point at 220 °C and HHV of 28.35 MJ/kg – a 63.02 % increase over the feedstock. Additionally, absence of sulphur in bio–oil suggested its potential as a source of cleaner fuels and chemicals.

Parvej et al. (2022) explored the fuel potential of pyrolysis–derived bio–oil of *Eichhornia crassipes*. The bio–oil exhibited density (0.97 – 1.08 Kg/L) and viscosity (1.33 – 1.80 cSt) lower than conventional diesel, implying enhanced fuel atomization. The bio–oil also showed an appreciable HHV of 33.32 MJ/Kg with low MC % (1.5 – 1.97 wt.%) displaying better combustion and engine compatibility. The findings supported the use of *E. crassipes* as a renewable fuel source.

Clemente–Castro et al. (2023) evaluated the physiochemical properties of bio–oil produced from pyrolysis of *Leucaena leucocephala*. HHV of *L. leucocephala* bio–oil was 18.87 MJ/Kg. The physical properties of *L. leucocephala* bio–oil, included low sulfur and AC % (0.04 and 0.12 wt.%, respectively), reduced viscosity (13.56 mm$^2$/s), a suitable density (1.22 Kg/L) and a moderately low pH (2.67). Furthermore, chemical characterization from GC–MS analysis revealed the presence of furans, aldehydes and phenols highlighting its potential application as a chemical feedstock.

Chen et al. (2024) comprehensively evaluated the thermochemical conversion of reed straw waste. The pyrolysis–derived bio–oil yield ranged from 18.94 – 35.23 %, consisting primarily of aldehydes (5.54 – 11.10 %), alcohols (4.59 – 13.68 %), ketones (9.34 – 16.33 %), furans (8.84 – 14.46 %), acids (1.12 – 16.05 %) and phenols (30.88 – 46.04 %). The findings endorsed the potential of bio–oil for the production of bioenergy and valuable chemicals.

### 2.1.5. Economic analysis of IS–derived bio–oil

A meticulous literature review yielded only a single investigation done on economic analysis of pyrolytic bio–oil derived from IS biomass.

Calicioglu et al. (2021) evaluated the challenges and potentials associated with large–scale biorefineries utilizing wastewater–derived duckweed to advance a circular bioeconomy. The study indicated Minimum Selling Price (MSP) for duckweed of $ 7.69/Mg of dry matter. The construction of duckweed ponds and harvesting of duckweed represented the predominant portion of capital (55.6 %) and operating costs (90.4 %), respectively.

### 2.1.6. Value–addition of pyrolysis–derived bio–oil

Despite the growing interest in biomass valorisation, there remains dearth of scientific exploration specifically addressing the bioactivity of IS–derived bio–oil. Previous investigations have emphasized the bioactive efficacy of bio–oils sourced from an array of feedstocks, establishing a strong foundation for their bioactive potential. This suggests that bio–oil from IS, which remains largely unexplored, may similarly exhibit significant bioactivity. Investigation of such IS–derived bio–oils would offer an opportunity to uncover novel antimicrobial and antioxidant compounds with therapeutic potential. In this context, the present review displays existing evidences on the bioactivity of bio–oils obtained from various biomass sources, providing a rationale for extending this line of inquiry to IS–derived bio–oil.

Patra et al. (2015) investigated sawdust bio–oil from *Pinus densiflora* to evaluate its volatile compounds and free radical combating potential. GC–MS identified 29 volatiles, accounting 97.6 % of the bio–oil's total volatile compounds. The antioxidant capacity of bio–oil displayed $IC_{50}$ value of 48.44 µg/mL and 1,1–diphenyl–2–picrylhydrazyl radical combating ability of 89.52 µg/mL. Bio–oil exhibited a phenol content of 5.7 % expressed as gallic acid equivalent. The results demonstrated the application of *P. densiflora* bio–oil as a potential antioxidant source showcasing its applicability in cosmetic, food and pharmaceutical sectors.

Chandrasekaran et al. (2016) investigated the slow pyrolysis of birch wood to generate bio–oil. Residence time of 2 h and optimum temperature of 450 °C facilitated bio–oil yield of up to 56 %. The antioxidant assay revealed the phenolic compounds displayed similar antioxidant efficacy with butylated hydroxytoluene. The findings of the study underscored the potential of phenolic extracts generated from bio–oil as sustainable source of bio–based antioxidants.

Lu et al. (2021) investigated the antioxidant potential of aqueous layer bio–oil, obtained from hydrothermal treatment (HTT) and pyrolysis of Chinese fir sawdust biomass. HTT enhanced phenolic content (61.68 %) particularly 2–methoxyphenol and its derivatives. HTT treated sample exhibited higher antioxidant property with a 0.402 mg/mL $IC_{50}$ value compared to commercial antioxidants. Higher antioxidant capability was exhibited by short carbon chains phenols (4–methyl–2–methoxyphenol > 4–ethyl–2– methoxyphenol, 2–methylphenol > 2–methoxyphenol). The findings demonstrated the applicability of aqueous bio–oil as an alternative antioxidant offering new insights into its efficient utilization.

Scheibe et al. (2022) evaluated the antibacterial activity of pyrolysis–derived bio–oil of textile sludge (HHV of > 20 MJ/Kg). The bio–oil showed significant efficacy against *Klebsiella pneumoniae*, *Pseudomonas aeruginosa* and *Staphylococcus aureus* at concentrations >17 mg/mL. The findings indicated the prospective application of bio–oil as an inexpensive antibacterial agent and as alternative fuel sources for bioenergy production.

Dias et al. (2023) investigated the water–soluble portion of Eucalyptus bio–oil for its antimicrobial, antioxidant and chemical configuration. Liquid–liquid fractionation efficiently separated pyrolytic lignin identifying high–value chemicals such as levoglucosan, catechol and vanillin. The phenolic–rich composition considerably favoured the bio–oil's bioactive capacity. The study highlighted the potential of aqueous bio–oil beyond its fuel uses, with promising bio–based applications.

Malagón–Romero et al. (2023) evaluated the antioxidant potential of bio–oil obtained from the pyrolysis of coffee grounds. GC–MS analysis identified 11.31 % aromatics, 31.65 % linear hydrocarbons and 50.86 % fatty acids. High phenolic content (TPC of 362 ± 44 mg GA $g^{-1}$) and notable antioxidant capacity (DPPH of 24.8 ± 2; Trolox equivalents of 108.5 ± 13.6 mg $L^{-1}$) highlights it as a source of bioactive compounds.

## 2.2. Work done in India

India's crude oil dependency rose to 88.2 % during April 2024 – February 2025 (fiscal year 2025). In March 2025, India's net import bill for gas and oil surged to $ 11.6 billion (Petroleum Planning and Analysis Cell, 2025), highlighting the economic strain of continued reliance on fossil fuel imports. This growing reliance poses a severe threat to the national security and economic resilience. To address this pressing issue, a trajectory shift towards the adoption of indigenous feedstocks is imperative, aligning with the goals outlined in the National Policy on Biofuels. In this context, IS offers considerable promise as an alternative bioenergy source owing to its largely untapped potential. However, IS – based biofuel research in India remains in its infancy. The substantial amount of IS biomass in the country has not been comprehensively explored for its bioenergy applications. Only a limited number of scientific research have explored this avenue, resulting in a significant research gap. Consequently, advanced IS – based biofuel research with experimental backing may aid in fully harnessing this underutilized resource while contributing towards national energy security.

### 2.2.1. Population assessment of IS

Kumar et al. (2020) assessed the impact of *Ageratina adenophora* and *Lantana camara* on species richness and understory vegetation in *Pinus roxburghii* forest of central Himalaya. Study plots were categorised as *Ageratina adenophora*–invaded, *Lantana camara* – invaded and non–invaded. IS caused a 29 – 40 % decline in native shrub and herbs species, significantly altering native vegetation. The study

addresses concerns over the need for immediate attention to protect native flora and maintain ecological and socio–economic balance.

Verma et al. (2022) conducted a population study on *A. adenophora* in Sikkim Himalaya, revealing a significant expansion from 2018 and 2021. The species showed increased basal cover (42.54 $cm^2$/100 $m^2$), density (58.41 ind./100 $m^2$), and frequency (99.96 %), with notable expansion at higher elevations (2400 – 2700 m) where it was previously unrecorded. This indicated its enhanced vigor and adaptability. Consequently, the study highlighted the urgent need for targeted management to mitigate its impact on native flora.

Hansda et al. (2024) conducted a field survey employing quadrat method to study the coupling effect of *L. camara* invasion and disturbance on soil properties and vegetation in Aravali hills, Delhi. The statistical data showed the site with maximum relative density of *L. camara* possessed significant soil organic carbon, high soil moisture, nitrogen, and microbial biomass carbon.

Kaushik et al. (2024) investigated the invasive potential of *Gliricidia sepium* in the tropical dry deciduous forests of Central India. Data from forty plots revealed significantly basal area (6.32 $m^2$ $ha^{-1}$), elevated density (37.2 individuals $ha^{-1}$), and IVI (95.8) of *G. sepium* distinctly indicating strong suppression of native forest species at the invaded sites. The findings revealed *G. sepium*'s robust proliferation and ecological impact, highlighting the need for prompt detection and proactive management to curb its nationwide spread.

Ranjini et al. (2024) investigated IS flora and ground plant composition in a coconut plantation with varying spacings at ICAR–CPCRI in Kasaragod, Kerala. Three plots with varying spacings (4 × 4 m, 6 × 6 m, and 7.5 × 7.5 m) were analyzed with 4 × 4 m spacing plot displaying the highest IS variety and 6 × 6 m displaying the highest density. 7.5 × 7.5 m had the lowest IS presence. The study highlighted the substantial influence of parameters including available temperature, shade, sun exposure and space on IS. The findings recommended species and site–specific IS management practices to enhance plantation health and efficiency.

Haq et al. (2024) assessed IS diversity in rice fields across five districts of Kashmir Valley, Jammu and Kashmir. Random sampling documented forty–seven IS species with Asteraceae (13 %) emerging as the dominant family. Major IS included *Echinochloa colona*, *Ranunculus sceleratus*, *Persicaria hydropiper* and *Poa annua*. IVI revealed substantial differences in IS diversity among rice fields. The findings provided valuable insights for enhancing IS management tactics to reduce crop losses and boost rice productivity.

Negi et al. (2024) employed stratified random sampling to document the alterations in *Ageratina adenophora* density across various topographies in Nainital, Uttarakhand. Triplicate transects (50 × 2 m) revealed that density of *A. adenophora* reduced with increasing distance from highways, while soil moisture and abundant sunlight positively influenced its growth. The findings underscored the necessity for restoration techniques, including soil enhancement and IS management, to curtail its proliferation in mountainous regions.

Joshi et al. (2024) investigated the ecological impacts and local perception of invasive *L. camara* and *A. adenophora* within the Western Himalaya Forest ecosystems. Using 150 randomly placed quadrats (5 × 5 m) across Chir–pine, Banj–oak and Sal forests, the findings recorded significant decline in native vegetation. *L. camara* and *A. adenophora* exhibited highest density of 512 ind/ha and 3168 ind/ha, respectively, in Chir–pine forest and exhibited contagious distribution in all forest stands. The study underlined the urgent need for conservation efforts, policy action and community engagement to mitigate biological invasion and sustain Himalayan Forest ecosystems.

### 2.2.2. Pyrolysis of IS biomass

Saikia et al. (2015) produced bio–oil from *Ipomoea carnea* through thermal pyrolysis at 350 – 600 °C (heating rate: 10 °C/min). Maximum yield (41.17 %, with 11.45 % oil phase), was achieved at 550 °C. FTIR, GC–MS and NMR identified various alcohols and hydrocarbons. Bio–oil's H/C ratio of 1.49 closely resembled that of petroleum–derived fuel, indicating its applicability as a fuel for industrial furnaces.

Nonetheless, its high oxygen content (35.86 %) contributes to acidity, requiring upgrading for utilization in contemporary internal combustion engines.

Suriapparao et al. (2015) investigated microwave pyrolysis of *Prosopis juliflora* for biochar, biogas and bio–oil production. Peak bio–oil yield (40 %) was achieved at 500 °C, with 59 % energy recovery and 51% deoxygenation (O/C ratio of 0.24). The bio–oil contained furan derivatives, ketones, carboxylic acids, aromatic hydrocarbons, cyclopentanones and phenolics. Lignin breakdown markedly affected the production of $C_2$ – $C_5$ oxygenates and non–condensable gases. The results demonstrated microwave pyrolysis as an efficient technique for converting *P. juliflora* biomass into valuable fuel intermediates.

Bhattacharjee & Biswas (2018) pyrolyzed *Alternanthera philoxeroides* at temperatures ranging from 350 – 550 °C (heating rate of 25 °C/min). Peak bio–oil yield (43.15 %) was obtained at 450 °C. High oxygen content lowered the HHV of bio–oil (8.88 MJ/kg). The elevated HHV of bio–char (20.41 MJ/kg) exceeds that of bio–oil, indicating its suitability as a solid fuel. TGA determined the thermal degradation profile of *A. philoxeroides*. Bio–oil characterisation included ultimate analysis, FTIR and GC–MS. Chemical analysis revealed bio–oil's potential as a transportation fuel upon upgrading or blending.

Bhattacharjee & Biswas (2019) pyrolyzed *Ageratum conyzoides* in a semi–batch reactor. The effects of $N_2$ flow rate (0.1 – 0.5 L $min^{-1}$), heating rate (25 – 100 °C $min^{-1}$) and temperature (350 – 600 °C) on product yield were examined. Peak bio–oil yield (37.55 %) was attained at a 525 °C (heating rate of 75 °C/min). Characterization included ultimate analysis, FTIR, TG–DTG, GC–MS and $^1$H NMR. The biochar and bio–oil derived from *A. conyzoides* possessed HHV of 22.93 MJ/Kg and 17.79 MJ/Kg, respectively. The study demonstrated the viability of *A. conyzoides* pyrolysis products as a sustainable and renewable energy source.

Gopal et al. (2019) optimized pyrolysis conditions for *Saccharum ravannae*, achieving peak bio–oil yield (45.69 %) at 505 °C, 311 ml/min $N_2$ flow rate and a heating rate of 6.36 °C/min in a fixed bed pyrolyzer. Elevated temperature (> 510 °C)

enhanced syngas production while lower temperature (< 300 °C) favoured char formation. Furthermore, high $N_2$ flow rate (300 – 350 ml/min) with moderate heating rate (5 – 20 °C/min) at temperature ranging from 470 – 510 °C displayed improved bio–oil yield. The findings identified temperature as the predominant influence on product yield, followed by $N_2$ flow rate and heating rate.

Sahoo et al. (2020) investigated the thermogravimetric characteristics of *Prosopis juliflora* and *Lantana camara* under dynamic pyrolysis (20 – 900 °C) at varying heating rates (5, 10, 20, and 40 °C/min). *L. camara* demonstrated lesser oxygen (44.82 %) and higher carbon content (48.87 %) with a slightly higher HHV of 18.92 MJ/kg than *P. juliflora* (18.2 MJ/Kg). Thermal degradation occurred in three distinct phases: dehydration (25 – 200 °C), devolatilization (200 – 450 °C), and char formation (> 450 °C). Peak product generation occurred during the devolatilization phase. Higher heating rates shifted decomposition to higher temperatures but diminished the overall weight loss. These findings aid in optimizing pyrolysis parameters for effective transformation of IS into bioenergy resources.

Venkatachalam et al. (2020) investigated the feedstock potential of *Prosopis juliflora* at temperatures ranging from 250 – 374 °C. TGA, ultimate analysis, proximate analysis and GC–MS were employed to characterize the bio–oil and biomass. The findings indicated the optimal bio–oil output of 3.65 % was achieved at 277 °C. The resultant bio–oil demonstrated the presence of phenols, amines, carboxylic acids, ketones and long–chain alkanes.

Saynik & Moholkar (2021) examined the effect of chemical pretreatment on pyrolysis characteristics of *Arundo donax*, focusing on the consequent changes in bio–oil composition. GC–MS analysis categorized the compounds in bio–oil into heterocyclic, non–aromatic and aromatics. NaOH treatment enhanced bio–oil yield, with an improvement ranging from 10.1 – 49.2 % while $H_3PO_4$ demonstrated an increase in furan production (21.2 % v/v). The findings offered valuable insights for optimizing large–scale pyrolysis systems to improve bio–oil yield and quality through targeted chemical treatment.

Ramesh & Murugavelh (2022) examined bio–oil generation and energy potential of *Prosopis juliflora*. Ultimate analysis and calorific value of *P. juliflora* biomass were determined along with thermogravimetric investigation at five distinct heating rates ranging. Pyrolysis at 500 °C with 0.5 mm particle size yielded maximum bio–oil (17.4 %). GC–MS analysis revealed traces of petroleum constituents in the bio–oil. The study's outcomes demonstrated the prospects of *P. juliflora* for effective waste management and sustainable energy generation.

Sahoo et al. (2022) valorised *Vachellia nilotica* through pyrolysis examining the influence of particle size (0.1 – 1 mm), heating rate (10 – 50 °C/min) and temperature (350 – 550 °C) on product output. Optimal condition of 500 °C at 25 °C/min with particle size of 0.4 mm was experimentally validated. Ultimate analysis, FTIR and GC–MS identified dehydroacetic acid, furfural and phenolics compounds as major bio–oil components. The study highlighted *V. nilotica*'s promising thermochemical conversion potential for sustainable bioenergy generation.

Suriapparao et al. (2023) performed microwave–assisted pyrolysis of *Prosopis juliflora* at 200 °C, 350 °C, and 500 °C to optimize bio–oil yield. The influence of conductive heat loss, specific microwave energy, power, reaction time and heating rate on product distribution were assessed. Gas, char and bio–oil yield ranged from 35 – 40 wt.%, 25 – 35 wt.% and 25 – 40 wt.%, respectively. The resulting bio–oil rich in methoxy phenols exhibited calorific value of 26 – 28 MJ/kg. Furthermore, analysis of carbon numbers indicated an elevated occurrence of $C_5$ – $C_9$ compounds.

### 2.2.3. Bioactivity of IS–derived bio–oil

In a nutshell, bioactivity studies on pyrolytic bio–oil from IS biomass has been rarely attempted. While investigations on the bioactive potential of pyrolysis–derived bio–oil remains sparse, only few investigations showcased the emerging interest in bioactivity of IS bio–oil (non–energy prospects) complementing its conventional application as fuel (energy prospects). Building on the established bioactivity of bio–oil derived from various sources (as mentioned in section 2.1.6), these preliminary findings contribute incrementally towards research in this fascinating domain.

Chandran et al. (2020) examined the pyrolysis–derived bio–oil of *Prosopis juliflora* at 450 °C analysing its component and thermal behaviour using TGA, FTIR, GC–MS, $^{1}H$ NMR and $^{13}C$ NMR. TGA revealed 6 % moisture with complete degradation starting at 360 °C. The bio–oil contained around 20 organic chemicals, including toluene, furfural, carbonyl and phenolics. A 35 % bio–oil–diesel blend performed slightly better than pure fossil diesel under full load conditions and exhibited antibacterial properties. The results affirmed the bio–oil's potential as a diesel additive and for antibacterial applications.

Chongloi et al. (2024) evaluated *Lantana camara* biomass for bioenergy production as part of its management. Pyrolysis yielded 62.58 % energy output with 64.95 % carbon content, confirming its biofuel potential. TG–DTG showed brief decomposition profile while spectroscopic analyses revealed numerous organic components including aromatics, aliphatics, aldehydes, ketones and phenols. Bio–oil displayed strong antimicrobial property [maximum zone of inhibition (ZOI) against C*andida albicans* (31.02 mm)] and notable antioxidant activity. The study highlighted *L. camara*'s multifaceted utility in the field of pharmaceuticals, chemical and bioenergy, supporting global sustainability objectives.

### 2.2.4. Molecular docking

Albeit, a handful of *in silico* molecular docking (MD) studies on certain feedstock derived bio–oil are available in the scientific repositories, a meticulous literature survey could yield only one result (self–publication) on *in–silico* MD experiments conducted using IS derived bio–oil.

Chongloi et al. (2025) investigated the therapeutic potential of bioactive compounds in invasive *Stachytarpheta jamaicensis*–derived bio–oil. The thermochemical conversion of biomass was initiated by pyrolysis ranging from ambient to 700 °C, at a heating rate of 30 °C/min. As a part of *in silico* drug discovery the compounds, identifiable by GC–MS, were docked against NUDT5 protein. MD studies identified key bioactive ligands such as 3,5–dimethoxy–4–hydroxytoluene and phenol, 2–methoxy– that mirrored notable binding affinities to well–established breast

cancer therapeutics such as anastrozole and letrozole. The study demonstrated the potential for therapeutic breakthroughs and futuristic drug discovery from repurposed IS biomass.

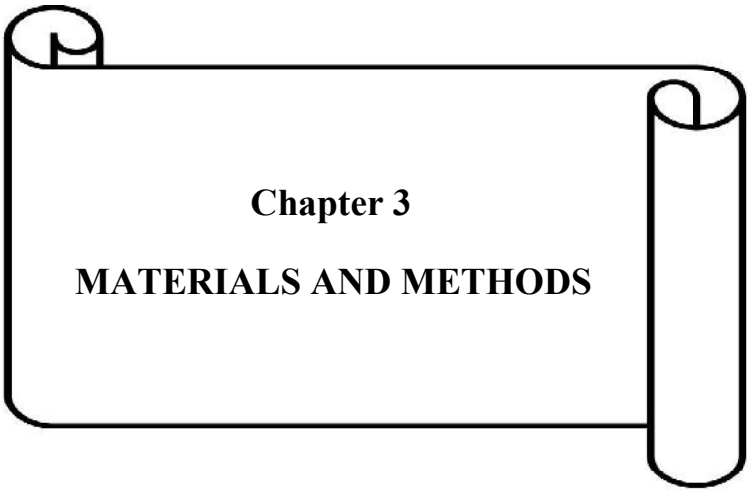

# Chapter 3

# MATERIALS AND METHODS

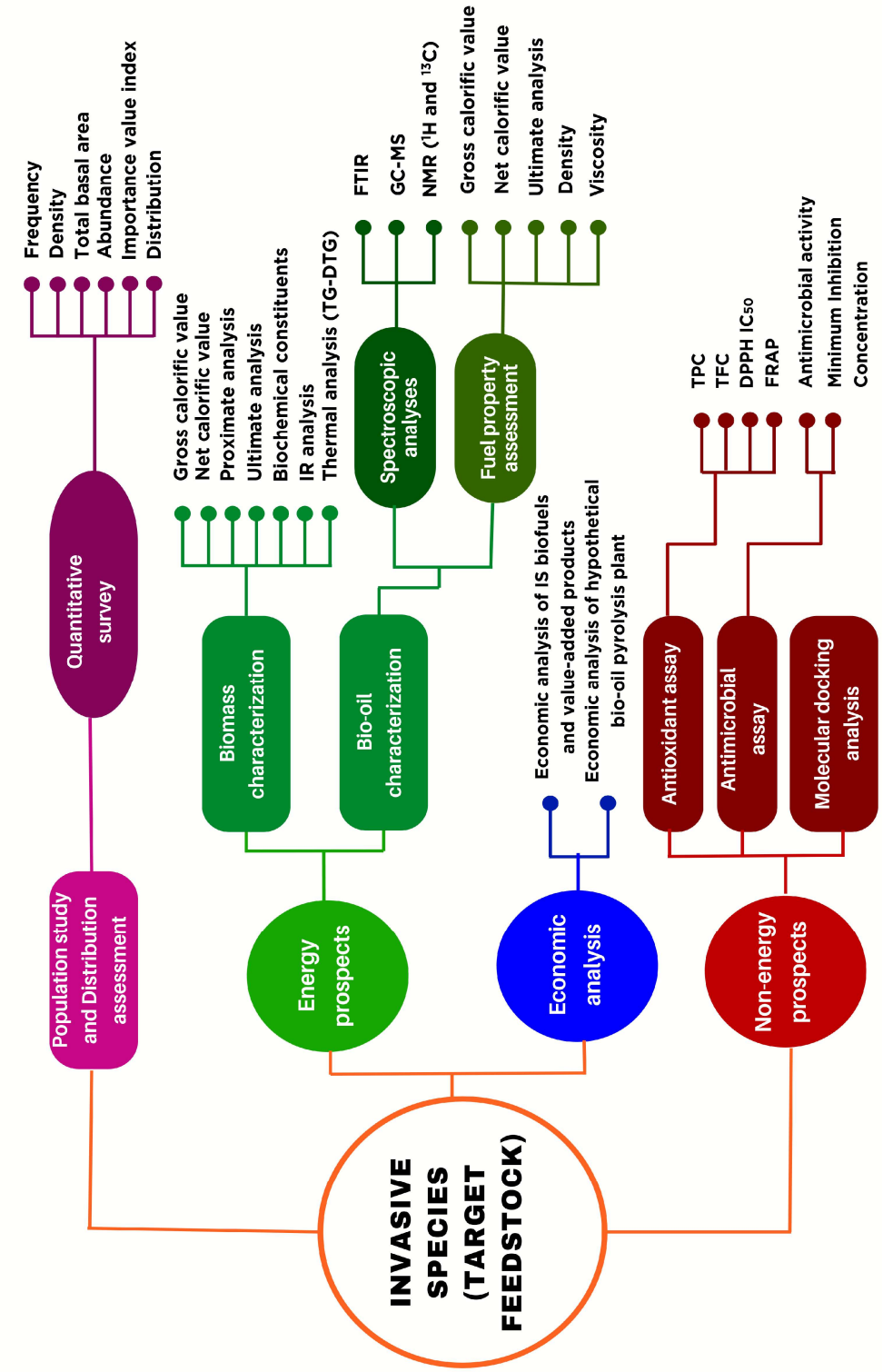


**Fig. 3.1.** Schematic flow chart of material and methods

# Chapter 3

# MATERIALS AND METHODS

## 3.1. Plastic/glassware used

The polystyrene tubes were acquired from Tarson, India and all glassware was obtained from Borosil, India.

## 3.2. Chemicals used

The chemicals and reagents for this study were of analytical grade and sourced from Sigma Aldrich, Merck India Ltd., Loba Chemie Pvt. Ltd., Thermo Fischer Scientific India and Himedia Laboratories.

## 3.3. Equipment used

The following equipment were utilized in the present study

1. Digital weighing balance – Sartorius
2. UV spectrophotometer – Systronics, UV–Vis double beam spectrophotometer 2202
3. pH meter – Labtronics
4. Laminar air flow – Labard Instruchem
5. Muffle furnace – IKON Instrument
6. Hot air oven – IKON Instrument
7. Water bath – IKON Instrument
8. Heating mantle – Symax, India
9. Magnetic stirrer with hot plate – IKON Instrument
10. Magnetic stirrer – Labard Instruchem
11. Electric grinder – Philips HL7759/00
12. Vortexer – Remi
13. Distillation unit – Borosil

14. Incubator shaker – Remi elektrotechnik
15. Deep freezer – Celfrost
16. Autoclave – Labard Instruchem
17. Centrifuge – IKON Instruchem
18. Bomb calorimeter – Labard Instruchem, Model LI–BOMB–A201
19. Refrigerator – L.G Electronics
20. CHNS/O Analyzer – Perkin Elmer 2400 Series II
21. Fourier Transformed Infrared Spectrophotometer (FTIR) – Spectrum Two, Perkin Elmer, USA
22. Thermogravimetric Analyzer (TGA) – TGA7, Perkin Elmer
23. Rheometer – Anton Paar's Modula (MCR–102)
24. GC–MS– Perkin Elmer Clarus 680 gas chromatograph (GC) coupled with a Perkin Elmer Clarus 600C mass spectrometer (MS)
25. NMR – Avance III 500 MHz FT–NMR Spectrometer

### 3.4. Study site

This study was carried out in the Kohima district (Fig. 3.2) (at 25°40' 28.81" N latitude and 94°06' 39.56" E longitude) of Nagaland, India. Kohima, the capital of Nagaland, lies in the southern region at an elevation between 800 – 1500 m above sea level and spans an area of 1,463 sq. km. The district shares borders with Chumoukedima and Peren districts to the west, Zunheboto and Phek districts to the east, the state of Manipur to the south, and Tseminyu district to the north. Kohima experiences a relatively moderate humid subtropical climate. December and January are the coldest months, characterised by frequent frost and snowfall at elevated altitudes. In the peak summer months of July and August, temperatures ascend to 30 °C. The area experiences substantial precipitation during summer, with rainy season lasting from May to September. Consequently, given its rich biodiversity, favourable climatic conditions, agricultural and cultural practices, increasing anthropogenic activities (urbanization and infrastructure development) and limited resources for IS management, among other factors, Kohima serves as an ideal environment for the proliferation of IS.

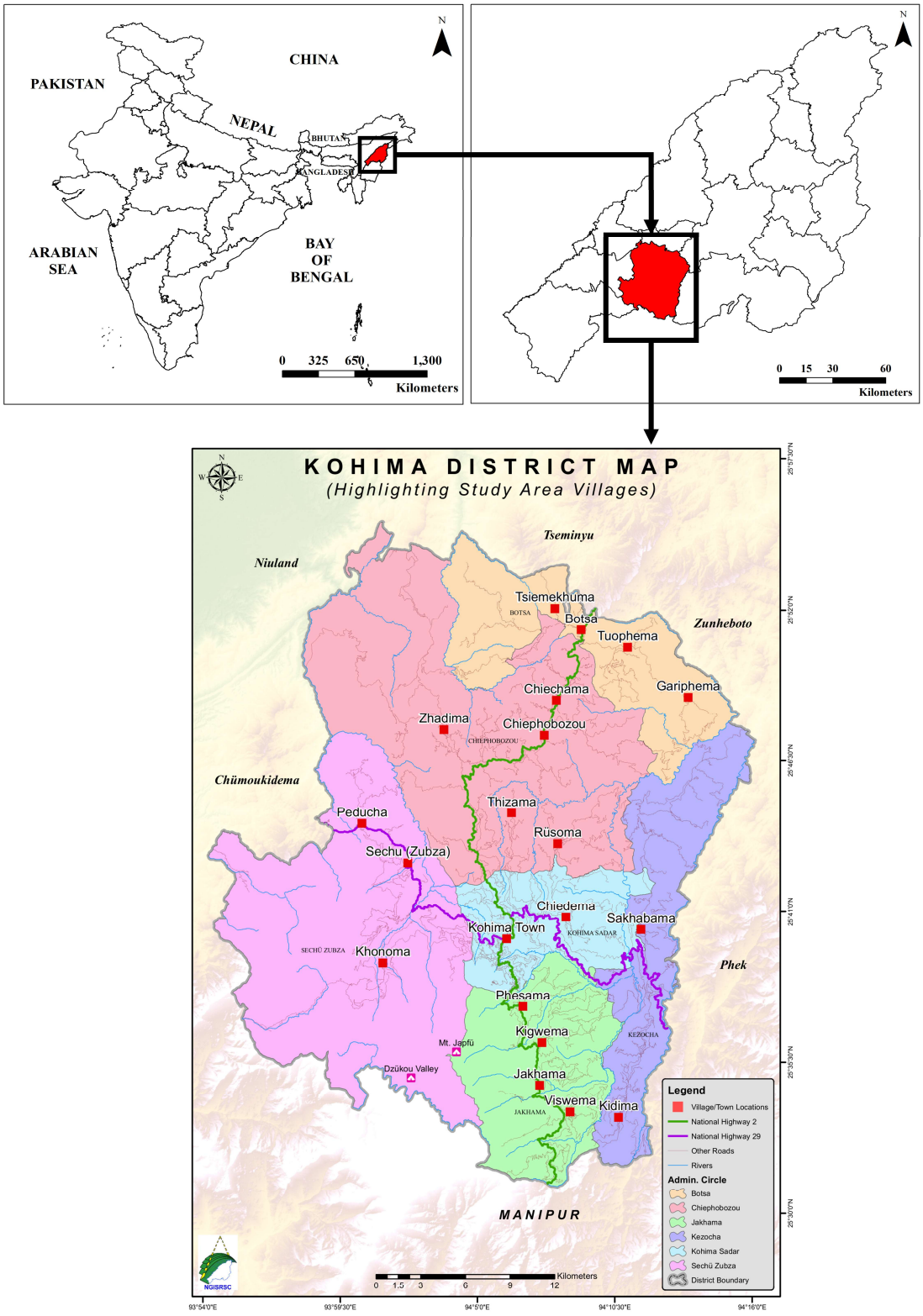


**Fig. 3.2.** Map of Kohima district highlighting sampling locations (villages).

### 3.5. Screening of invasive species (IS) for biofuel generation

Initially, twenty (20 Nos.) invasive species (IS) were randomly selected based on criteria such as visual prominence, abundance driven by aggressive growth, ease of collection, ecological impact, and management challenges. The screening process was based on their energy content, measured as Gross Calorific Value (GCV) in MJ/kg (only top three species in terms of GCV).

### 3.6. Population study of IS

Population study using quantitative surveys are essential for an in–depth comprehension of the plant population in a given area as numerical data highlights the species richness within the studied region. A detailed survey was conducted to study the population and distribution of invasive *Ageratina adenophora*, *Lantana camara* and *Stachytarpheta jamaicensis* in Kohima district, Nagaland during December 2019, February–March 2020, September–October 2020, February–March 2021, and June–July 2021). The species were selected based on their visual prominence and ease of identification in the field, facilitating accurate and efficient data collection. Twenty (20 Nos.) villages were surveyed for the study, with ten quadrates measuring 3m × 3m established per village using the random sampling approach. The location was recorded with the help of a Global Positioning System (GPS) and presented in Table 3.1. At each instance, the occurrences of *A. adenophora*, *L. camara*, and *S. jamaicensis* within the quadrant were enumerated and documented. The species count in each quadrate was conducted by individually measuring the collar diameter of the shrubs using a digital calliper. The reasoning behind the selection of the villages/sites were

1. The IS were abundant (massively visually obvious) in the study sites/villages
2. The villages were accessible by road ensuring ease of transportation and logistics
3. The selected villages covered all directions – north, east, south, west – within the district
4. The villages encompassed diverse land–use types such as human inhabited areas, agricultural fields and secondary forest among others

**Table 3.1.** GPS coordinates of sampling villages with altitude

| Sampling site code | Site | Latitude | Longitude | Altitude |
|---|---|---|---|---|
| S – 1 | Botsa | 25.85593 | 94.15486 | 1414 m |
| S – 2 | Chedema | 25.68309 | 94.0364 | 1167 m |
| S – 3 | Chiechama | 25.80608 | 94.13740 | 1421 m |
| S – 4 | Chiephobozou | 25.79400 | 94.13078 | 1338 m |
| S – 5 | Gariphema | 25.81496 | 94.2253 | 1087 m |
| S – 6 | Jakhama | 25.58706 | 94.12699 | 1622 m |
| S – 7 | Khonoma | 25.64819 | 94.01682 | 1425 m |
| S – 8 | Kidima | 25.55456 | 94.17857 | 1457 m |
| S – 9 | Kigwema | 25.56883 | 94.14516 | 1596 m |
| S – 10 | Kohima town | 25.70669 | 94.10493 | 1352 m |
| S – 11 | Peducha | 25.74566 | 94.0062 | 1029 m |
| S – 12 | Phesama | 25.63168 | 94.11658 | 1574 m |
| S – 13 | Rusoma | 25.73429 | 94.15043 | 1334 m |
| S – 14 | Sakhabama | 25.67693 | 94.19411 | 1064 m |
| S – 15 | Sechu (Zubza) | 25.70710 | 94.03549 | 1075 m |
| S – 16 | Thizama | 25.73824 | 94.10955 | 1358 m |
| S – 17 | Tsiemekhuma | 25.86838 | 94.13893 | 1298 m |
| S – 18 | Tuophema | 25.84451 | 94.17792 | 1487 m |
| S – 19 | Viswema | 25.56406 | 94.14388 | 1633 m |
| S – 20 | Zhadima | 25.80467 | 94.06235 | 1261 m |

### 3.6.1. Data analysis techniques

The data collected was quantitatively analyzed for frequency, density, total basal area (TBA), abundance and distribution (Phillips, 1959). The Importance Value Index (IVI) was calculated for the three IS following method described by Curtis and McIntosh (1950).

#### *i. Frequency*

Frequency is an essential parameter in quantitative analysis, indicating the distribution, frequency, or dissemination of a species within a specified area, expressed in percentage. The below mentioned formula was used to calculate the % frequency

$$\%\ Frequency = \frac{Total\ no.of\ quadrates\ in\ which\ the\ species\ occured}{Total\ no.of\ quadrates\ studied} \times 100 \qquad (3.1)$$

The following formula was used to determine the relative frequency (RF),

$$\%\ Relative\ frequency = \frac{Frequency\ of\ \text{the}\ species}{Total\ frequencies\ of\ all\ the\ species} \times 100 \qquad (3.2)$$

#### *ii. Density*

Density refers to the count of individuals of a particular species within a given area.

$$Density = \frac{Total\ no.of\ individuals\ of\ a\ species}{Total\ no.of\ quadrates\ studied} \qquad (3.3)$$

Relative density (RD) examines the numerical abundance of a species in proportion to the total population of all species. RD was determined using the below mentioned formula

$$\%\ Relative\ density = \frac{Density\ of\ the\ species}{Total\ density\ of\ all\ species} \times 100 \qquad (3.4)$$

### *iii. Total basal area (TBA)*

TBA refers to the sum of cross – sectional areas of all plant stems within a specified plot. It is measured at ground level or just above the root collar for shrubs and is typically expressed in $m^2$/ha.

$$Basal\ area = \frac{\pi}{4} \times (Diameter)^2 \quad (3.5)$$

$$Dominance = Total\ basal\ area\ of\ the\ species\ per\ unit\ area \quad (3.6)$$

While dominance quantifies the TBA per unit area, relative dominance (RD') represents the proportion of a species' basal area in relation to the aggregate basal area of all species.

$$\%\ Relative\ dominance = \frac{Total\ basal\ area\ of\ the\ species}{Total\ basal\ area\ of\ all\ the\ species} \times 100 \quad (3.7)$$

### *iv. Abundance*

Abundance refers to the aggregate population of a specific species within the study area and was calculated as per the below mentioned equation

$$Abundance = \frac{Total\ number\ of\ individuals\ of\ the\ species}{Total\ number\ of\ quadrats\ in\ which\ the\ species\ occured} \quad (3.8)$$

### *v. Distribution*

The abundance–to–frequency ratio was used to determine the distribution pattern of the species. A ratio < 0.025 denotes a regular distribution, whereas ratios between 0.025 – 0.050 imply a random distribution. Ratios > 0.050 indicated contagious distribution (Whitford, 1949).

### *vi. Importance Value Index (IVI)*

IVI is a statistical metric that provides a comprehensive assessment of a species' significance within a community. It considers the comparative values of frequency, density and species dominance in a specified area (Curtis and McIntosh, 1950). It

therefore encompasses three critical parameters that reflects the diversity, productivity and dispersion of each species. IVI was determined using the below mentioned formula

$$\%\ IVI = Relative\ frequency + Relative\ density + Relative\ dominance \quad (3.9)$$

The sum of the IVI should be equal to 300.

### 3.7. Sample collection and preparation

Fresh plants were collected from various locations in the study area. The entire shrub was used as the sample/feedstock for the study. The sample was thoroughly rinsed with distilled water (DW). Following this, the sample was oven–dried for 12 h at 100°C ± 2°C. An electric grinder was used to finely ground the feedstock. The sample was then passed through a sieve (0.25 mm) to attain uniform particle size (Jacqueline et al., 2022). The powdered samples were then packaged and stored in sealed containers for further analysis.

### 3.8. Gross Calorific Value (GCV) determination

GCV is a crucial factor in fuel selection, that signifies the heat generated during combustion and reflects the fuel's available energy (Ghazali et al., 2015). Model LI–BOMB–A201, automatic bomb calorimeter, was used to measure the GCV. The samples were combusted with an oxygen pressure of 3.4 Mpsi in an adiabatic bomb chamber. The final GCV was calculated as the average of three replicates.

### 3.9. Biochemical analysis

#### 3.9.1. Carbohydrate estimation

The Anthrone method (Yemm and Willis, 1954) was used for the quantitative estimation of carbohydrate in the sample. The test sample (100 mg) was hydrolyzed by treating it with 2.5 N HCl (5 ml) and boiling the mixture in a water bath for 3 h and subsequently neutralized using $Na_2CO_3$. Following centrifugation, the resulting supernatant was collected for analysis. Glucose standards (20 – 100 µg/ml) were prepared by diluting a stock solution. 1 ml of each blank (DW), standard, and sample was mixed with 4 ml of freshly prepared Anthrone reagent (0.2 % Anthrone in

concentrated $H_2SO_4$) in test tubes. The tubes were incubated in a boiling water bath for 10 min to commence the reaction and then cooled rapidly in an ice bath to stabilize the green colour formed. Absorbance was measured at 620 nm using a spectrophotometer (UV–Vis double beam spectrophotometer 2202), with the blank serving as the reference. A standard curve was plotted using absorbance values of glucose standards, and the carbohydrate content of the sample was calculated using the curve.

$$C_{glc} = \frac{1}{0.005}(OD_{620} - 0.017) \quad (3.10)$$

Where, $C_{glc}$, and $OD_{620}$ represents the concentration of glucose (in mg/ml) and optical density at 620 nm, respectively.

### 3.9.2. Protein estimation

Protein estimation was performed following the Lowry method (Lowry et al., 1951). 500 mg of the sample was grinded in a mortar and pestle containing 10 ml of phosphate buffer. Following centrifugation of the sample for 10 min, the supernatant was collected for further analysis. The reagents were prepared as follows: Reagent A consisted of 2 % $Na_2CO_3$ in 0.1 N NaOH; Reagent B was 100 ml of DW with 0.5 % $CuSO_4$ and 1 % $CuSO_4$; Alkaline copper solution (Reagent C) was made by combining 50 ml of Reagent A with 1 ml of Reagent B; and FC reagent was prepared by diluting the Folin–Ciocalteu reagent (FCR) with an equal volume of DW (1:1). The protein standard was prepared by dissolving 10 mg of bovine serum albumin (BSA) in 10 ml of DW. To estimate protein concentrations, varying concentrations (0.2, 0.4, 0.6, 0.8, 1 and 1.2 ml) of the working standard were pipetted into a series of labelled test tubes. 1 ml of the sample was introduced into a separate test tube. The volume in all the test tubes were adjusted to 2 ml with DW. 2 ml of DW served as the blank. To each test tube (blank and sample), 4 ml of Reagent C was added followed by vortexing and a 10 min incubation at ambient temperature. Subsequently, 0.5 ml of FC reagent was added, followed by immediate mixing. The tubes were then incubated at 37 °C in the dark for 30 min. Absorbance was recorded at 660 nm using a UV–Vis spectrophotometer. The relationship between BSA concentration ($C_{bsa}$, mg/ml) and optical density was expressed by the following equation

$$C_{bsa} = \frac{1}{0.001}(OD_{660} - 0.435) \quad (3.11)$$

### 3.9.3. Determination of total lipids

Soxhlet extraction method was used to calculate the total lipid (Manirakiza et al., 2001). A thimble with 5 g of the finely powdered sample was placed into a Soxhlet apparatus. Petroleum ether, with a boiling point range of 60 – 80 °C, was used as the solvent for lipid extraction. The sample was extracted under continuous reflux until the solvent became colourless. Subsequently, the condenser unit was detached, and the extraction apparatus was allowed to cool. The solvent was then evaporated to obtain the lipid fraction. The extracted lipids were dried and weighed to determine the lipid content of the sample.

$$\%\ Lipid = \frac{Weight\ of\ lipid}{Weight\ of\ the\ dried\ sample} \times 100 \quad (3.12)$$

### 3.9.4. Determination of lignin, cellulose and hemicellulose

Following the Lin et al. (2010) outlined method, cellulose, lignin and hemicellulose contents were estimated. To determine hemicellulose content, 1 g of extractive–free biomass was treated with 30 ml of 0.5 M NaOH solution and heated at 80 °C for 3.5 h. The mixture was then filtered, and the residue was thoroughly washed with deionized water. The residue was dried in hot air oven at 105 °C, and the hemicellulose content was calculated as the difference in sample weight before and after treatment.

For lignin content analysis, 1 g of dried extractive–free biomass was treated with 30 ml of 98 wt. % $H_2SO_4$ and allowed to undergo hydrolysis at ambient temperature for 24 h with intermittent shaking. The sample was subsequently boiled at 100 °C for 60 min and then filtered. The residue was washed with deionized water and dried at 105 °C to a constant weight. Ash content was determined by incinerating the dried residue at 525 °C ± 25 °C in a muffle furnace. Lignin content was calculated as the residue weight after subtracting the ash content. Cellulose was estimated by difference assuming the biomass consisted solely of ash, extractives, hemicellulose and lignin.

$$Cellulose = 100 - \%\,(Extractive + lignin + hemicellulose + ash) \quad (3.13)$$

The mean values are reported based on the results of three sets of tests.

## 3.10. Proximate analysis

### 3.10.1. Moisture Content (MC) determination

MC % was determined in accordance with the ASTM D 3173 methodology. 1g sample was added to a pre–weighed crucible, which was then kept in a hot air oven at 105 ± 3°C until a constant weight was achieved. The following equation was used to determine the MC %

$$MC\ \% = \frac{Initial\ weight\ of\ the\ sample - Oven\ dry\ weight}{Initial\ weight\ of\ the\ sample} \times 100 \quad (3.14)$$

### 3.10.2. Volatile Matter (VM) determination

VM % was determined following the ASTM D 3175 protocol. Briefly, 1g of the oven dried sample was kept in a pre–weighed crucible and subjected to heating at 950 ºC for 2 min in a muffle furnace. The crucible was then left to cool for approximately 5 min. The sample was subsequently placed in a desiccator for 15 min to ensure complete cooling. VM contents were determined through a two–step calculation process. Initially, sample weight loss was determined using Eq. (3.15) followed by the calculation of VM % using Eq. (3.16)

$$Weight\ loss\ \% = \frac{weight\ of\ the\ sample\ plus\ crucible - weight\ of\ the\ sample\ and\ crucible\ after\ heating}{initial\ weight\ of\ the\ sample} \times 100 \quad (3.15)$$

$$VM\ \% = Weight\ loss\ (\%) - MC\ \% \quad (3.16)$$

In Eq. (3.16), weight loss corresponds to the value calculated in Eq. (3.15), while the MC % is derived from Eq. (3.14).

### 3.10.3. Ash Content (AC) determination

AC % was determined according to ASTM D 3174 protocol. Briefly, 1 g of oven dried sample was kept in a pre–weighed crucible and subjected to heating at 525 °C ±

25 °C for 3 h. The below mentioned formula was used to calculate the same

$$AC\ \% = \frac{\text{initial weight of the sample plus crucible} - \text{weight of the sample and crucible after heating}}{\text{weight of the biomass sample}} \times 100 \quad (3.17)$$

### 3.10.4. Fixed Carbon (FC) determination

FC % of the biomass sample was determined mathematically according to the equation furnished below

$$FC\ \% = 100 - (MC\% + VM\ \% + AC\ \%) \quad (3.18)$$

Only the average value obtained from the three assays are presented.

## 3.11. Ultimate analysis

Ultimate analysis was conducted in a Perkin Elmer 2400 Series II CHNS/O Analyzer. Weight percentages of hydrogen (H), carbon (C) and nitrogen (N) were determined. Oxygen (O) % was calculated mathematically (by difference)

$$O\ \% = 100 - (C\ \% + H\ \% + N\ \%) \quad (3.19)$$

## 3.12. Estimation of Net Calorific Value (NCV)

The NCV was determined using the equation (Evald et al., 2008)

$$\text{NCV} = \text{GCV} \times \left(1 - \frac{w}{100}\right) - 2.444 \times \left(\frac{w}{100}\right) - 2.444 \left(\frac{H}{100}\right) \times 8.936 \times \left(1 - \frac{w}{100}\right) \text{ ; (MJ/Kg, w.b.)} \quad (3.20)$$

Where, GCV denotes the Gross calorific value

2.444 = Enthalpy difference between gaseous and liquid water at 25°C

$8.936 = \frac{M_{H2O}}{M_{H2}}$, the molecular mass ratio between $H_2O$ and $H_2$

H is the weight % of hydrogen concentration *w* is the weight % of MC of the fuel

### 3.13. Fourier Transformed Infrared Spectroscopy (FTIR) Analysis

The samples were analyzed for their functional groups at ambient temperature of 28 ± 2 °C in an IR Spectrometer (Spectrum Two, Perkin Elmer, USA). Prior to analysis, the sample was amalgamated with KBr powder followed by its compression into tablets. Mid–infrared range (4000 – 400 $cm^{-1}$) with a 4 $cm^{-1}$ resolution recorded the IR spectra of the samples.

### 3.14. Thermogravimetric Analysis (TGA)

TGA was performed to investigate the samples' degradation profile. TGA was conducted at varying heating rates (10 °C/min and 30 °C/min, respectively) in nitrogen environment. 10 mg sample was heated from ambient to 700 °C at the specified heating rates. The analysis was conducted using a TGA7 Thermogravimetric Analyzer (Perkin Elmer), with a purity of 99.99 % nitrogen. The flow rate was 50 ml/min.

### 3.15. Pyrolysis of IS biomass

Pyrolysis of IS biomass (40 g) was carried out in a vertical tubular custom–built lab–scale pyrolyzer. A schematic representation of the pyrolyzer is provided in Fig. 3.3. The experiment was conducted in nitrogen atmosphere (flow rate of 100 ml/min) from ambient to 600°C, with a heating rate of 30 °C/min. The heating rate and operating temperature for pyrolysis was based on previous literature (Cheng et al., 2019; Maulinda et al., 2023). The temperature throughout the pyrolysis process was monitored and regulated using a Ni–Cr–Ni thermocouple. The volatiles produced during the process were condensed through a water circulating condenser functioning at 8 °C. The reactor held the sample at the final temperature for approximately 30 min (de Abreu Neto et al., 2020). The resulting condensate exhibited heterogeneity, comprising of an aqueous layer (high polar constituent) and a heavy oil layer (low polar constituent). The condensed liquid product was recovered using $C_2H_5OC_2H_5$. A separating funnel using gravity separation process was used to separate the two fractions. The organic phase was desiccated using anhydrous sodium sulfate, filtered, and subsequently evaporated in a rotary evaporator at 30 °C to eliminate $C_2H_5OC_2H_5$ (Bordoloi et al., 2015). The bio–oil (heavy oil fraction) was collected and weighed. The bio–oil obtained was stored in a

glass vial and sealed with parafilm to avoid unwanted reactions at 4 °C in a refrigerator. The biochar (solid residue) in the reactor was weighed after being cooled to ambient temperature.

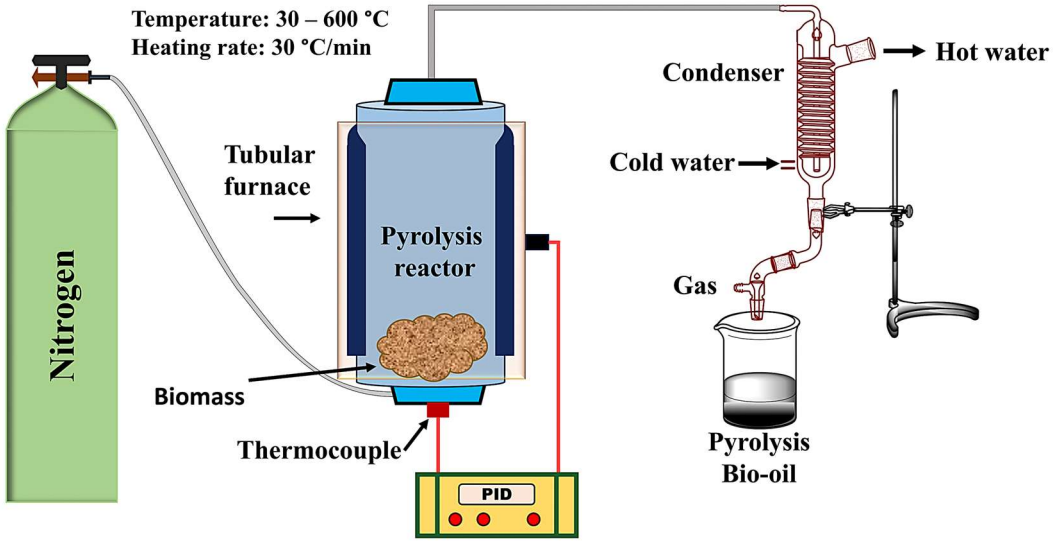


**Fig. 3.3.** Schematic diagram of the pyrolyzer used for thermochemical conversion.

### 3.16. Mass and Energy Yields of the products

For each product, Eqs. (3.21) and (3.22) were used to calculate the percentages of mass yield and energy yield (Akhtar et al., 2021)

$$\%\ mass\ yield\ (wt.\%) = \frac{Mass\ of\ the\ pyrolytic\ product}{Mass\ of\ biomass} \times 100\% \qquad (3.21)$$

$$\%\ energy\ yield = \frac{Mass\ of\ the\ pyrolytic\ product}{Mass\ of\ the\ biomass} \times \frac{GCV\ of\ the\ pyrolytic\ product}{GCV\ of\ the\ biomass} \times 100\% \qquad (3.22)$$

% mass yield of the gaseous product was estimated by difference.

### 3.17. Density and Viscosity of bio–oil

Density of bio–oil was measured using a pycometer at ambient temperature according to ASTM D 1217 protocol

$$Density = \frac{Mass\ of\ the\ bio-oil}{Volume\ of\ the\ bio-oil} \quad (3.23)$$

Anton Paar's Modula compact Rheometer (MCR–102) at 40 °C was used to determine the viscosity of the bio–oil samples.

### 3.18. Gas Chromatography–Mass Spectroscopy (GC–MS) analysis

Perkin Elmer Clarus 680 GC coupled with a mass spectrometer was used for GC–MS analysis of the bio–oil. A DB5–MS capillary column (30 m × 0.25 mm × 0.25 µm) was used for gas chromatography. The temperature in the oven was set to rise at a rate of 10 °C/min, beginning at 70 °C (2 min hold) up to 300 °C. High purity helium (99.99 %) at a flow rate of 1 ml/min was used as the carrier gas. The mass spectrometer functioned across a mass range of 40 – 1000 m/z. The interface temperature was set to 240 °C. The compounds in the samples were identified by comparing the mass spectrum with the NIST library.

### 3.19. Nuclear Magnetic Resonance (NMR)

Avance III 500 MHz FT–NMR Spectrometer was used to record the $^{13}C$ and $^{1}H$ NMR spectra of the bio–oil with Tetramethylsilane (TMS) as the internal standard. Dissolved in $CDCl_3$, the chemical shift values in the bio–oil, relative to intensity, were used to analyze the spectrum. Spectral data integration was performed using MestReNova software.

### 3.20. Economic analysis for IS biofuel and value–added products

The economic viability of biofuel production from IS biomass were analyzed in accordance with existing literature (Chisti, 2008; Phukan et al., 2019). The energy content of a barrel of crude petroleum is equivalent to approximately M tons of IS biomass, determined using the following calculation

$$M = \frac{E_{Petroleum}}{ywE_{bio-oil} + qE_{syngas}x_{syngas} + E_{biochar}x_{biochar}} \quad (3.24)$$

Where, $E_{Petroleum}$ (~6100 MJ) is the calorific value of a barrel of petroleum (Chisti, 2008); $y$ the yield of biomass converted to bio–oil, expressed as weight fractions; $w$ represents the weight fractions of fuels and value–added products that can be derived from biomass (or bio–oil); $E_{biochar}$, $E_{bio-oil}$, and $E_{syngas}$ represent the energy content of biochar, bio–oil and syngas respectively; $x_{syngas}$ and $x_{biochar}$ are the weight fractions of derived syngas and biochar; syngas volume generated for each ton of biomass (in $m^3$/ton) is represented as q. M is calculated based on bio–oil's varying conversion efficiencies ($w$) into fuels and value–added products.

Given that the cost of transforming M tons of biomass into various biofuels and value–added products through pyrolysis parallels the conversion of several products from a barrel of petroleum, the maximum permissible price for the IS biofuels (along with other bio–oil derived value–added products) can be determined as follows

$$Acceptable\ price\ of\ IS\ biofuel = \frac{Price\ of\ a\ barrel\ of\ petroleum}{M} \quad (3.25)$$

## 3.21. Economic analysis of a hypothetical pyrolysis facility

Economic analysis was carried out to evaluate the viability and profitability of a hypothetical bio–oil pyrolysis facility encompassing cost structure analysis, financial evaluation and sensitivity analysis to identify key factors influencing profitability. The current theoretical assessment indicates that each IS contributes around six million Kg/year, which represents the minimum requirement to initiate processing operations for the proposed plant. According to our theoretical findings, the three species under investigation, have reached the established threshold of six million Kg/year. As a result, no particular IS was selected for the present study; the focus was on the broadly dominant IS within the research area.

### 3.21.1. Data collection

The data required for the economic feasibility analysis were acquired through primary and secondary sources. The primary source comprised of field interviews and surveys aimed at evaluating the availability of IS in the study area. Secondary data included relevant financial and technical statistics. This encompassed governmental

reports and policy documents (e.g., Ministry of Rural Development), previous scientific literature focused on the financial assessment of biomass processing facilities, particularly those utilising pyrolysis technology, as well as case studies featuring analogous economic evaluations. The data were carefully gathered and integrated into a financial modelling framework to assess the economic feasibility.

### 3.21.2. Pyrolysis of IS biomass for the hypothetical pyrolysis plant

The pyrolysis process for bio–oil production is estimated to utilise a feedstock capacity of 5000 Kg per run. The operation processes 20000 Kg of feedstock daily, conducting four runs each day. The total feedstock processing reaches six million Kg annually, operating on a schedule of 300 days each year. This configuration seeks to achieve a steady throughput alongside optimal use of IS biomass, all while investigating the maximum potential of the biomass processing facility.

### 3.21.3. Cost structure analysis

The cost structure of the pyrolysis plant was analyzed by categorizing expenses into Capital Expenditure (CAPEX) and Operational Expenditure (OPEX).

#### *i. Capital Expenditure (CAPEX)*

The CAPEX is estimated by summing the various cost components outlined below

$$CAPEX = C_{lc} + C_c + C_{iu} + C_{pc} + C_p + C_{su} \quad (3.26)$$

Where, $C_{lc}$ represents the cost of land required for plant establishment, $C_c$ denotes the plant's construction cost, $C_{iu}$ is expenses associated with infrastructure and utilities, $C_{pc}$ signifies cost related to permits and compliance, $C_p$ indicates cost of pyrolizer and $C_{su}$ represents cost of establishing one storage unit. Due to the absence of standardized rates for capital assets, including land, construction materials, and machinery, the average prevailing market prices were considered in the formulation of CAPEX.

### *ii. Operational Expenditure (OPEX)*

The OPEX is similarly estimated by adding the various cost components outlined below

$$C_r = C_{ul} + C_t \quad (3.27)$$

Where, $C_r$ denotes expenses associated with raw materials. $C_{ul}$ represents the remuneration allocated to unskilled labourers, calculated as the wage rate multiplied by the number of labourers while $C_t$ denotes the cost of transportation. The total is calculated by multiplying the rate per trip by the number of trips.

$$C_{sl} = W_r \times nE \quad (3.28)$$

Where, $C_{sl}$ represents the expense associated with skilled labour, the remuneration disbursed to skilled labourers engaged in the plant's functioning, $W_r$ represents the average wage rate of skilled employees and nE is the number of employees.

Thus, the OPEX can be expressed as,

$$OPEX = C_e + C_r + C_{sl} \quad (3.29)$$

$C_e$ represents the annual cost of electricity consumption.

The wage rate for unskilled labourers was determined as per the Mahatma Gandhi National Rural Employment Guarantee Act (MGNREGA). The act guarantees a legal entitlement to paid work for one hundred days each financial year for adults in rural households willing to engage in unskilled physical labour (Ministry of Rural Development, 2024).

### *iii. Financial evaluation*

The economic feasibility of the pyrolysis facility was assessed using three key financial metrics

*Payback Period (PBP):* An investment project's PBP refers to the duration required for the cumulative anticipated net returns to equal the initial investment expenditure (Seboka, 2009). The calculation for PBP is outlined below

$$PBP = T - 1 + \frac{|\mathrm{CNCF_{T-1}}|}{\mathrm{NCF_T}} \quad (3.30)$$

Where, T is the specific year of cumulative net cash flow, $NCF_T$ is net cash flow for year T, and $CNCF_{T-1}$ is cumulative net cash flow in year T − 1 (Zhang et al., 2017).

*Net Present Value (NPV):* NPV is the difference between incoming cash flows and expected future cash outflows discounted to today's value (López–Marín et al., 2020). It represents the present value of all future cash flows from an investment. The formula for NPV is expressed as

$$NPV = \sum_{t=0}^{n} \frac{(C_1 - C_0)}{(1-r)^t} \quad (3.31)$$

Where, $n$ is the project's operational period, $C_1$ and $C_0$ are the annual cash inflows and outflows, respectively, $r$ is the capital expenditure, and $t$ represents time.

Positive NPV indicated project feasibility, while a negative value necessitated rejection (Bora, 2015).

*Internal Rate of Return (IRR):* IRR is the annual rate of returns of an investment. It is the rate of return which equates the present value of all cash flows to zero in a discounted cash flow analysis (Bora, 2015). In other words, it is the discount rate that makes the NPV of a project zero. The formula for IRR is given as

$$0 = NPV = \sum_{t=0}^{n} \frac{(CF_t)}{(1-IRR)^t} \quad (3.32)$$

Where, $CF_t$ is the annual net cash flow, $n$ is the project duration, and $t$ represents time.

### 3.21.4. Sensitivity analysis

To evaluate the robustness of profitability, sensitivity analysis was conducted to assess the impact of variations in operational costs and product pricing on NPV and IRR. Operational costs, initially set at $ 0.2361/Kg, encompassing expenses for feedstock acquisition, transportation, labour, electricity, and salaries, were hypothetically varied between $ 0.2196 – 0.2774/Kg with $ 0.01 increments to observe their effect on the IRR. The IRR threshold was identified when profitability dropped below an 8 % cost of capital (COC). Similarly, product pricing was adjusted from $ 0.2427 – 0.3005/Kg with $ 0.01 increment, to assess its influence on IRR and NPV. This analysis identified critical cost and pricing parameters essential for maintaining project profitability under variable market and operational conditions.

## 3.22. Antioxidant activity of bio–oil

### 3.22.1. Total Phenolic Content (TPC)

TPC of bio–oil was estimated following the Folin–Ciocalteu method (Kähkönen, 1999). To 100 µl of each standard solutions of gallic acid (0.25 – 1.50 mg/ml) and sample extract, 0.5 ml of FC reagent was added, followed by vortexing. After 4 min of incubation, 1.5 ml of 7.5 % $Na_2CO_3$ solution was added to the mixture. $CH_3OH$ (100 µl) served as the blank. This was followed by a 2 h incubation of the reaction mixture at ambient temperature in the dark. UV–Vis spectrophotometer recorded the absorbance at 765 nm with blank as the reference. Gallic acid at various concentrations was used to plot the standard curve. From the standard curve equation, the TPC of the bio–oil samples were determined and presented as mg GAE/ml of bio–oil. Only the average value obtained from three assays is presented.

### 3.22.2. Total Flavonoid Content (TFC)

TFC of the bio–oil was estimated following the Aluminium Chloride method (Chang et al., 2002). 100 µl each of the sample extract, standards of quercetin (25 – 200 µg/ml in $CH_3OH$) and $CH_3OH$ (blank) were mixed with 1 ml of 10 % $AlCl_3$ and vortexed, followed by the addition of 1 ml of 1M $CH_3COONa$ solution. This was

followed by incubation for 45 min at ambient temperature in the dark and subsequent vortexing. Absorbance of the reaction mixture was recorded at 415 nm with blank as the reference. A standard curve equation was generated by plotting the absorbance values against the various quercetin concentrations. The result of the TFC was expressed as mg QE/ml of bio–oil. Only the mean value derived from three assays is presented.

### 3.22.3. 1, 1–diphenyl–2–picrylhydrazyl (DPPH) free radical scavenging capability

Bio–oil's ability to scavenge DPPH free radicals was assessed using the Lu et al. (2021) method. Briefly, 3.9 ml of $CH_3OH$ solution of DPPH (0.1 mM/L) was added to 100 µl of bio–oil, vortexed, followed by a 30 min incubation in the dark at ambient temperature. At 517 nm, the absorbance was measured for both the sample and the blank mixture (100 µl of $CH_3OH$ and 3.9 ml of DPPH reagent). The antioxidant potential of the bio–oil was compared using ascorbic acid as a standard antioxidant agent. The DPPH free radical scavenging activity (% RSA) was calculated using the following equation

$$(\%)\ DPPH\ radical\ scavenging\ activity\ (RSA) = \frac{Abs_{blank} - Abs_{sample}}{Abs_{blank}} \times 100 \quad (3.33)$$

Where, $Abs_{blank}$ represents the absorbance of DPPH solution in $CH_3OH$, $Abs_{sample}$ represents the absorbance of DPPH radical + sample extract.

From the regression curve obtained by plotting % RSA value against various concentrations of bio–oil, $IC_{50}$ value of the bio–oil was calculated. Results are expressed as the mean value of triplicate assays.

### 3.22.4. Ferric Reducing Antioxidant Power (FRAP) assay

The Benzie and Strain (1996) method was used to carry out the FRAP assay of the bio–oil. 100 µl of bio–oil diluted with $CH_3OH$ was combined with 3 ml of FRAP reagent (mixture of acetic acid buffer, 10 mM/L TPTZ solution, and 20 mM/L of $FeCl_3$ solution at a ratio of 10:1:1). The mixture was incubated for 15 min at 37 °C in the dark and the absorbance was measured at 593 nm. The ascorbic acid equivalent of the bio–oil was determined by plotting a standard curve using ascorbic acid concentrations

ranging from 0.2 – 1.0 µM/ml. The final FRAP value of the bio–oil was calculated from the equation

$$FRAP\ value\ (\mu M\ AAE/ml) = \frac{AAE\ x\ V}{W} \quad (3.34)$$

Where, AAE = Ascorbic acid equivalent in µmol/ml, V = volume of test sample, w = concentration of the bio–oil in the test sample.

Data reported represent the mean value of triplicates.

### 3.23. Antimicrobial activity of bio–oil

#### 3.23.1. Agar well diffusion method

The agar well diffusion method was used for the antimicrobial assay (Balouiri et al., 2016). The bio–oil's antimicrobial activity was evaluated against gram–positive bacteria (*Staphylococcus aureus* MTCC740 and *Bacillus cereus* MTCC8361), gram–negative bacteria (*Salmonella enterica* MTCC1164 and *Escherichia coli* MTCC593), and fungus (*Candida albicans* MTCC13013). The Mueller Hinton Agar (MHA) served as the culture medium for bacteria, while for fungus MHA was enriched with glucose and methylene blue. The media were sterilized and poured into sterile petri plates. After the agar solidified, a standardized microbial inoculum prepared by matching the test organisms' turbidity to the 0.5 McFarland standard, was evenly spread across the solidified agar. 8 mm wells were bored using a sterile borer. Dimethyl sulfoxide (DMSO) served as negative control. 100 µl of DMSO (negative control) and bio–oil (test sample) was added to each well. Fluconazole (25 µg) and ciprofloxacin (5 µg) discs served as positive controls for fungus and bacteria, respectively. Incubation was carried out at 37 °C for 48 h for fungal culture and 24 h for bacterial culture. Following incubation, the diameter of zone of inhibition (ZOI) was measured in millimetres to determine the antimicrobial efficacy of the bio–oil.

#### 3.23.2. Minimum Inhibitory Concentration (MIC)

MIC was determined employing the microbroth dilution method (Tekwu et al., 2012). 96–well sterile microplates were used for the assay. The bio–oil stock solution

was prepared at a concentration of 50 µl /ml in DMSO. Standardized microbial inocula was prepared by matching the test organisms' turbidity to the 0.5 McFarland standard. 100 µl of Mueller Hinton Broth (MHB) was added to each well for bacteria, while MHB, enriched with 10 % glucose and 0.05 % phenol red, was used for fungus. In column 1, 100 µl of the bio–oil stock solution was introduced to the wells in rows A through H. A multichannel pipette was employed to transfer 100 µl from column 1 to column 2, ensuring thorough mixing of the well contents. The approach of serial 1:2 dilutions was carried out until column 10, with 100 µl of surplus medium removed from column 10. In rows A to H in columns 1 to 11, 5–10 µl of the inoculum suspension was introduced to the wells. Azithromycin (for bacteria) and fluconazole (for fungus) at a concentration of 1mg/ml was used as the positive controls. DMSO (1 %) served as negative control for all the test samples. The microplates were sealed and incubated at 37 °C for 24 h. The red colouration of the well was interpreted as indicative of no growth, whereas wells exhibiting a distinct yellow colour were documented as positive, signifying microbial growth.

### 3.24. Molecular docking simulation

Molecular docking simulations were conducted to investigate potential therapeutic ligands for breast cancer, adhering to a standardized and systematic protocol. Ligands were initially screened for availability in reputable chemical databases such as PubChem and ChemSpider. Once validated, the Simplified Molecular Input Line Entry System (SMILES) strings of the selected ligands were imported into PerkinElmer ChemDraw 3D software for structural optimization. The Merck Molecular Mechanics (MM2) force field was applied to refine the geometries and compute potential energy profiles, ensuring optimal molecular conformations. This process of ligand preparation, encompassing geometry optimization and energy minimization, was critical for achieving reliable docking results.

A comprehensive literature review identified relevant protein targets and standards used in breast cancer computational studies. Selected protein structures were retrieved from the Research Collaboratory for Structural Bioinformatics (RCSB) Protein Data Bank (PDB) after rigorous cross–validation of parameters, including experimental

method, resolution, mutations, and structural integrity. Protein preparation was carried out in Biovia Discovery Studio by removing non–essential entities such as chains, crystallographic water, and heteroatoms. Polar hydrogen atoms were added to enhance hydrogen bonding, improve electrostatic interaction calculations, and ensure force field compatibility. Geometry optimization was performed to reduce steric hindrance and maintain structural fidelity for subsequent docking simulations.

Prepared ligands and proteins were loaded into PyRx for molecular docking simulations using Autodock Vina. Charges were assigned to the ligands for minimization, and proteins were designated as docking targets. Grid boxes were carefully defined to encompass the binding site, guided by active pocket coordinates identified through cavity prediction algorithms in Molegro Virtual Docker. The selected docking conformations were visualized and analyzed using advanced molecular visualization tools, including Biovia Discovery Studio, UCSF Chimera, and Avogadro. These analyses provided detailed insights into ligand–protein interaction profiles, validating the docking results and supporting the identification of potential therapeutic candidates.

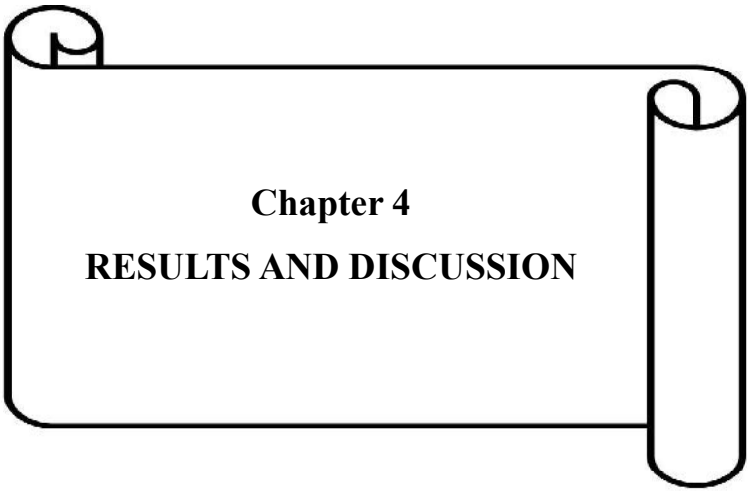

# Chapter 4

# RESULTS AND DISCUSSION

# Chapter 4

# RESULTS AND DISCUSSION

## 4.1. Screening of invasive species (IS) for biofuel generation

A total of twenty (20 Nos.) IS were shortlisted for the current investigation. The cardinal objective was to investigate their feasibility as feedstock for thermochemical conversion (pyrolysis). Initially, their Gross calorific values (GCV) were determined using a bomb calorimeter. The top three species with the highest energy content (*Stachytarpheta jamaicensis* (17.06 MJ/Kg) > *Ageratina adenophora* (16.63 MJ/Kg) > *Lantana camara* (16.49 MJ/Kg) were finally selected for the present study. Following this, a quantitative survey was conducted to assess the abundance, distribution patterns, and biomass availability of these three species in the study sites. This step was essential to evaluate the practical feasibility of biomass collection for utilization of these IS for bioenergy generation and subsequent value–addition studies.

## 4.2. Population study of selected IS

The study presents key ecological parameters viz. frequency, density, total basal area (TBA), abundance, distribution and Importance Value Index (IVI) for three species (*A. adenophora*, *L. camara*, and *S. jamaicensis*) across multiple sites in Kohima district, Nagaland. The IS have high acclimatization ability and ubiquitous growth which supports their luxuriant proliferation in the study sites in Kohima district, Nagaland. Fig. 4.1 displays the frequency of the three IS while Fig. 4.2, Fig. 4.3 and Fig. 4.4 represents their density, TBA and IVI, respectively. *A. adenophora* was recorded in all 20 surveyed villages, with frequency ranging from 60 % – 100 %. Notably, 9 villages exhibited 100 % frequency of occurrence. The results of this study are consistent with the findings of Verma et al. (2022), who reported the presence of *A. adenophora* across all altitudinal gradients studied, highlighting its ability to thrive in diverse ecosystems. The significant density (131000 – 622000 Ind./ha.), TBA

(16.83 – 46.32 m sq./ha.) and IVI (41.3 – 112.79) of *A. adenophora* across all surveyed sites signifies its ecological success in the study area. Furthermore, the distribution trends of IS across diverse ecosystems provide essential insights into their proliferation and establishment in varying ecological niches (Santamarina et al., 2023). Distribution study, as depicted in Table 4.1, revealed *A. adenophora* exhibited contagious distribution in all surveyed sites. This may be attributed to its robust reproductive capacity and its potential in overshadowing its native associates thereby further reinforcing its superiority in the ecosystem (Verma et al., 2022). A key factor driving the rapid spread of *A. adenophora* is its strong allelopathic properties, which enable it to outcompete native species (Inderjit et al., 2011). The prevalence of this species in the hilly Kohima district, highlights the vulnerability of mountain ecosystem to biological invasions. These invasions are primarily driven by increasing anthropogenic activity (such as agricultural expansion, urbanization, travel and trade) and climate change (Gu et al., 2021).

In comparison, *L. camara* showed moderate to high frequencies (10 – 90 %), in several sites (17 surveyed villages). This may be attributed to the fact that while it can endure partial shade, *L. camara* is shade–intolerant thriving in ecosystems with open canopies (Mandal & Joshi, 2015). This characteristic explains its rarity in closed–canopy forest and its predominance in open–disturbed areas within the study sites. Additionally, numerous studies have demonstrated the proliferation of *L. camara* to be associated with its physiological and ecological traits. For instance, the species have been reported to alter certain soil properties such as increasing phosphorous and carbon contents, to facilitate its proliferation (Ruwanza & Shackleton, 2016; Mhlongo et al., 2024). However, these alterations may not consistently support its dominance or expansion across all sites. *L. camara* exhibited random distribution in majority of the surveyed sites. The species also exhibited lower densities (1000 – 24000 Ind./ha.) across most sites, indicating that while it is widespread, it is less dominant compared to *A. adenophora*.

*S. jamaicensis*, meanwhile, had limited presence, with noticeable frequencies only in sites S – 16 (60 %), S – 20 (10 %), and S – 10 (60 %). *S. jamaicensis* thrives in tropical and sub–tropical regions, although it demonstrates stronger affinity towards

tropical ecosystem (Liew & Yong, 2016). This preference may account for its reduced prevalence in the study area, which falls within the subtropical zone highlighting its specific habitat preference. Nonetheless, its presence in certain sites within the study area indicate its ability to acclimatize to varied environmental factors despite its tropical inclination (Finch et al., 2021). *S. jamaicensis* exhibited moderate density (1000 – 8000 Ind./ha.) with relatively low TBA [S – 16 (7.31) > S – 10 (5.12) > S – 20 (0.32) m sq./ha.] and IVI ranging between 2.24 – 26.14, suggesting that while present, it does not significantly impact the overall vegetation structure.

IS, recognised for their extensive temperature tolerances, leverage daily temperature variations to exploit favourable environments while enduring sub–optimal ones (Finch et al., 2021). This versatility enables them to colonise varied habitats, allowing them to surpass less adaptable species (Waller et al., 2020). This biological invasion modifies essential nutrients and trophic interactions. Furthermore, IS are fast gaining resilience and proliferating as forest ecosystems have steadily deviated from their original state exhibiting alterations including modification in soil nutrients, reduced understory biomass, canopy gaps, etc (Mandal & Joshi, 2015; Knapp et al., 2023). Additionally, the disturbance regime in an area is a critical determinant influencing the success of IS (Davis et al., 2000). Habitats exposed to natural or anthropogenic disturbances are particularly susceptible to invasion (Jauni et al., 2014). The findings highlight that human–induced disturbances play a key role in facilitating the invasion of *A. adenophora* and *L. camara*, which proliferate in such environments. This trend is further evidenced by the contagious distribution of *S. jamaicensis*, which, despite its limited presence in other areas, displayed 60 % frequency in sites S–10 and S–16, both of which experience significant anthropogenic disturbances. IS in urban environments frequently develop characteristics that enhances their survival in human–altered ecosystems (Ansong & Pickering, 2014). Likewise, IS in agricultural areas have significant traits that enable their survival despite advancements in agricultural approaches (Grime, 2006). Consequently, this leads to the predominance of IS that are better adapted to survive and colonize in these habitats than their counterparts (Macchia & Benvenuti, 2003).

The swift proliferation of IS presents a considerable risk to native biodiversity. Its influence on global ecosystem is significant and multifaceted requiring management strategies with emphasis on utilization over elimination. This study effectively utilizes quantitative survey to identify hotspots of IS (typically regarded as an environmental waste) for efficient biomass collection. This approach promotes waste valorization as a potential means of IS management. The findings revealed notable distribution and abundance of IS across Kohima district. This is indicative of sufficient IS biomass availability for collection and utilization as envisioned in the present study.

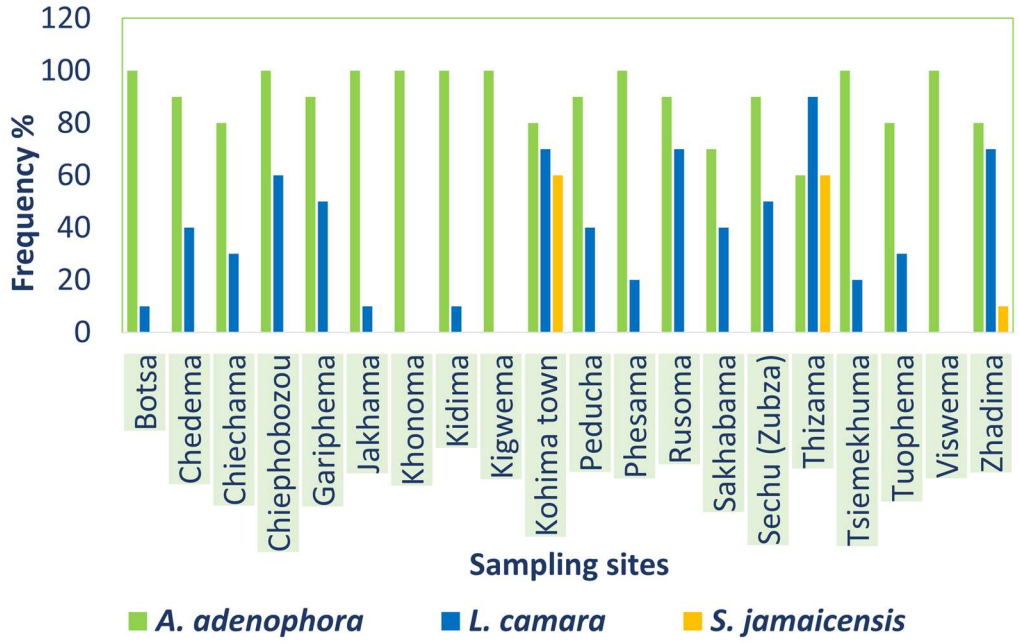


**Fig. 4.1.** Frequency of IS in Kohima district.

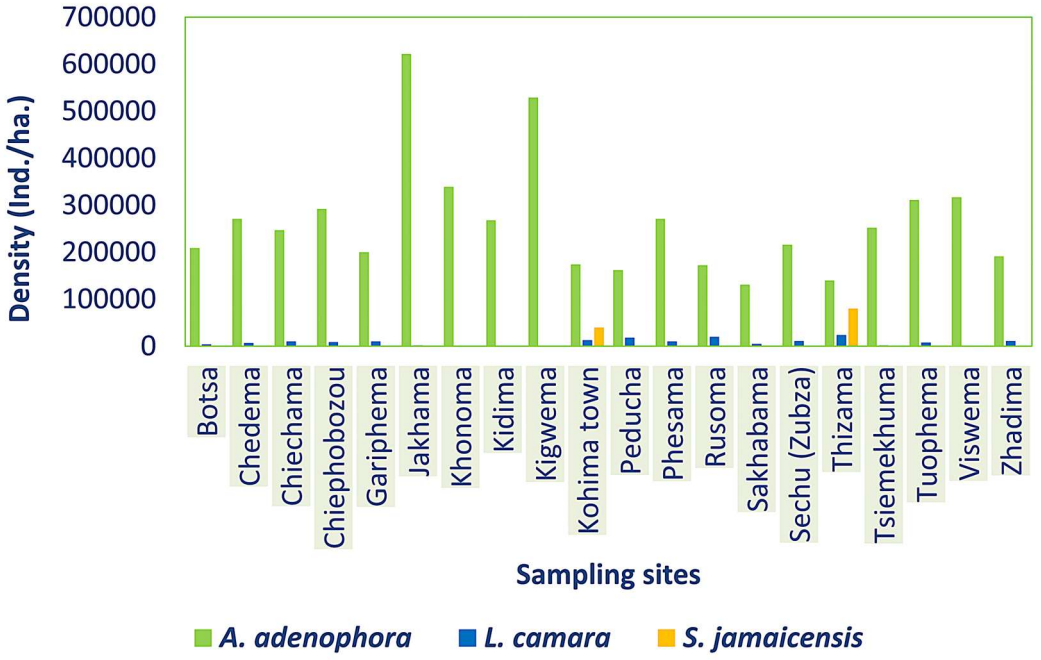


**Fig. 4.2.** Density of IS in Kohima district.

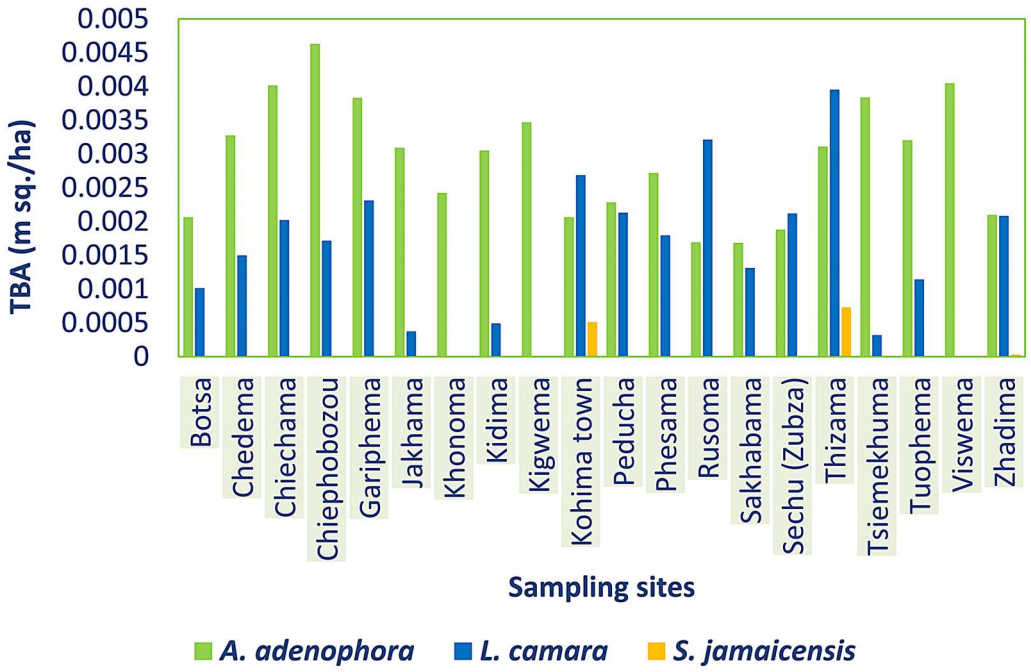


**Fig. 4.3.** Total basal area (TBA) of IS in Kohima district.

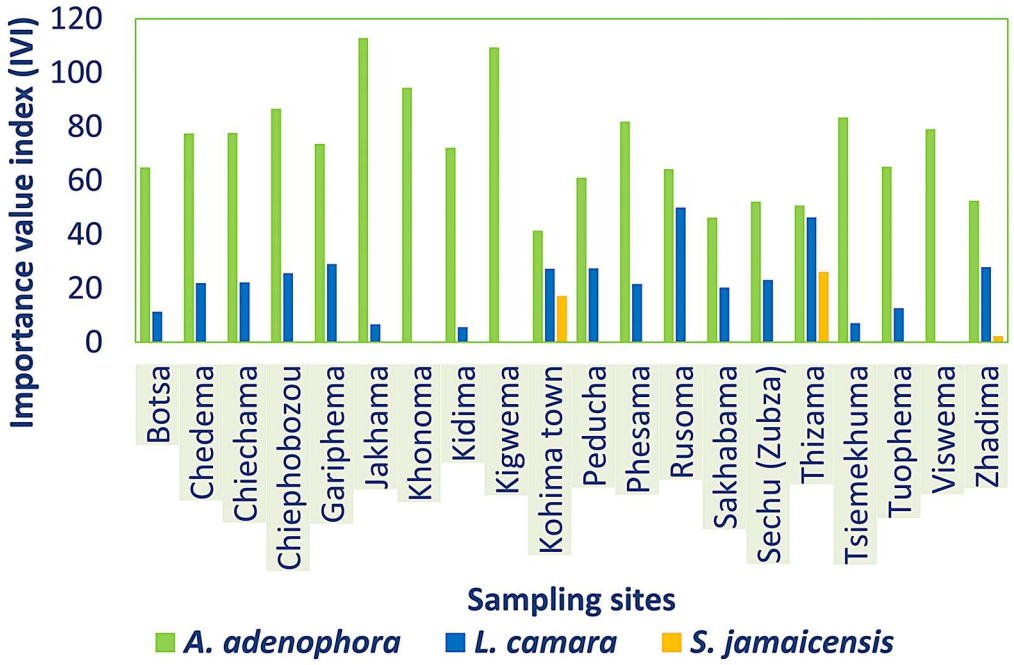


**Fig. 4.4.** Importance value index (IVI) of IS in Kohima district.

**Table 4.1.** Distribution of IS in study area.

| Sampling site code | Locations | *A. adenophora* | *L. camara* | *S. jamaicensis* |
|---|---|---|---|---|
| S – 1 | Botsa | Contagious | Contagious | – |
| S – 2 | Chedema | Contagious | Random | – |
| S – 3 | Chiechama | Contagious | Contagious | – |
| S – 4 | Chiephobozou | Contagious | Random | – |
| S – 5 | Gariphema | Contagious | Random | – |
| S – 6 | Jakhama | Contagious | Contagious | – |
| S – 7 | Khonoma | Contagious | – | – |
| S – 8 | Kidima | Contagious | Contagious | – |
| S – 9 | Kigwema | Contagious | – | – |
| S – 10 | Kohima town | Contagious | Random | Contagious |
| S – 11 | Peducha | Contagious | Contagious | – |
| S – 12 | Phesama | Contagious | Contagious | – |
| S – 13 | Rusoma | Contagious | Random | – |
| S – 14 | Sakhabama | Contagious | Random | – |
| S – 15 | Sechu (Zubza) | Contagious | Random | – |
| S – 16 | Thizama | Contagious | Random | Contagious |
| S – 17 | Tsiemekhuma | Contagious | Random | – |
| S – 18 | Tuophema | Contagious | Contagious | – |
| S – 19 | Viswema | Contagious | – | – |
| S – 20 | Zhadima | Contagious | Regular | Contagious |

## 4.3. Characterization of IS biomass, bio–oil and biochar

Biomass lies in the vanguard of bioenergy research. Numerous biomass feedstocks such as agricultural waste, forestry residues, bagasse, switchgrass, mosses, algae, ferns, IS etc. are rigorously investigated to be used as feedstock for bioenergy generation and subsequent biorefining. This interest is driven by growing concerns over carbon emission and fossil fuel depletion. Currently, biomass contributes approximately 14 % of the world's total energy consumption (Parikka, 2004). Its potential as a biofuel feedstock is largely determined by its inherent chemical and physical properties. Biomass properties such as calorific value, moisture content (MC), and other physico–chemical parameters directly influence the conversion efficiency and fuel yield (Azargohar et al., 2014). Accordingly, comprehensive biomass characterization forms the basis for selecting suitable conversion processes suited to the demands of biomass conversion technologies.

Table 4.2 furnishes the biomass properties of *A. adenophora*, *L. camara* and *S. jamaicensis* along with their average characteristic composition. MC is a key parameter influencing the conversion efficiency, product yield and its energy content. The link between MC and conversion technology is fairly straightforward. A low MC (< 15 %) is preferable for thermochemical conversion (Pandey & Kumar, 2020) with < 10 % threshold reported for efficient heat transfer during pyrolysis (Choudhury et al., 2014). On the contrary, high MC advocates for biochemical conversion (which rely on microbial activity). MC in *A. adenophora* (5.4 %), *L. camara* (4.67 %) and *S. jamaicensis* (4.9 %) were low indicating their biomass suitability for thermochemical conversion of pyrolysis. Ash content (AC) of biomass also plays a critical role as the alkalis in ash can catalyse undesirable cracking reactions during pyrolysis leading to reduced bio–oil yield (Oyebanji et al., 2017). Additionally, ash may potentially cause operational challenges such as slag formation at elevated temperatures, hence diminishing process efficiency and escalating economic costs (Nanda et al., 2012). The obtained low values of AC in *A. adenophora* (4.68 %), *L. camara* (4.15 %) and *S. jamaicensis* (4.43 %) biomasses are favourable and comparable to the value of 4.9 % reported by Onokwai et al. (2022) for invasive *Chromolaena odorata*. Volatile matter (VM) was relatively high for all the three species indicating their favourable thermal

reactivity. High proportion of VM coupled with low AC is known to significantly enhance the combustion characteristics and thermal degradation behaviour (Bordoloi et al., 2015). The VM (68.97 % for *A. adenophora*, 69.49 % for *L. camara* and 69.23 for *S. jamaicensis*) is in close proximity with previous investigations (Cai et al., 2017; Fernández et al., 2024). The FC:VM ratio (fuel ratio), signifies the combustion characteristics. Pattanayak et al. (2020) reported that a FC:VM ratio < 1.5 implies ease of combustion while > 1.5 implies difficulty during combustion. Accordingly, FC:VM ratio of 0.3 (for all three IS biomass), revealed its suitability for biofuel applications following effective combustion.

Ultimate analysis of biomass revealed high carbon (C) content of 44.47 % (*A. adenophora*), 45.74 % (*L. camara*) and 44.59 % (*S. jamaicensis*). The obtained C content supported the resultant GCV of 16.63 MJ/Kg (*A. adenophora*), 16.49 MJ/Kg (*L. camara*) and 17.06 MJ/Kg (*S. jamaicensis*). The biochemical (structural) composition of biomass revealed varying amounts of lignin, cellulose and hemicellulose along with minor proportion of extractives. The relative proportion of lignin and cellulose in IS biomass play a decisive role in determining their biofuel potential (McKendry, 2002). Owing to its appreciable heating value, lignin aids in enhancing the thermochemical conversion processes. However, it hinders biochemical conversion processes by inhibiting ethanol generation through phenolic lignin degradation products (Williams et al., 2015). Conversely, the polysaccharides (cellulose, hemicellulose and carbohydrate) in biomass are conducive for its efficient transformation into simple monomeric sugars via fermentation for bioethanol generation (Ho et al., 2011), while lipids transform into biodiesel via transesterification (Muh et al., 2019). The lignin, cellulose and hemicellulose content of *A. adenophora, L. camara* and *S. jamaicensis* biomass is furnished in Table 4.2. Excluding the hemicellulose content, the lignin and cellulose content in our study were in close proximity with Gonçalves et al. (2021). The lignin and cellulose content as reported by Gonçalves et al. (2021) on *Cyperus giganteus* was in the range 17.3 – 26.8 % and 27.8 – 32.6 %, respectively.

The fuel properties of bio–oils derived from *A. adenophora*, *L. camara* and *S. jamaicensis* biomass are furnished in Table 4.3. The bio–oil yields from the three IS

exceeded 30 % which is comparable to yields reported in previous findings (Reza et al., 2019; Fardi et al., 2023). Among the three IS, *A. adenophora* displayed higher bio–oil yield of 34.5 % and energy yield 69.87 %, suggesting its superior potential for liquid fuel production.

Density of bio–oil obtained from all three IS (1461 $kgm^{-3}$ for *A. adenophora*, 1150 $kgm^{-3}$ for *L. camara* and 1023 $kgm^{-3}$ for *S. jamaicensis*) were observed to be higher than that of commercial diesel (820 – 860 $kgm^{-3}$). This may be attributed to the presence of substantial quantities of O and water containing macromolecules including oligomeric phenolics, carboxylic acids, sugars, hydroxyketones and hydroxyaldehydes, which reduces the bio–oil's heating value in comparison to hydrocarbon fuels (Oasmaa & Czernik, 1999). Fuel viscosity significantly impacts the design and functioning of a fuel injection system, the quality of atomization and the resulting combustion characteristics (Lehto et al., 2013). The viscosity of the bio–oils (17.03 cSt for *A. adenophora*, 21.64 cSt for *L. camara* and 24.32 cSt for *S. jamaicensis*) were higher than that of diesel (2.0 – 4.5 cSt). This variation maybe based on the feedstock and its processing conditions.

Complete chemical characterization of bio–oil is challenging owing to the presence of pyrolytic lignin. Nevertheless, ultimate analysis, GCV, empirical formula, H/C and O/C molar ratio were determined. Ultimate analysis of bio–oil showed negligible difference between the three species. CHNO analysis revealed the carbon (C) rich composition of the three samples in the order: *A. adenophora* (68.42 %) > *S. jamaicensis* (65.58 %) > *L. camara* (64.95 %). Elemental analysis of bio–oils displayed reduced oxygen (O) contents that are comparatively lower than their original feedstock. These decrease in O contents is favourable since elevated O content is not conducive for generation of transportation fuel (Bordoloi et al., 2015). Furthermore, presence of O leads to reduced energy density, increased acidity, and immiscibility with hydrocarbon fuels (Czernik & Bridgwater, 2004). Elevated elemental C has been associated with elevated calorific value (Ahmed et al., 2018). The elevated GCV of bio–oils (33.7 MJ/Kg for *A. adenophora*, 30.99 MJ/Kg for *L. camara* and 30.18 MJ/Kg for *S. jamaicensis*) obtained can thus be attributed to its elevated C content endorsing their suitability for combustion and biofuel applications. The higher GCV

coupled with higher percentages of C and H and low O content in *A. adenophora* bio–oil corroborates its better fuel properties than *L. camara* and *S. jamaicensis* bio–oil. Findings in this study are in close proximity with the findings of Chen et al. (2019). The empirical formulae for *A. adenophora*, *L. camara* and *S. jamaicensis* bio–oil in this study were $C_{15.4}H_{25.5}NO_{2.86}$, $C_{15.03}H_{24.67}NO_{3.67}$ and $C_{18.83}H_{28.67}NO_{4.72}$, respectively.

H/C molar ratio in bio–oil was 1.65, 1.64 and 1.52 for *A. adenophora*, *L. camara* and *S. jamaicensis*, respectively and is comparable with the 1.86 H/C molar ratio of petroleum–sourced sulphur–free diesel as reported by Saikia et al. (2015). Combustion with low $CO_2$ emissions and high energy content of the fuel may be attributed to the elevated H/C ratio (Gopalakrishnan et al., 2019). Notably, bio–oil's C–rich profile endorses the potential of secondary treatment approaches to produce liquid fuels comparable to conventional fuels (diesel or petrol) (Özyuğuran & Yaman, 2017).

Furthermore, the properties of biochar obtained as co–product from pyrolysis of IS biomass is shown in Table 4.4. Notably, biochar from IS revealed reduced VM and high FC compared to the original biomass feedstock. The C content in the three IS biochar increased while the O level decreased when compared to their biomass. High C content of 52.09 % (*A. adenophora*), 56.06 % (*L. camara*) and 65.33 % (*S. jamaicensis*) is suggestive of their potential use as a soil amendment. Analogous to the trend observed for O, H content similarly decreased in biochar. Atomic H/C and O/C ratios serve as indicators of aromaticity and degree of carbonation in biochar. The decrease in these ratios in comparison to their respective feedstocks is likely attributed to processes such as decarbonylation, decarboxylation and dehydration (Kim et al., 2011). Additionally, the biochars exhibited higher GCV (20.71 MJ/Kg for *A. adenophora*, 20.12 MJ/Kg for *L. camara* and 25.26 MJ/Kg for *S. jamaicensis*), compared to their respective feedstocks. This increase is likely due to their lower H and O content relative to C. The GCV values align well with those reported by Nanda et al. (2012), who observed a range of 22 – 28 MJ/Kg for biochars. This increase in energy value is because C–C bonds contain more energy than C–O and C–H bonds. Although the total accessible energy within the biomass remains constant regardless of the conversion method used (pyrolysis, gasification, combustion, mechanical

extraction or fermentation); however, the form and quantity of energy recovered will vary depending on the various conversion processes employed (McKendry, 2002).

**Table 4.2.** Biomass properties of *A. adenophora*, *L. camara* and *S. jamaicensis*

| **Properties** | | ***A. adenophora*** | ***L. camara*** | ***S. jamaicensis*** |
|---|---|---|---|---|
| Gross calorific value (MJ/Kg) | | 16.63 | 16.49 | 17.06 |
| Net calorific value (MJ/Kg) | | 14.33 | 14.23 | 14.74 |
| Empirical formulae | | $C_{16.82}H_{28.45}NO_{13.14}$ | $C_{15.24}H_{26.44}NO_{11.04}$ | $C_{14.27}H_{25}NO_{10.88}$ |
| H/C molar ratio | | 1.69 | 1.73 | 1.75 |
| O/C molar ratio | | 0.78 | 0.72 | 0.76 |
| Ultimate analysis (%) | Carbon | 44.47 | 45.74 | 44.59 |
| | Hydrogen | 6.26 | 6.61 | 6.50 |
| | Nitrogen | 3.04 | 3.51 | 3.61 |
| | Oxygen (By difference) | 46.23 | 44.14 | 45.3 |
| Proximate analysis (%) | Moisture content | 5.4±1.2 | 4.67±0.3 | 4.9 ± 1.4 |
| | Ash content | 4.68±0.4 | 4.15±0.15 | 4.43 ± 0.8 |
| | Volatile matter | 68.97±0.9 | 69.49±0.2 | 69.23 ±0.18 |
| | Fixed carbon | 21.05 | 21.69 | 21.44 |
| Biochemical analysis (%) | Carbohydrate | 22.78±0.3 | 24.09±0.7 | 29.86 ± 0.4 |
| | Protein | 2.9±0.06 | 3±0.09 | 2.94 ± 0.2 |
| | Lipid content | 8.3±0.2 | 6.55±0.3 | 5.24 ± 0.03 |
| | Lignin | 20.9±0.4 | 19.9±0.4 | 20.4 ± 0.5 |
| | Cellulose | 40.62 | 41.37 | 41.01 |
| | Hemicellulose | 19.44±0.1 | 24.44±0.1 | 21.9 ± 1.2 |

**Table 4.3.** Fuel properties of *A. adenophora*, *L. camara* and *S. jamaicensis* bio–oil.

| **Properties** | | ***A. adenophora*** | ***L. camara*** | ***S. jamaicensis*** |
|---|---|---|---|---|
| Gross calorific value (MJ/Kg) | | 33.7 | 30.99 | 30.18 |
| Net calorific value (MJ/Kg) | | 31.62 | 29.04 | 28.35 |
| Mass yield (%) | | 34.5 | 32.71 | 31.8 |
| Energy yield (%) | | 69.87 | 62.58 | 56.25 |
| Density($kgm^{-3}$) | | 1461 at 30°C | 1150 at 30°C | 1023 at 30°C |
| Viscosity(cSt) | | 17.03 at 40°C | 21.64 at 40°C | 24.32 at 40°C |
| Empirical formulae | | $C_{15.4}H_{25.5}NO_{2.86}$ | $C_{15.03}H_{24.67}NO_{3.67}$ | $C_{18.83}H_{28.67}NO_{4.72}$ |
| H/C molar ratio | | 1.65 | 1.64 | 1.52 |
| O/C molar ratio | | 0.19 | 0.24 | 0.25 |
| Ultimate analysis (%) | Carbon | 68.42 | 64.95 | 65.58 |
| | Hydrogen | 9.44 | 8.88 | 8.31 |
| | Nitrogen | 5.2 | 5.09 | 4.15 |
| | Oxygen (By difference) | 16.94 | 21.08 | 21.96 |

**Table 4.4.** Properties of *A. adenophora*, *L. camara* and *S. jamaicensis* biochar.

| **Properties** | | ***A. adenophora*** | ***L. camara*** | ***S. jamaicensis*** |
|---|---|---|---|---|
| Gross calorific value (MJ/Kg) | | 20.71 | 20.12 | 25.26 |
| Net calorific value (MJ/Kg) | | 19.8 | 18.65 | 23.47 |
| Mass yield (%) | | 37.37 | 35.93 | 38.8 |
| Energy yield (%) | | 46.07 | 45.96 | 57.42 |
| Empirical formulae | | $C_{20.67}H_{4.74}NO_{12.48}$ | $C_{58.38}H_{68.37}NO_{29.13}$ | $C_{52.31}H_{54.44}NO_{17.12}$ |
| H/C molar ratio | | 0.71 | 1.17 | 1.04 |
| O/C molar ratio | | 0.6 | 0.5 | 0.33 |
| Ultimate analysis (%) | Carbon | 52.09 | 56.06 | 65.33 |
| | Hydrogen | 3.1 | 5.47 | 5.66 |
| | Nitrogen | 2.88 | 1.14 | 1.46 |
| | Oxygen (By difference) | 41.93 | 37.33 | 27.55 |
| Proximate analysis (%) | Moisture content | 1.2 ± 0.4 | 1.3 ± 0.2 | 1.8 ± 0.3 |
| | Ash content | 19 ± 0.6 | 18 ± 0.12 | 17.4 ± 0.3 |
| | Volatile matter | 18.4 ± 0.15 | 16.4 ± 0.15 | 16.3 ± 0.22 |
| | Fixed carbon | 61.4 | 64.3 | 64.5 |

## 4.4. Fourier Transformed Infrared Spectroscopy (FTIR) analysis

FTIR analyses was conducted to identify the functional groups present in the biomass and the resulting bio–oil of *A. adenophora*, *L. camara* and *S. jamaicensis*. This analysis revealed the structural transformation that occurred during pyrolysis of the three IS. The biomass spectra exhibited characteristic peaks corresponding to functional groups associated with key structural components (lignin, cellulose and hemicellulose). The peaks associated with bio–oil showed evidence of depolymerization of the structural components. Notably, all three IS exhibited similar patterns for both biomass and bio–oil. The analyses highlighted the common functional groups across all samples, primarily O–H group, aliphatic C–H, carbonyl (C=O), ether (C–O–C), and aromatic (C=C) bonds. Despite this overall similarity, species–specific variations in peak intensity, breadth, and presence reflect differing thermal decomposition behaviours. Fig. 4.5 illustrates the FTIR spectra of the IS biomass and Fig. 4.6 displays the FTIR spectra of the IS bio–oil. The identified functional groups are listed in Table 4.5 for biomass and Table 4.6 for bio–oil.

Broad transmittance % for biomass was observed in the region between 3800 – 3170 $cm^{-1}$ (*A. adenophora*), 3701 – 3066 $cm^{-1}$ (*L. camara*) and 3691 – 3201 $cm^{-1}$ (*S. jamaicensis*). This is indicative of hydroxyl groups engaged in polymeric structures and correspond to bonded O–H stretching vibration typically found in carbohydrates (holocellulose) and lignin (Bilba et al., 2007). Absorbance peaks from 2951 – 2851 $cm^{-1}$ in *A. adenophora*, 2996 – 2829 $cm^{-1}$ in *L. camara* and 2951 – 2916 $cm^{-1}$ in *S. jamaicensis* biomass are linked to the presence of lipids, particularly $CH_2$ asymmetric stretching typical of lipids (Romero–Anaya et al., 2011). Peaks observed between 1683 – 1530 $cm^{-1}$, 1705 – 1506 $cm^{-1}$ and 1650 – 1615 $cm^{-1}$ in *A. adenophora*, *L. camara* and *S. jamaicensis*, respectively, represent a blend of vibrational modes including stretching of carbonyl (C=O) in hemicellulose, absorbed water deformation vibrations (H-O-H bending) and stretching vibration of aromatics (C=C) (Zhuang et al., 2020). Lignin exhibits aromatic skeletal vibration (C=C) within this range (Kumar et al., 2024). C–H deformation vibration in the region 1450 – 1360 $cm^{-1}$ (*A. adenophora*), 1485 – 1353 $cm^{-1}$ (*L. camara*) and 1458 – 1387 $cm^{-1}$ (*S. jamaicensis*)

indicates presence of terminal $CH_3$ group (Silverstein et al., 2015) while those at 1277 – 1231 $cm^{-1}$, 1322 – 1216 $cm^{-1}$ and 1285 – 1239 $cm^{-1}$ for *A. adenophora*, *L. camara* and *S. jamaicensis*, respectively, signifies the existence of C-O-C ether linkages in cellulose (Cheng et al., 2019). Absorptions in region 1060 – 960 $cm^{-1}$ (*A. adenophora*), 1190 – 933 $cm^{-1}$ (*L. camara*) and 1165 - 970 $cm^{-1}$ (*S. jamaicensis*) are associated to stretching vibrations of C–O, C–O–C, C–C and C–O–P, primarily linked with polysaccharides (Pavia et al. 2015) along with $CH_2$ and $CH_3$ rocking modes (Wolpert & Hellwig, 2006). Peaks from 771 – 592 $cm^{-1}$, 687 – 526 $cm^{-1}$ and 827 – 572 $cm^{-1}$ for *A. adenophora*, *L. camara* and *S. jamaicensis*, respectively, are linked to aromatic rings C=C stretching (Pavia et al. 2015).

The weak absorbance of peaks in range 3800 – 3100 $cm^{-1}$, 3699 – 3093 and 3368 – 3201 for *A. adenophora*, *L. camara* and *S. jamaicensis* bio-oils, respectively, in comparison to biomass indicates depolymerization of cellulose, hemicellulose and lignin during the conversion processes (Lu et al., 2009). This range corresponds to alcohols and phenols in bio–oil representing intramolecular hydrogen bond (Saikia et al., 2015). A slight difference in *L. camara* bio–oil is the presence of a specific peak between 2991 – 2823 $cm^{-1}$. This is attributed to the retention of C–H aliphatic in the bio–oil (Saikia et al., 2015). The aliphatics in this region are indicative of saturated hydrocarbons, contributing towards the bio–oil's energy and combustion characteristics (Lachos–Perez et al., 2023). Absorbance from 1760 – 1510 (*A. adenophora*), 1701 – 1542 $cm^{-1}$ (*L. camara*) and 1640 – 1615 (*S. jamaicensis*) represents C=O stretching vibrations signifies the presence of conjugated systems such as aldehyde, quinone, ketone groups, etc. and C=C stretching vibrations indicating the existence of aromatics and alkenes (Ogunkanmi et al., 2018). C–H deformation of $CH_3$ group remains visible in peaks within 1460 – 1340 $cm^{-1}$, 1487 – 1324 $cm^{-1}$and 1448 – 1387 $cm^{-1}$ for *A. adenophora*, *L. camara* and *S. jamaicensis* bio-oils, respectively (Silverstein et al., 2015). C–O vibrations indicating the presence of carbonyl groups (alcohols, esters, carboxylic acids, and ethers) are observed within the range (Ogunkanmi et al., 2018). Additionally, the weakened peaks in the regions 1050 – 930 $cm^{-1}$ (*A. adenophora*), 1050 – 963 $cm^{-1}$ (*L. camara*) and 1165–970 $cm^{-1}$ (*S. jamaicensis*) reflect the presence of aliphatic and alcohol–based C–O bonds formed

during the pyrolytic conversion of the biomass (Pavia et al., 2015). Furthermore, absorption in the range 780 – 590 $cm^{-1}$, 783 – 542 $cm^{-1}$ and 681 - 542 $cm^{-1}$ for *A. adenophora*, *L. camara* and *S. jamaicensis* bio-oils, respectively, maybe attributed to single, polycyclic and branched aromatics (Özçimen & Ersoy-Meriçboyu, 2010). Notably, there is weak absorbance of peaks in bio-oil when compared with biomass spectra. This may be attributed to the breakdown of organic structures, originally present in biomass, into oxygenates in bio-oil.

An intriguing aspect of bio–oil lies in its composition, which includes oxygenated functional groups such as O–H, C=O, C–O, etc. and aromatic compounds. These compounds make the bio–oil highly oxygenated, reduce the heating value, and heighten corrosiveness in bio–oils. Moreover, the bio–oil's potential to function as an energy source is often enhanced by the inclusion of hydrocarbons (C=C, C–H) (Saikia et al., 2015). Studies performed by Kumar et al. (2024), Zhou et al. (2021), Ogunkanmi et al. (2018) and Ayaa et al. (2022) revealed the presence of similar functional groups (such as alcohols, phenols, aliphatics, aromatics, esters, ethers, alkanes, alkenes, ketones, aldehydes, etc.) showcasing their candidature as a bioenergy and chemical feedstock potential. The study showcased bio–oil's candidature as a bioenergy and chemical feedstock potential.

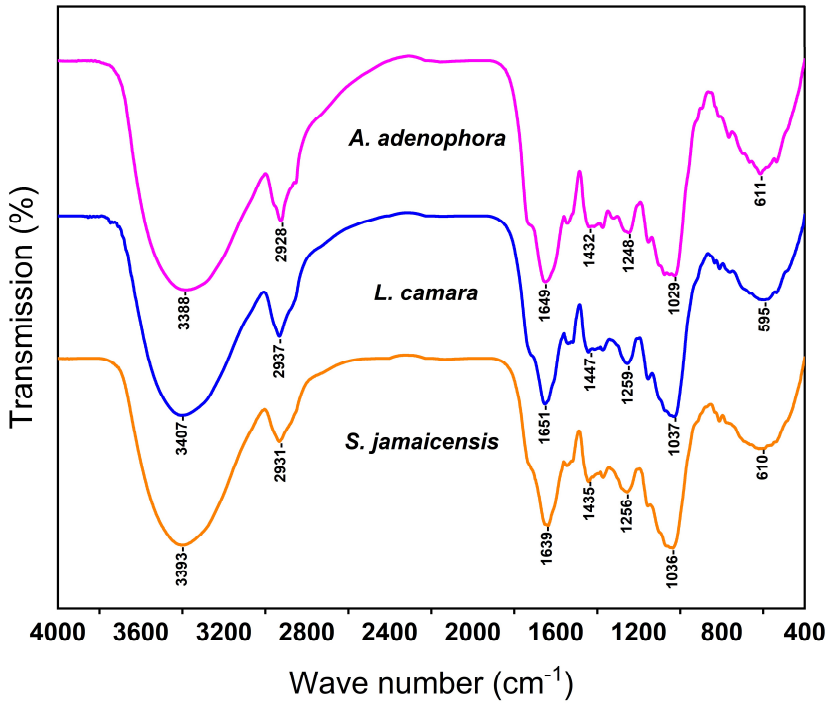


**Fig. 4.5.** FTIR spectra of *A. adenophora, L. camara and S. jamaicensis* biomass.

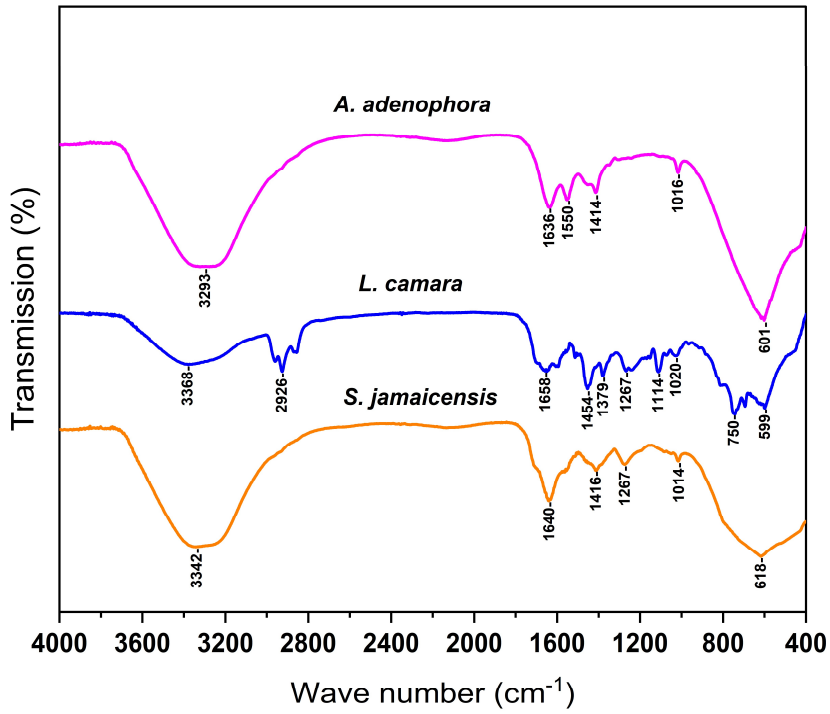


**Fig. 4.6.** FTIR spectra of *A. adenophora, L. camara and S. jamaicensis* bio–oil.

**Table 4.5.** Functional group identified by FTIR spectroscopy in IS biomass.

| Wave number ($cm^{-1}$) | | | Functional group assignment | Compound class |
|---|---|---|---|---|
| ***A. adenophora*** | ***L. camara*** | ***S. jamaicensis*** | | |
| 3800 – 3170 | 3701 – 3066 | 3691 – 3201 | O–H stretching vibration | Carbohydrates |
| 2951 – 2851 | 2996 – 2829 | 2951 – 2916 | C–H stretching vibration | Lipids |
| 1683 – 1530 | 1705 – 1506 | 1650 – 1615 | Stretching of C=O, C=C, H–O–H deformation | Carbonyl group, Alkenes and Aromatics |
| 1450 – 1360 | 1485 – 1353 | 1458 – 1387 | C–H deformation | Methyl group |
| 1277 – 1231 | 1322 – 1216 | 1285 – 1239 | C–O–C stretching | Alcohol and Phenol |
| 1060 – 960 | 1190 – 933 | 1165 – 970 | C–O, C–O–C, C–O–P stretching | Polysaccharides |
| 771 – 592 | 687 – 526 | 827 – 572 | C=C stretching | Aromatic rings |

**Table 4.6.** Functional group identified by FTIR spectroscopy in IS bio–oil.

| Wave number ($cm^{-1}$) | | | Functional group assignment | Compound class |
|---|---|---|---|---|
| ***A. adenophora*** | ***L. camara*** | ***S. jamaicensis*** | | |
| 3800 – 3100 | 3699 – 3093 | 3368 – 3201 | O–H stretching vibration | Alcohol and Phenol |
| – | 2991 – 2823 | – | C–H stretching vibration | Aliphatics |
| 1760 – 1510 | 1701 – 1542 | 1640 – 1615 | C=O, C=C stretching vibrations | Aromatics and Alkenes |
| 1460 – 1340 | 1487 – 1324 | 1448 – 1387 | C–H deformation | Methyl group and Alkanes |
| 1300 – 1080 | 1305 – 1067 | 1285 – 1239 | C–O vibration | Carbonyl groups |
| 1050 – 930 | 1050 – 963 | 1165 – 970 | C–O stretching | Aliphatic ethers and Alcohol |
| 780 – 590 | 783 – 542 | 681 – 542 | C=C stretching | Aromatic rings |

## 4.5. Thermogravimetric Analysis (TGA)

TGA was performed to study the degradation profile of *A. adenophora*, *L. camara* and *S. jamaicensis* biomass. The analysis was conducted at two varying heating rates (10 °C/min and 30 °C/min). The degradation profile revealed three distinct stages of weight loss from ambient temperature to 700 °C. The initial weight loss (first stage) is associated with moisture evaporation and loss of light volatiles. This was followed by the devolatization of biomass (second stage) where maximum weight loss occurred. These stages of initial weight loss and devolatization of biomass is designated as the zone of active pyrolysis. Following this, is the third zone, designated as the zone of passive pyrolysis and primarily characterized by continual and slow lignin degradation (Kumar et al., 2024). Minimal mass loss is evident beyond this zone continuing up to 700 °C, indicating the conclusion of biomass combustion with subsequent reactions involving the char. The findings evident from TG–DTG analysis of *A. adenophora*, *L. camara* and *S. jamaicensis* biomass are presented below, displaying the thermal degradation stages along with the corresponding heating rates

(a) *A. adenophora* biomass (Fig. 4.7)

*First stage*: From ambient to 130 °C and 160 °C for 10 °C/min and 30 °C/min heating rate, respectively

*Second stage*: From 175 – 480 °C and 190 – 500 °C for 10 °C/min and 30 °C/min, respectively with maximum mass loss of 50 % and 56.68 % for 10 °C/min and 30 °C/min heating rate, respectively

Temperature ranges 130 – 480 °C and 160 – 500 °C for 10 °C/min and 30 °C/min, respectively (designated as the zone of active pyrolysis)

*Third stage*: Beyond 480 °C and 500 °C/min for 10 °C/min and 30 °C/min, respectively (designated as the zone of passive pyrolysis)

(b) *L. camara* biomass (Fig. 4.8)

*First stage*: From ambient to 120 °C and 170 °C for 10 °C/min and 30 °C/min heating rate, respectively

*Second stage*: From 170 – 490 °C and 220 – 540 °C for 10 °C/min and 30 °C/min, respectively

Temperature ranges 120 – 490 °C and 170 – 540 °C for 10 °C/min and 30 °C/min, respectively (designated as the zone of active pyrolysis) with maximum mass loss of 51.77 % and 53.53 % for 10 °C/min and 30 °C/min heating rate, respectively

*Third stage*: Beyond 490 °C and 540 °C/min for 10 °C/min and 30 °C/min, respectively (designated as the zone of passive pyrolysis)

(c) *S. jamaicensis* biomass (Fig. 4.9)

*First stage*: From ambient to 120 °C and 170 °C for 10 °C/min and 30 °C/min heating rate, respectively

*Second stage*: From 160 – 490 °C and 195 – 550 °C for 10 °C/min and 30 °C/min, respectively with maximum mass loss of 49.65 % and 50.24 % for 10 °C/min and 30 °C/min heating rate, respectively

Temperature ranges 120 – 490 °C and 170 – 550 °C for 10 °C/min and 30 °C/min, respectively (designated as the zone of active pyrolysis)

*Third stage*: Beyond 490 °C and 550 °C/min for 10 °C/min and 30 °C/min, respectively (designated as the zone of passive pyrolysis)

It is noteworthy that both the pyrolysis zones (active and passive) shift to higher temperature ranges with rise in heating rate (Slopiecka et al., 2012). With an increase in heating rate, the rate of devolatization also increases. A higher heating rate simultaneously promotes a swift reaction, leading to an elevated peak temperature owing to acceleration in the breakdown of bonds in the investigated samples (Chong et al., 2019). As numerous reactions occurred in a condensed timeframe, DTG peak evidently rose with higher heating rate (30 °C/min), leading to a swift decline in the initial mass of feedstock. However, the peak reaction rate declines as biomass undergoes gradual decomposition over a wider temperature range (Zhang et al., 2019). Gašparovič et al. (2010) conducted a comparable study that focused on thermogravimetric pyrolysis of wood and its constituents. The study identified three distinct stages: water evaporation, zones of active and passive pyrolysis. Lignin degradation was apparent in both the zones while zone of active pyrolysis predominantly involved degradation of hemicellulose and cellulose. Hu et al. (2016) reported that lignin breakdown occurred from 160 – 900 °C temperature range.

Nonetheless, this degradation occurs at a gradual rate in comparison to holocellulose break down. Furthermore, the findings of this study are consistent with those reported by Zapata et al. (2019) who reported that at temperature range from 200 – 260 °C, hemicellulose decomposition produces less char and more volatiles in comparison to cellulose. Findings with similar devolatization with various feedstocks have been reported by Chong et al. (2019), Lu et al. (2021), Kumar et al. (2024). *A. adenophora*, *L. camara* and *S. jamaicensis* biomass with their short thermal degradation profile make them promising feedstocks for thermochemical conversion processes.

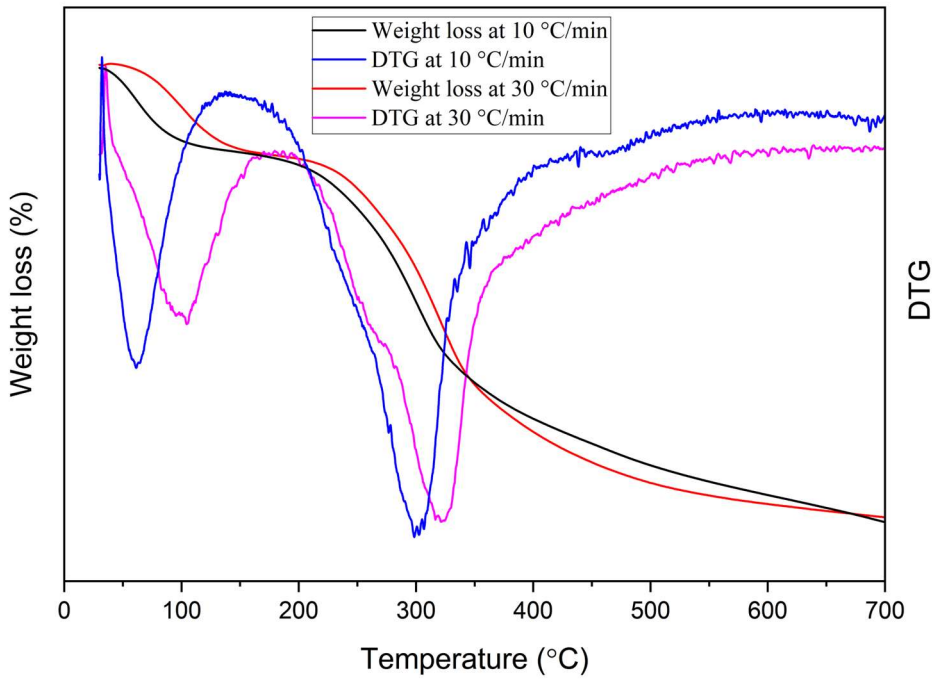


**Fig. 4.7.** TG–DTG profile of *A. adenophora* biomass at heating rates 10 °C and 30 °C/min.

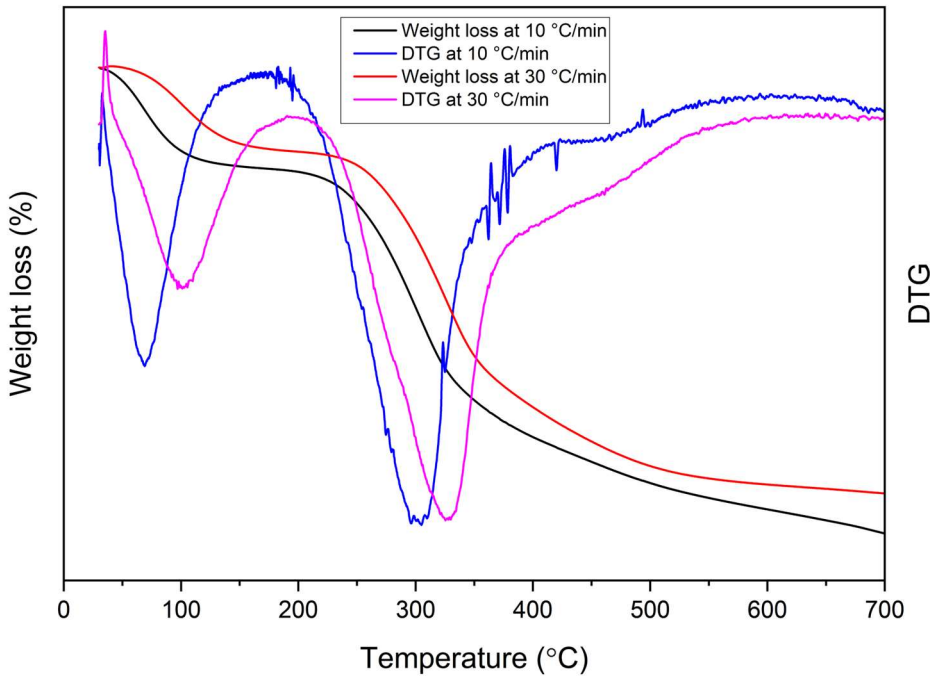


**Fig. 4.8.** TG–DTG profile of *L. camara* biomass at heating rates 10 °C and 30 °C/min.

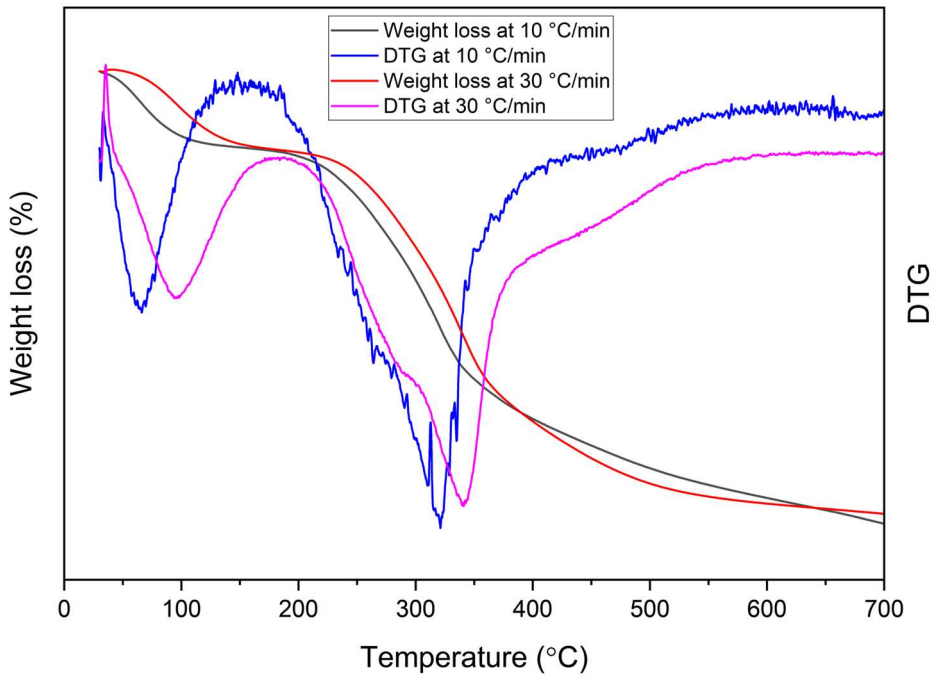


**Fig. 4.9.** TG–DTG profile of *S. jamaicensis* biomass at heating rates 10 °C and 30 °C/min.

## 4.6. Gas Chromatography–Mass Spectroscopy (GC–MS) analysis

GC–MS analysis was performed to identify the chemical compounds in the bio–oil of *A. adenophora*, *L. camara* and *S. jamaicensis*. The GC–MS analysis of bio–oil does not serve as a definitive test for compounds. Nonetheless, it provides valuable insight into the most probable compounds utilizing standard library. In the present study, mass spectra of identified compounds were matched with those listed in NIST library. The identification and characterization of compounds detected was based on GC retention time.

GC–MS analysis of *A. adenophora* bio–oil revealed the existence of organic compounds ranging from $C_5$ – $C_{37}$. Table 4.7 presents the details of compounds identified along with retention time, area (%), chemical formula and molecular weight. The TIC of the *A. adenophora* bio–oil is provided in Fig. 4.10. The compounds detected comprised of branched/long chains, aldehydes, esters, cycloalkenes, phenols, hydrocarbons, N–containing compounds, various aromatics, mixed acids, ketones and sugars. The major chemical components identified were acids and phenols. Acids such as Methylenecyclopropanecarboxylic acid (8.82 %), Phosphonic acid, (p–hydroxyphenyl)– (6.75 %), 5–Clorovaleric acid, 2–dimethylaminoethyl ester (4.85 %) constituted major portions of the bio–oil. Phenols such as Phenol, 2–methoxy– (1.20 %), Phenol, 2,6–dimethoxy (1.14 %) and Phenol, 3–methyl– (1.05 %) represented significant fractions of the bio–oil.

Compounds detected for *L. camara* bio–oil ranged from $C_6$ – $C_{37}$ indicating a complex blend of chemical composition. This composed primarily of branched/long chains hydrocarbon, esters, phenols, N–containing compounds and various aromatics (Table 4.8). The TIC of the *L. camara* bio–oil is displayed in Fig. 4.11. Toluene (5.96 %) represented the most abundant compound in *L. camara* bio–oil followed by Phosphonic acid, (p–hydroxyphenyl)– (3.68 %), Phenol, 3–ethyl– (2.99 %) and Phenol, 3–methyl– (2.93 %).

The organic compounds detected in *S. jamaicensis* bio–oil are presented in Table 4.9. The TIC of the *S. jamaicensis* bio–oil is shown in Fig. 4.12. The compounds

detected displayed C–chain lengths varying from $C_5$ – $C_{37}$. The compounds detected comprised of branched/long chains, ketones, sulfoxide derivatives, aromatics, hydrocarbon, mixed acids, ester derivatives, cyclopentenone, phenols, and sugars. Sugar–derived compound such as 1,4:3,6–Dianhydro–.alpha.–d–glucopyranose accounted for 6.18% of total identified compounds. Phenol, 2,6–dimethoxy– (lignin–derived phenolic compound) represented 4.92 %, Methylenecyclopropanecarboxylic acid (a carboxylic acid derivative) accounted for 3.61 % while 2–Ethyly–5–propylcyclopentanone (a ketone compound) made up 2.86 % among the major constituents in bio–oil.

The compounds identified indicated a highly intricate mixture of chemical composition of bio–oil. This is also evident from FTIR and NMR analyses. Majority of the compounds detected in the bio–oil from all three species, predominantly stems from lignin and holocellulose degradation during thermal conversion. For instance, the occurrence of esters is attributed to holocellulose decomposition (Li et al., 2017) while degradation of lignin with impurities in water fosters an increased proportion of phenols (Bhattacharjee & Biswas, 2018). Thermal breakdown of lignin leads to the formation of aromatic compounds including hydrocarbons while breakdown of cellulose, a polymer of glucose, is frequently associated with sugar derivatives evident in bio–oil (Alvarez–Chavez et al., 2019). Furthermore, the dehydration and aromatization of holocellulose structural units aid in the production of oxygenates and aromatic compounds (Gollakota & Savage, 2018). These findings are in close proximity with the findings of Cheng et al. (2019), Sugumaran et al. (2017), Alagöz et al. (2023) and Suraiya et al. (2023). The detection of hydrocarbons including aliphatic, aromatic, and oxygenates highlights the potential of bio–oils to be used as a potential chemical feedstock.

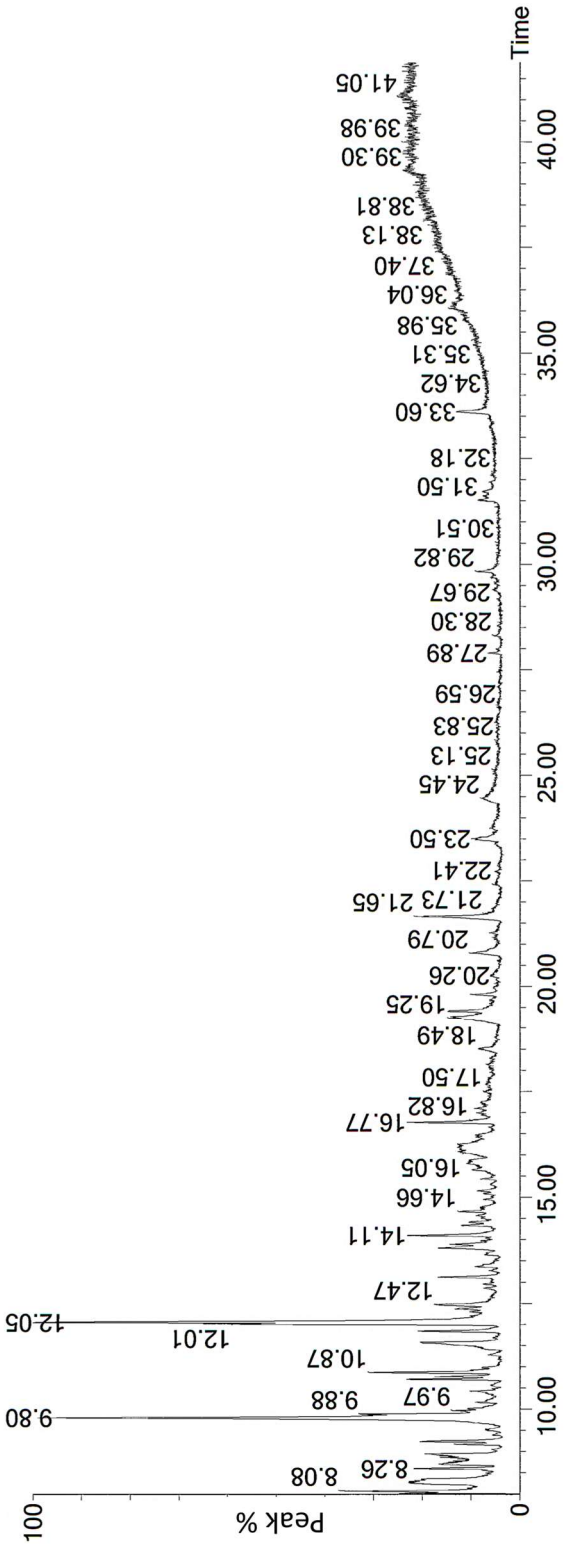


**Fig. 4.10.** TIC of *A. adenophora* bio–oil.

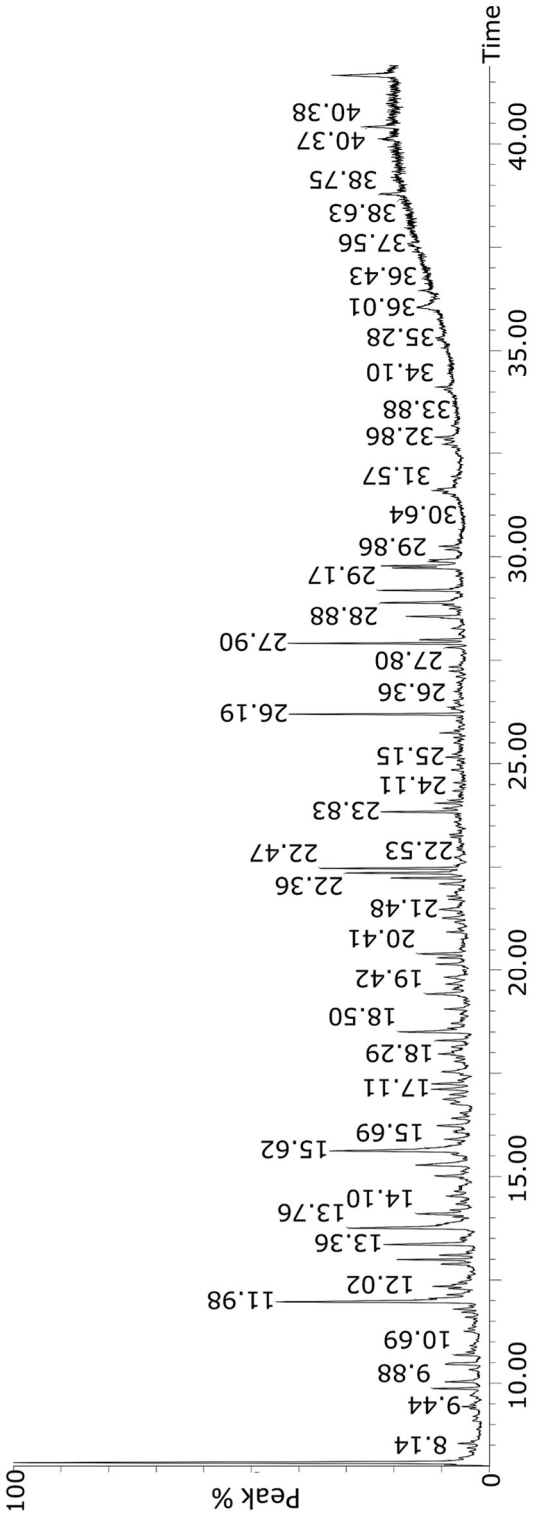


**Fig. 4.11.** TIC of *L. camara* bio–oil.

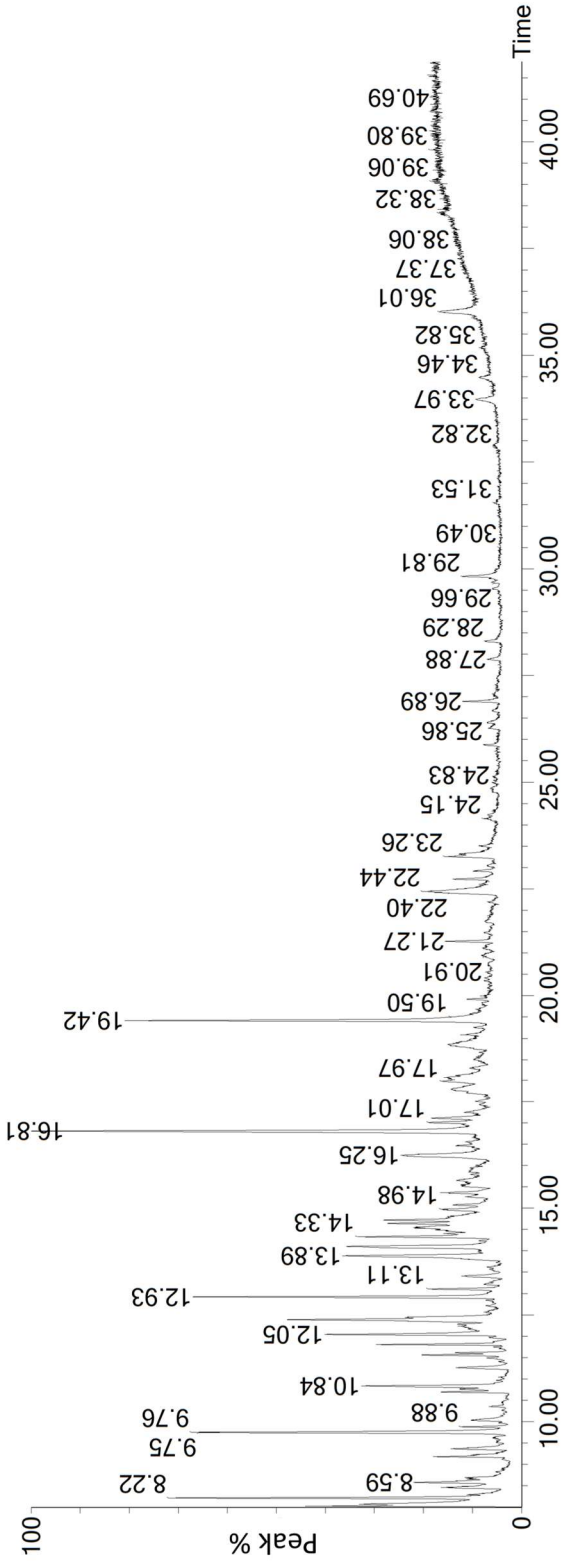


**Fig. 4.12.** TIC of *S. jamaicensis* bio–oil.

**Table 4.7.** Chemical compounds in *A. adenophora* bio–oil.

| Sl. No | Retention time | Area (%) | Compounds detected | Chemical formula |
|---|---|---|---|---|
| 1 | 8.08 | 3.06 | Spiro[2,4]hepta–4,6–diene | $C_7H_8$ |
| 2 | 8.30 | 4.85 | 5–Clorovaleric acid, 2–dimethylaminoethyl ester | $C_9H_{18}ClNO_2$ |
| 3 | 9.80 | 8.82 | Methylenecyclopropanecarboxylic acid | $C_5H_6O_2$ |
| 4 | 9.89 | 1.16 | .beta.–L–Arabinopyranoside, methyl | $C_6H_{12}O_5$ |
| 5 | 9.97 | 0.44 | Butanoic acid, 2–methyl– | $C_5H_{10}O_2$ |
| 6 | 10.71 | 0.75 | 2–Cyclopenten–1–one, 2–methyl– | $C_6H_8O$ |
| 7 | 10.87 | 1.38 | Clofexamide | $C_{14}H_{21}ClN_2O_2$ |
| 8 | 12.05 | 6.75 | Phosphonic acid, (p–hydroxyphenyl)– | $C_6H_7O_4P$ |
| 9 | 12.48 | 0.82 | 2,4,6–Cycloheptatrien–1–one, 2–hydroxy– | $C_7H_6O_2$ |
| 10 | 13.12 | 0.74 | Cyclopentene, 1–(1–methylethyl)– | $C_8H_{14}$ |
| 11 | 13.81 | 1.05 | Phenol, 3–methyl– | $C_7H_8O$ |
| 12 | 14.11 | 1.20 | Phenol, 2–methoxy– | $C_7H_8O_2$ |
| 13 | 14.66 | 0.54 | 1,2–Cyclobutanedicarboxylic acid, cis– | $C_6H_8O_4$ |
| 14 | 16.18 | 2.27 | Trans,cis–1,8–dimethylspiro[4.5]decane | $C_{12}H_{22}$ |
| 15 | 16.77 | 1.52 | 1,4:3,6–Dianhydro–.alpha.–d–glucopyranose | $C_6H_8O_4$ |
| 16 | 18.51 | 0.58 | Indole | $C_8H_7N$ |
| 17 | 19.41 | 1.14 | Phenol, 2,6–dimethoxy | $C_8H_{10}O_3$ |
| 18 | 19.81 | 0.39 | Boraneamine, n–ethyl–1,1–dipropyl– | $C_8H_{20}BN$ |
| 19 | 20.79 | 0.93 | Pyrimidine–2,4(1H,3H)–dione, 1–(5–aminomethyl–2–tetrahydrofuryl)–5–methyl | $C_{10}H_{15}N_3O_3$ |

| | | | | |
|---|---|---|---|---|
| 20 | 21.65 | 1.94 | Furaltadone | $C_{13}H_{16}N_4O_6$ |
| 21 | 23.50 | 0.97 | Morpholine, 4–octadecyl– | $C_{22}H_{45}NO$ |
| 22 | 24.46 | 0.70 | Cyclopentanecarboxylic acid, 3,3–dimethyl–4–oxo– | $C_8H_{12}O_3$ |
| 23 | 29.82 | 0.71 | Z,Z–6,28–Heptatriactontadien–2–one | $C_{37}H_{70}O$ |
| 24 | 33.60 | 0.86 | 5,6,7,4'–Tetramethoxyflavanone | $C_{19}H_{20}O_6$ |

**Table 4.8.** Chemical compounds in *L. camara* bio–oil.

| Sl. No. | Retention time | Area (%) | Compounds detected | Chemical formula |
|---|---|---|---|---|
| 1 | 8.09 | 5.96 | Toluene | $C_7H_8$ |
| 2 | 9.88 | 0.48 | Ethylbenzene | $C_8H_{10}$ |
| 3 | 10.47 | 0.62 | 2–Phenethyl–.beta.–phenylpropionate | $C_{17}H_{18}O_2$ |
| 4 | 11.98 | 3.68 | Phosphonic acid, (p–hydroxyphenyl)– | $C_6H_7O_4P$ |
| 5 | 12.35 | 0.68 | Mesitylene | $C_9H_{12}$ |
| 6 | 13.00 | 0.75 | D–limonene | $C_{10}H_{16}$ |
| 7 | 13.36 | 1.43 | Phenol, 2–methyl– | $C_7H_8O$ |
| 8 | 13.76 | 2.93 | Phenol, 3–methyl– | $C_7H_8O$ |
| 9 | 14.10 | 0.86 | Formic acid, 2–methoxyphenyl ester | $C_8H_8O_3$ |
| 10 | 15.28 | 1.11 | Phenol, 2,3–dimethyl– | $C_8H_{10}O$ |
| 11 | 15.62 | 2.99 | Phenol, 3–ethyl– | $C_8H_{10}O$ |
| 12 | 16.23 | 0.69 | Fumaric acid, 3,4–dimethylphenyl octyl ester | $C_{20}H_{28}O_4$ |
| 13 | 17.11 | 0.55 | Phenol, 4–ethyl–2–methyl– | $C_9H_{12}O$ |
| 14 | 17.53 | 0.62 | Phenol, 3–propyl– | $C_9H_{12}O$ |
| 15 | 18.29 | 0.41 | 6–Methylheptyl 2–methylbutanoate | $C_{13}H_{26}O_2$ |
| 16 | 18.50 | 1.14 | Indole | $C_8H_7N$ |
| 17 | 19.42 | 0.60 | Phenol, 2,6–dimethoxy– | $C_8H_{10}O_3$ |
| 18 | 20.17 | 0.38 | 3–n–Hexylthiolane, S,S–dioxide | $C_{10}H_{20}O_2S$ |
| 19 | 20.41 | 0.57 | Indolizine, 7–methyl– | $C_9H_9N$ |
| 20 | 22.24 | 0.78 | Hentriacontane | $C_{31}H_{64}$ |
| 21 | 22.36 | 1.33 | Benzene, 4–ethenyl–1,2–dimethyl– | $C_{10}H_{12}$ |
| 22 | 22.47 | 1.32 | Butylated hydroxytoluene | $C_{15}H_{24}O$ |
| 23 | 23.84 | 0.81 | Naphthalene, 1,4,6–trimethyl– | $C_{13}H_{14}$ |
| 24 | 26.19 | 1.66 | 1R,2c,3t,4t–Tetramethyl–cyclohexane | $C_{10}H_{20}$ |
| 25 | 27.90 | 1.56 | Neophytadiene | $C_{20}H_{38}$ |
| 26 | 28.88 | 1.19 | Z–28–Heptatriaconten–2–one | $C_{37}H_{72}O$ |
| 27 | 29.17 | 0.88 | Methyl 11–methyl–dodecanoate | $C_{14}H_{28}O2$ |
| 28 | 29.71 | 0.64 | 9,12–Octadecadienoic acid (z,z)– | $C_{18}H_{32}O_2$ |
| 29 | 29.76 | 0.75 | Z,Z–6,28–Heptatriactontadien–2–one | $C_{37}H_{70}O$ |

| | | | | |
|---|---|---|---|---|
| 30 | 38.75 | 1.02 | Cyclotrisiloxane, hexamethyl– | $C_6H_{18}O_3Si_3$ |
| 31 | 41.62 | 1.27 | Eicosyl isopropyl ether | $C_{23}H_{48}O$ |

**Table 4.9.** Chemical compounds in *S. jamaicensis* bio–oil.

| Sl. No | Retention time | Area (%) | Compounds detected | Chemical formula |
|---|---|---|---|---|
| 1 | 8.22 | 2.47 | Trifluoromethyl t–butyl disulfide | $C_5H_9F_3S_2$ |
| 2 | 9.19 | 0.94 | Pyridine, 2–methyl– | $C_6H_7N$ |
| 3 | 9.76 | 3.61 | Methylenecyclopropanecarboxylic acid | $C_5H_6O_2$ |
| 4 | 10.70 | 0.60 | 2–Cyclopenten–1–one, 2–methyl– | $C_6H_8O$ |
| 5 | 10.85 | 2.09 | Clofexamide | $C_{14}H_{21}ClN_2O_2$ |
| 6 | 11.57 | 0.75 | 1,2–Ethanediol, dipropanoate | $C_8H_{14}O_4$ |
| 7 | 11.82 | 1.12 | 2–Cyclopenten–1–one, 3–methyl– | $C_6H_8O$ |
| 8 | 12.05 | 1.80 | Phosphonic acid, (p–hydroxyphenyl)– | $C_6H_7O_4P$ |
| 9 | 12.93 | 2.86 | 2–Ethyl–5–propylcyclopentanone | $C_{10}H_{18}O$ |
| 10 | 13.89 | 2.45 | 2–Isobornyloxy–tetrahydropyran | $C_{15}H_{26}O_2$ |
| 11 | 14.11 | 2.27 | Phenol, 2–methoxy– | $C_7H_8O_2$ |
| 12 | 14.33 | 1.31 | 1,3–Propanediol, 2–methyl–, dipropanoate | $C_{10}H_{18}O_4$ |
| 13 | 14.65 | 1.02 | Z,Z–6,28–Heptatriactontadien–2–one | $C_{37}H_{70}O$ |
| 14 | 14.72 | 1.63 | 4–n–Hexylthiane, S,S–dioxide | $C_{11}H_{22}O_2S$ |
| 15 | 16.25 | 2.04 | 6,6,9a–Trimethyl–decahydronaphtho[1,2–c]furan–1,4–dione | $C_{15}H_{22}O_3$ |
| 16 | 16.81 | 6.18 | 1,4:3,6–Dianhydro–.alpha.–d–glucopyranose | $C_6H_8O_4$ |
| 17 | 17.97 | 0.82 | Hydroquinone | $C_6H_6O_2$ |
| 18 | 18.86 | 1.63 | 3–n–Butylthiolane, S,S–dioxide | $C_8H_{16}O_2S$ |
| 19 | 19.42 | 4.92 | Phenol, 2,6–dimethoxy– | $C_8H_{10}O_3$ |
| 20 | 21.28 | 0.49 | 3,5–Dimethoxy–4–hydroxytoluene | $C_9H_{12}O_3$ |
| 21 | 22.44 | 1.90 | D–Allose | $C_6H_{12}O_6$ |
| 22 | 23.26 | 0.63 | Sedoheptulosan | $C_7H_{12}O_6$ |

| | | | | |
|---|---|---|---|---|
| 23 | 33.97 | 0.58 | (1r,3as,5as,8ar)–1,3a,5a–Trimethyl–4–methylenedecahydrocyclopenta[c]pentalene | $C_{15}H_{24}$ |
| 24 | 36.01 | 1.33 | Eicosane, 1–iodo– | $C_{20}H_{41}I$ |

## 4.7. Nuclear Magnetic Resonance (NMR)

A comprehensive understanding of chemical components in *A. adenophora* bio–oil, involves the $^{1}H$ and $^{13}C$ NMR investigations performed within a well–defined chemical shift range (Table 4.10). $^{1}H$ NMR spectrum [Fig. 4.13 (a)] revealed presence of aliphatic hydrocarbon attached to carbon atoms observed within 0.6 – 1.7 ppm. The integrated region from 1.7 – 3.2 ppm represents 48.3 % of resonating proton corresponding to aliphatics adjacent to olefinic and aromatic structures by a C=C bond further contributing towards to elevated energy value of bio–oil. Region 3.2 – 4.2 ppm is associated with protons on C atoms adjacent to aliphatic compounds attached to methoxy, hydroxyl (OH) group and oxygen, while 4.2 – 6.6 ppm correspond to methylene or methane, olefinic protons or phenolic hydroxyl further reinforcing the complexity of bio–oil. The spectral region between 6.6 – 8.2 ppm revealed 50.4 % of total hydrogen corresponded to carboxylics, carbohydrates, conjugated olefin and high aromatics. The heightened proportion of aromatics in bio–oil is a consequence of methoxy phenols derived from lignin. This is further supported by its significant calorific value (33.7 MJ/Kg) (Chutia et al., 2014). $^{13}C$ NMR spectrum offers enhanced detail with complementary information owing to their extensive chemical shift region [Fig. 4.13 (b)]. Signals in the 1 – 48 ppm range signifies the existence of aliphatic carbon atoms. The range 48 – 107 ppm represents carbohydrates, phenolic methoxy, esters and alcohols, typically with carbon adjacent to heteroatoms. Signals within 107 – 145 ppm is associated with the presence of phosphonic acid, indole, olefinic and aromatic structures. Esters are evident in the 145 – 157 ppm range while 157 – 197 ppm indicates the presence of amides, carboxylic acids, aldehydes and ketones.

Similarly, Table 4.11 displays the chemical shift range for *L. camara* bio–oil. $^{1}H$ NMR spectrum of *L. camara* bio–oil [Fig. 4.14 (a)] revealed the region 0.7 – 2.2 ppm comprised of long–chain aliphatic hydrocarbons. Protons in alkyl groups linked to double–bonded olefinic or aromatic rings resonated within range 2.3 – 2.8 ppm, while region 2.89 – 4.38 ppm was characteristic of naphthalene derivatives. Elevated phenolic and aliphatics were evident in the integrated region from 4.4 – 7.5 ppm. These phenolic and aliphatic compounds enhance the calorific value (30.99 MJ/Kg) of bio–oil (Chongloi et al., 2024). Bio–oil's aromatic fraction is observed within the integrated

region 7.5 – 8.2 ppm, potentially featuring aromatic structures, possibly with carbohydrate protons and conjugated double bonds. The $^{13}C$ NMR spectrum [Fig. 4.14 (b)] signifies the existence of long, branch and short aliphatics (1 – 56 ppm); indoles, olefines, esters and methoxys (57 – 146 ppm); phenol, carboxylic acid, esters (147 – 158 ppm); and aldehydes and ketones (159 – 206 ppm).

Furthermore, Table 4.12 displays the chemical shift range for *S. jamaicensis* bio–oil. $^{1}H$ NMR spectrum [Fig. 4.15 (a)] of *S. jamaicensis* bio–oil revealed the presence of aliphatics in the region 0.6 – 3.2 ppm (Chandran et al., 2020). The integrated region 1.1 – 2.0 ppm displayed aliphatics with alkynes or alkenes adjacent to aromatics while OH groups or methoxy are observed in the region between 2.1 – 2.9 ppm. The region between 2.9 – 3.2 ppm (47.9 % of total proton) corresponds to aliphatics attached to acetylenes or aromatics or adjacent to OH or methoxy groups. The spectral region from 3.2 – 8.4 ppm corresponds to carboxylic protons, aromatics, carbohydrates, phenols and olefins (Bordoloi et al., 2015) with the range 5.0 – 7.2 ppm highlighting a high phenolic content of 38.7 %. Valuable insights of *S. jamaicensis* bio–oil are revealed in $^{13}C$ NMR spectrum, illustrated in Fig. 4.15 (b). The region between 1 – 49 ppm reveals long, short and branched– chain aliphatics while furans, pyran, methoxys, phenolics, thianes and thiolanes are evident in the region 50 – 100 ppm. Signals from 101 – 145 ppm range signifies sulfides, olefins, aromatics and phosphonic acids. Region 145 – 159 ppm corresponds with the presence of pyridines, esters and phenols while amides, carboxylic acids, aldehydes and ketones were observed in region 160 – 175 ppm. These findings are consistent with the FTIR analysis results.

Pyrolytic liquids have been known to exhibit acidic characteristic. This bio–oil is rendered unsuitable as fuel due to its high oxygen content along with unsaturated and phenolic compounds. Subsequently, the elevated oxygen content, varying from 30 – 40 %, results in immiscibility, decreased energy density, and heightened acidity and overall instability of bio–oil (Runnebaum et al., 2011). Consequently, these factors enhance the corrosive characteristic of bio–oil simultaneously surging its viscosity and molecular weight accompanied by potential obstruction in fuel systems (Hu et al., 2012). Oxygenates such as carbonyl, aldehydes, ketones, carboxylic acid, and esters

are deemed responsible for the acidic and corrosive nature of bio–oil (Czernik & Bridgwater, 2004; Masudi et al., 2022). As a result, the direct application of bio–oil is challenging, necessitating the implementation of effective refining techniques. One such upgradation technique, hydrodeoxygenation (HDO), involves upgrading bio–oil into high–value hydrocarbon fuel (Michailos & Bridgwater, 2019). This involves the stabilization and deoxygenation of bio–oil (Demirbas, 2011). Oxygen is eliminated as $H_2O$, CO or $CO_2$ (Michailos & Bridgwater, 2019). Thereafter, the deoxygenated bio–oil undergoes cracking using a zeolite catalyst to produce short–chain hydrocarbons (Wang et al., 2013), ultimately yielding hydrocarbon biofuels comparable to gasoline and diesel (Ma et al., 2023). Other upgrading techniques include fluid catalytic cracking (FCC) (Agblevor et al., 2012), super critical fluid (SCFs) (Baloch et al., 2018), decarboxylation (Zhang et al., 2017b), emulsification and esterification (Baloch et al., 2018) to enhance optimal utilization of bio–oil. Implementation of these processes is expected to enhance heating value and decrease corrosiveness, enhancing its suitability as a prospective liquid fuel (Saikia et al., 2015). These processes, however, ultimately elevate the overall cost of product, subsequently diminishing its competitiveness with fossil fuels. The intricate spectrum of compounds detected in bio–oil underscores its chemical feedstock potential while its aliphatic and aromatic hydrocarbons, in particular, enhances its prospects for conversion into biofuel. Furthermore, the existence of bioactive compounds in bio–oil highlights its application and significance in the pharmaceutical domain. Chemical compounds reported in the current investigation are consistent with previous studies on pyrolysis–derived bio–oil (Bordoloi et al., 2015).

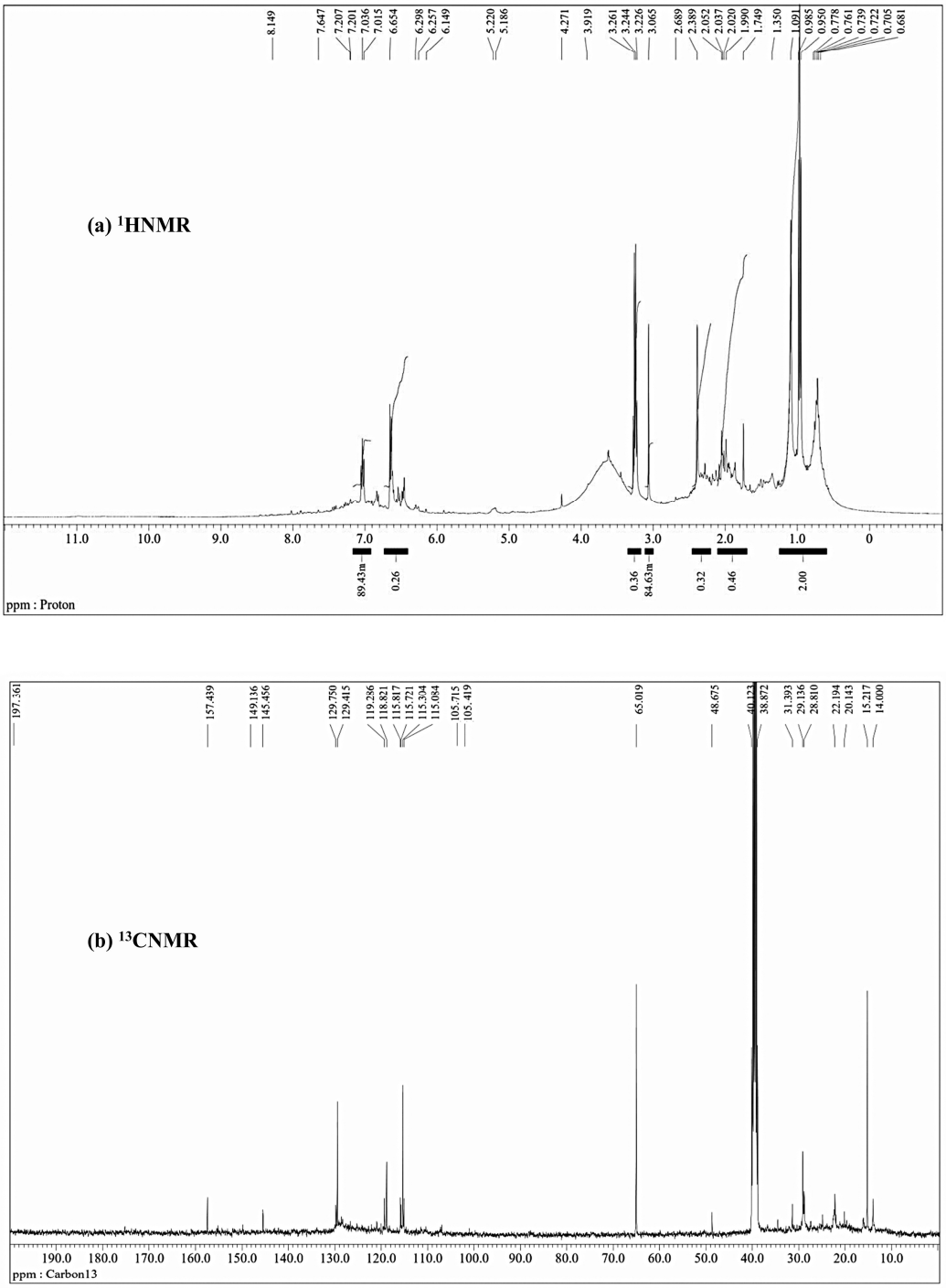


**Fig. 4.13 (a)** $^{1}$H–NMR and **(b)** $^{13}$C–NMR of *A. adenophora* bio–oil.

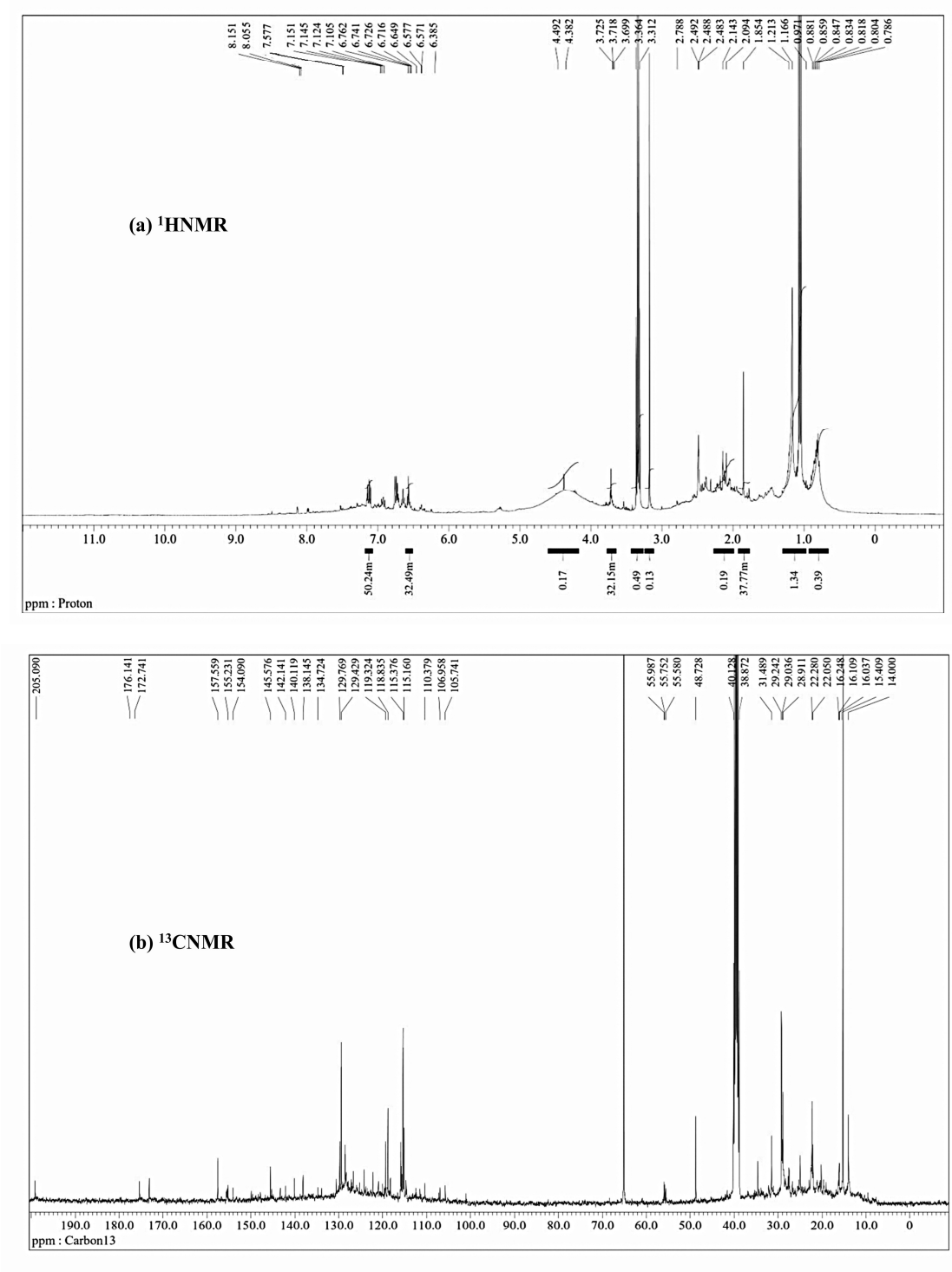


**Fig. 4.14 (a)** $^{1}$H–NMR and **(b)** $^{13}$C–NMR of *L. camara* bio–oil.

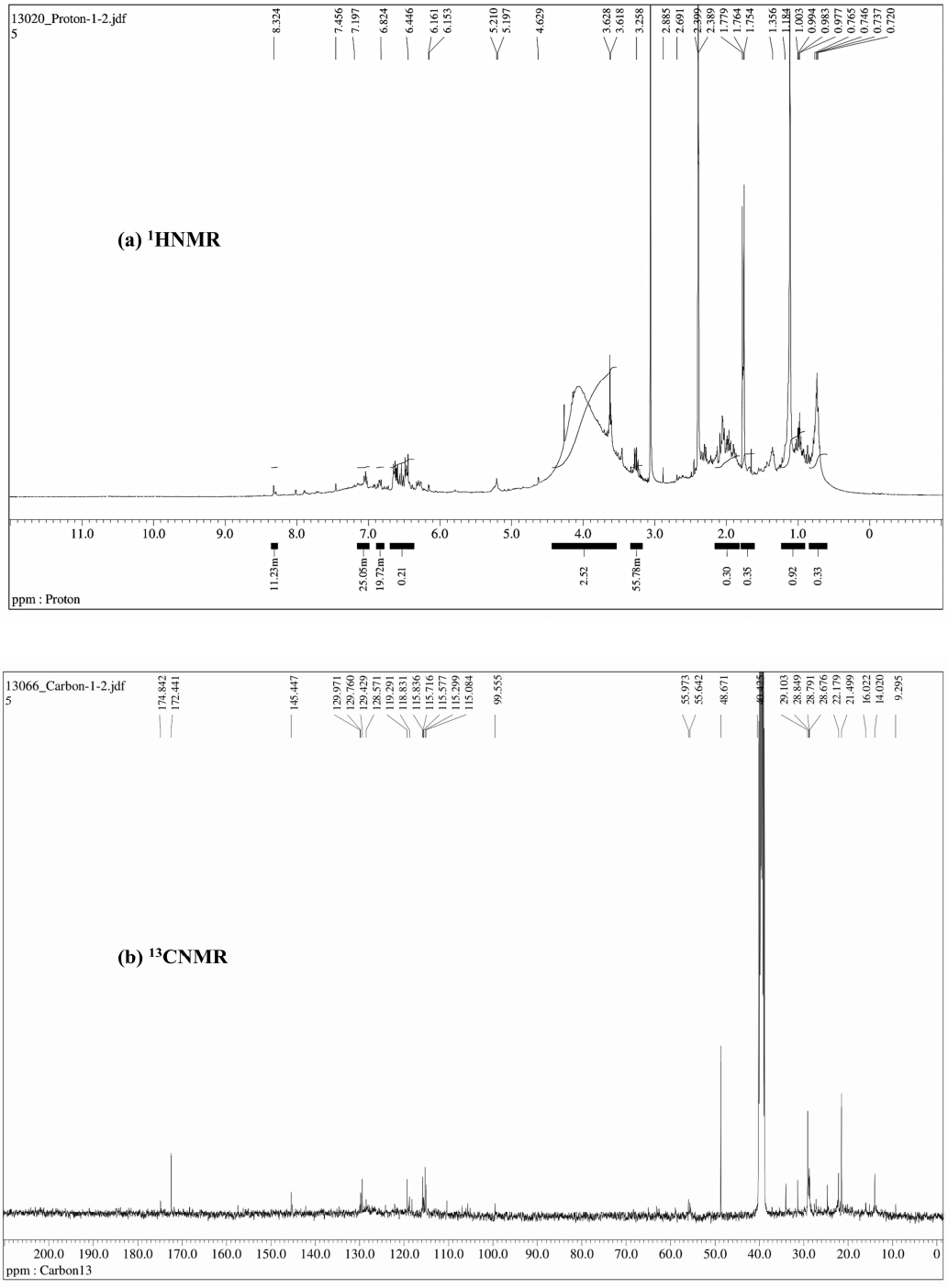


**Fig. 4.15 (a)** $^{1}$H–NMR and **(b)** $^{13}$C–NMR of *S. jamaicensis* bio–oil.

**Table 4.10.** Chemical compounds in *A. adenophora* bio–oil from $^{1}H$ and $^{13}C$–NMR spectral analyses.

| | Type of proton | Type of carbon | Total hydrogen percentage (%) |
|---|---|---|---|
| Chemical shifts range(ppm) | | | |
| 0.6–1.7 | Other Aliphatic such as alkanes, further from the aromatic ring | – | 1.4 |
| 1.7–3.2 | Aliphatic adjacent to aromatic, Olefinic | – | 48.1 |
| 3.2–4.2 | Aliphatic attached to oxygen/hydroxyl group or methoxy | – | 0.2 |
| 4.2–6.6 | Phenolic, olefinic, methylene or methane | – | 0.15 |
| 6.6–8.2 | Aromatic, conjugated olefin, carbohydrates, carboxylic proton | – | 50.4 |
| 1–48 | – | Aliphatic | |
| 48–107 | – | Alcohols, esters, phenolic methoxy, carbohydrate sugar | |
| 107–145 | – | Aromatic and olefinic, indole, phosphonic acid | |
| 145–157 | – | Esters | |
| 157–197 | – | Ketones, aldehydes, carboxylic acids, amide | |

**Table 4.11.** Chemical compounds in *L. camara* bio–oil from $^{1}H$ and $^{13}C$–NMR spectral analyses.

| | Type of proton | Type of carbon | Total hydrogen percentage (%) |
|---|---|---|---|
| Chemical shifts range(ppm) | | | |
| 0.7–2.2 | Aliphatic, further from the aromatic ring | – | 25.5 |
| 2.3–2.8 | Aliphatic adjacent to aromatic, Olefinic | – | 0.1 |
| 2.89–4.38 | Aliphatic attached to naphthalene, aliphatic attached to hydroxy group | – | 21.1 |
| 4.4–7.5 | Phenolic, olefinic, methylene, methane or methoxy | – | 21 |
| 7.5–8.2 | Aromatic, conjugated olefin, carbohydrates | – | 32.3 |
| 1–56 | – | Short, long, and branched aliphatics, siloxanes, sulphurous anhydrides | |
| 57–146 | – | Esters, methoxys, olefines, indoles | |
| 147–158 | – | Esters, carboxylics, phenols | |
| 159–206 | – | Ketones and aldehydes | |

**Table 4.12.** Chemical compounds in *S. jamaicensis* bio–oil from $^{1}H$ and $^{13}C$–NMR spectral analyses.

| | Type of proton | Type of carbon | Total hydrogen percentage (%) |
|---|---|---|---|
| Chemical shifts range(ppm) | | | |
| 0.6–1.1 | Aliphatic (γ) or further away from aromatic ring | – | 0.3 |
| 1.1–2.0 | Aliphatic and alkene or alkyne, adjacent to aromatic, olefinic | – | 1.1 |
| 2.1–2.9 | Aliphatic attached to methoxy or hydroxyl groups | – | 0.3 |
| 2.9–3.2 | Aliphatic attached to methoxy or hydroxyl groups, or attached to aromatic group or acetylene | – | 47.9 |
| 3.2–4.7 | Olefinic, methylene, methane or methoxy | – | 2.2 |
| 5.0–7.2 | Phenols, non–conjugated olefins | – | 38.7 |
| 7.2–8.4 | Aromatic, conjugated olefins, carbohydrates, carboxylic proton | – | 9.7 |
| 1–49 | – | Short, long and branched aliphatics | |
| 50–100 | – | Thiolanes, thianes, phenolic metgoxys, pyran, furan | |
| 101–145 | – | Phosphonic acid, aromatic, olefins, sulfide | |

| | | |
|---|---|---|
| 145–159 | – | Phenols, esters, pyridine |
| 160–175 | | Ketone, aldehyde, carboxylic acids, amides |

## 4.8. Economic analysis of IS biofuels and value–added products

The economic analysis was undertaken to evaluate the cost–competitiveness and commercial feasibility of producing biofuels from IS biomass in comparison to conventional petroleum fuels. According to data presented in Table 4.3 and Table 4.4 for *A. adenophora*, y = 0.3450, $x_{biochar}$ = 0.3737, $x_{syngas}$ = 0.2813, $E_{bio-oil}$ = 33,700 MJ/ton, $E_{biochar}$ = 20,710 MJ/ton, $E_{syngas}$ = 15 MJ/m$^3$ based on previous literature (Hu et al., 2013), q = 1050 m$^3$/ton (considering density as 0.95 kg/m$^3$) and $E_{Petroleum}$ = 6100 MJ (Chisti, 2008; Phukan et al, 2019). Accordingly, Eq. (3.24) is expressed as

$$M = \frac{6100}{11626.5w+12169.802} \quad (4.1)$$

From data in Table 4.3 and Table 4.4 for *L. camara*, $E_{Petroleum}$ = 6100, y=0.3271, $E_{bio-oil}$=30,990 MJ/ton, q = 1050 m$^3$/ton, $E_{syngas}$ = 15 MJ/m$^3$, $x_{syngas}$=0.3136, $E_{biochar}$=20,120 MJ/ton and $x_{biochar}$=0.3593. Accordingly, Eq. (3.24) becomes

$$M = \frac{6100}{10136.829w+1216\ .316} \quad (4.2)$$

Similarly, from Table 4.3 and Table 4.4 for *S. jamaicensis,* y = 0.3180, $x_{biochar}$ = 0.3880, $x_{syngas}$ = 0.2940, $E_{bio-oil}$ = 30,180 MJ/ton, $E_{biochar}$ = 25,260 MJ/ton, $E_{syngas}$ = 15 MJ/m$^3$, q = 1050 m$^3$/ton and $E_{Petroleum}$ = 6100 MJ. Accordingly, Eq. (3.24) becomes:

$$M = \frac{6100}{9597.24w+14431.38} \quad (4.3)$$

The predicted price of *A. adenophora* biofuel is estimated from Eqs. (3.24), (3.25), and (4.1), respectively, while the projected cost for *L. camara* biofuel is calculated from Eqs. (3.24), (3.25), and (4.2), respectively. Similarly, estimated cost for *S. jamaicensis* biofuel is estimated based on Eqs. (3.24), (3.25), and (4.3). These estimations consider crude oil prices up to $ 1000/barrel and for *w* ranging from 10 – 100 % (furnished in Fig. 4.16 for *A. adenophora*, Fig. 4.17 for *L. camara* and Fig. 4.18 for *S. jamaicensis*). The acceptable competitive price of biofuel relative to petroleum (per barrel) elevated as *w* i.e., bio–oil conversion percentage, increased. Biofuel derived from the three IS with 100 % conversion to bio–oil (to fuel and value–added products), is deemed economically viable at < $ 390.104 ton$^{-1}$ to be positioned in competition against petroleum priced at $ 100/barrel. In comparison, biofuels from *L.*

*camara* and *S. jamaicensis* are economically feasible at < $ 361.86 ton$^{-1}$ and < $ 393.91 ton$^{-1}$, respectively. Accordingly, taking consideration of production cost of biofuel at $ 1000 ton$^{-1}$, the production cost of *A. adenophora, L. camara* and *S. jamaicensis* biofuel needs to be reduced by a factor of ~3.

The present analysis may be conducive in providing new perspectives into prospective market viability of IS biofuel across varied scenarios serving as a guide for investors and policymakers in the bioenergy domain. Nevertheless, implementation of integrated biorefinery approach coupled with advancement in biomass conversion technologies could further curb down the production costs of syngas, bio–oils and biochar derived from the three IS. An integrated strategy for bioenergy generation and developing value–added products possess potential to reduce the economics of feedstock utility (Phukan et al., 2019) associated with IS management while also supporting the essential shift towards bio–based economy Consequently, successful commercialization following large–scale implementation of IS biomass conversion technologies requires comprehensive techno–economic analyses and life cycle assessments (LCA) to be deemed sustainable and economically feasible.

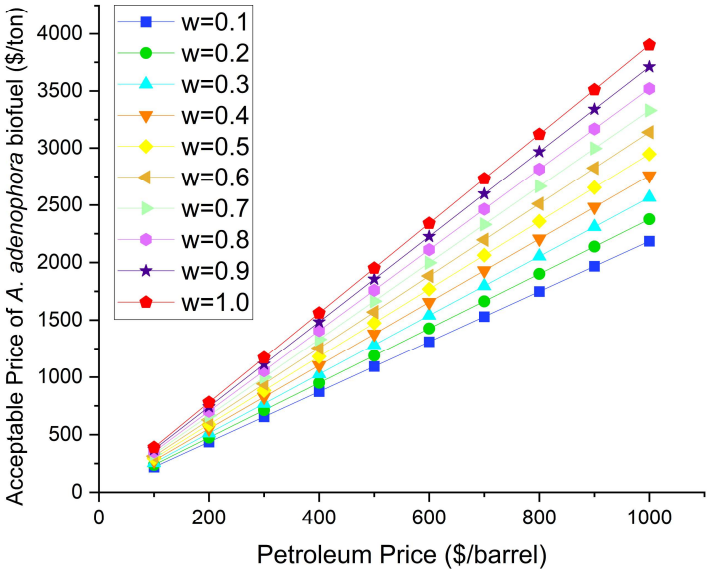


**Fig. 4.16.** Competitiveness of *A. adenophora* biofuel with petroleum prices.

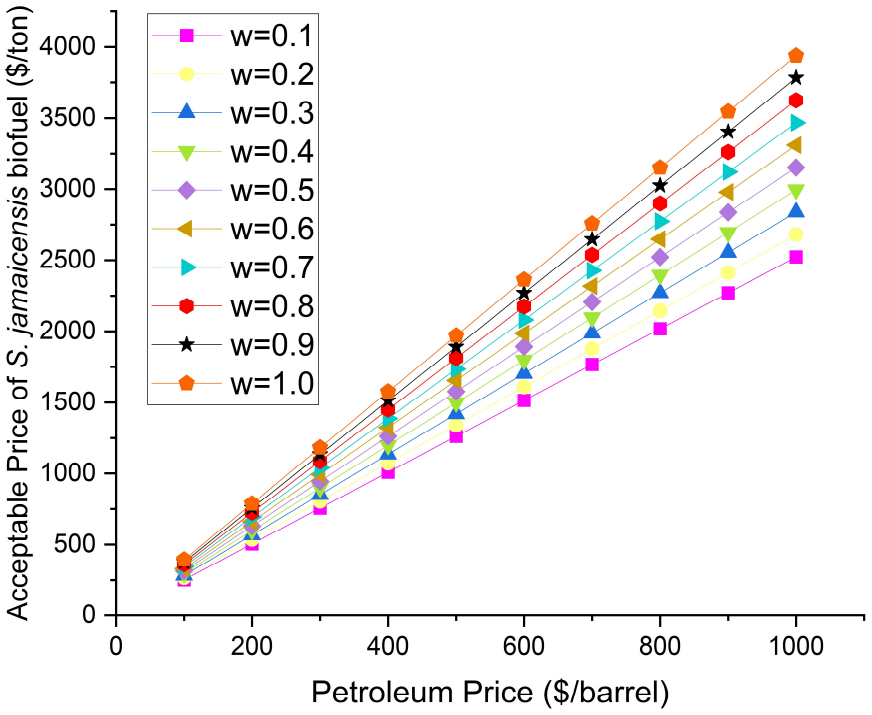


**Fig. 4.17.** Competitiveness of *L. camara* biofuel with petroleum prices.

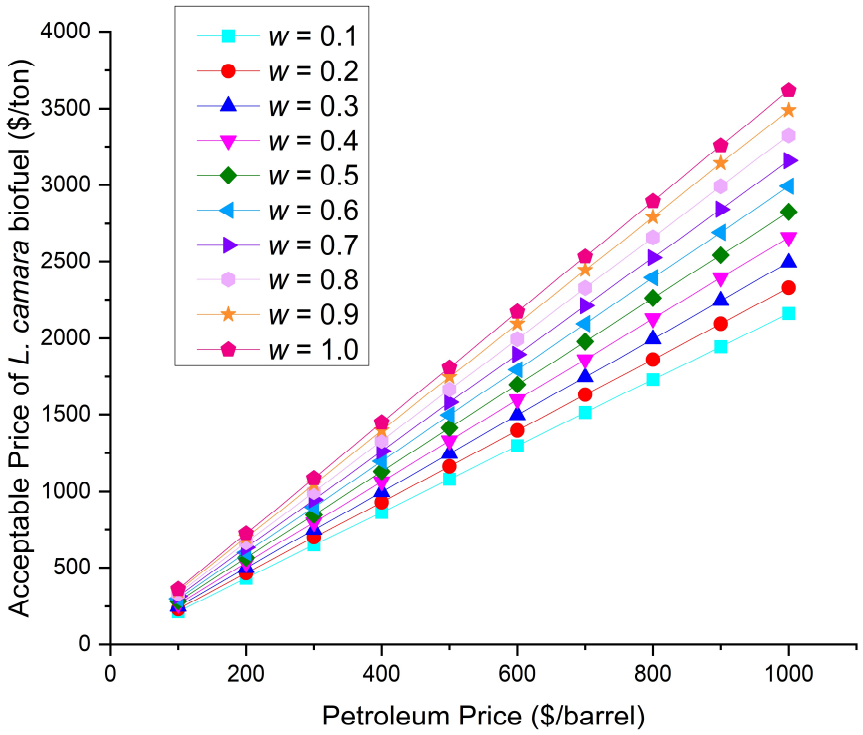


**Fig. 4.18.** Competitiveness of *S. jamaicensis* biofuel with petroleum prices.

## 4.9. Economic analysis of bio–oil pyrolysis plant

### 4.9.1. Pyrolysis of IS biomass for hypothetical pyrolysis plant

The yearly output of bio–oil derived from IS biomass is projected to be 1800000 Kg, calculated on a yield of approximately 30 % in relation to the feedstock input. This yield confirms the effectiveness of the pyrolysis process under the defined operating conditions and reinforces the financial viability of the biomass processing facility.

### 4.9.2. Cost structure analysis

The estimation of capital costs in the early stages of plant development is significantly affected by the installation factors associated with the selected methodology. The way these installation parameters respond to the price of individual equipment has a substantial effect on the overall cost of plant. This establishes which type of capital cost each strategy is most effective for, whether it calls for an upgrade project or the construction of a whole new plant (Aromada et al., 2021). Capital expenditure (CAPEX) survey data, obtained from Eq. (3.26), are presented in Fig. 4.19. Emphasizing the significant investment necessary for the plant's infrastructure, the construction cost stands at 53.6 %, constituting the predominant segment of CAPEX while land acquisition, comprising of 26.8 % of CAPEX, ranks as the second–largest contributor. Accounting for 10.7 % of CAPEX, is the pyrolyzer unit, a crucial element demonstrating its technological sophistication and implications in the overall plant design. The current study corroborates the conclusions of (Aromada et al., 2021) with both the studies highlighting the importance of equipment prices – in this case, the pyrolyzer unit – in the total CAPEX. By meticulously evaluating the equipment installation costs, both studies concentrate on analysing how installation parameters influence the total plant cost (TPCo). Infrastructure and utilities represented 5.4 %, followed by storage units at 3 %, while permits and compliance accounted for 0.5 % of CAPEX. These ratios highlight prospects where cost–optimisation strategies such as opting for alternative sites or negotiating enhanced construction contracts, could possibly reduce initial capital costs.

Operational expenditure (OPEX) refers to the daily recurring expenses associated with the operation of the plant. This encompasses raw material acquisition

(labour and transportation), salary and electricity. Predominantly influenced by labour and transportation, raw material procurement expenses constituted 70.3 % of OPEX, ensuring a steady supply of feedstock for plant processing. Additionally, electricity cost and employees' salaries accounted for 1.9 % and 27.8 % of OPEX, respectively. The OPEX data were obtained from Eqs. (3.27), (3.28) and (3.29) and presented in Fig. 4.20. These electricity cost could significantly be reduced employing energy–efficient approaches (Can et al., 2022). These data synergistically signify the necessity to augment worker productivity, optimization of supply chain logistics, and implementation of energy–efficient approaches to boost the overall cost effectiveness and project profitability. Ji et al. (2017) demonstrated that 20 % variation in unit feedstock expense results in a 10.59 % alteration in the overall production cost. This aligns with the present finding, which highlights the substantial impact of raw material acquisition (70.3 %) on the total production cost. This highlights the necessity to effectively manage feedstock expenses to reduce operational expenses and maintain economic stability. The overall project investment and annual revenue generated from bio–oil sales are furnished in Table 4.13.

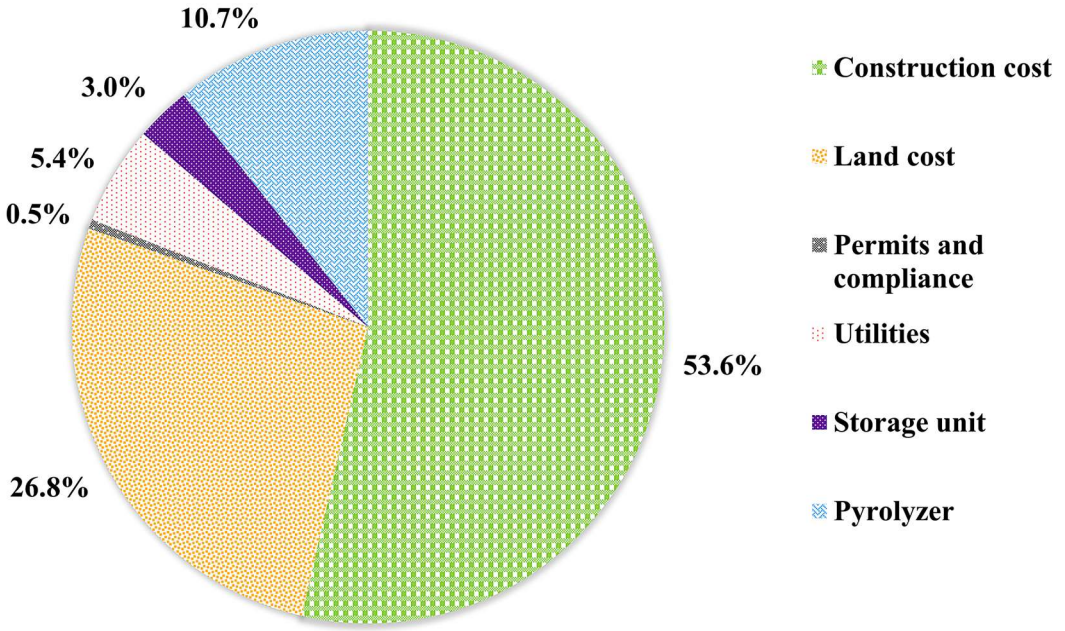


**Fig. 4.19.** Estimated CAPEX.

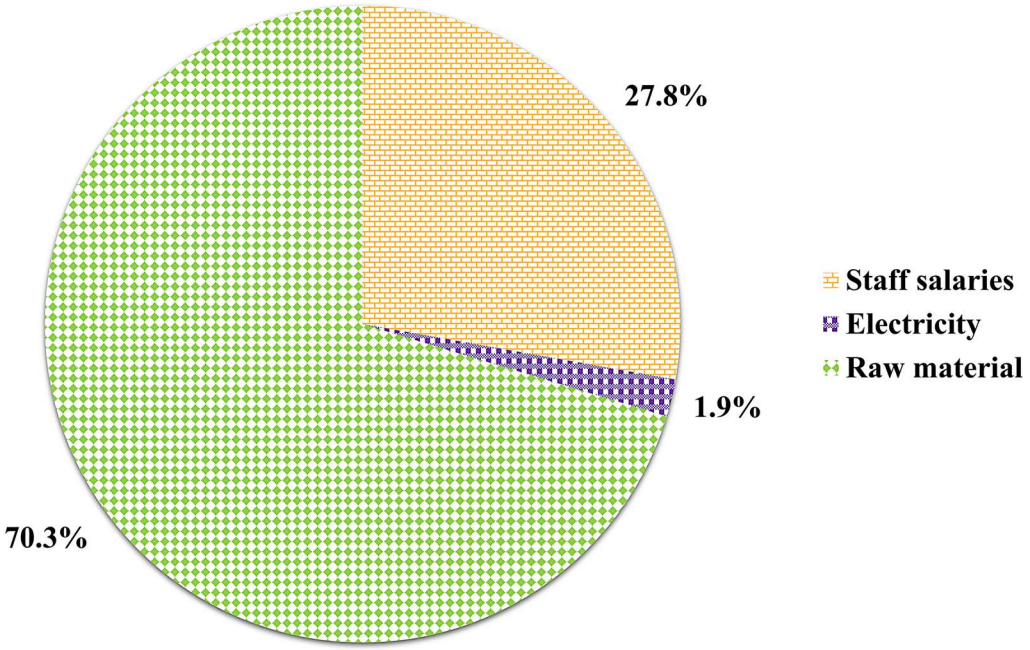


**Fig. 4.20.** Estimated OPEX.

**Table 4.13.** Total project investment and revenue breakdown.

| Item | Quantity |
|---|---|
| **Cost–benefit Analysis** | |
| Net Present Value | $ 378,912.829 |
| Internal Rate of Return | 21 % |
| Payback Period (in years) | 5.19 |
| Capital expenditure (CAPEX) | |
| Land cost | $ 1,15,580.21 |
| Construction cost | $ 2,31,160.43 |
| Infrastructure and utilities | $ 23,404.99 |
| Permits and compliance | $ 2,253.81 |
| Cost of pyrolyzer | $ 46,232.09 |
| Cost of setting up 1 storage unit | $ 12,771.61 |
| **Total CAPEX** | $ 4,31,403.14 |
| Operational expenditure (OPEX) | |
| Electricity consumption per year | $ 11,092.93 |
| Cost of raw materials (labour cost + transport cost) | $ 4,14,048.32 |
| Staff salaries | $ 1,63,627.61 |
| **Total OPEX** | $ 5,88,769 |
| **Bio–oil production cost** | |
| Feedstock capacity per run | 5000 Kg |
| No. of runs per day | 4 |
| Total operational days per year | 300 |
| Feedstock capacity per year | 6000000 Kg |
| Bio–oil yield at 30 % of feedstock | 1800000 Kg/year |
| **Annual revenue ($0.2543/Kg)** | **$ 457,740** |

### 4.9.3. Finance evaluation

Underpinned by crucial financial indicators that underlines its sustainability and profitability, the financial evaluation confirmed the bio–oil pyrolysis plant as an effective and financially feasible investment with a modest risk profile. A low payback period (PBP) often indicates quick retrieval of investment by investors (Zhang et al., 2017a). With a 30 % yield of bio–oil leading to an annual production of 18000 tons, Eq. (3.30) calculated the investment project's PBP to be 5.19 years signifying its attractive profit potential. This PBP is considered appropriate considering the 15–year operational duration of the project indicating a modest risk profile and promising potential for long–term profitability (Udomsri et al., 2010). Zhang et al. (2017a) conducted a comparable study estimating a PBP of 2.58 years for bamboo–biochar plants in China. Additionally, internal rate of return (IRR) and net present value (NPV) were assessed to deliver a thorough evaluation of the investment's viability.

Eq. (3.31) yielded an NPV of $ 378,912.829 highlighting the financial strength of the pyrolysis plant. Even when future revenues are discounted at the usual cost of capital (COC) of 8 %, a positive NPV not only validates the project's capacity to provide returns that surpass the initial investment, but also accounts for the time worth of money, making it a wise investment (Bora, 2015). This evaluation further supports the project's economic feasibility by demonstrating its capacity to continuously generate value over time. Fig. 4.21 demonstrates the relevant NPVs at different years.

Furthermore, IRR of 21 % as yielded from Eq. (3.32), is a persuasive indicator, significantly surpassing the COC (8 %). This substantial margin underscores the project's capacity to yield returns significantly exceeding the conventional benchmark for financial feasibility. IRR of 21 % exceeding the COC (8 %) by more than two–fold demonstrated that the pyrolysis plant is both financially viable and extremely competitive when compared to alternate investment options, especially in renewable energy domain. A similar study with a lower NPV ($1,969,614) but higher IRR (35 %) was documented by (Badger et al., 2010). Nonetheless, both studies suggest the capability and competitiveness of financially feasible pyrolysis projects in the renewable energy domain. Moreover, IRR of 21 % exceeding the COC corroborates

the findings of Badger et al. (2010) that pyrolysis system can independently compete in the energy domain without support from the government (subsidiary here).

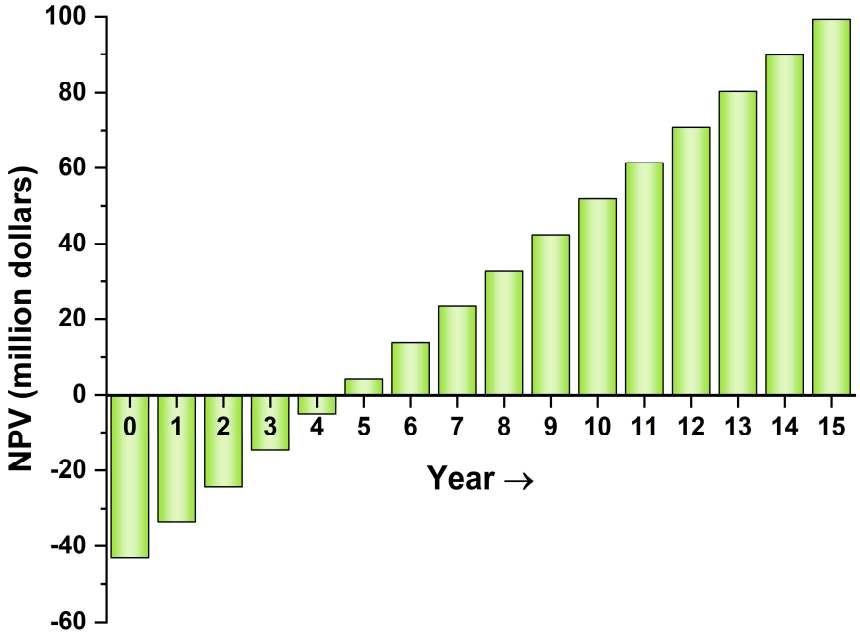


**Fig. 4.21.** NPV at different years.

### 4.9.4. Sensitivity Analysis

From the producer's perspective, for a project to be commercially successful and lucrative, cost must be reduced, as escalating expenses lead to declining returns. The price must be established at a level that adequately covers manufacturing expenses and yields a reasonable profit. A decrease in price results in reduced returns, while an increase in price yields increased returns. A sensitivity analysis is thus undertaken to assess the influence of uncertainty in several cost parameters on the production cost of liquid fuel. This analysis elucidates how variations in a particular cost component can impact the entire assessment of the cost of liquid biofuel production (Zhang et al., 2013). The production cost of one kilogram of bio–oil was evaluated to ascertain its effect on the project's profitability. The assessment analysed the effect of pricing and

operational expenses on the project's NPV and IRR. The project generated an IRR of 18 % at the base operational cost of $ 0.2427 /Kg. The IRR is estimated to rise to 23 % with a lower hypothetical rate of $ 0.2311/Kg. However, the IRR gradually decreased as operational costs increased. Evidently, the rise in operational cost/unit to $ 0.2543/Kg resulted in a decrease of IRR to 12 %. The IRR further drops to 5 % as the cost increases to $ 0.2658/Kg. At this juncture, the IRR still exceeds the COC. However, an increase of operational cost to $ 0.2774/Kg reduced the IRR to merely 4%. IRR at this point falls below the COC (8 %), rendering the project unfeasible.

Comparable patterns were observed in the pricing analysis. Negative IRR yielded from hypothetical prices up to $ 0.2427/Kg signified financial impracticability. A positive IRR of 2 % resulted when the price was set at $ 0.2543/Kg. However, this is still below the COC making it unfavourable when considering the project's long–term viability. IRR exceeds the COC achieving favourable rates of 9 %, 15 % and 21 % when the price is increased to $ 0.2658/Kg, $ 0.2774/Kg and $ 0.2889/Kg, respectively. IRR of 21 % achieved when the price is set to $ 0.2889/Kg substantiates the project's viability. The product price was henceforth set at this rate. A crucial threshold of $ 0.2543 – 0.2658/Kg, where both cost and price align, was identified by a sensitivity analysis. The threshold represented the maximum permissible cost and minimal sustainable price for ensuring a favourable IRR. Any decline in product price below $ 0.2543/Kg or escalation in operational cost above $ 0.2658/Kg yields a negative NPV. This demonstrates that for the project to be deemed financially sustainable, it is essential to maintain price and cost within these limits. Fig. 4.22 furnishes the sensitivity analysis of operational cost and IRR %, Fig. 4.23 presents the operational cost and NPV, Fig. 4.24 presents the product price and IRR % and Fig. 4.25 shows the product price and NPV. Bio–oil price of $ 0.2889/Kg (approximately $ 1.09/gallon) is substantially less than the estimated 2025 fuel prices for diesel ($ 3.61/gallon) and gasoline ($ 3.19/gallon) and the anticipated 2026 prices for diesel ($ 3.70 /gallon) and gasoline ($ 3.14/gallon) (Analysis & Projections, 2023). This price difference suggest that bio–oil, following suitable upgradation, could be a viable alternative to conventional fuels if production cost are further reduced or maintained at the existing level. An investigation by (Ji et al., 2017) indicated that production costs

are minimally impacted by water and electricity expenses, operating days per year and transportation and liquid fuel storage cost; moderately affected by labour project investments and labour costs; and significantly influenced by alterations in fuel yield and feedstock expenses. This is consistent with the current findings which emphasizes the crucial impact of feedstock cost and bio–oil yield on the plant's economic viability. Additionally, the sensitivity analysis emphasizes the significance of maintaining feedstock costs and improving the yield. This further supports the conclusions drawn from both studies regarding the key factors affecting biofuel production costs. A comparable study was documented by Wright et al. (2010).

Minimum Selling Price (MSP), the minimum price at which the product can be sold to guarantee a desired degree of profitability, was ascertained using the Discounted Cash Flow Rate of Return (DCFROR) analysis (Sarker et al., 2023). DCFROR determined MSP to be $ 0.2617/Kg (Fig. 4.26). Dealing below this price would render the project unprofitable, resulting in financial deficit. Consequently, $ 0.2617/Kg functions as a pivotal benchmark for market pricing, guaranteeing the project's long–term economic feasibility. The MSP of bio–oil determined in the current study contrasts with the MSP of $ 6.25/gallon reported by Carrasco et al. (2017). This can be ascribed to the reduced feedstock cost ($ 0.2543/Kg operational cost) in conjunction with regional disparities in labour expenses, utilities, market conditions, etc. Another study by Meyer et al. (2020) encompassing several biomass feedstocks procured MSP between 6.57 – 9.05 CNY/L for a plant with processing capacity of 2000 t/d of dry feedstock.

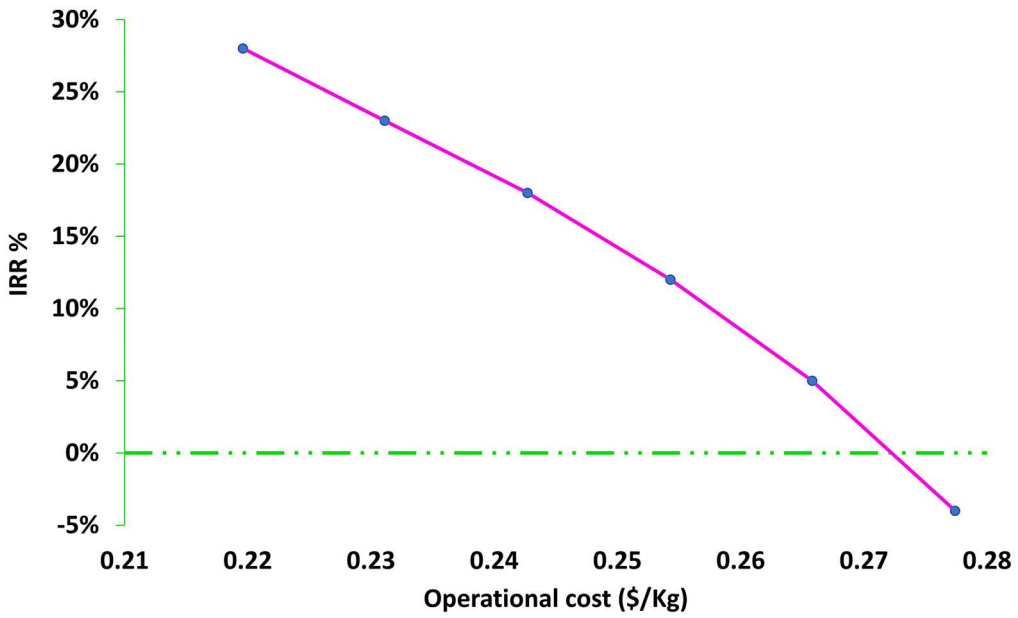


**Fig. 4.22.** Sensitivity analysis of operational cost and IRR %.

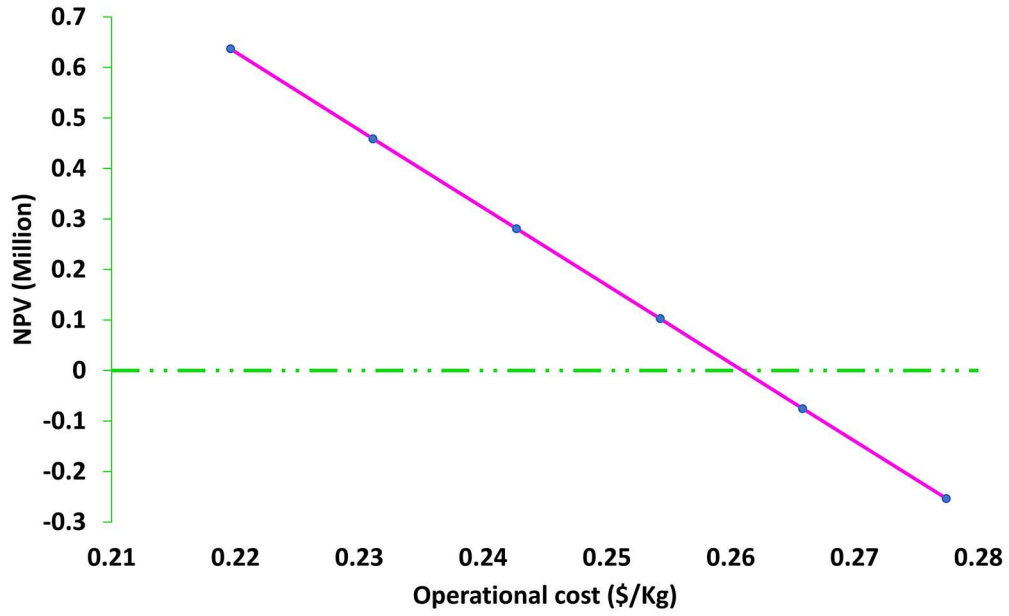


**Fig. 4.23.** Sensitivity analysis of operational cost and NPV.

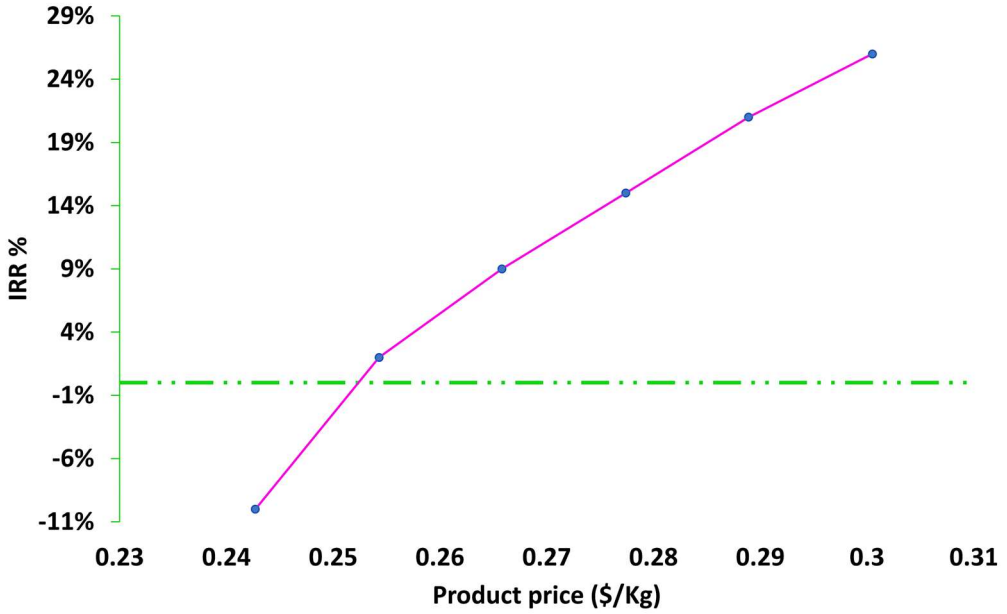


**Fig. 4.24.** Sensitivity analysis of product price and IRR %.

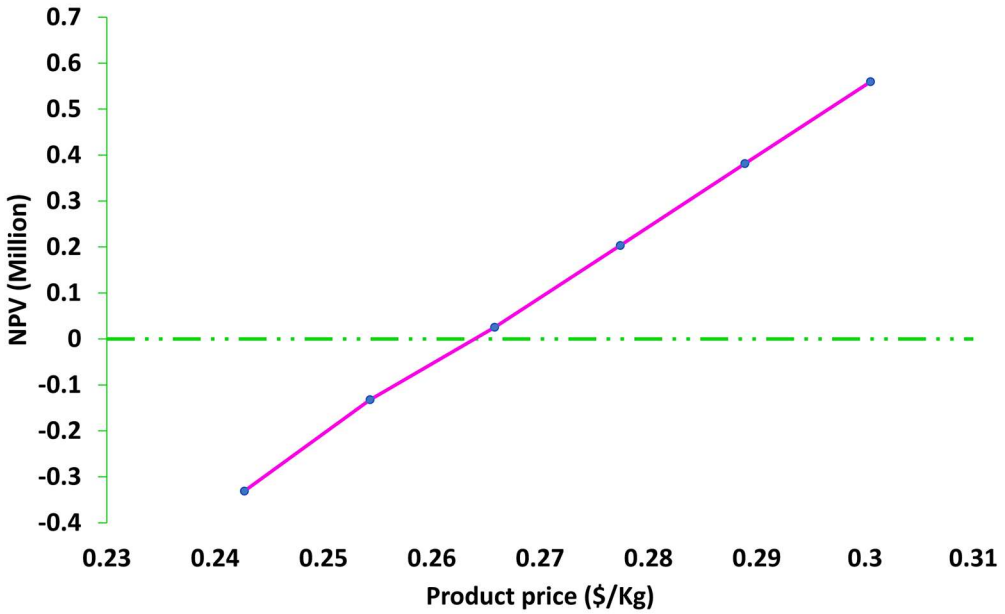


**Fig. 4.25.** Sensitivity analysis of product price and NPV.

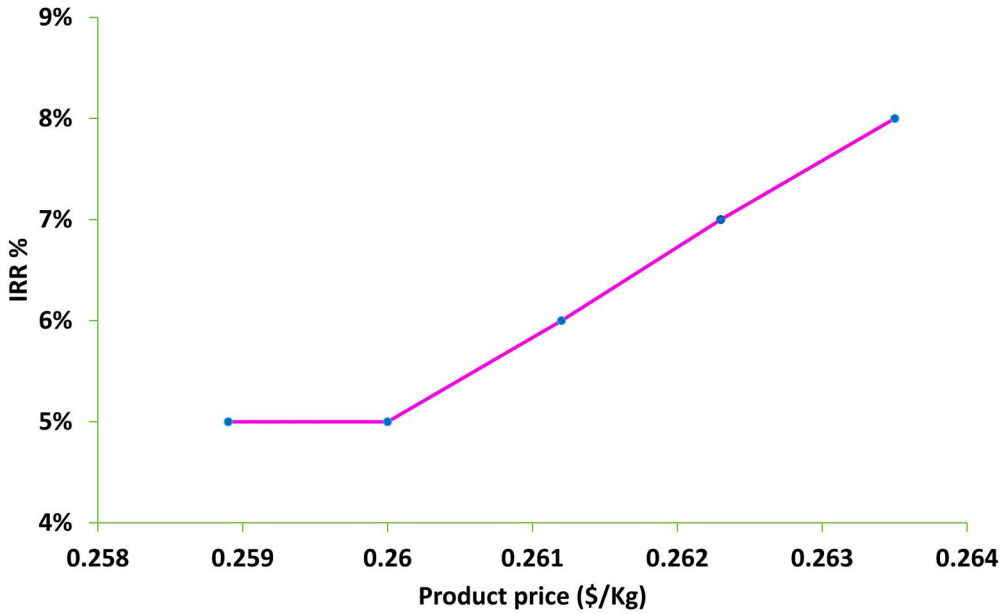


**Fig. 4.26.** MSP of product estimated using Discounted Cash Flow Rate of Return (DCFROR) analysis.

## 4.10. Antioxidant activity of bio–oil

Pyrolysis–derived bio–oil contains a complex mixture of organic compounds including high – value bioactives. These bioactives, especially phenolics, significantly contribute to its antioxidant efficacy. Identified within the chemical composition of bio–oil, these compounds serve multiple functional roles such as free radical scavenging, deactivating singlet oxygen, reducing activity and metal chelation (Sousa et al., 2015). The reducing potential of phenolic compounds inhibits the development of superoxide anion radicals ($O_2^-$) (Bursal & Gülçin, 2011). Similarly, the bioactive compounds help minimize viscosity changes, thereby extending the shelf life of bio–oil (Udomsap et al., 2011). Nonetheless, further research with technological advancements is warranted to enhance efficiency and facilitate large–scale adoption (Lødeng & Bergem, 2018). Furthermore, the outcomes of our experimental findings demonstrate the need for leveraging and repurposing IS–derived bio–oil.

In the current investigation, bio–oil from the three species, viz., *A. adenophora*, *L. camara* and *S. jamaicensis* were evaluated for their antioxidant properties using total phenolic content (TPC), total flavonoid content (TFC), 1, 1–diphenyl–2–picrylhydrazyl (DPPH) free radical scavenging capability and ferric reducing antioxidant power (FRAP) assay. The details of the assessment are presented in Table 4.14. The linear regression curves to quantify the TPC and TFC are displayed in Fig. 4.27 and Fig. 4.28, respectively. The *L. camara* bio–oil exhibited superior phenolic content of 96.5 ± 1.2 mg GAE/ml while TPC of *A. adenophora* and *S. jamaicensis* bio–oils were 71.17 ± 1.6 and 62.71 ± 1.3 mg GAE/ml, respectively. These phenolic components form a significant category of natural products that are extensively found throughout the plant kingdom (Míguez et al., 2022). They boost antioxidant activity by transferring electrons or hydrogen atoms to stabilize free radicals (Shon, 2003). Various biomass components, specifically lignin, are prominent sources of phenolic compounds (Alcazar–Ruiz et al., 2023; Pinheiro et al., 2024). Thus, the phenolic content evident in the bio–oils may be attributed to the lignocellulosic IS biomass used as feedstock for bio–oil production. The free radicals undergo saturation with phenolic compounds through its interaction with the hydrogen atom in the OH group of the

phenolic compounds (Bendary et al., 2013). The flavonoid content of *A. adenophora*, *L. camara* and *S. jamaicensis* bio–oils were 14.75 ± 1.2, 17.7 ± 1.1 and 12.45 ± 0.8 mg QE/ml, respectively. The role of these flavonoids is crucial in comprehending the antioxidant efficacy owing to their potential in effectively reducing metals, scavenging radicals, and chelating ions contributing towards OH radical production (Rodríguez–Arce & Saldías, 2021). Evidently, the bio–oils demonstrated clear potential to counter balance heightened levels of reactive nitrogen species (RNS) and reactive oxygen species (ROS) owing to the synergistic activity of phenolic and flavonoids in them. These work together to minimize oxidative stress linked with degenerative and chronic ailments (Tungmunnithum et al., 2018).

Furthermore, DPPH and FRAP assay, used to determine the bio–oils' free radical scavenging activity validated its antioxidant potential. The linear regression graph for FRAP assay is presented in Fig. 4.29. The linear regression curve for DPPH $IC_{50}$ for *A. adenophora*, *L. camara* and *S. jamaicensis* is displayed in Fig. 4.30, Fig. 4.31 and Fig. 4.32, respectively. Reducing power is a crucial metric for evaluating the antioxidant potential (Lu et al., 2021). The findings of DPPH $IC_{50}$ and FRAP are presented in Table 4.14. DPPH $IC_{50}$ (half–maximal inhibitory concentration) values of *A. adenophora*, *L. camara* and *S. jamaicensis* bio–oils were 211.4 ± 1.2, 233.72 ± 0.2 and 232.42 ± 1.1 µg/ml, respectively. FRAP values of *A. adenophora*, *L. camara* and *S. jamaicensis* bio–oils were 121.39 ± 0.6, 122.45 ± 1.9 and 114.96 ± 1.8 µM AAE/ml, respectively. The results revealed that the bio–oils possessed substantial antioxidant activity. Yang et al. (2016) examined Butylated Hydroxytoluene (BHT), an established antioxidant, for its antioxidant effectiveness, employing the DPPH assay. The study reported an $IC_{50}$ value of 175 µg/ml which lies in close proximity to the findings of the current study. Furthermore, $IC_{50}$ acts as an indicator of antioxidant efficacy where lower values signify stronger antioxidant capacity (Lu et al., 2021). Thus, the lower DPPH $IC_{50}$ value of 211.4 ± 1.2 µg/ml of *A. adenophora* bio–oil obtained in this study signifies stronger antioxidant capacity when compared to the DPPH $IC_{50}$ value (257 µg /ml) of its petroleum ether extract (Zheng–qiang et al., 2024). In contrast, crude extracts of *L. camara* leaf and flower investigated by Mansoori et al. (2020) exhibited more potent antioxidant potential with $IC_{50}$ value of 172.03 ± 1.73 and 144.94 ± 1.36

µg/ml, respectively, when compared to *L. camara* bio–oil (233.72 ± 0.2 µg/ml). Methanolic extract of *S. jamaicensis* leaf as studied by Fatmawati et al. (2023) displayed $IC_{50}$ value of 539.17 µg/ml implying the stronger antioxidant activity of *S. jamaicensis* bio–oil (232.42 ± 1.1 µg/ml) investigated in the present study. Consequently, the prominent role of phenolic components in counteracting free radicals is evident from its DPPH scavenging ability.

**Table 4.14.** Antioxidant activity of IS bio–oil derived from *A. adenophora*, *L. camara* and *S. jamaicensis.*

| Species | Total phenolic content (mg GAE/ml) | Total flavonoid content (mg QE/ml) | Ferric Reducing Antioxidant Power (FRAP) Assay (µM AAE/ml) | DPPH $IC_{50}$ value (µg/ml) |
|---|---|---|---|---|
| *A. adenophora* | 71.17 ± 1.6 | 14.75 ± 1.2 | 121.39 ± 0.6 | 211.4 ± 1.2 |
| *L. camara* | 96.5 ± 1.2 | 17.7 ± 1.1 | 122.45 ± 1.9 | 233.72 ± 0.2 |
| *S. jamaicensis* | 62.71 ± 1.3 | 12.45 ± 0.8 | 114.96 ± 1.8 | 232.42 ± 1.1 |

Several compounds in the bio–oils (as detected in GC–MS analyses and shown in section 4.6) have been previously reported to exhibit bioactivity, viz., antioxidant, anti–inflammatory, anti–cancer and antimicrobial activities. For instance, compounds detected in *A. adenophora* bio–oil such as Phenol, 3–methyl–, Furaltadone, Phenol, 2–methoxy–, 2–cyclopenten–1–one and Phenol, 2,6–dimethoxy have been reported for their antioxidant properties (Wang et al., 2015). Similarly, compounds in *L. camara* bio–oil (D–limonene, indole, neophytadiene, Z,Z–6,28–Heptatriacontadien–2–one, Z–28–Heptatriaconten–2–one) (Deepak et al., 2017; Yu et al., 2017) and *S. jamaicensis* bio–oil (Z,Z–6,28–Heptatriactontadien–2–one, Phenol, 2,6–dimethoxy–, Eicosane, 1–iodo–) (Adelakun et al., 2012; Chen et al., 2022; Ralte et al., 2022) have been noted

for their antioxidant potential. Previous investigations have highlighted the ability of D–limonene to inhibit lipid peroxidation (Murali & Saravanan, 2012) along with its anti–cancer and antioxidant effects (Yu et al., 2017). D–Allose and hydroquinone have been reported to exhibit promising potential in cancer treatments (Lim & Oh, 2011; Maldonado et al., 2024). Phenol, 2–methoxy– has been reported for its cardioprotective effects (Aqeel et al., 2023). Furthermore, Indole has been documented to exhibit analgesic, antimicrobial and anti–inflammatory properties (Zhang et al., 2021). The findings here necessitate further explorations into the antioxidant capacities of *A. adenophora, L. camara* and *S. jamaicensis* bio–oil along with its chemical feedstock prospects. This calls for in–depth research efforts, incorporating advanced bioactive assays and molecular docking studies, to gain a better comprehensive understanding of its underlying molecular mechanisms. The results of this study unveil the antioxidant potential of IS–derived bio–oils, exploring their potential as a chemical feedstock and as source of high–value compounds for potential pharmaceutical applications. The recovery or isolation of bioactive compounds for application in pharmaceuticals requires efficient separation techniques. The current techniques or mechanisms for retrieval of these compounds include: (1) Microwave–assisted extraction (MAE) (Shi et al., 2022) (2) vacuum filtration (Iftekhar et al., 2023), (3) solvent extraction (Singh et al., 2024b), (4) two–step molecular distillation (Kim, 2015), (4) liquid–liquid extraction (del Pozo et al., 2018), etc. Hossain et al. (2017) conducted a study aimed at enhancing the yield of antioxidants, proposing a two–stage mechanically fluidised reactor (MFR) process that demonstrated favourable outcomes through the regulation of condenser and reactor temperatures.

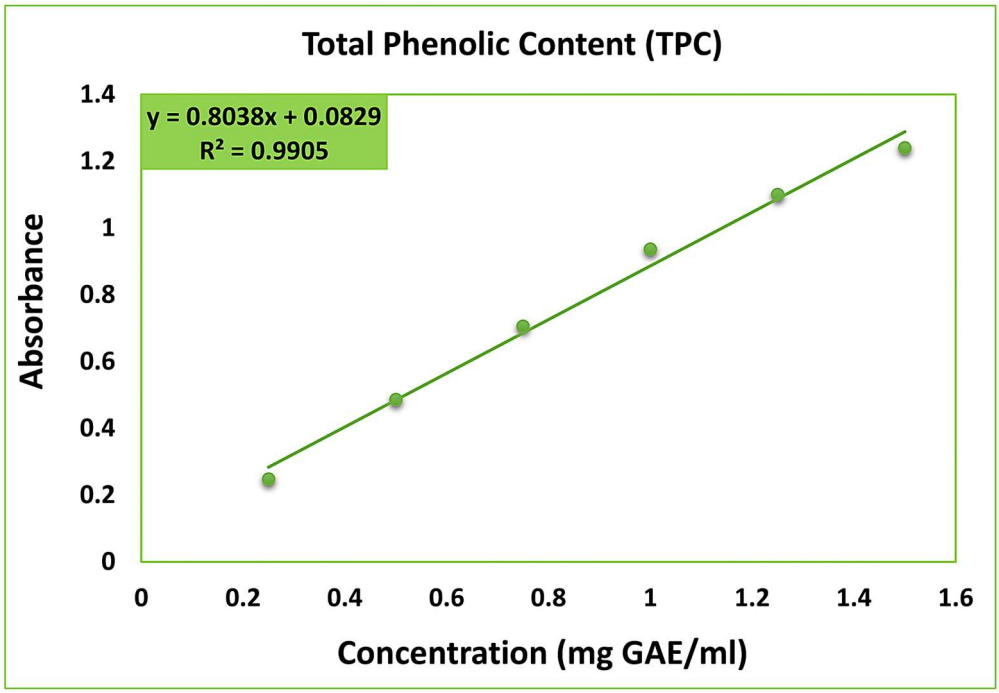


**Fig. 4.27.** Linear regression curve to quantify TPC of IS bio–oil.

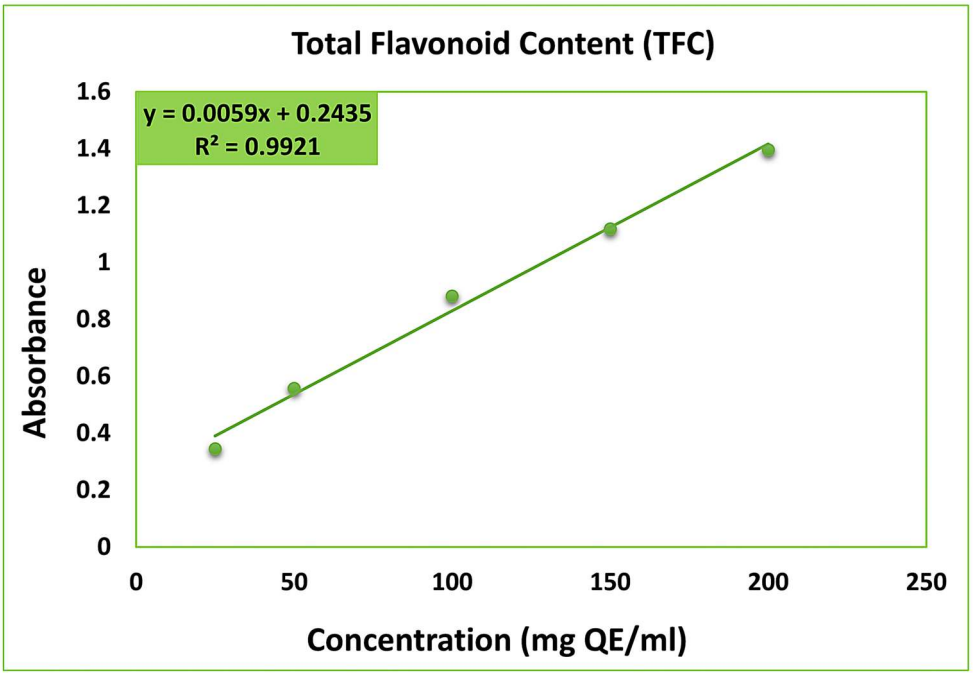


**Fig. 4.28.** Linear regression curve to quantify TFC of IS bio–oil.

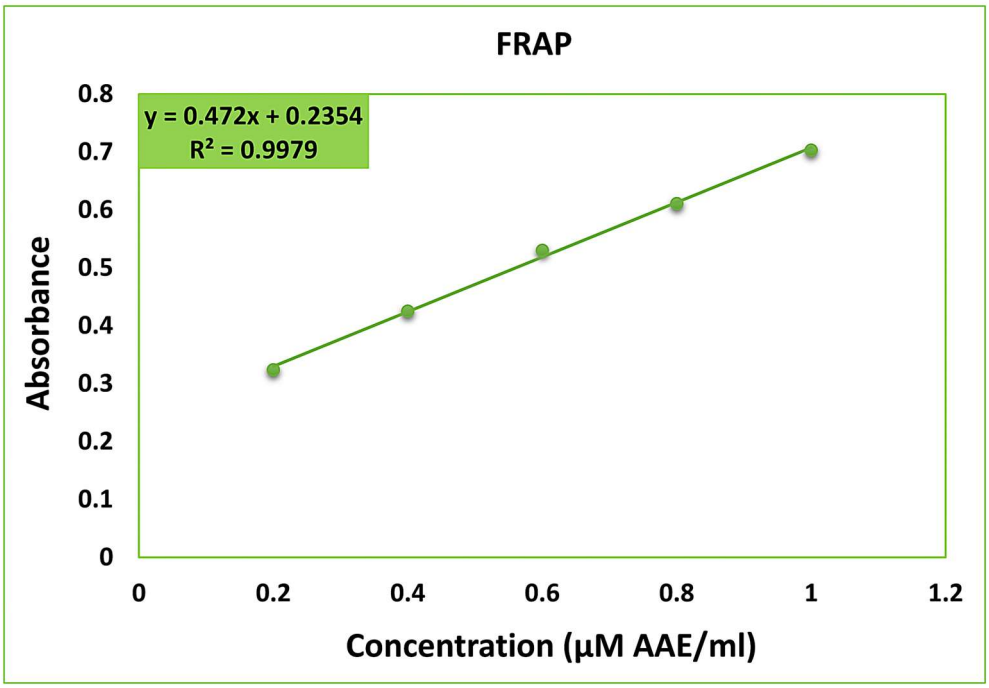


**Fig. 4.29.** Linear regression curve to quantify FRAP of IS bio–oil.

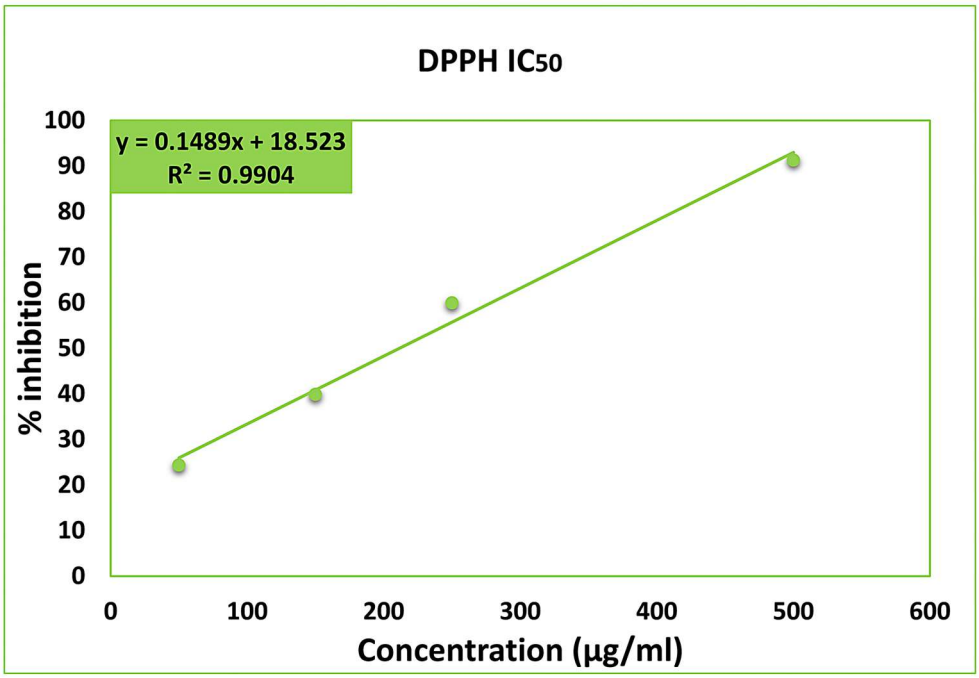


**Fig. 4.30.** Linear regression curve to quantify DPPH $IC_{50}$ of *A. adenophora* bio–oil.

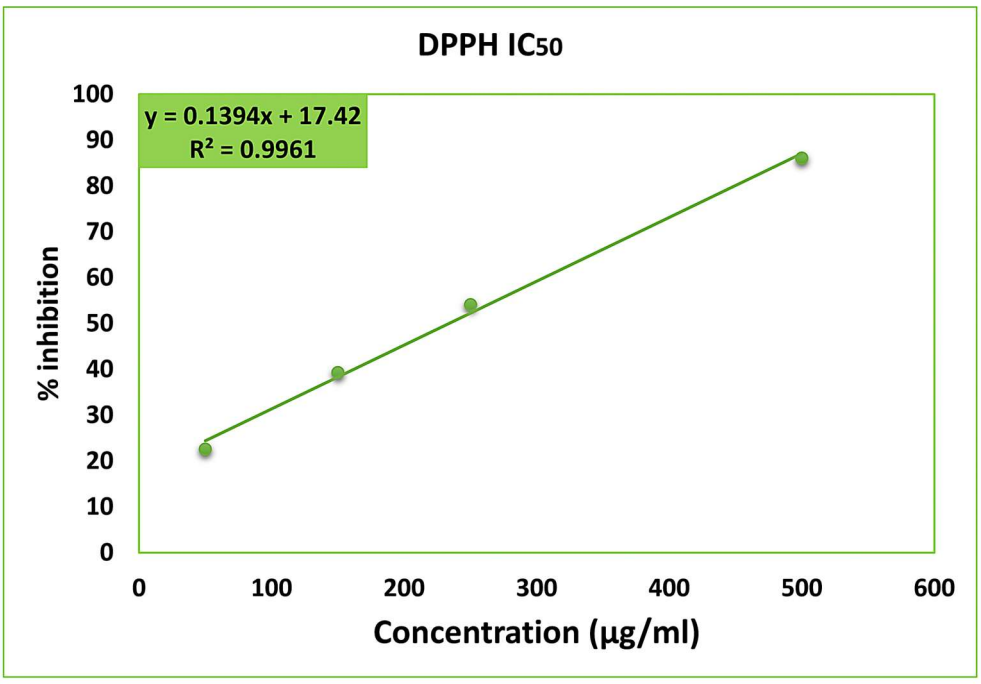


**Fig. 4.31.** Linear regression curve to quantify DPPH $IC_{50}$ of *L. camara* bio–oil.

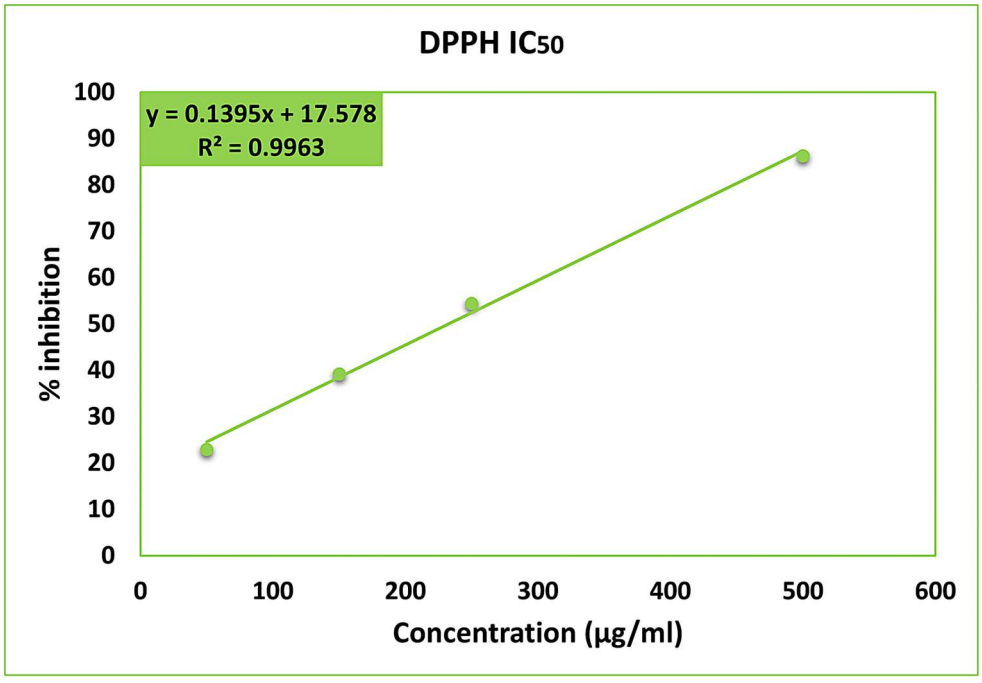


**Fig. 4.32.** Linear regression curve to quantify DPPH $IC_{50}$ of *S. jamaicensis* bio–oil.

## 4.11. Antimicrobial activity of bio–oil

Antimicrobial resistance (AMR) represents critical global health issues stemming from inappropriate over–utilization of antibiotics, prompting the emergence of resistant pathogens. This misuse of antibiotics in both human and animal health signals a looming "Silent Pandemic", driven by rapid spread of resistance genes, that could surpass other causes of mortality by 2050 (Ahmed et al., 2024). This situation underscores the urgency of investigating alternate approaches to address the microbial contagions.

Given the complex composition of organic compounds in the bio–oil, this study sought to investigate its antimicrobial activity. Consequently, agar–well diffusion and microbroth dilution method were used to assess the antimicrobial efficacy of *A. adenophora*, *L. camara* and *S. jamaicensis* bio–oil. Among the test microorganisms, all three bio–oils exhibited highest zone of inhibition (ZOI) against fungus *Candida albicans*. ZOI of the bio–oils against *C. albicans* (descending order) was *L. camara* (31.02 ± 0.9 mm) > *A. adenophora* (27.7 ± 0.2 mm) > *S. jamaicensis* (19.48 ± 0.8 mm). *L. camara* bio–oil exhibited superior antifungal potency. Table 4.15 details the antimicrobial efficacy of the bio–oils against the tested microbes. Fig. 4.33, Fig. 4.34 and Fig. 4.35 displays the antimicrobial assay of *A. adenophora*, *L. camara* and *S. jamaicensis*, respectively. Furthermore, a quantitative analysis employing MIC evaluated the minimum concentration of bio–oil vital to suppress microbial growth (Data presented in Table 4.15). Fig. 4.36, Fig. 4.37, Fig. 4.38 and Fig. 4.39 displays the MIC of *A. adenophora*, *L. camara*, *S. jamaicensis*, and antibiotics, respectively. Bio–oil from *A. adenophora* and *S. jamaicensis* demonstrated notable antimicrobial potency exhibiting MIC value of 6.25 µg/ml against all tested microbes which aligns in close proximity with the established antibiotics range from 3.125 – 25 µg/ml. *L. camara* bio–oil displayed superior performance here as well against *C. albicans* achieving MIC value of 3.125 µg/ml, while maintaining similar effectiveness against bacteria at 6.25 µg/ml. The antimicrobial property of bio–oil stems from its intricate range of compounds, which play significant role in inhibiting microbial growth. Aromatic hydrocarbons and N–containing compounds evident from spectroscopic analyses (FTIR, GC–MS and NMR) have been previously reported for their biocidal

activity in countering bacterial growth (Scheibe et al., 2022). Compounds detected during GC–MS, such as Phenol, 2–methoxy–, Phenol, 2,6–dimethoxy–, Pyridine, 2–methyl–, 2–methyl–, and 2–Cyclopenten–1–one are widely acknowledged for their antimicrobial activity (Nandhini et al., 2021; Scheibe et al., 2022). Additionally, Eicosane, 1–iodo– detected in *S. jamaicensis* bio–oil have been documented to exhibit antifungal activity (Bhat et al., 2024). Presence of organic acids, phenolic derivatives and acid carbonyls in bio–oil effectively suppresses microbial growth and activity (Mattos et al., 2019). Furthermore, the bio–oil's antimicrobial activity may be a consequence of the structural vulnerability of gram–positive bacteria with its mono cytoplasmic membrane and thick peptidoglycan wall as well as its interaction with intracellular $Ca^{2+}$ in gram–negative bacteria metabolism making them susceptible to injury (Suresh et al., 2016). An alternative explanation demonstrates phenolic chemicals in bio–oil causes the constituents of bacterial cell to leak through cell membrane, modify permeability and inhibit key enzymes (Savoia, 2012; Dias et al., 2023). There are reports on antimicrobial activity of extracts from *A. adenophora* (Ren et al., 2022), *L. camara* (Gowda et al., 2022) and *S. jamaicensis* (Utami et al., 2022; Fatmawati et al., 2023). However, till date there are no reports on antimicrobial activity of pyrolytic bio–oil sourced from these plants. Bio–oil contain a plethora of organic compounds and it is quite arguable to expect the discovery of potential pharmaceuticals from bio–oil for futuristic drug discovery. Extraction methods (including distillation, solvent extraction) and purification and separation techniques [such as capillary electrophoresis (CE), gas chromatography (GC), high–performance liquid chromatography (HPLC), supercritical fluid chromatography (SFC), and thin–layer chromatography (TLC)], may be further employed to analyse the antimicrobial compounds in the bio–oils. Advanced purification and separation techniques will further contribute significantly towards developing potential strategies to source antimicrobial agents from the bio–oils.

Plant–derived compounds remain a crucial focus for the discovery of novel bioactive compounds that can combat antibiotic resistant genes, despite the widespread availability of synthetic antimicrobial agents (Vaou et al., 2021). In light of the increasing concerns encompassing antibiotic resistance, the application of *A.*

*adenophora*, *L. camara* and *S. jamaicensis* bio–oil could offer innovative strategies for developing novel antimicrobial drugs. Additional investigation is crucial to assess their suitability and determine their effectiveness in clinical settings.

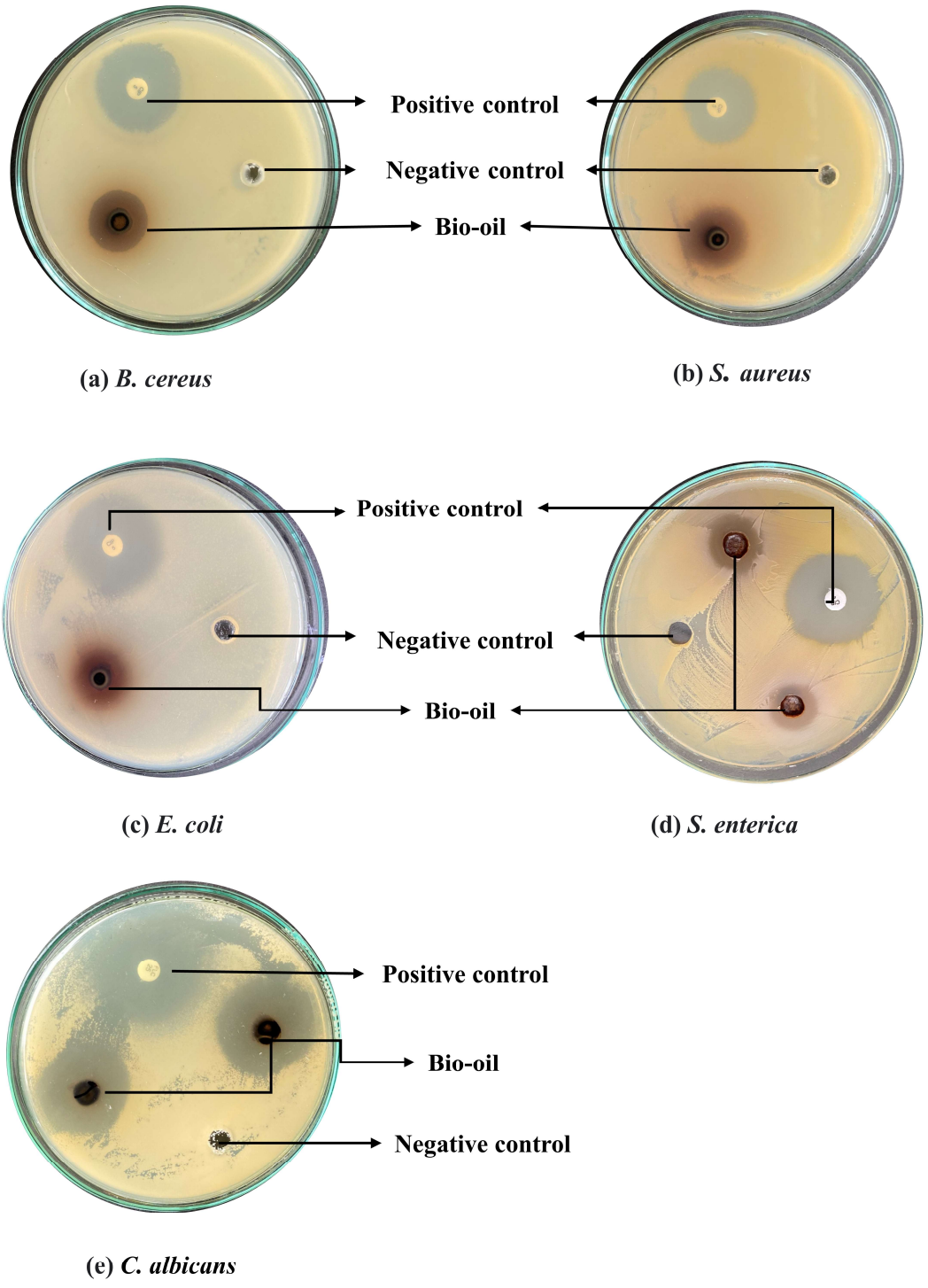


**Fig. 4.33.** ZOI of *A. adenophora* bio–oil against (a) *Bacillus cereus* (b) *Staphylococcus aureus* (c) *Escherichia coli* (d) *Salmonella enterica* and (e) *Candida albicans*

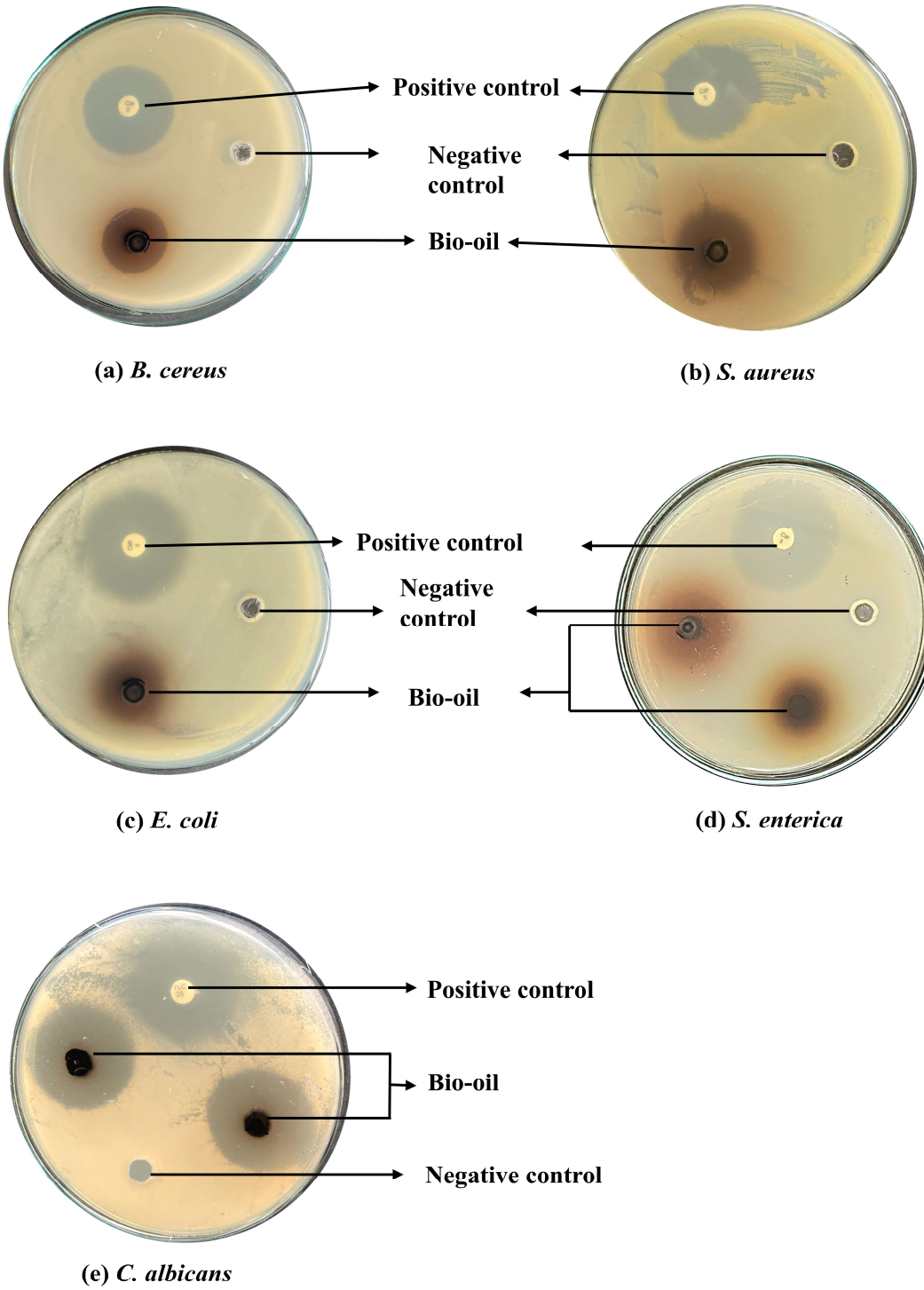


**Fig. 4.34.** ZOI of *L. camara* bio–oil against (a) *Bacillus cereus* (b) *Staphylococcus aureus* (c) *Escherichia coli* (d) *Salmonella enterica* and (e) *Candida albicans*

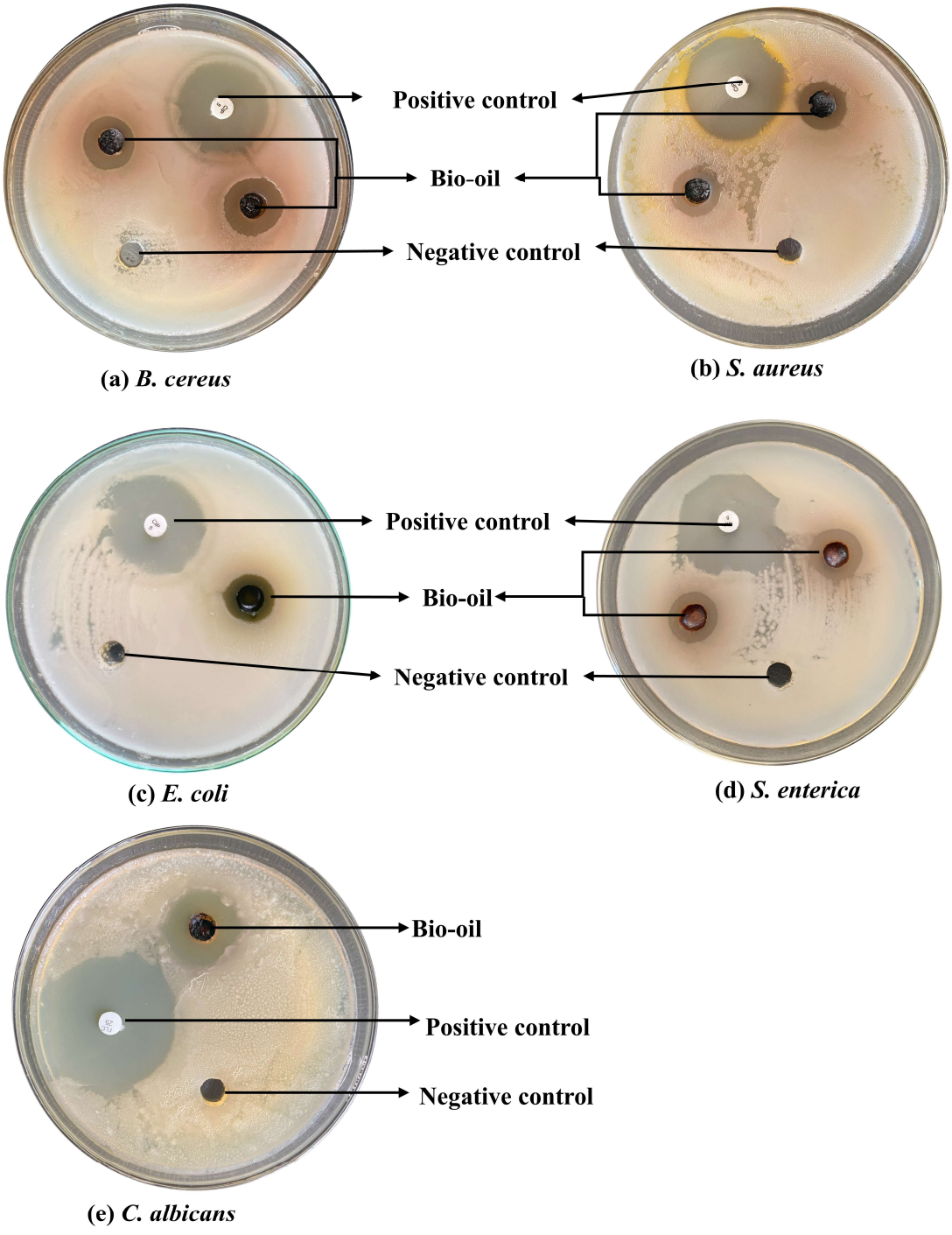


**Fig. 4.35.** ZOI of *S. jamaicensis* bio–oil against (a) *Bacillus cereus* (b) *Staphylococcus aureus* (c) *Escherichia coli* (d) *Salmonella enterica* and (e) *Candida albicans*

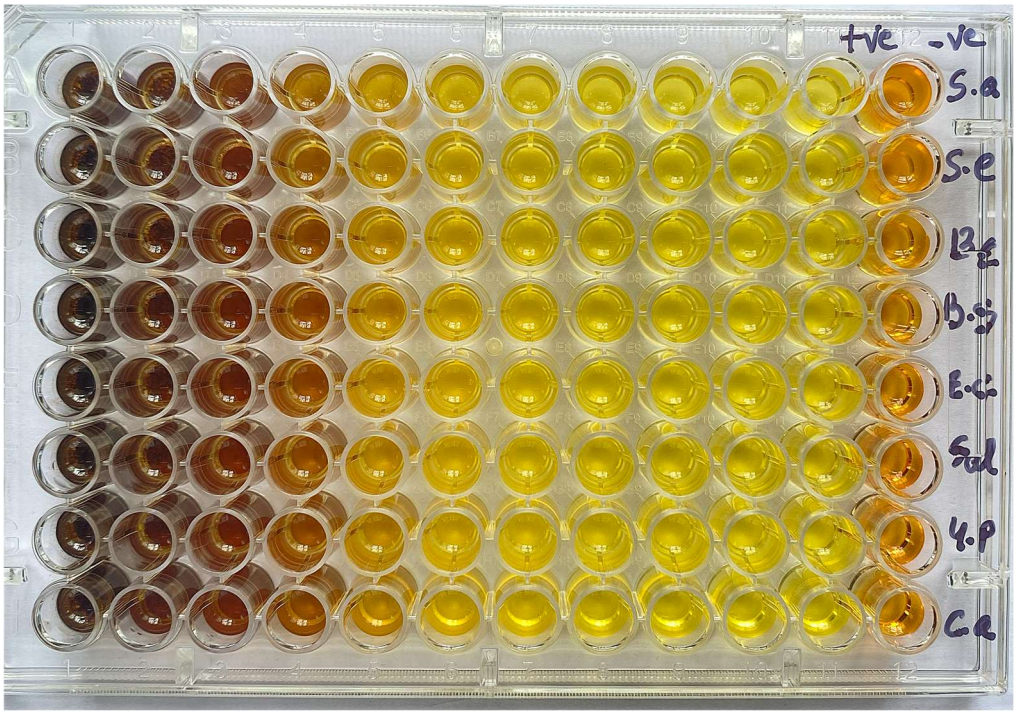


**Fig. 4.36.** MIC of *A. adenophora* bio–oil.


**Fig. 4.37.** MIC of *L. camara* bio–oil.

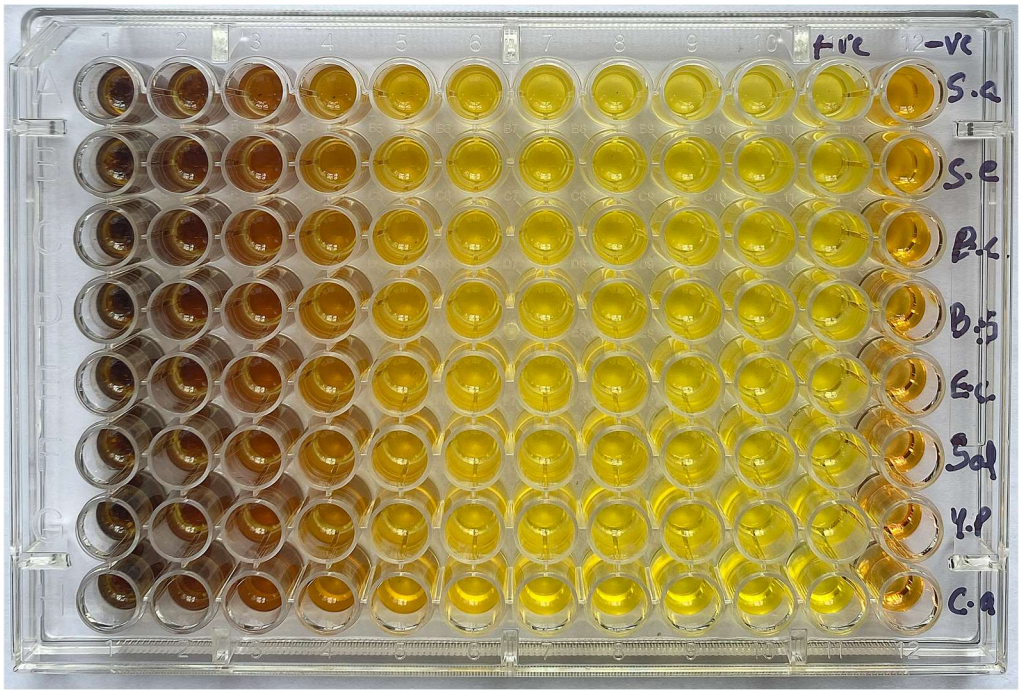


**Fig. 4.38.** MIC of *S. jamaicensis* bio–oil.


**Fig. 4.39.** MIC of antibiotics Azithromycin (bacteria) and Flucanozole (fungus).

**Table 4.15.** Antimicrobial activity of IS bio–oil.

| Species | Test microorganisms | ZOI of bio–oil (mm) | Positive control (mm) | MIC (µg/ml) |
|---|---|---|---|---|
| *A. adenophora* | *S. aureus* | 24.46±0.8 | 28.13±0.6 | 6.25 |
| | *B. cereus* | 17.86±0.7 | 27.16±0.5 | 6.25 |
| | *S. enterica* | 14.51±1.1 | 29.64±0.8 | 6.25 |
| | *E. coli* | 22.78±0.5 | 29.29±0.2 | 6.25 |
| | *C. albicans* | 27.7±0.2 | 32.39±0.4 | 6.25 |
| *L. camara* | *S. aureus* | 20.96±1.4 | 27.04±0.5 | 6.25 |
| | *B. cereus* | 20.75±0.6 | 26.33±0.6 | 6.25 |
| | *S. enterica* | 17.16±1.2 | 28.98±0.4 | 6.25 |
| | *E. coli* | 19.68±0.3 | 28.19±0.5 | 6.25 |
| | *C. albicans* | 31.02±0.9 | 32.9±0.8 | 3.125 |
| *S. jamaicensis* | *S. aureus* | 15.35 ± 0.2 | 30.74 ± 0.6 | 6.25 |
| | *B. cereus* | 17.28 ± 0.14 | 25.92 ±1.1 | 6.25 |
| | *S. enterica* | 14.6 ± 0.07 | 31.67 ± 1.3 | 6.25 |
| | *E. coli* | 12.82 ± 1.1 | 29.75 ± 0.3 | 6.25 |
| | *C. albicans* | 19.48 ± 0.8 | 36.35 ± 1.4 | 6.25 |
| Antibiotics | *S. aureus* | | | 6.25 |
| | *B. cereus* | | | 6.25 |
| | *S. enterica* | | | 6.25 |
| | *E. coli* | | | 3.125 |
| | *C. albicans* | | | 25 |

*Positive control (for bacteria) = Ciprofloxacin; Positive control (for fungus) = Fluconazole.

*Antibiotic (for bacteria) = Azithromycin; Antibiotic (for fungus) = Fluconazole.

## 4.12. Molecular docking analysis

### 4.12.1. Homology modelling of NUDT5 Protein

Homology modelling was performed to generate NUDT5 protein for use in subsequent molecular docking studies. Six models were generated through homology modelling of the 5NWH protein using Swiss Model web server based on its FASTA sequence. Model 3, among the generated models, with its superior GMQE value (Waterhouse et al., 2024) and QMEANDisCo Global Score (Studer et al., 2019) of 0.89 and 0.86 ± 0.05, respectively, emerged as the leading and most reliable model. Table 4.16 presents the outcomes of the generated models.

With a minimal 0.98 % outliers (e.g., BI76 ASN and A66 PRO), Ramachandran plot for Model 3 (Fig. 4.40) suggested precise backbone dihedral angles, displaying 96.81 % of residues positioned in favoured regions. A minor geometric concern was indicated due to a single C–beta deviation (A71 THR) while no bad bonds were apparent. With a low MolProbity score complemented by an excellent clash score (1.32 and 0.78, respectively), suggesting negligible steric clashes, MolProbity analysis further validated the quality of the modelled protein structure (Chen et al., 2009). Q mean based structure validation is presented in Fig. 4.41. The figure underscores the high quality of generated model, featuring a red star that represents the NUDT5 protein structure, which aligns with the score range noted in a nonredundant set of PDB structures of comparable size. ProSA–Z score of homology modelling–generated NUDT5 protein model is illustrated in Fig. 4.42 while Swiss Model–generated local quality estimate graph is displayed in Fig. 4.43 to offer comprehensive insights into model quality. Fig. 4.44 presents the final modelled structure of NUDT5. Overall, the structure demonstrated high accuracy rendering it appropriate for subsequent docking studies.

**Table 4.16.** Homology modelling of 5NWH protein**.**

| MODELS | GMQE | QSQE | METHOD | OLIGO STATE |
|---|---|---|---|---|
| **MODEL 1** | 0.86 | 0.85 | X–Ray, 2.50 Å | Homo Dimer |
| **MODEL 2** | 0.88 | 0.83 | X–Ray, 2.50 Å | Homo Dimer |
| **MODEL 3** | 0.89 | 0.82 | X–Ray, 2.50 Å | Homo Dimer |
| **MODEL 4** | 0.88 | 0.82 | X–Ray, 2.50 Å | Homo Dimer |
| **MODEL 5** | 0.85 | 0.82 | X–Ray, 2.20 Å | Homo Dimer |
| **MODEL 6** | 0.85 | 0.82 | X–Ray, 2.20 Å | Homo Dimer |

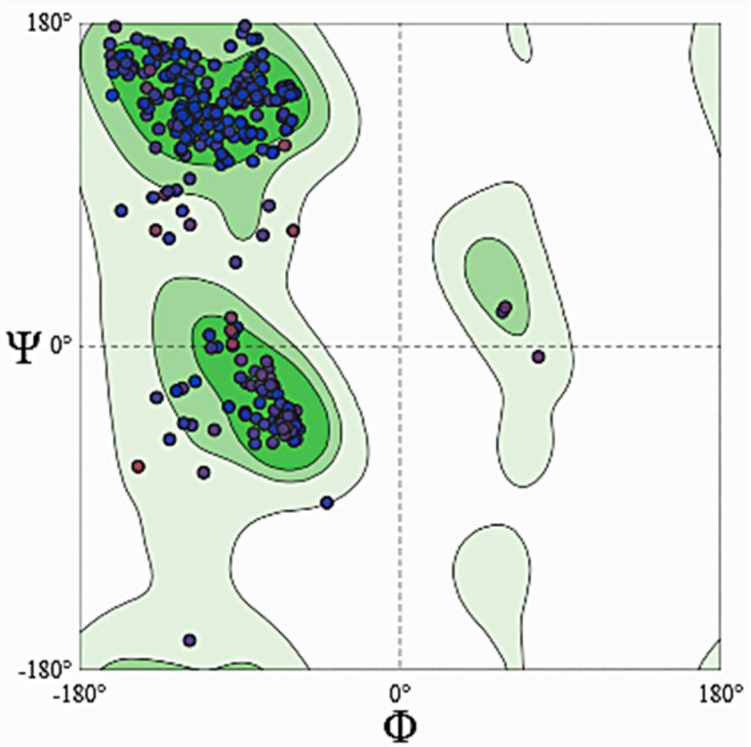


**Fig. 4.40.** The Ramachandran plot of NUDT5 protein (Model 03).

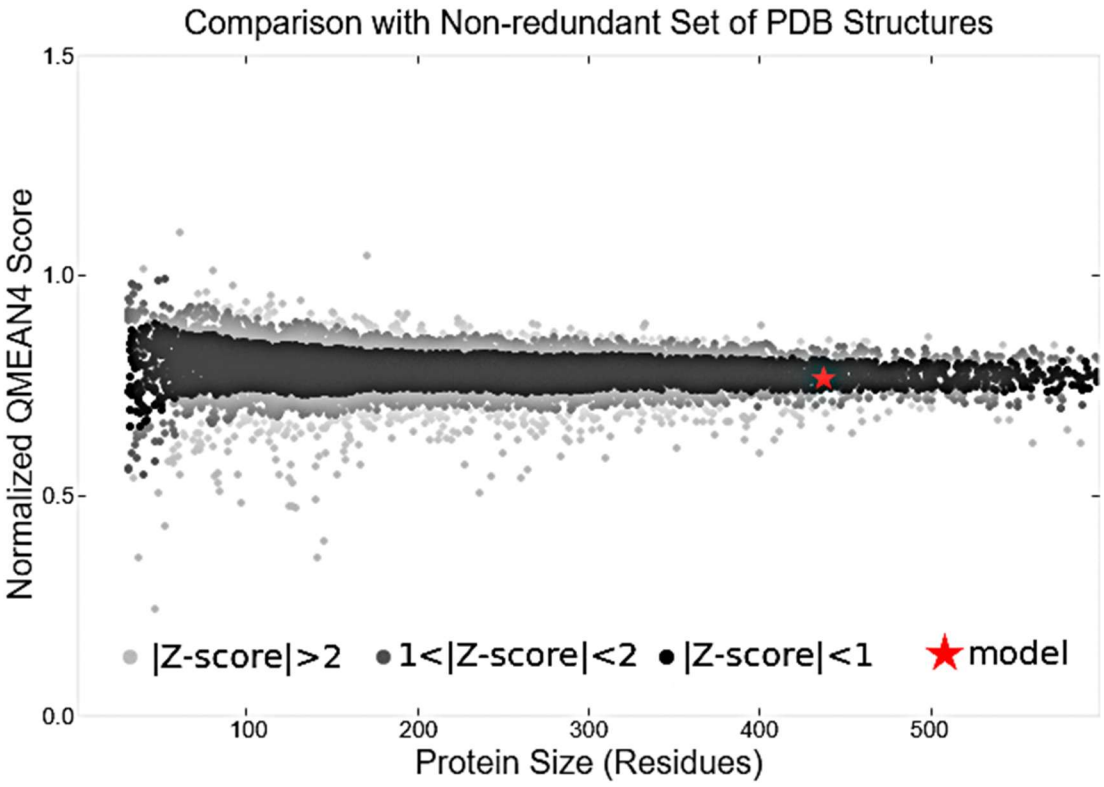


**Fig. 4.41.** Q mean based structure validation, the NUDT5 structure, represented by a red star, falls within the range of scores observed for a nonredundant set of PDB structures of similar size, highlighting its good quality.

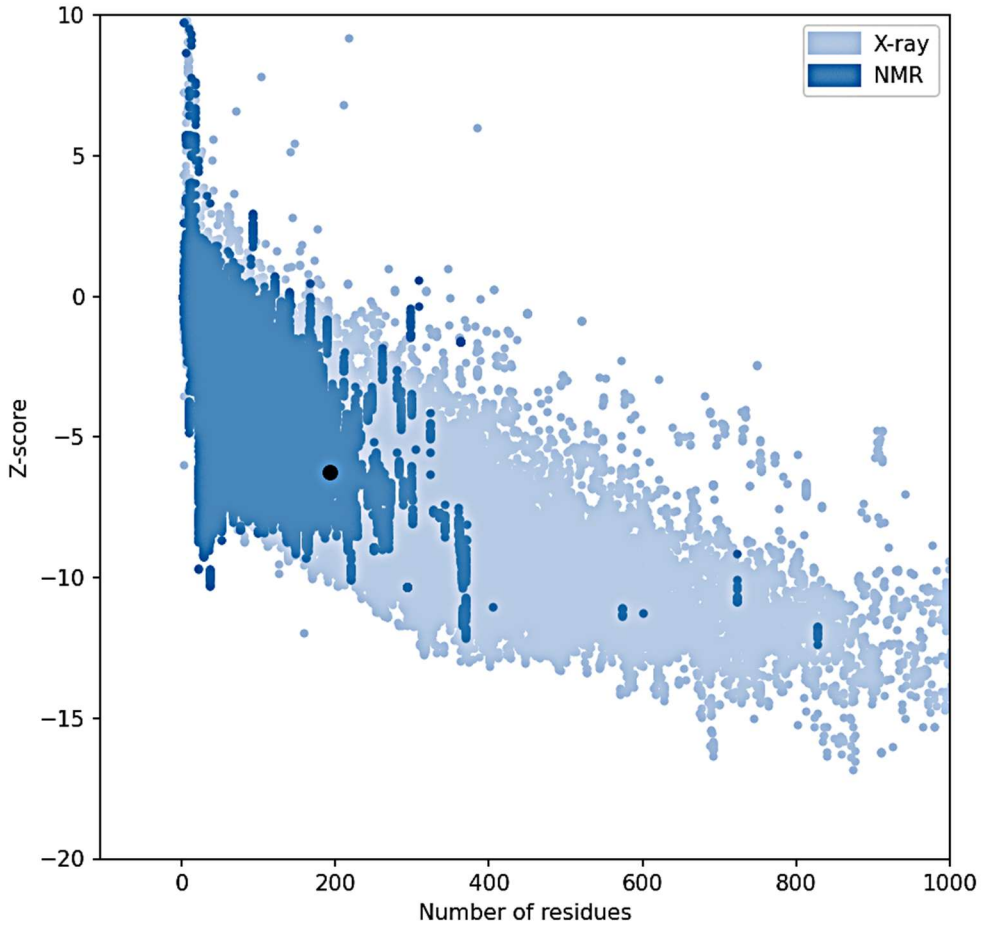


**Fig. 4.42.** Prosa Z score of NUTD5 protein (model 03).

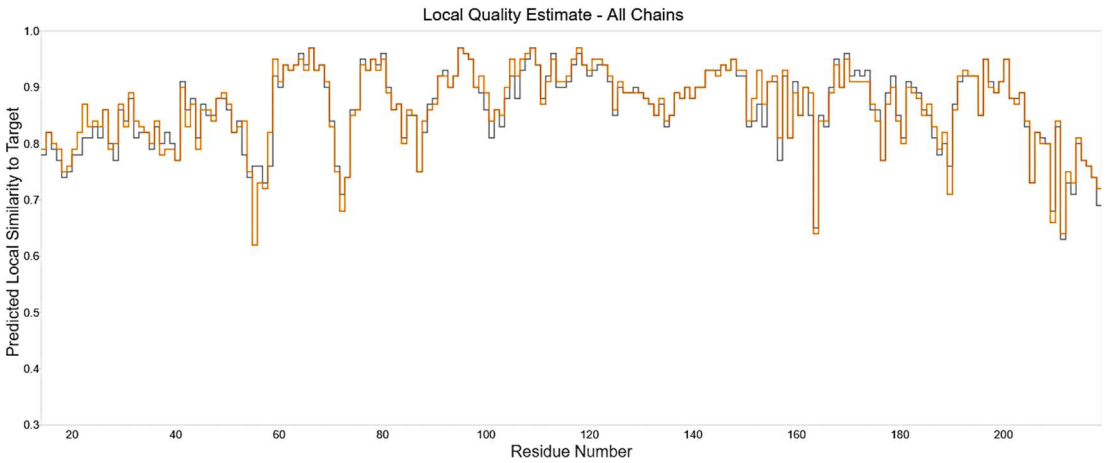


**Fig. 4.43.** Local quality estimate of NUDT5 protein (model 03).

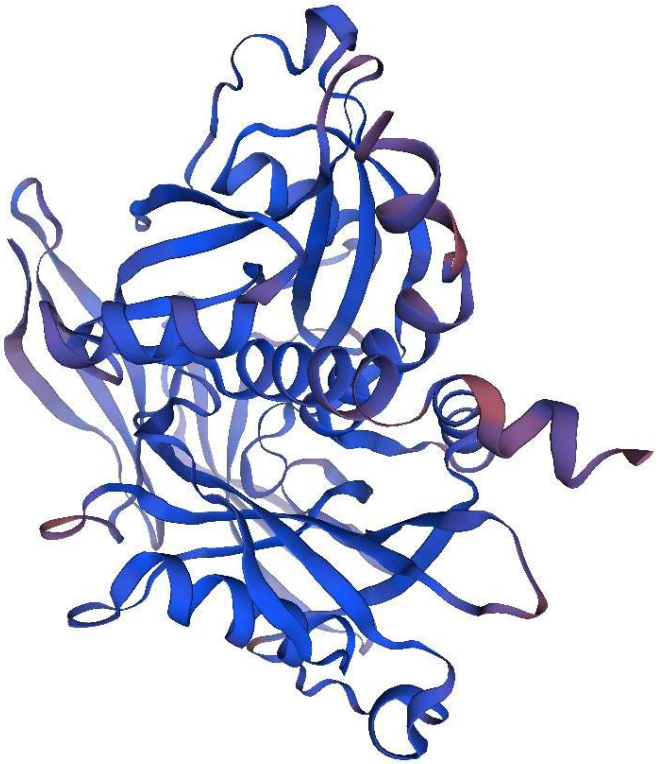

**Fig. 4.44.** Model 03 generated for NUDT5 protein.

### 4.12.2. Molecular Docking

Molecular docking simulations were performed to explore potential ligands targeting NUDT5 protein for breast cancer therapy. The molecular docking score for compounds detected in *A. adenophora*, *L. camara* and *S. jamaicensis* bio–oil with NUDT5 protein have been furnished in Table 4.17, Table 4.18 and Table 4.19, respectively. Molecular docking was performed for *A. adenophora* (27 ligands: 24 GC–MS detected compounds and 3 standard compounds) (Table 4.20), *L. camara* (34 ligands: 31 GC–MS detected compounds and 3 standard compounds) (Table 4.21) and *S. jamaicensis* bio–oil (27 ligands: 24 GC–MS detected compounds detected and 3 standard compounds) (Table 4.22) with Model 3 of NUDT5 protein (Fig. 4.44). The findings revealed significant binding affinities (BA) of several ligands with key residues within the active site, demonstrating varying degrees of interaction. The analysis and visualization docking results along with identification of specific interaction types were conducted using Biovia DS. BA were assessed along with Root mean square deviation (RMSD) to evaluate the binding stability.

Among the standard drugs, Letrozole and Exemestane each displayed the highest binding affinity (− 6.2 kcal/mol), closely followed by Anastrozole (− 5.6 kcal/mol). Despite this, it is noteworthy that these standards displayed widely varying RMSD values (Anastrozole: 16.57 – 18.89 Å; Exemestane: 15.29 − 17.04 Å), which might indicate less favourable binding pose stability or increased conformational deviation in some cases. Letrozole, however, showed a relatively lower RMSD range (1.18 − 6.08 Å), suggesting more reliable binding conformations. While the standard compounds exhibited comparatively higher BA and established interactions with multiple key residues within the active site, several test ligands also demonstrated compelling interaction patterns, underscoring their therapeutic potential. Exemestane, despite its high binding energy, showed no notable residue interactions (likely due to steric hindrance or conformational mismatch), the bioactive compounds displayed both favourable docking scores and meaningful interaction profiles, reinforcing their therapeutic potential.

Several test ligands from *A. adenophora* bio–oil demonstrated promising interactions. Among the tested ligands, Furaltadone with the strongest BA (– 6.4

kcal/mol), emerged as the most potent compound, surpassing the standard drugs. It formed multiple hydrogen bonds with Ala A:195, Gly A:97, Val A:62, Arg A:196, Glu A:93 along with π–alkyl interaction with Ala A:96. The compound maintained a moderately stable RMSD range (5.982 − 8.643 Å). Other notable ligands, for instance, Pyrimidine–2,4(1H,3H)–dione, 1–(5–aminomethyl–2–tetrahydrofuryl)–5–methyl (BA: −5.1 kcal/mol, RMSD: 2.534 − 5.809 Å) exhibited three similar binding residues with Anastrozole and Letrozole, 5,6,7,4'–Tetramethoxyflavanone (BA of – 5.6 kcal/mol, RMSD: 4.817 − 10.48 Å) shared three residue similarity with Anastrozole and two with Letrozole while Clofexamide (− 4.8 kcal/mol, RMSD: 2.691 − 3.559 Å) exhibited two and three common binding residues with Anastrozole and Letrozole, respectively. Despite their slightly lower BA values, these compounds demonstrated favourable binding poses and displayed significant overlap in interaction patterns with known therapeutics. Regardless of binding modes of interaction, a comparison between interaction of standards and ligands with residues revealed Ala A:96 as the most prominent residues. This finding demonstrated Ala A:96 established interactions with 14 of the docked compounds, underscoring its crucial role in ligand stabilization. Other prevalent residues noted as common interacting residues included Leu A:98, Arg A:196 and Gly A:97 emphasizing the potential candidature of compounds in focus for breast cancer treatment.

Molecular docking of *L. camara* revealed numerous compounds displaying significant interactions with NUDT5 protein. For instance, Phosphonic acid, (p–hydroxyphenyl)– (BA: − 4.5 kcal/mol, RMSD: 3.109 − 4.425 Å), Phenol, 4–ethyl–2–methyl– (BA: − 4.2 kcal/mol, RMSD: 2.371 − 4.086 Å), Indole (BA: − 3.9 kcal/mol, RMSD: 14.384 − 16.02 Å) and Toluene (BA: − 3.2 kcal/mol, RMSD: 13.386 − 14.772 Å), among others, each demonstrated three similar binding residues with Letrozole. Ala A:96 was a recurring interacting residue, establishing interactions with 21 of the docked compounds, emerged as the key residue, highlighting its significance in ligand stabilization. Occurrence of Ala A:96 highlighting their prominence in BA and specificity, was notable in the interaction profiles of standard Letrozole and Anastrozole, respectively. Other key residues included Leu A:98, Arg A:84 and Gly A:97. These findings suggest that many *L. camara* compounds, despite their lower

BA, target the same active site residues as standard drugs, indicating potential therapeutic relevance.

Numerous ligands derived from *S. jamaicensis* bio–oil exhibited favourable interactions. For instance, 3,5–Dimethoxy–4–hydroxytoluene (BA: −4.3 kcal/mol, RMSD: 0.66 – 3.71 Å) and 2–methoxyphenol (BA: −4.0 kcal/mol, RMSD: 3.36 – 4.61 Å) demonstrated interactions with critical residues such as Leu A:98, Gly A:97, Ala A:96 and Arg A:84, which are evidently significant in the standards' binding profiles. Arg A:84 was identified as the most frequently interacting residue within the ligand repertoire, engaging with 18 compounds and significantly contributing to ligand stabilization. Arg A:84 is also crucial in the binding of Anastrozole, underscoring its importance as a therapeutic target. Residues such as Ala A:96, Leu A:98, Arg A:51, Gly A:97 and Arg A:196 were consistently observed across several ligand interactions, indicating a conserved binding hotspot within the active site of NUDT5 protein. Additional ligands, Clofexamide (BA: − 4.8 kcal/mol), D–Allose (BA: − 4.8 kcal/mol) and 6,6,9a–Trimethyl–decahydronaphtho[1,2–c] furan–1,4–dione (BA: − 5.2 kcal/mol) engaged with many critical residues, signifying distinct pharmacological significance.

Although the standard compounds exhibited enhanced BA due to their clinically optimized structures, the docked compounds demonstrated interactions with residues (Arg A:51, Arg A:196, Arg A:84, Arg A:111, Glu A:112, Glu A:166, Ala A:96, Gly A:97 and Leu A:98), with some sharing similar binding sites with the established standards. These binding affinities to crucial residues within the active site mimicked the interactions evident with recognised breast cancer therapeutics including Letrozole and Anastrozole. Furthermore, several test ligands had low RMSD values, often below 3.0 Å, implying consistent and stable docking poses that further strengthen their candidature for drug development. Among the standards, Anastrozole showed notable binding to significant residues such as Glu A:166, Glu A:112, Arg A:84, Arg A:196 and Arg A:51 while Letrozole displayed interactions with Gly A:97, Ala A:96, Leu A:98, Arg A:111 and Arg A:196 highlighting their high interaction properties. Contrastingly, no notable interaction was exhibited by Exemestane, possibly due to structural incompatibility or steric hindrances that obstructed its access to binding

pocket. The crucial role of specific residues in encouraging binding within active site of NUDT5 protein is underscored through the comparative analysis of residue interaction with docked ligands and standard compounds. A comparable investigation by Ruswanto et al. (2022), identified Leu A:98 and Arg A:84 as crucial residues involved in interaction with target NUDT5 protein, highlighting their prominence in BA and specificity. The outcomes highlight the prospects of identified ligands of *A. adenophora*, *S. jamaicensis* and *L. camara* bio–oil as effective NUDT5 inhibitors, presenting a promising avenue in the development of novel breast cancer therapeutics. These results collectively indicate that these natural ligands, albeit having lower BA, are not inherently inferior in therapeutic efficacy, relative to their binding mechanisms. Owing to their consistent interaction with critical residues and favourable RMSD values, these ligands emerge as promising candidates for use as adjunctive or synergistic agents in combination therapies. Their advancement into in–vivo and in–vitro validation studies, whether independently or in conjunction with established drugs like Anastrozole or Letrozole etc, may facilitate novel NUDT5–targeting approaches in breast cancer therapy. Investigations conducted by Page et al. (2018) and Sultana (2019) identified NUDT5 as a promising candidate for drug targeting breast cancer therapy.

It is noteworthy that while the compounds detected in the bio–oil have previously been extracted from other sources and well–documented for their bioactive assays, the current study presents a distinct approach by utilizing a different feedstock that is both cost–effective and abundantly available. Consequently, this study offers a sustainable and economically viable approach demonstrating the potential of bio–oil as a valuable and underutilized source of bioactive compounds which may be extracted from it through suitable techniques [solvent extraction, liquid–liquid extraction, molecular distillation, microwave–assisted extraction (MAE) and chromatographic techniques such as gas chromatography (GC), capillary electrophoresis (CE), thin–layer chromatography (TLC), high–performance liquid chromatography (HPLC), and supercritical fluid chromatography (SFC)]. This further enhances its pharmacological and commercial significance.

**Table 4.17**. Molecular docking score for compounds detected in *A. adenophora* bio–oil with NUDT5 protein.

| COMPOUNDS | BA | RMSD LB | RMSD UB |
|---|---|---|---|
| Furaltadone | –6.4 | 5.982 | 8.643 |
| LETROZOLE | –6.2 | 1.182 | 6.086 |
| EXEMESTANE | –6.2 | 15.297 | 17.041 |
| ANASTROZOLE | –5.6 | 16.572 | 18.895 |
| 5,6,7,4'–Tetramethoxyflavanone | –5.6 | 4.817 | 10.48 |
| Pyrimidine–2,4(1H,3H)–dione, 1–(5–aminomethyl–2–tetrahydrofuryl)–5–methyl | –5.1 | 2.534 | 5.809 |
| Clofexamide | –4.8 | 2.691 | 3.559 |
| Cyclopentanecarboxylic acid, 3,3–dimethyl–4–oxo– | –4.8 | 1.553 | 2.195 |
| Phosphonic acid, (p–hydroxyphenyl)– | –4.5 | 0.863 | 2.195 |
| Trans,cis–1,8–dimethylspiro[4.5]decane | –4.4 | 14.568 | 16.42 |
| .beta.–L–Arabinopyranoside, methyl | –4.2 | 1.808 | 3.271 |
| 2,4,6–Cycloheptatrien–1–one, 2–hydroxy– | –4.2 | 1.777 | 2.797 |
| 1,2–Cyclobutanedicarboxylic acid, cis– | –4.2 | 1.716 | 2.78 |
| Phenol, 2,6–dimethoxy | –4.2 | 0.024 | 3.838 |
| 1,4:3,6–Dianhydro–.alpha.–d–glucopyranose | –4.1 | 1.159 | 1.995 |
| Morpholine, 4–octadecyl– | –4 | 15.568 | 17.614 |
| Phenol, 3–methyl– | –3.9 | 0.776 | 2.316 |
| Phenol, 2–methoxy– | –3.9 | 2.615 | 3.628 |
| Indole | –3.8 | 15.39 | 16.44 |
| Methylenecyclopropanecarboxylic acid | –3.7 | 2.084 | 3.019 |
| Z,Z–6,28–Heptatriactontadien–2–one | –3.6 | 1.593 | 2.496 |
| 5–Clorovaleric acid, 2–dimethylaminoethyl ester | –3.5 | 1.976 | 2.766 |
| Butanoic acid, 2–methyl– | –3.5 | 1.504 | 2.542 |
| 2–Cyclopenten–1–one, 2–methyl– | –3.4 | 11.618 | 12.471 |
| Cyclopentene, 1–(1–methylethyl)– | –3.4 | 13.252 | 15.419 |

| | | | |
|---|---|---|---|
| Spiro[2,4]hepta–4,6–diene | –3.3 | 13.583 | 15.054 |
| Boraneamine, n–ethyl–1,1–dipropyl– | –2.8 | 13.51 | 15.14 |

**Table 4.18**. Molecular docking score for compounds detected in *L. camara* bio–oil with NUDT5 protein.

| COMPOUNDS | BA | RMSD LB | RMSD UB |
|---|---|---|---|
| LETROZOLE | –6.2 | 1.182 | 6.086 |
| EXEMESTANE | –6.2 | 15.297 | 17.041 |
| ANASTROZOLE | –5.6 | 16.572 | 18.895 |
| Naphthalene, 1,4,6–trimethyl– | –5.1 | 2.009 | 3.821 |
| Butylated hydroxytoluene | –4.7 | 15.238 | 16.928 |
| Neophytadiene | –4.7 | 2.86 | 7.734 |
| Phosphonic acid, (p–hydroxyphenyl)– | –4.5 | 3.109 | 4.425 |
| 2–Phenethyl–beta–phenylpropionate | –4.2 | 14.849 | 16.527 |
| Phenol, 3–propyl– | –4.2 | 15.678 | 16.869 |
| Phenol, 4–ethyl–2–methyl– | –4.2 | 2.371 | 4.086 |
| 9,12–Octadecadienoic acid (z,z)– | –4.1 | 13.441 | 15.185 |
| Phenol, 2,6–dimethoxy | –4.1 | 0.098 | 3.903 |
| Phenol, 3–ethyl– | –4.1 | 2.471 | 3.43 |
| Cyclotrisiloxane, hexamethyl– | –4.1 | 0.06 | 4.06 |
| 1R,2c,3t,4t–Tetramethyl–cyclohexane | –4 | 12.836 | 15.691 |
| Indolizine, 7–methyl– | –4 | 14.003 | 15.656 |
| 6–Methylheptyl 2–methylbutanoate | –3.9 | 14.176 | 17.432 |
| Formic acid, 2–methoxyphenyl ester | –3.9 | 2.343 | 3.356 |
| Fumaric acid, 3,4–dimethylphenyl octyl ester | –3.9 | 1.841 | 3.348 |
| Indole | –3.9 | 14.384 | 16.02 |
| Phenol, 2,3–dimethyl– | –3.9 | 1.094 | 2.615 |
| Phenol, 3–methyl– | –3.9 | 0.77 | 2.35 |
| 3–n–Hexylthiolane, S,S–dioxide | –3.8 | 14.862 | 15.98 |
| D–limonene | –3.8 | 14.1 | 17.351 |
| Methyl 11–methyl–dodecanoate | –3.8 | 14.327 | 16.372 |
| Benzene, 4–ethenyl–1,2–dimethyl– | –3.7 | 12.378 | 14.224 |
| Hentriacontane | –3.7 | 2.543 | 7.45 |
| Mesitylene | –3.7 | 12.29 | 14.689 |
| Phenol, 2–methyl– | –3.7 | 13.805 | 14.587 |
| Z–28–Heptatriaconten–2–one | –3.7 | 1.65 | 3.867 |

| | | | |
|---|---|---|---|
| Z,Z–6,28–Heptatriactontadien–2–one | –3.6 | 1.787 | 7.89 |
| EthylBenzene | –3.5 | 14.658 | 15.82 |
| Eicosyl isopropyl ether | –3.4 | 14.62 | 16.453 |
| Toluene | –3.2 | 13.386 | 14.772 |

**Table 4.19**. Molecular docking score for compounds detected in *S. jamaicensis* bio–oil with NUDT5 protein.

| COMPOUNDS | BA | RMSD LB | RMSD UB |
|---|---|---|---|
| LETROZOLE | –6.2 | 1.182 | 6.086 |
| EXEMESTANE | –6.2 | 15.297 | 17.041 |
| ANASTROZOLE | –5.6 | 16.572 | 18.895 |
| 6,6,9a–Trimethyl–decahydronaphtho[1,2–c]furan–1,4–dione | –5.2 | 15.463 | 18.011 |
| 2–Isobornyloxy–tetrahydropyran | –4.8 | 1.517 | 2.764 |
| Clofexamide | –4.8 | 2.566 | 3.127 |
| D–Allose | –4.8 | 1.785 | 3.284 |
| Sedoheptulosan | –4.8 | 1.492 | 3.822 |
| Phosphonic acid, (p–hydroxyphenyl)– | –4.5 | 2.808 | 4.65 |
| (1r,3as,5as,8ar)–1,3a,5a–Trimethyl–4–methylenedecahydrocyclopenta[c]pentalene | –4.4 | 13.711 | 15.715 |
| 3,5–Dimethoxy–4–hydroxytoluene | –4.3 | 0.666 | 3.718 |
| Phenol, 2,6–dimethoxy– | –4.2 | 0.067 | 3.838 |
| 1,4 3,6–Dianhydro–.alpha.–d–glucopyranose | –4.1 | 1.051 | 2.233 |
| 4–n–Hexylthiane, S,S–dioxide | –4.1 | 14.306 | 15.655 |
| 2–Ethyl–5–propylcyclopentanone | –4 | 14.514 | 16.216 |
| Phenol, 2–methoxy– | –4 | 3.367 | 4.611 |
| Hydroquinone | –3.9 | 0.055 | 3.23 |
| Z,Z–6,28–Heptatriactontadien–2–one | –3.8 | 1.804 | 5.537 |
| 3–n–Butylthiolane, S,S–dioxide | –3.7 | 14.655 | 15.932 |
| 1,2–Ethanediol, dipropanoate | –3.6 | 3.693 | 4.628 |
| Methylenecyclopropanecarboxylic acid | –3.6 | 2.804 | 3.488 |
| 1,3–Propanediol, 2–methyl–, dipropanoate | –3.5 | 3.821 | 5.649 |
| 2–Cyclopenten–1–one, 2–methyl– | –3.4 | 13.269 | 13.669 |
| 2–Cyclopenten–1–one, 3–methyl– | –3.4 | 13.333 | 14.825 |
| Eicosane, 1–iodo– | –3.4 | 10.742 | 13.992 |

| | | | |
|---|---|---|---|
| Pyridine, 2–methyl– | –3.3 | 12.715 | 13.768 |
| Trifluoromethyl t–butyl disulfide | –3.1 | 14.548 | 15.998 |

**Table 4.20.** Interaction of ligands in *A adenophora* bio–oil with residues.

| Sl. No | Compound Name | Interactions | Residues |
|---|---|---|---|
| 1. | Anastrazole | *Conventional Hydrogen Bond* | Arg A:51, Arg A: 196 |
| | | *Carbon Hydrogen Bond* | Glu A:112 |
| | | *Pi–Cation* | Arg A:84 |
| | | *Pi–Anion* | Glu A:166 |
| 2. | Exemestane | *No Interactions* | |
| | | *Conventional Hydrogen Bond* | Arg A:196, Arg A:111 |
| 3. | Letrozole | *Pi–Donor Hydrogen Bond* | Leu A:98 |
| | | *Amide Pi–Stacked* | Ala A:96, Gly A:97 |
| | | *Pi–Alkyl* | Ala A:96, Gly A:97 |
| 4. | 5,6,7,4'–Tetramethoxyflavanone | *Conventional Hydrogen Bond* | Arg A:51, Arg A:84, Leu A:98, Arg A:111 |
| | | *Carbon Hydrogen Bond* | Asp A:100 |
| | | *Pi–Anion* | Glu A:112 |
| | | *Alkyl* | Met A:132, Ile A:141 |
| 5. | Pyrimidine–2,4(1H,3H)–dione, 1–(5–aminomethyl–2–tetrahydrofuryl)–5–methyl | *Conventional Hydrogen Bond* | Glu A:166, Arg A:196 |
| | | *Pi–Cation* | Arg A:84 |
| | | *Pi–Alkyl* | Ala A:96, Leu A:98 |
| 6. | Clofexamide | *Conventional Hydrogen Bond* | Arg A:84, Arg A:196 |

| | | | |
|---|---|---|---|
| | | *Pi–Sigma* | Gly A:97 |
| | | *Alkyl* | Leu A:98 |
| | | *Pi–Alkyl* | Leu A:98 |
| 7. | Cyclopentanecarboxylic acid, 3,3–dimethyl–4–oxo– | *Conventional Hydrogen Bond* | Arg A:84, Gly A:97 |
| | | *Carbon Hydrogen Bond* | Gly A:61 |
| 8. | Phosphonic acid, (p–hydroxyphenyl)– | *Conventional Hydrogen Bond* | Gly A:97, Val A:62 |
| | | *Carbon Hydrogen Bond* | Gly A:61 |
| | | *Amide Pi–Stacked* | Ala A:96 |
| | | *Pi–Alkyl* | Leu A:98 |
| 9. | Trans,cis–1,8–dimethylspiro[4.5]decane | *Alkyl* | Leu A:98, Ala A:96 |
| 10. | .beta.–L–Arabinopyranoside, methyl | *Conventional Hydrogen Bond* | Arg A:51, Arg A:196, Glu A:97 |
| 11. | 2,4,6–Cycloheptatrien–1–one, 2–hydroxy– | *Conventional Hydrogen Bond* | Arg A:196, Arg A:84, Glu A:93 |
| | | *Pi–Alkyl* | Ala A:96 |
| 12. | 1,2–Cyclobutanedicarboxylic acid, cis– | *Conventional Hydrogen Bond* | Val A:62, Gly A:97, Arg A:51 |
| 13. | Phenol, 2,6–dimethoxy | *Conventional Hydrogen Bond* | Arg A:84 |
| | | *Carbon Hydrogen Bond* | Glu A:166, Glu A:93 |
| | | *Alkyl* | Ala A:96 |
| | | *Pi–Alkyl* | Leu A:98, Ala A:96 |
| 14. | 1,4:3,6–Dianhydro–.alpha.–d–glucopyranose | *Conventional Hydrogen Bond* | Gly A:97, Val A:62 |
| 15. | Morpholine, 4–octadecyl– | *Alkyl* | Met A:132, Pro A:86, Met A:87, |

| | | | |
|---|---|---|---|
| | | | Arg A:84, Cys A:91 |
| 16. | Phenol, 3–methyl– | *Conventional Hydrogen Bond* | Val A:62 |
| | | *Pi–Alkyl* | Ala A:96 |
| 17. | Phenol, 2–methoxy– | *Conventional Hydrogen Bond* | Val A:62 |
| | | *Alkyl* | Cys A:139, Ile A:141 |
| | | *Pi–Alkyl* | Ala A:96, Leu A:98 |
| 18. | Indole | *Amide Pi–Stacked* | Ala A:96, Gly A:97 |
| | | *Pi–Alkyl* | Leu A:98 |
| 19. | Methylenecyclopropanecarboxylic acid | *Conventional Hydrogen Bond* | Arg A:196, Gly A:97 |
| | | *Alkyl* | Ile A:141, Leu A:98 |
| 20. | Z,Z–6,28–Heptatriactontadien–2–one | *Alkyl* | Arg A:84, Cys A:139, Met A:87, Ala A:195, Cys A:91, Met A:132, Pro A:86 |
| 21. | 5–Clorovaleric acid, 2–dimethylaminoethyl ester | *Alkyl* | Ala A:96 |
| 22. | Butanoic acid, 2–methyl– | *Conventional Hydrogen Bond* | Gly A:97 |
| 23. | 2–Cyclopenten–1–one, 2–methyl– | *Conventional Hydrogen Bond* | Arg A:196 |
| 24. | Cyclopentene, 1–(1–methylethyl)– | *Alkyl* | Leu A:98, Ala A:96 |
| 25. | Spiro[2,4]hepta–4,6–diene | *Alkyl* | Ala A:96, Ile A:141 |

| | | | |
|---|---|---|---|
| 26. | Boraneamine, n–ethyl–1,1–dipropyl– | *Hydrophobic Interaction* | Leu A:98, Ile A:141, Ala A:96, Ala A:63, Met A:132 |
| 27. | Furaltadone | *Conventional Hydrogen Bond* | Ala A:195, Gly A:97, Val A:62, Arg A:196 |
| | | *Carbon Hydrogen Bond* | Glu A:93 |
| | | *Pi–Alkyl* | Ala A:96 |

**Table 4.21.** Interaction of ligands in *L. camara* bio–oil with residues.

| Sl. No | Compound Name | Interactions | Residues |
|---|---|---|---|
| 1. | Anastrozole | *Conventional Hydrogen Bond* | Arg A:51, Arg A: 196 |
| | | *Carbon Hydrogen Bond* | Glu A:112 |
| | | *Pi–Cation* | Arg A:84 |
| | | *Pi–Anion* | Glu A:166 |
| 2. | Exemestane | *No Interactions* | |
| 3. | Letrozole | *Conventional Hydrogen Bond* | Arg A:196, Arg A:111 |
| | | *Pi–Donor Hydrogen Bond* | Leu A:98 |
| | | *Amide Pi–Stacked* | Ala A:96, Gly A:97 |
| | | *Pi–Alkyl* | Ala A:96, Gly A:97 |
| 4. | Naphthalene, 1,4,6–trimethyl– | *Alkyl* | Ala A:203, Ile A:65, Phe A:94, Arg A:196 |
| | | *Pi–Alkyl* | Arg A:196, Ile A:143 |
| 5. | Butylated hydroxytoluene | *Conventional Hydrogen Bond* | Asp A:194 |
| | | *Pi–Anion* | Glu A:93 |
| | | *Pi–Sulfur* | Met A:87 |
| | | *Alkyl* | Pro A:86, Arg A:84 |
| | | *Pi–Alkyl* | Arg A:84, Cys A:91 |
| 6. | Neophytadiene | *Alkyl* | Val A:130, Tyr A:200, Ala A:203 |
| | | *Pi–Alkyl* | Val A:130, Ile A:143, Tyr A:200, Arg A:196, Ala A:203 |
| 7. | Phosphonic acid, (p–hydroxyphenyl)– | *Conventional Hydrogen Bond* | Gly A:97, Val A:62, Arg A:196 |

| | | | |
|---|---|---|---|
| | | *Amide Pi–Stacked* | Ala A:96, Gly A:97 |
| | | *Pi–Alkyl* | Leu A:98 |
| 8. | 2–Phenethyl–beta–phenylpropionate | *Conventional Hydrogen Bond* | Ala A:195 |
| | | *Carbon Hydrogen Bond* | Asp A:194 |
| | | *Pi–Anion* | Glu A:93 |
| | | *Pi–Sulfur* | Met A:37 |
| | | *Pi–Alkyl* | Pro A:86, Cys A:91, Arg A:84 |
| 9. | Phenol, 3–propyl– | *Conventional Hydrogen Bond* | Ala A:96, Arg A:84 |
| | | *Pi–Sigma* | Gly A:97 |
| | | *Alkyl* | Ile A:141, Leu A:98 |
| | | *Pi–Alkyl* | Leu A:98 |
| 10. | Phenol, 4–ethyl–2–methyl– | *Conventional Hydrogen Bond* | Arg A:196, Val A:62 |
| | | *Alkyl* | Ala A:96, Leu A:98 |
| | | *Pi–Alkyl* | Ala A:96 |
| 11. | 9,12–Octadecadienoic acid (z,z)– | *Conventional Hydrogen Bond* | Gly A:97, Val A:62 |
| | | *Alkyl* | Cys A:91, Pro A:86, Met A:87, Arg A:84 |
| 12. | Phenol, 2,6–dimethoxy | *Conventional Hydrogen Bond* | Arg A:84 |
| | | *Carbon Hydrogen Bond* | Glu A:166, Glu A:93 |
| | | *Alkyl* | Ala A:96 |
| | | *Pi–Alkyl* | Ala A:96, Leu A:98 |
| 13. | Phenol, 3–ethyl– | *Pi–Sigma* | Ala A:96 |
| | | *Alkyl* | Leu A:98, Ile A:141 |

| | | | |
|---|---|---|---|
| 14. | Cyclotrisiloxane, hexamethyl– | *Hydrophobic Interaction* | Met A:132, Leu A:98, Ala A:96, Ile A:141, Ala A:63 |
| 15. | 1R,2c,3t,4t–Tetramethyl–cyclohexane | *Alkyl* | Ala A:96 |
| 16. | Indolizine, 7–methyl– | *Pi–Cation* | Arg A:51 |
| | | *Amide Pi–Stacked* | Gly A:97 |
| | | *Alkyl* | Leu A:98, Ile A:141 |
| | | *Pi Alkyl* | Ala A:96 |
| 17. | 6–Methylheptyl 2–methylbutanoate | *Alkyl* | Ala A:96 |
| 18. | Formic acid, 2–methoxyphenyl ester | *Conventional Hydrogen Bond* | Arg A:51 |
| | | *Carbon Hydrogen Bond* | Val A:62 |
| | | *Alkyl* | Met A:132, Ile A:141, Ala A:96 |
| | | *Pi–Alkyl* | Leu A:98, Ala A:96 |
| 19. | Fumaric acid, 3,4–dimethylphenyl octyl ester | *Conventional Hydrogen Bond* | Arg A:196 |
| | | *Alkyl* | Met A:132 |
| | | *Pi–Alkyl* | Arg A:84, Met A:87, Cys A:91 |
| 20. | Indole | *Amide Pi–Stacked* | Gly A:97, Ala A:96 |
| | | *Pi–Alkyl* | Leu A:98 |
| 21. | Phenol, 2,3–dimethyl– | *van der Walls* | Leu A:98 |
| | | *Conventional Hydrogen Bond* | Arg A:84 |
| | | *Amide Pi–Stacked* | Gly A:97 |
| | | *Pi–Alkyl* | Ala A:96 |
| 22. | Phenol, 3–methyl– | *Conventional Hydrogen Bond* | Gly A:97 |
| | | *Alkyl* | Leu A:98 |
| | | *Pi–Alkyl* | Ala A:96 |

| | | | |
|---|---|---|---|
| 23. | 3–n–Hexylthiolane, S,S–dioxide | *Conventional Hydrogen Bond* | Arg A:84, Arg A:196 |
| | | *Alkyl* | Cys A:91 |
| 24. | D–limonene | *Alkyl* | Ala A:96, Ile A:141, Leu A:98 |
| 25. | Methyl 11–methyl–dodecanoate | *Conventional Hydrogen Bond* | Arg A:196 |
| | | *Alkyl* | Arg A:84, Pro A:86, Met A:87, Cys A:91 |
| 26. | Benzene, 4–ethenyl–1,2–dimethyl– | *Pi–Anion* | Glu A:93 |
| | | *Alkyl* | Pro A:86, Met A:87, Arg A:84 |
| | | *Pi–Alkyl* | Arg A:84, Cys A:91 |
| 27. | Hentriacontane | *Alkyl* | Ala A:195, Arg A:196, Cys A:91, Met A:87, Arg A:84, Met A:132, Leu A:136, Pro A:86 |
| 28. | Mesitylene | *Alkyl* | Leu A:98, Ile A:141 |
| | | *Pi–Alkyl* | Ala A:96 |
| 29. | Phenol, 2–methyl– | *Conventional Hydrogen Bond* | Gly A:97 |
| | | *Pi–Sigma* | Met A:132 |
| | | *Pi–Alkyl* | Ala A:96 |
| 30. | Z–28–Heptatriaconten–2–one | *Conventional Hydrogen Bond* | Gly A:97 |
| | | *Alkyl* | Met A:132, Cys A:91, Pro A:86, Leu A:98 |

| | | | |
|---|---|---|---|
| 31. | Z,Z–6,28–Heptatriactontadien–2–one | *Conventional Hydrogen Bond* | Arg A:51 |
| | | *Alkyl* | Cys A:91, Arg A:84, Pro A:86, Ala A:96, Met A:132, Met A:87, Leu A:98 |
| 32. | EthylBenzene | *Amide Pi–Stacked* | Ala A:96, Gly A:97 |
| | | *Alkyl* | Ile A:141, Leu A:98 |
| | | *Pi–Alkyl* | Ala A:96, Gly A:97 |
| 33. | Eicosyl isopropyl ether | *Carbon Hydrogen Bond* | Ala A:96 |
| | | *Alkyl* | Met A:132, Cys A:91, Arg A:84, Met A:87 |
| 34. | Toluene | *Amide Pi–Stacked* | Ala A:96, Gly A:97 |
| | | *Alkyl* | Leu A:98, Ile A:141 |
| | | *Pi–Alkyl* | Leu A:98 |

**Table 4.22.** Interaction of ligands of *S. jamaicensis* bio–oil with residues.

| Sl. No. | Compound Name | Interactions | Residues |
|---|---|---|---|
| 1. | Anastrozole | *Conventional Hydrogen Bond* | Arg A:51, Arg A: 196 |
| | | *Carbon Hydrogen Bond* | Glu A:112 |
| | | *Pi–Cation* | Arg A:84 |
| | | *Pi–Anion* | Glu A:166 |
| 2. | Exemestane | *No interactions* | |
| 3. | Letrozole | *Conventional Hydrogen Bond* | Arg A:196, Arg A:111 |
| | | *Pi–Donor Hydrogen Bond* | Leu A:98 |
| | | *Amide Pi–Stacked* | Ala A:96, Gly A:97 |
| | | *Pi–Alkyl* | Ala A:96, Gly A:97 |
| 4. | (1r,3as,5as,8ar)–1,3a,5a–Trimethyl–4–methylenedecahydrocyclopenta[c]pentalene | *Alkyl* | Arg A:84 |
| 5. | 1,2–Ethanediol, dipropanoate | *Conventional Hydrogen Bond* | Arg A:196 |
| 6. | 1,3–Propanediol, 2–methyl–, dipropanoate | *Conventional Hydrogen Bond* | Arg A:84 |
| 7. | 1,4 3,6–Dianhydro–.alpha.–d–glucopyranose | *Conventional Hydrogen Bond* | Gly A:97, Val A:62 |
| 8. | 2–Cyclopenten–1–one, 2–methyl– | *Conventional Hydrogen Bond* | Arg A:51 |
| 9. | 2–Cyclopenten–1–one, 3–methyl– | *Conventional Hydrogen Bond* | Arg A:84 |
| | | *Alkyl* | Ala A:96, Ile A:141, Met A:132 |
| 10. | 2–Ethyl–5–propylcyclopentanone | *Alkyl* | Ile A:141, Leu A:98 |
| 11. | 2–Isobornyloxy–tetrahydropyran | *Conventional Hydrogen Bond* | Arg A:51 |

| | | | |
|---|---|---|---|
| | | *Alkyl* | Leu A:98, Ala A:96 |
| 12. | 3,5–Dimethoxy–4–hydroxytoluene | *Conventional Hydrogen Bond* | Ala A:96, Arg A:84 |
| | | *Carbon Hydrogen Bond* | Glu A:93 |
| | | *Amide Pi–Stacked* | Gly A:97 |
| | | *Alkyl* | Leu A:98 |
| | | *Pi–Alkyl* | Leu A:98 |
| 13. | 3–n–Butylthiolane, S,S–dioxide | *Conventional Hydrogen Bond* | Arg A:84, Arg A:196 |
| | | *Alkyl* | Met A:87, Cys A:91 |
| 14. | 4–n–Hexylthiane, S,S–dioxide | *Conventional Hydrogen Bond* | Arg A:84 |
| | | *Alkyl* | Cys A:91 |
| 15. | 6,6,9a–Trimethyl–decahydronaphtho[1,2–c]furan–1,4–dione | *Conventional Hydrogen Bond* | Ala A:195, Arg A:196 |
| | | *Carbon Hydrogen Bond* | Asp A:194 |
| 16. | Clofexamide | *Conventional Hydrogen Bond* | Arg A:196 |
| | | *Alkyl* | Leu A:98, Ala A:96 |
| | | Pi–Alkyl | Leu A:98, Ala A:96 |
| 17. | D–Allose | Conventional Hydrogen Bond | Gly A:97 |
| 18. | Eicosane, 1–iodo– | Alkyl | Cys A:91, Met A:87, Arg A:84, Pro A:86, Met A:132, Ala A:96, Ile A:141, Leu A:98 |
| 19. | Hydroquinone | Conventional Hydrogen Bond | Arg A:51, Gly A:97 |
| | | Pi–Alkyl | Ala A:96 |

| | | | |
|---|---|---|---|
| 20. | Methylenecyclopropanecarboxylic acid | Conventional Hydrogen Bond | Arg A:196, Glu A:93 |
| | | Alkyl | Ile A:141, Ala A:96 |
| 21. | Phenol, 2,6–dimethoxy– | Conventional Hydrogen Bond | Arg A:84 |
| | | Carbon Hydrogen Bond | Glu A:166, Glu A:93 |
| | | Alkyl | Ala A:96 |
| | | Pi–Alkyl | Leu A:98, Ala A:96 |
| 22. | Phenol, 2–methoxy– | Conventional Hydrogen Bond | Arg A:84, Glu A:166 |
| | | Amide Pi–Stacked | Gly A:97 |
| | | Alkyl | Ala A:96 |
| | | Pi–Alkyl | Ala A:96, Leu A:98 |
| 23. | Phosphonic acid, (p–hydroxyphenyl)– | Conventional Hydrogen Bond | Gly A:97, Arg A:84 |
| | | Pi–Alkyl | Ala A:96 |
| 24. | Pyridine, 2–methyl– | Conventional Hydrogen Bond | Arg A:196 |
| | | Pi–Anion | Glu A:93 |
| | | Pi–Sulfur | Cys A:91 |
| | | Alkyl | Cys A:91 |
| | | Pi–Alkyl | Arg A:84 |
| 25. | Sedoheptulosan | Conventional Hydrogen Bond | Glu A:93, Glu A:166, Arg A:84 |
| 26. | Trifluoromethyl t–butyl disulfide | Conventional Hydrogen Bond | Arg A:84 |
| | | Halogen (Flourine) | Glu A:93 |
| | | Alkyl | Cys A:91, Pro A:86 |
| 27. | Z,Z–6,28–Heptatriactontadien–2–one | Conventional Hydrogen Bond | Arg A:51 |

| | | |
|---|---|---|
| | Alkyl | Cys A:91, Pro A:86, Arg A:84, Met A:87, Met A:132, Cys A:139, Leu A:136 |

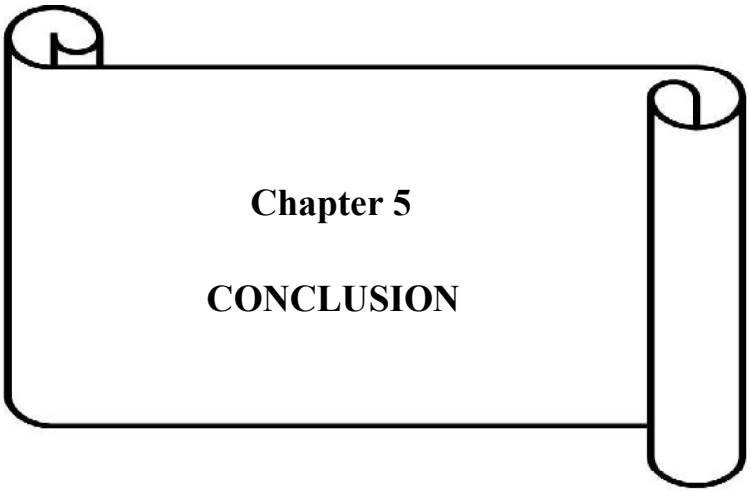

# Chapter 5

# CONCLUSION

# Chapter 5
# CONCLUSION

The unique climatic profile and topography of Nagaland supports the luxuriant, rampant and ubiquitous growth of IS. However, their vast scientific and economic potential remains largely unexplored due to limited research. Currently, there is paucity of research on bioenergy generation and subsequent value–addition from IS biomass. The current investigation presents an alternative and environmental management approach for IS biomass through bioenergy generation and value–addition to bridge this knowledge gap. The study's uniqueness stems from its thorough approach to assess the feasibility of thermochemical conversion (pyrolysis). Economic analysis is further included in the study for a better comprehensive understanding of pyrolytic bio–oil production from IS biomass. Antioxidant and antimicrobial studies of the pyrolytic bio–oil were carried out as a part of value–enhancement. Additionally, *in–silico* drug discovery was another important facet of the study.

The following conclusions were drawn from the study

1. Population study identified *A. adenophora* as the predominant IS among the three species under investigation. *A. adenophora* was documented in all 20 surveyed villages of Kohima district, Nagaland. The findings displaying highest frequency (100 %), density (131000 – 622000 Ind./ha.) and TBA (16.83 – 46.32 m sq./ha.). The IVI of 112.79 of *A. adenophora* further validated its ecological success in the study area.

2. Distribution study exhibited a contagious distribution pattern of *A. adenophora* in all the sampling sites, while *L. camara* predominantly displayed random distribution in nine out of seventeen sites where it occurred. Albeit, *S. jamaicensis*, exhibited limited presence, it displayed contagious distribution in the three surveyed sites.

3. The biomass properties (low MC %, high VM % and appreciable energy content) of *A. adenophora*, *L. camara* and *S. jamaicensis,* suggest their feasibility for thermochemical conversion (pyrolysis) for bio–oil generation.

4. The short thermal degradation profile of all the three investigated biomasses viz. *A. adenophora, L. camara* and *S. jamaicensis*, projects their candidature as an ideal feedstock for thermochemical conversion.

5. Pyrolysis effectively transformed the biomass of *A. adenophora*, *L. camara* and *S. jamaicensis* into bio–oil (GCV: 33.7 MJ/Kg, 30.99 MJ/Kg and 30.18 MJ/Kg, respectively) endorsing their candidature for futuristic bioenergy generation.

6. The appreciable holocellulose content of *A. adenophora* (60.06 %), *L. camara* (65.81 %) and *S. jamaicensis* (62.91 %) offers lucrative prospect for fermentation (production of bioethanol).

7. Spectroscopic analyses (FTIR and GC–MS) demonstrated the presence of varying organic compounds such as straight and branched chain hydrocarbons, aromatics, aliphatics, ketones, esters, aldehydes phenols, etc. in the bio–oil, confirming their viability as a potential chemical feedstock.

8. NMR ($^{1}H$ and $^{13}C$) of IS bio–oil confirmed the presence of high fraction of aliphatics and aromatics which contributes towards their appreciable energy content (calorific value).

9. Theoretical analysis further suggests that IS biomass conversion technologies may demonstrate potential economic viability compared to petroleum refining. Biofuel derived from the three IS with 100 % conversion to bio–oil (to fuel and value–added products), is deemed economically viable at < $ 390.104 $ton^{-1}$ (*A. adenophora*), < $ 361.86 $ton^{-1}$ (*L. camara*) and < $ 393.91 $ton^{-1}$ (*S. jamaicensis*) to be positioned in competition against petroleum priced at $ 100/barrel.

10. Economic assessment validated the bio–oil pyrolysis facility in Kohima district as a financially sound and lucrative investment, featuring PBP of 5.19 years, a robust NPV of $ 378,912.829 and remarkable IRR of 21 %, with MSP of $

0.2617/Kg serving as the essential benchmark for market pricing, thereby guaranteeing the project's sustainability and economic feasibility.

11. DPPH $IC_{50}$ (half–maximal inhibitory concentration) values of *A. adenophora*, *L. camara* and *S. jamaicensis* bio–oils were 211.4 ± 1.2, 233.72 ± 0.2 and 232.42 ± 1.1 µg/ml, respectively. FRAP values of *A. adenophora*, *L. camara* and *S. jamaicensis* bio–oils were 121.39 ± 0.6, 122.45 ± 1.9 and 114.96 ± 1.8 µM AAE/ml, respectively. The results revealed that the bio–oils possessed substantial antioxidant activity

12. The bio–oils revealed appreciable antimicrobial activity with all three species exhibiting highest ZOI against fungus *C. albicans*. ZOI of the bio–oils against *C. albicans* were in order: 31.02 ± 0.9 mm for *L. camara* > 27.7 ± 0.2 mm for *A. adenophora* > 19.48 ± 0.8 mm for *S. jamaicensis* bio–oil.

13. MIC of IS bio–oil revealed superior performance of *L. camara* bio–oil against *C. albicans* achieving MIC value of 3.125 µg/ml, while maintaining efficacy against bacteria at 6.25 µg/ml.

14. Molecular docking investigation documented key compounds from *A. adenophora*, *L. camara* and *S. jamaicensis* bio–oil, which exhibited binding patterns analogous to breast cancer therapeutics Letrozole and Anastrozole, highlighting their latent potential in inhibiting NUDT5 protein.

15. Furaltadone in *A. adenophora* bio–oil emerged as the most effective compound, with the strongest BA of – 6.4 kcal/mol, and outperforming the standard drugs Letrozole and Exemestane (− 6.2 kcal/mol), closely followed by Anastrozole (− 5.6 kcal/mol).

Biofuel production from IS in the context of Nagaland, India, is at its infantile stage and consequently warrants strenuous research endeavours to explore its full potential. Consequently, adopting/establishing an integrated biorefinery approach could markedly enhance the efficiency and sustainability of resource utilization transforming this often neglected IS into lucrative biofuels or bio–based products.

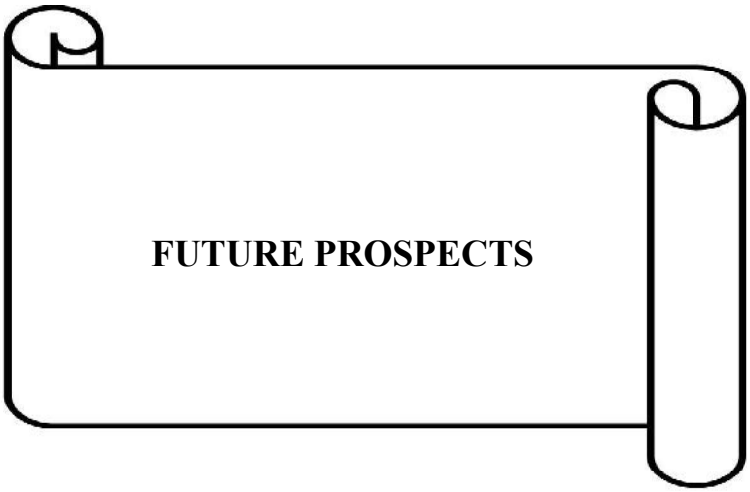
FUTURE PROSPECTS

# FUTURE PROSPECTS

In context of the present investigation, the below mentioned may be undertaken as a part of futuristic research activity (probability of carrying out the work beyond the tenure of Ph.D. or as a part of planned future research activity).

1. Process and data–driven optimization for higher efficiency coupled with computational modelling for enhanced bio–oil yield and quality.
2. Upgradation and refining of bio–oil via enhanced upgradation techniques such as hydrodeoxygenation (HDO) and catalytic cracking involving novel catalysts for improved fuel properties.
3. Real–world testing of upgraded bio–oil for engine performance evaluation for prospective large–scale applicability.
4. Prospects for investigating the feasibility of production of bioethanol from IS biomass (biochemical conversion).
5. Implementation of zero–waste biorefinery approach for simultaneous production of biofuels and biochemicals from IS feedstock, wherein any waste product generated automatically becomes the feedstock for the next product.
6. Extraction of fine biochemicals from IS–biomass derived bio–oil.
7. Antimicrobial studies of bio–oils against pathogenic and multidrug resistant strains of microbes and elucidating their mode of action.
8. Exploring the application of biochar (derived from thermochemical conversion of IS feedstock) as soil amendment through field trials.

The suggested research bears direct relevance to the progression of bio–refining applications and the promotion of a zero–waste biorefinery. Strategic optimization of process parameters, alongside cost–effective production methods and co–product utilization, can markedly improve the commercial feasibility of bio–oil sourced from IS.

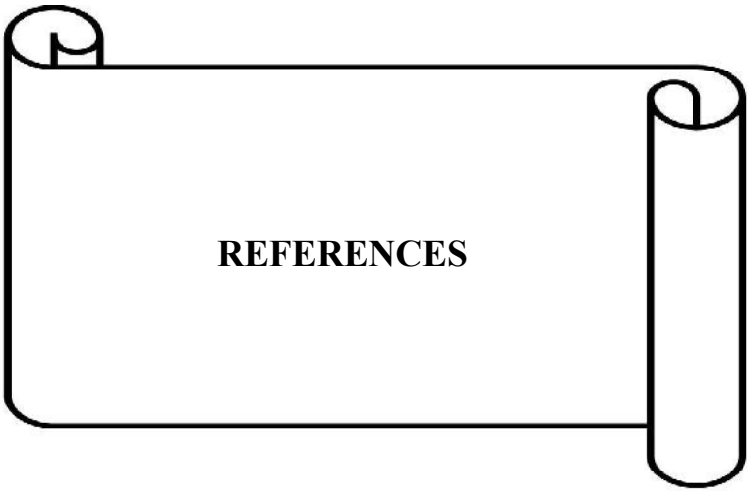

# REFERENCES

# REFERENCES

Adelakun, O. E., Kudanga, T., Green, I. R., le Roes–Hill, M., & Burton, S. G. (2012). Enzymatic modification of 2,6–dimethoxyphenol for the synthesis of dimers with high antioxidant capacity. *Process Biochemistry*, *47*(12), 1926–1932. https://doi.org/10.1016/j.procbio.2012.06.027

Adelino, J. R. P., Heringer, G., Diagne, C., Courchamp, F., Faria, L. D. B., & Zenni, R. D. (2021). The economic costs of biological invasions in Brazil: a first assessment. *NeoBiota*, *67*, 349–374. https://doi.org/10.3897/neobiota.67.59185

Adhikari, P., Lee, Y. H., Adhikari, P., Poudel, A., Choi, S. H., Yun, J. Y., Lee, D.–H., Park, Y.–S., & Hong, S. H. (2024). Global invasion risk assessment of *Lantana camara*, a highly invasive weed, under future environmental change. *Global Ecology and Conservation*, *55*, e03212. https://doi.org/10.1016/j.gecco.2024.e03212

Agblevor, F. A., Mante, O., McClung, R., & Oyama, S. T. (2012). Co–processing of standard gas oil and biocrude oil to hydrocarbon fuels. *Biomass and Bioenergy*, *45*, 130–137. https://doi.org/10.1016/j.biombioe.2012.05.024

Ahmad, T., Jabran, K., Cheema, Z. A., Bajwa, A. A., & Farooq, M. (2023). A global perspective of education in weed science. *Weed Science*, *71*, 1–13. https://doi.org/10.1017/wsc.2023.49

Ahmed, A., Bakar, M. S. A., Razzaq, A., Hidayat, S., Jamil, F., Amin, M. N., Sukri, R. S., Shah, N. S., & Park, Y.–K. (2021). Characterization and Thermal Behavior Study of Biomass from Invasive *Acacia mangium* Species in Brunei Preceding Thermochemical Conversion. *Sustainability*, *13*(9), 5249. https://doi.org/10.3390/su13095249

Ahmed, A., Hidayat, S., Abu Bakar, M. S., Azad, A. K., Sukri, R. S., & Phusunti, N. (2018). Thermochemical characterisation of *Acacia auriculiformis* tree parts via

proximate, ultimate, TGA, DTG, calorific value and FTIR spectroscopy analyses to evaluate their potential as a biofuel resource. *Biofuels*, 1–12. https://doi.org/10.1080/17597269.2018.1442663

Ahmed, S. K., Husein, S., Qurbani, K., Ibrahim, R. H., Fareeq, A., Mahmood, K. A., & Mohamed, M. G. (2024). Antimicrobial resistance: Impacts, challenges, and future prospects. *Journal of Medicine Surgery and Public Health*, *2*, 100081–100081. https://doi.org/10.1016/j.glmedi.2024.100081

Akatov, V. V., Akatova, T. V., Eskina, T. G., Sazonets, N. M., & Chefranov, S. G. (2022). Frequency of Occurrence and Level of Dominance of Alien and Native Species in Synanthropic Plant Communities of Southern Russia. *Russian Journal of Biological Invasions*, *13*(4), 399–411. https://doi.org/10.1134/s2075111722040026

Akhtar, J., Imran, M., Ali, A. M., Nawaz, Z., Muhammad, A., Butt, R. K., Jillani, M. S., Naeem, H. A. (2021) Torrefaction and Thermochemical Properties of Agriculture Residues. *Energies*, *14*, 4218. https://doi.org/10.3390/en14144218

Alagöz, O., Yılmaz, N., & Dilek, M. (2023). Obtaining bio–oil and activated carbon from waste pomegranate peels by pyrolysis. *Environmental Science and Pollution Research*, *30*(54), 115037–115049. https://doi.org/10.1007/s11356–023–30527–3

Alcazar–Ruiz, A., Dorado, F., & Sanchez–Silva, L. (2023). Bio–phenolic compounds production through fast pyrolysis: Demineralizing olive pomace pretreatments. *Food and Bioproducts Processing*, *137*, 200–213. https://doi.org/10.1016/j.fbp.2022.12.002

Alhumade, H., da Silva, J. C. G., Ahmad, M. S., Çakman, G., Yıldız, A., Ceylan, S., & Elkamel, A. (2019). Investigation of pyrolysis kinetics and thermal behavior of Invasive Reed Canary (*Phalaris arundinacea*) for bioenergy potential. *Journal of Analytical and Applied Pyrolysis*, *140*, 385–392. https://doi.org/10.1016/j.jaap.2019.04.018

Alvarez–Chavez, B. J., Godbout, S., Palacios–Rios, J. H., Le Roux, É., & Raghavan, V. (2019). Physical, chemical, thermal and biological pre–treatment technologies in fast pyrolysis to maximize bio–oil quality: A critical review. *Biomass and Bioenergy*, *128*, 105333. https://doi.org/10.1016/j.biombioe.2019.105333

Analysis & Projections – *U.S. Energy Information Administration (EIA)*. (2023). Eia.gov. https://www.eia.gov/analysis. Accessed 16 March 2025

Ansong, M., & Pickering, C. (2014). Weed seeds on clothing: A global review. *Journal of Environmental Management*, *144*, 203–211. https://doi.org/10.1016/j.jenvman.2014.05.026

Aqeel, M. T., Rahman, N., Khan, A., Khan, M. T., Ashraf, Z., Hassan, Bungau, S. G., & Majid, M. (2023). Cardioprotective effect of 2–methoxy phenol derivatives against oxidative stress–induced vascular complications: An integrated in vitro, in silico, and in vivo investigation. *Biomedicine & Pharmacotherapy*, *165*, 115240–115240. https://doi.org/10.1016/j.biopha.2023.115240

Aref, I. M., Salem, M. Z., Shetta, N. D., Alshahrani, T. S., & Nasser, R. A. (2016). Possibility of using three invasive non–forest tree species as an alternative source for energy production. *Journal of Wood Science*, *63*(1), 104–114. https://doi.org/10.1007/s10086–016–1599–7

Arias, E. R., Bertero, M., Jozami, E., Feldman, S. R., Falco, M., & Sedran, U. (2019). Pyrolytic conversion of perennial grasses and woody shrubs to energy and chemicals. *SN Applied Sciences*, *2*(1). https://doi.org/10.1007/s42452–019–1911–4

Aromada, S. A., Eldrup, N. H., & Erik Øi, L. (2021). Capital cost estimation of $CO_2$ capture plant using Enhanced Detailed Factor (EDF) method: Installation factors and plant construction characteristic factors. *International Journal of Greenhouse Gas Control*, *110*, 103394. https://doi.org/10.1016/j.ijggc.2021.103394

Ayaa, F., Lubwama, M., Kirabira, J. B., & Jiang, X. (2022). Potential of invasive shrubs for energy applications in Uganda. *Energy, Ecology and Environment*, *7*(6), 563–576. https://doi.org/10.1007/s40974–022–00255–4

Azargohar, R., Nanda, S., Kozinski, J. A., Dalai, A. K., & Sutarto, R. (2014). Effects of temperature on the physicochemical characteristics of fast pyrolysis bio–chars derived from Canadian waste biomass. *Fuel*, *125*, 90–100. https://doi.org/10.1016/j.fuel.2014.01.083

Badger, P., Badger, S., Puettmann, M., Steele, P., & Cooper, J. (2010). Techno–economic analysis: Preliminary assessment of pyrolysis oil production costs and material energy balance associated with a transportable fast pyrolysis system. *BioResources*, *6*(1), 34–47. https://doi.org/10.15376/biores.6.1.34–47

Bajgai, R. C., Tamang, D. T., Kushwaha, A., & Goswami, L. (2021). Strategic consideration as feedstock resource for biofuel production as a holistic approach to control invasive plant species. *Elsevier EBooks*, 245–268. https://doi.org/10.1016/b978–0–323–85387–3.00007–0

Baloch, H. A., Nizamuddin, S., Siddiqui, M. T. H., Riaz, S., Jatoi, A. S., Dumbre, D. K., Mubarak, N. M., Srinivasan, M. P., & Griffin, G. J. (2018). Recent advances in production and upgrading of bio–oil from biomass: A critical overview. *Journal of Environmental Chemical Engineering*, *6*(4), 5101–5118. https://doi.org/10.1016/j.jece.2018.07.050

Balouiri, M., Sadiki, M., & Ibnsouda, S. K. (2016). Methods for in vitro evaluating antimicrobial activity: a review. *Journal of Pharmaceutical Analysis*, *6*(2), 71–79. https://doi.org/10.1016/j.jpha.2015.11.005

Bang, A., Cuthbert, R. N., Haubrock, P. J., Fernandez, R. D., Moodley, D., Diagne, C., Turbelin, A. J., Renault, D., Dalu, T., & Courchamp, F. (2022). Massive economic costs of biological invasions despite widespread knowledge gaps: a dual setback for India. *Biological Invasions*, *24*(7), 2017–2039. https://doi.org/10.1007/s10530–022–02780–z

Bendary, E., Francis, R. R., Ali, H. M. G., Sarwat, M. I., & El Hady, S. (2013). Antioxidant and structure–activity relationships (SARs) of some phenolic and

anilines compounds. *Annals of Agricultural Sciences*, *58*(2), 173–181. https://doi.org/10.1016/j.aoas.2013.07.002

Benzie, I. F. F., & Strain, J. J. (1996). The Ferric Reducing Ability of Plasma (FRAP) as a Measure of "Antioxidant Power": The FRAP Assay. *Analytical Biochemistry*, *239*(1), 70–76. https://doi.org/10.1006/abio.1996.0292

Bhat, M. P., Raju, S. K., Chakraborty, B., Nagaraja, S. K., Babu, K. G., & Nayaka, S. (2024). Eicosane: An antifungal compound derived from *Streptomyces* sp. KF15 exhibits inhibitory potential against major phytopathogenic fungi of crops. *Environmental Research*, *251*, 118666–118666. https://doi.org/10.1016/j.envres.2024.118666

Bhattacharjee, N., & Biswas, A. B. (2018). Pyrolysis of *Alternanthera philoxeroides* (alligator weed): Effect of pyrolysis parameter on product yield and characterization of liquid product and bio char. *Journal of the Energy Institute*, *91*(4), 605–618. https://doi.org/10.1016/j.joei.2017.02.011

Bhattacharjee, N., & Biswas, A. B. (2019). Pyrolysis of *Ageratum conyzoides* (goat weed). *Journal of Thermal Analysis and Calorimetry*, *139*(2), 1515–1536. https://doi.org/10.1007/s10973–019–08437–9

Bilba, K., Arsene, M., & Ouensanga, A. (2007). Study of banana and coconut fibers Botanical composition, thermal degradation and textural observations. *Bioresource Technology*, *98*(1), 58–68. https://doi.org/10.1016/j.biortech.2005.11.030

Bora, B. (2015). Comparison between net present value and internal rate of returns. *International Journal of Research in Finance and Marketing*, *5*, 61–71.

Bora, P., Konwar, L. J., Phukan, M. M., Deka, D., & Konwar, B. K. (2015). Microemulsion based hybrid biofuels from *Thevetia peruviana* seed oil: Structural and dynamic investigations. *Fuel*, *157*, 208–218. https://doi.org/10.1016/j.fuel.2015.04.075

Bordoloi, N., Narzari, R., Chutia, R. S., Bhaskar, T., & Kataki, R. (2015). Pyrolysis of *Mesua ferrea* and *Pongamia glabra* seed cover: Characterization of bio–oil and its sub–fractions. *Bioresource Technology*, *178*, 83–89. https://doi.org/10.1016/j.biortech.2014.10.079

Borges, A., Ferreira, C., Saavedra, M. J., & Simões, M. (2013). Antibacterial Activity and Mode of Action of Ferulic and Gallic Acids Against Pathogenic Bacteria. *Microbial Drug Resistance*, *19*(4), 256–265. https://doi.org/10.1089/mdr.2012.0244

Bradley, B. A. (2013). Remote detection of invasive plants: a review of spectral, textural and phenological approaches. *Biological Invasions*, *16*(7), 1411–1425. https://doi.org/10.1007/s10530–013–0578–9

Bridgwater, A. V. (2003). Renewable fuels and chemicals by thermal processing of biomass. *Chemical Engineering Journal*, *91*(2–3), 87–102. https://doi.org/10.1016/s1385–8947(02)00142–0

Bridgwater, A. V. (2012). Review of fast pyrolysis of biomass and product upgrading. *Biomass and Bioenergy*, *38*, 68–94. https://doi.org/10.1016/j.biombioe.2011.01.048

Bridgwater, A. V., Czernik, S., & Piskorz, J. (2008). An Overview of Fast Pyrolysis. *Blackwell Science Ltd EBooks*, 977–997. https://doi.org/10.1002/9780470694954.ch80

Bursal, E., & Gülçin, İ. (2011). Polyphenol contents and in vitro antioxidant activities of lyophilised aqueous extract of kiwifruit (*Actinidia deliciosa*). *Food Research International*, *44*(5), 1482–1489. https://doi.org/10.1016/j.foodres.2011.03.031

Cai, J., He, Y., Yu, X., Banks, S. W., Yang, Y., Zhang, X., Yu, Y., Liu, R., & Bridgwater, A. V. (2017). Review of physicochemical properties and analytical characterization of lignocellulosic biomass. *Renewable and Sustainable Energy Reviews*, *76*, 309–322. https://doi.org/10.1016/j.rser.2017.03.072

Cai, W., Zhu, X., Kumar, R., Zhu, Z., Ye, J., & Zhao, J. (2024). Catalytic Pyrolysis of Biomass Waste using Montmorillonite–Supported Ultrafine Iron Nanoparticles for Enhanced Bio–Oil Yield and Quality. *Green Energy and Resources*, 100085–100085. https://doi.org/10.1016/j.gerr.2024.100085

Calicioglu, O., Femeena, P. V., Mutel, C. L., Sills, D., Richard, T. L., & Brennan, R. C. (2021). Techno–economic Analysis and Life Cycle Assessment of an Integrated Wastewater–Derived Duckweed Biorefinery. *ACS Sustainable Chemistry & Engineering*, *9*(28), 9395–9408. https://doi.org/10.1021/acssuschemeng.1c02539

Cam, T., Tran, T. V., Thi, T., Nguyen, D. H., Alhassan, M., & Lee, T. (2022). New frontiers of invasive plants for biosynthesis of nanoparticles towards biomedical applications: A review. *Science of the Total Environment*, *857*, 159278–159278. https://doi.org/10.1016/j.scitotenv.2022.159278

Can, S. de la R. du, Letschert, V., Agarwal, S., Park, W. Y., & Kaggwa, U. (2022). Energy efficiency improves energy access affordability. *Energy for Sustainable Development*, *70*, 560–568. https://doi.org/10.1016/j.esd.2022.09.003

Carrasco, J. L., Gunukula, S., Boateng, A. A., Mullen, C. A., DeSisto, W. J., & Wheeler, M. C. (2017). Pyrolysis of forest residues: An approach to techno–economics for bio–fuel production. *Fuel*, *193*, 477–484. https://doi.org/10.1016/j.fuel.2016.12.063

Carregosa, I. S. C., Carregosa, J. de C., Silva, W. R., Santos, T. M., & Wisniewski Jr, A. (2023). Thermochemical conversion of aquatic weed biomass in a rotary kiln reactor for production of bio–based derivatives. *Journal of Analytical and Applied Pyrolysis*, *173*, 106048. https://doi.org/10.1016/j.jaap.2023.106048

Cesari, L., Mutelet, F., & Canabady–Rochelle, L. (2019). Antioxidant properties of phenolic surrogates of lignin depolymerisation. *Industrial Crops and Products*, *129*, 480–487. https://doi.org/10.1016/j.indcrop.2018.12.010

Chandran, R., Kaliaperumal, R., Balakrishnan, S., Britten, A. J., MacInnis, J., & Mkandawire, M. (2020). Characteristics of bio–oil from continuous fast pyrolysis

of *Prosopis juliflora*. *Energy*, *190*, 116387. https://doi.org/10.1016/j.energy.2019.116387

Chandrasekaran, S. R., Murali, D., Marley, K. A., Larson, R. A., Doll, K. M., Moser, B. R., Scott, J., & Sharma, B. K. (2016). Antioxidants from Slow Pyrolysis Bio–Oil of Birch Wood: Application for Biodiesel and Biobased Lubricants. *ACS Sustainable Chemistry & Engineering*, *4*(3), 1414–1421. https://doi.org/10.1021/acssuschemeng.5b01302

Chang, C.–C., Yang, M.–H., Wen, H.–M., & Chern, J.–C. (2020). Estimation of total flavonoid content in propolis by two complementary colometric methods. *Journal of Food and Drug Analysis*, *10*(3). https://doi.org/10.38212/2224–6614.2748

Chapple, D. G., Naimo, A. C., Brand, J. A., Michelangeli, M., Martin, J. M., Goulet, C. T., Brunton, D. H., Sih, A., & Wong, B. B. M. (2022). Biological invasions as a selective filter driving behavioural divergence. *Nature Communications*, *13*(1), 5996. https://doi.org/10.1038/s41467–022–33755–2

Chen, G., Pan, F., Gao, Y., Li, H., Qin, X., Jiang, Y., Qi, J., Xie, J., & Jia, S. (2022). Analysis of Components and Properties of Extractives from *Alnus cremastogyne* Pods from Different Provenances. *Molecules*, *27*(22), 7802–7802. https://doi.org/10.3390/molecules27227802

Chen, L., Wang, H., Tu, Z., Hu, J., & Wu, F. (2024). Renewable fuel and value–added chemicals potential of reed straw waste (RSW) by pyrolysis: Kinetics, thermodynamics, products characterization, and biochar application for malachite green removal. *Renewable Energy*, *229*, 120724–120724. https://doi.org/10.1016/j.renene.2024.120724

Chen, V. B., Arendall, W. B., Headd, J. J., Keedy, D. A., Immormino, R. M., Kapral, G. J., Murray, L. W., Richardson, J. S., & Richardson, D. C. (2009). MolProbity: all–atom structure validation for macromolecular crystallography. *Acta Crystallographica Section D Biological Crystallography*, *66*(1), 12–21. https://doi.org/10.1107/s0907444909042073

Chen, W.–H., Lin, Y.–Y., Liu, H.–C., Chen, T.–C., Hung, H.–C., & Chen, C.–H. (2019). Analysis of physicochemical properties of liquefaction bio–oil from food waste. *Energy Procedia*, *158*, 61–66. https://doi.org/10.1016/j.egypro.2019.01.036

Chen, X., Lan, W., & Xie, J. (2023). Natural phenolic compounds: Antimicrobial properties, antimicrobial mechanisms, and potential utilization in the preservation of aquatic products. *Food Chemistry*, *440*, 138198–138198. https://doi.org/10.1016/j.foodchem.2023.138198

Cheng, S., Shu, J., Wang, S., Zhang, L., Peng, J., Li, C., Jiang, X., & Zhang, Q. (2019). Pyrolysis of Crofton weed for the production of aldehyde rich bio–oil and combustible matter rich bio–gas. *Applied Thermal Engineering*, *148*, 1164–1170. https://doi.org/10.1016/j.applthermaleng.2018.12.009

Chisti, Y. (2008). Biodiesel from microalgae beats bioethanol. *Trends in Biotechnology*, *26*(3), 126–131. https://doi.org/10.1016/j.tibtech.2007.12.002

Chong, C. T., Mong, G. R., Ng, J.–H., Chong, W. W. F., Ani, F. N., Lam, S. S., & Ong, H. C. (2019). Pyrolysis characteristics and kinetic studies of horse manure using thermogravimetric analysis. *Energy Conversion and Management*, *180*, 1260–1267. https://doi.org/10.1016/j.enconman.2018.11.071

Chongloi, V., Gogoi, P. P., Sangma, S. R., Sinha, U. B., Bora, P., & Phukan, M. M. (2025). Antioxidant, antimicrobial and in silico investigations on pyrolytic bio–oil from invasive *Stachytarpheta jamaicensis*. *Environmental Science and Pollution Research*. https://doi.org/10.1007/s11356–025–36741–5

Chongloi, V., Phukan, M. M., & Bora, P. (2024). Miscellaneous prospects of invasive *Lantana camara* biomass—a standpoint on bioenergy generation and value addition. *Environmental Science and Pollution Research*, *31*. https://doi.org/10.1007/s11356–024–35042–7

Choudhury, N. D., Chutia, R. S., Bhaskar, T., & Kataki, R. (2014). Pyrolysis of jute dust: effect of reaction parameters and analysis of products. *Journal of Material*

*Cycles and Waste Management*, *16*(3), 449–459. https://doi.org/10.1007/s10163–014–0268–4

Chukwuneke, J. L., Ewulonu, M. C., Chukwujike, I. C., & Okolie, P. C. (2019). Physico–chemical analysis of pyrolyzed bio–oil from swietenia macrophylla (mahogany) wood. *Heliyon*, *5*(6), e01790. https://doi.org/10.1016/j.heliyon.2019.e01790

Chutia, R. S., Kataki, R., & Bhaskar, T. (2014). Characterization of liquid and solid product from pyrolysis of *Pongamia glabra* deoiled cake. *Bioresource Technology*, *165*, 336–342. https://doi.org/10.1016/j.biortech.2014.03.118

Clemente–Castro, S., Palma, A., Ruiz–Montoya, M., Giráldez, I., & Díaz, M. J. (2023). Optimizing pyrolysis parameters and product analysis of a fluidized bed pilot plant for *Leucaena leucocephala* biomass. *Environmental Sciences Europe*, *35*(1). https://doi.org/10.1186/s12302–023–00800–w

Collard, F.–X., & Blin, J. (2014). A review on pyrolysis of biomass constituents: Mechanisms and composition of the products obtained from the conversion of cellulose, hemicelluloses and lignin. *Renewable and Sustainable Energy Reviews*, *38*, 594–608. https://doi.org/10.1016/j.rser.2014.06.013

Crall, A. W., Jarnevich, C. S., Young, N. E., Panke, B. J., Renz, M., & Stohlgren, T. J. (2015). Citizen science contributes to our knowledge of invasive plant species distributions. *Biological Invasions*, *17*(8), 2415–2427. https://doi.org/10.1007/s10530–015–0885–4

Curtis, J. T., & McIntosh, R. P. (1950). The Interrelations of Certain Analytic and Synthetic Phytosociological Characters. *Ecology*, *31*(3), 434–455. https://doi.org/10.2307/1931497

Czernik, S., & Bridgwater, A. V. (2004). Overview of Applications of Biomass Fast Pyrolysis Oil. *Energy & Fuels*, *18*(2), 590–598. https://doi.org/10.1021/ef034067u

Dai, J., Roberts, D. A., Stow, D. A., An, L., Hall, S. J., Yabiku, S. T., & Kyriakidis, P. C. (2020). Mapping understory invasive plant species with field and remotely sensed data in Chitwan, Nepal. *Remote Sensing of Environment*, *250*, 112037. https://doi.org/10.1016/j.rse.2020.112037

Davis, M. A., Grime, J. P., & Thompson, K. (2000). Fluctuating resources in plant communities: a general theory of invasibility. *Journal of Ecology*, *88*(3), 528–534. https://doi.org/10.1046/j.1365–2745.2000.00473.x

Debella, H. A., Ancha, V. R., & Atnaw, S. M. (2023). Production, optimization, and characterization of Ethiopian variant *Prosopis juliflora* based biodiesel. *Heliyon*, *9*(5), e15721. https://doi.org/10.1016/j.heliyon.2023.e15721

Deepak, P., Sowmiya, R., Balasubramani, G., & Perumal, P. (2017). Phytochemical profiling of *Turbinaria ornata* and its antioxidant and anti–proliferative effects. *Journal of Taibah University Medical Sciences*, *12*(4), 329–337. https://doi.org/10.1016/j.jtumed.2017.02.002

de Abreu Neto, R., de Assis, A. A., Ballarin, A. W., & Hein, P. R. G. (2020). Effect of final temperature on charcoal stiffness and its correlation with wood density and hardness. *SN Applied Sciences*. https://doi.org/10.1007/s42452–020–2822–0

del Pozo, C., Bartrolí, J., Alier, S., Puy, N., & Fàbregas, E. (2020). Production of antioxidants and other value–added compounds from coffee silverskin via pyrolysis under a biorefinery approach. *Waste Management*, *109*, 19–27. https://doi.org/10.1016/j.wasman.2020.04.044

Diagne, C., Leroy, B., Vaissière, A.–C., Gozlan, R. E., Roiz, D., Jarić, I., Salles, J.–M., Bradshaw, C. J. A., & Courchamp, F. (2021). High and rising economic costs of biological invasions worldwide. *Nature*, *592*, 1–6. https://doi.org/10.1038/s41586–021–03405–6

Dias, I. A., Horta, R. P., Matos, M., Helm, C. V., Magalhães, W. L. E., de Lima, E. A., da Silva, B. J. G., de Muniz, G. I. B., & de Cademartori, P. H. G. (2023). Exploring the antioxidant and antimicrobial properties of the water–soluble fraction derived

from pyrolytic lignin separation in fast–pyrolysis bio–oil. *Biomass Conversion and Biorefinery*, *14*(19). https://doi.org/10.1007/s13399–023–04561–7

Dong, L., Tong, X., Li, X., Zhou, J., Wang, S., & Liu, B. (2019). Some developments and new insights of environmental problems and deep mining strategy for cleaner production in mines. *Journal of Cleaner Production*, *210*, 1562–1578. https://doi.org/10.1016/j.jclepro.2018.10.291

dos Santos, E. G., Inoue, M. H., Guimarães, A. C. D., Bastos, J. S. Q., Alcántara–de la Cruz, R., & Mendes, K. F. (2023). Influence of Chemical Control on the Floristic Composition of Weeds in the Initial and Pre–Harvest Development Stages of the Sunflower Crop. *Agrochemicals*, *2*(2), 193–202. https://doi.org/10.3390/agrochemicals2020014

Du, Y., Feng, Y., Shu, L., Ren, Z., Kong, Q., Xu, F., & Wang, Q. (2018). A mesoporous biochar from bio–invasion alligator weed for adsorption of rhodamine B from aqueous solution. *Desalination and Water Treatment*, *135*, 341–350. https://doi.org/10.5004/dwt.2018.22616

Elith, J., Kearney, M., & Phillips, S. (2010). The art of modelling range–shifting species. *Methods in Ecology and Evolution*, *1*(4), 330–342. https://doi.org/10.1111/j.2041–210x.2010.00036.x

Energy Transitions Commission. (2022). *Roadmap to India's 2030 Decarbonization Target – ETC*. Energy Transitions Commission. https://www.energy–transitions.org/publications/roadmap–to–indias–2030–decarbonization–target/. Accessed 18 January 2025

European Union. (2014). *Regulation (EU) No. 1143/2014 of the European Parliament and of the Council on the prevention and management of the introduction and spread of invasive alien species*. Www.fao.org. https://www.fao.org/faolex/results/details/en/c/LEX–FAOC140066. Accessed 23 January 2024

Evald, A., Koppejan, J., Livingston, W., Nussbaumer, T., Obernberger, I., Skreiberg, Q. (2008). Biomass fuel properties and basic principles of biomass combustion. In: Loo SV, Koppejan J, editors. Handbook of biomass combustion and co–firing. London: Earthscan. p. 7–53.

Fang, Y., Zhang, X., Wei, H., Wang, D., Chen, R., Wang, L., & Gu, W. (2020). Predicting the invasive trend of exotic plants in China based on the ensemble model under climate change: A case for three invasive plants of Asteraceae. *The Science of the Total Environment*, *756*, 143841–143841. https://doi.org/10.1016/j.scitotenv.2020.143841

Fardi, Z., Shahbeik, H., Nosrati, M., Motamedian, E., Tabatabaei, M., & Aghbashlo, M. (2023). Waste–to–energy: Co–pyrolysis of potato peel and macroalgae for biofuels and biochemicals. *Environmental Research*, *242*, 117614–117614. https://doi.org/10.1016/j.envres.2023.117614

Fatmawati, S., Auwaliyah, F., Yuliana, Hasanah, N., Putri, D. A., Kainama, H., & Choudhary, M. I. (2023). Antioxidant and α–glucosidase inhibitory activities of compound isolated from *Stachytarpheta jamaicensis* (L) Vahl. leaves. *Scientific Reports*, *13*(1), 18597. https://doi.org/10.1038/s41598–023–45357–z

Feng, Q., & Lin, Y. (2017). Integrated processes of anaerobic digestion and pyrolysis for higher bioenergy recovery from lignocellulosic biomass: A brief review. *Renewable and Sustainable Energy Reviews*, *77*, 1272–1287. https://doi.org/10.1016/j.rser.2017.03.022

Fernández, E., Amutio, M., Artetxe, M., López, G., Santamaria, L., López, J. E., Olazar, M., & Saldarriaga, J. F. (2024). Exploring the potential of fast pyrolysis of invasive biomass species for the production of chemicals. *Journal of Analytical and Applied Pyrolysis*, *183*, 106817–106817. https://doi.org/10.1016/j.jaap.2024.106817

Finch, D. M., Butler, J. L., Runyon, J. B., Fettig, C. J., Kilkenny, F. F., Jose, S., Frankel, S. J., Cushman, S. A., Cobb, R. C., Dukes, J. S., Hicke, J. A., & Amelon, S. K.

(2021). Effects of Climate Change on Invasive Species. *Invasive Species in Forests and Rangelands of the United States*, 57–83. https://doi.org/10.1007/978–3–030–45367–1_4

Fried, G., Chauvel, B., Reynaud, P., & Sache, I. (2017). *Impact of Biological Invasions on Ecosystem Services*. Springer International Publishing. https://doi.org/10.1007/978–3–319–45121–3

Gašparovič, L., Koreňová, Z., & Jelemenský, Ľ. (2010). Kinetic study of wood chips decomposition by TGA. *Chemical Papers*, *64*(2). https://doi.org/10.2478/s11696–009–0109–4

Gautam, P., Kumar, S., & Lokhandwala, S. (2019). Energy–Aware Intelligence in Megacities. In *Current Developments in Biotechnology and Bioengineering* (pp. 211–238). https://doi.org/10.1016/b978–0–444–64083–3.00011–7

Ghazali, W. N. M. W., Mamat, R., Masjuki, H. H., & Najafi, G. (2015). Effects of biodiesel from different feedstocks on engine performance and emissions: A review. *Renewable and Sustainable Energy Reviews*, *51*, 585–602. https://doi.org/10.1016/j.rser.2015.06.031

Gollakota, A., & Savage, P. E. (2018). Hydrothermal Liquefaction of Model Food Waste Biomolecules and Ternary Mixtures under Isothermal and Fast Conditions. *ACS Sustainable Chemistry & Engineering*, *6*(7), 9018–9027. https://doi.org/10.1021/acssuschemeng.8b01368

Gonçalves, E. C. B. M., Moura, F. J., & Teixeira, M. A. (2021). *Cyperus giganteus* pruning residues from constructed wetlands: Potential for energy production. *Journal of Cleaner Production*, *325*, 129319. https://doi.org/10.1016/j.jclepro.2021.129319

González–Trujillo, J. D., Escobar–Alba, M. R., Lara, D. E., & Carvajal–C, J. E. (2024). Mapping the threat: projecting invasive plant distribution in the tropical Andes under climate change. *Perspectives in Ecology and Conservation*, *22*(4), 348–357. https://doi.org/10.1016/j.pecon.2024.11.002

Gopal, P., Nadimpalli, G., Saikia, R., Sankari, H., Ratnam, R., Gogoi, N., Garg, A., Buragohain, P., & Kataki, R. (2019). Optimization of pyrolyzer design to produce maximum bio–oil from *Saccharum ravannae* L.: an integrated approach using experimental data and artificial intelligence. *Biomass Conversion and Biorefinery*, *9*(4), 727–736. https://doi.org/10.1007/s13399–019–00397–2

Gopalakrishnan, B., Khanna, N., & Das, D. (2019). Dark–Fermentative Biohydrogen Production. *Biohydrogen*, 79–122. https://doi.org/10.1016/b978–0–444–64203–5.00004–6

Gowda, N. A. N., Gurikar, C., Anusha, M. B., & Gupta, S. (2022). Ultrasound–Assisted and Microwave–Assisted Extraction, GC–MS Characterization and Antimicrobial Potential of Freeze–dried *L. camara* Flower. *Journal of Pure and Applied Microbiology*, *16*(1), 526–539. https://doi.org/10.22207/jpam.16.1.50

Grime, J. P. (2006). *Plant strategies, vegetation processes, and ecosystem properties*. Wiley, Chichester, UK.

Gu, C., Yanli, T., Liu, L., Bo, W., Zhang, Y., Haibin, Y., Xilong, W., Zhuoga, Y., Binghua, Z., & Bohao, C. (2021). Predicting the potential global distribution of *Ageratina adenophora* under current and future climate change scenarios. *Ecology and Evolution*, *11*(17), 12092–12113. https://doi.org/10.1002/ece3.7974

Gulzar, R., Ahmad, R., Hassan, T., Rashid, I., & Khuroo, A. A. (2024). Environmental and anthropogenic drivers of invasive plant diversity and distribution in the Himalaya. *Ecological Informatics*, *81*, 102586–102586. https://doi.org/10.1016/j.ecoinf.2024.102586

Gunaseelan, V. N. (1997). Anaerobic digestion of biomass for methane production: A review. *Biomass and Bioenergy*, *13*(1–2), 83–114. https://doi.org/10.1016/s0961–9534(97)00020–2

Hansda, P., Kumar, S., Singh, S., & Garkoti, S. C. (2024). Assessing the influence of invasion of *Lantana camara* on vegetation attributes and soil properties across

varied disturbance gradients in semi–arid forests of Aravali hills, Delhi. *Plant Ecology*, *225*. https://doi.org/10.1007/s11258–024–01441–6

Haq, S. M., Waheed, M., Bussmann, R. W., & Kumar, M. (2024). Trouble in the rice field: Distribution ecology and indicator value of weed species in the rice fields of Himalayan region. *Ecological Frontiers*, *44*(3), 507–516. https://doi.org/10.1016/j.chnaes.2023.07.012

Heshmati, I., Khorasani, N., Shams–Esfandabad, B., & Riazi, B. (2019). Forthcoming risk of *Prosopis juliflora* global invasion triggered by climate change: implications for environmental monitoring and risk assessment. *Environmental Monitoring and Assessment*, *191*(2). https://doi.org/10.1007/s10661–018–7154–9

Hingston, J. A., Collins, C. D., Murphy, R. J., & Lester, J. N. (2001). Leaching of chromated copper arsenate wood preservatives: a review. *Environmental Pollution*, *111*(1), 53–66. https://doi.org/10.1016/s0269–7491(00)00030–0

Ho, N. W. Y., Ladisch, M. R., Sedlak, M., Mosier, N., & Casey, E. (2011). Biofuels from Cellulosic Feedstocks. *Comprehensive Biotechnology*, 51–62. https://doi.org/10.1016/b978–0–08–088504–9.00155–0

Hossain, M. M., Scott, I. M., Berruti, F., & Briens, C. (2017). Application of Novel Pyrolysis Reactor Technology to Concentrate Bio–oil Components with Antioxidant Activity from Tobacco, Tomato and Coffee Ground Biomass. *Waste and Biomass Valorization*, *9*(9), 1607–1617. https://doi.org/10.1007/s12649–017–9943–8

Hu, M., Chen, Z., Wang, S., Guo, D., Ma, C., Zhou, Y., Chen, J., Laghari, M., Fazal, S., Xiao, B., Zhang, B., & Ma, S. (2016). Thermogravimetric kinetics of lignocellulosic biomass slow pyrolysis using distributed activation energy model, Fraser–Suzuki deconvolution, and iso–conversional method. *Energy Conversion and Management*, *118*, 1–11. https://doi.org/10.1016/j.enconman.2016.03.058

Hu, X., & Gholizadeh, M. (2019). Biomass pyrolysis: A review of the process development and challenges from initial researches up to the commercialisation

stage. *Journal of Energy Chemistry*, *39*, 109–143. https://doi.org/10.1016/j.jechem.2019.01.024

Hu, Z., Ma, X., & Li, L. (2013). The characteristic and evaluation method of fast pyrolysis of microalgae to produce syngas. *Bioresource Technology*, *140*, 220–226. https://doi.org/10.1016/j.biortech.2013.04.096

Hulme, P. E. (2021). Unwelcome exchange: International trade as a direct and indirect driver of biological invasions worldwide. *One Earth*, *4*(5), 666–679. https://doi.org/10.1016/j.oneear.2021.04.015

Iftekhar, S., Deb, A., Heidari, G., Sillanpää, M., Lehto, V.–P., Doshi, B., Hosseinzadeh, M., & Zare, E. N. (2023). A review on the effectiveness of nanocomposites for the treatment and recovery of oil spill. *Environmental Science and Pollution Research International*, *30*(7), 16947–16983. https://doi.org/10.1007/s11356–022–25102–1

Iliopoulou, E. F., Triantafyllidis, K. S., & Lappas, A. A. (2018). Overview of catalytic upgrading of biomass pyrolysis vapors toward the production of fuels and high–value chemicals. *Wiley Interdisciplinary Reviews: Energy and Environment*, *8*(1), e322. https://doi.org/10.1002/wene.322

Inderjit, Evans, H., Crocoll, C., Bajpai, D., Kaur, R., Feng, Y.–L., Silva, C., Carreón, J. T., Valiente–Banuet, A., Gershenzon, J., & Callaway, R. M. (2011). Volatile chemicals from leaf litter are associated with invasiveness of a Neotropical weed in Asia. *Ecology*, *92*(2), 316–324. https://doi.org/10.1890/10–0400.1

IPBES. (2019). Global assessment report on biodiversity and ecosystem services of the Intergovernmental Science–Policy Platform on Biodiversity and Ecosystem Services. *IPBES*. https://doi.org/10.5281/zenodo.6417333

IPBES. (2023). Summary for Policymakers of the Thematic Assessment Report on Invasive Alien Species and Their Control of the Intergovernmental Science–policy Platform on Biodiversity and Ecosystem Services. IPBES secretariat, Bonn, Germany.

IUCN. (2009). Guidelines on Biofuels and Invasive Species. *Gland: IUCN*.

Jacqueline, P.J., Muthuraman, V.S., Karthick, C., Alaswad, A., Velvizhi, G., Nanthagopal, K. (2022). Catalytic microwave preheated co–pyrolysis of lignocellulosic biomasses: A study on biofuel production and its characterization. *Bioresource Technology 347, 126382*. https://doi.org/10.1016/j.biortech.2021.126382

Jauni, M., Gripenberg, S., & Ramula, S. (2014). Non–native plant species benefit from disturbance: a meta–analysis. *Oikos*, *124*(2), 122–129. https://doi.org/10.1111/oik.01416

Jaureguiberry, P., Titeux, N., Wiemers, M., Bowler, D. E., Coscieme, L., Golden, A. S., Guerra, C. A., Jacob, U., Takahashi, Y., Settele, J., Díaz, S., Molnár, Z., & Purvis, A. (2022). The direct drivers of recent global anthropogenic biodiversity loss. *Science Advances*, *8*(45).

Ji, L.–Q., Zhang, C., & Fang, J.–Q. (2017). Economic analysis of converting of waste agricultural biomass into liquid fuel: A case study on a biofuel plant in China. *Renewable and Sustainable Energy Reviews*, *70*, 224–229. https://doi.org/10.1016/j.rser.2016.11.189

Jin, Y., Liu, S., Shi, Z., Wang, S., Wen, Y., Zaini, I. N., Tang, C., Hedenqvist, M. S., Lu, X., Kawi, S., Wang, C.–H., Jiang, J., Jönsson, P. G., & Yang, W. (2024). A novel three–stage ex–situ catalytic pyrolysis process for improved bio–oil yield and quality from lignocellulosic biomass. *Energy*, *295*, 131029–131029. https://doi.org/10.1016/j.energy.2024.131029

Joshi, V. C., Sundriyal, R. C., Khatri, K., & Arya, D. (2024). Unveiling the Ecological Alarm: People's perception towards Exploring the Impact of Invasive Plants on Biodiversity and Ecosystem Services in the Western Himalaya. *Environmental Challenges*, *16*, 100997–100997. https://doi.org/10.1016/j.envc.2024.100997

Kähkönen, M. P., Hopia, A. I., Vuorela, H. J., Rauha, J.–P., Pihlaja, K., Kujala, T. S., & Heinonen, M. (1999). Antioxidant Activity of Plant Extracts Containing Phenolic

Compounds. *Journal of Agricultural and Food Chemistry*, *47*(10), 3954–3962. https://doi.org/10.1021/jf9901461

Kan, T., Strezov, V., & Evans, T. J. (2016). Lignocellulosic biomass pyrolysis: A review of product properties and effects of pyrolysis parameters. *Renewable and Sustainable Energy Reviews*, *57*, 1126–1140. https://doi.org/10.1016/j.rser.2015.12.185

Karaeva, J., Timofeeva, S., Gilfanov, M., Slobozhaninova, M., Sidorkina, O., Luchkina, E., Panchenko, V., & Bolshev, V. (2023). Exploring the Prospective of Weed Amaranthus retroflexus for Biofuel Production through Pyrolysis. *Agriculture*, *13*(3), 687–687. https://doi.org/10.3390/agriculture13030687

Kaushik, P., Pati, P. K., Khan, M. L., & Khare, P. (2024). Effect of invasive species on forest composition in tropical dry forest: a case study of invasion by *Gliricidia sepium*. *Southern Forests: A Journal of Forest Science*, *86*(2), 1–16. https://doi.org/10.2989/20702620.2024.2322484

Khalid, Z., & Singh, B. (2023). Looking at moss through the bioeconomy lens: biomonitoring, bioaccumulation, and bioenergy potential. *Environmental Science and Pollution Research*, *30*(54), 114722–114738. https://doi.org/10.1007/s11356–023–30633–2

Kim, J.–S. (2015). Production, separation and applications of phenolic–rich bio–oil – A review. *Bioresource Technology*, *178*, 90–98. https://doi.org/10.1016/j.biortech.2014.08.121

Kim, K. H., Bai, X., Cady, S., Gable, P., & Brown, R. C. (2015). Quantitative Investigation of Free Radicals in Bio–Oil and their Potential Role in Condensed–Phase Polymerization. *ChemSusChem*, *8*(5), 894–900. https://doi.org/10.1002/cssc.201403275

Kim, P., Johnson, A., Edmunds, C. W., Radosevich, M., Vogt, F., Rials, T. G., & Labbé, N. (2011). Surface Functionality and Carbon Structures in Lignocellulosic–Derived

Biochars Produced by Fast Pyrolysis. *Energy & Fuels*, *25*(10), 4693–4703. https://doi.org/10.1021/ef200915s

Kim, T.–S., Kim, J.–Y., Kim, K.–H., Lee, S., Choi, D., Choi, I.–G., & Choi, J. W. (2012). The effect of storage duration on bio–oil properties. *Journal of Analytical and Applied Pyrolysis*, *95*, 118–125. https://doi.org/10.1016/j.jaap.2012.01.015

Knapp, L. S. P., Coyle, D. R., Dey, D. C., Fraser, J. S., Hutchinson, T., Jenkins, M. A., Kern, C. C., Knapp, B. O., Maddox, D., Pinchot, C., & Wang, G. G. (2023). Invasive plant management in eastern North American Forests: A systematic review. *Forest Ecology and Management*, *550*, 121517. https://doi.org/10.1016/j.foreco.2023.121517

Kocira, A., & Staniak, M. (2021). Weed Ecology and New Approaches for Management. *Agriculture*, *11*(3), 262. https://doi.org/10.3390/agriculture11030262

Kumar, A., Devnani, G. L., & Pal, D. B. (2024). Thermal kinetic analysis and characterization of water hyacinth biomass for renewable energy application. *Biomass Conversion and Biorefinery*. https://doi.org/10.1007/s13399–024–06285–8

Kumar, M., Verma, A. K., & Garkoti, S. C. (2020). *Lantana camara* and *Ageratina adenophora* invasion alter the understory species composition and diversity of chir pine forest in central Himalaya, India. *Acta Oecologica*, *109*, 103642. https://doi.org/10.1016/j.actao.2020.103642

Lachos–Perez, D., Martins–Vieira, J. C., Missau, J., Anshu, K., Siakpebru, O. K., Thengane, S. K., Morais, A. R. C., Tanabe, E. H., & Bertuol, D. A. (2023). Review on Biomass Pyrolysis with a Focus on Bio–Oil Upgrading Techniques. *Analytica*, *4*(2), 182–205. https://doi.org/10.3390/analytica4020015

Lehto, J., Oasmaa, A., Solantausta, Y., Kytö, M., & Chiaramonti, D. (2013). Fuel oil quality and combustion of fast pyrolysis bio–oils. *Espoo. VTT Technology*.

Li, R., Li, B., Kai, X., & Yang, T. (2017). Hydro–liquefaction of rice stalk in supercritical ethanol with in situ generated hydrogen. *Fuel Processing Technology*, *167*, 363–370. https://doi.org/10.1016/j.fuproc.2017.07.013

Liew, P. M., & Yong, Y. K. (2016). *Stachytarpheta jamaicensis* (L.) Vahl: From Traditional Usage to Pharmacological Evidence. *Evidence–Based Complementary and Alternative Medicine*, *2016*, 1–7. https://doi.org/10.1155/2016/7842340

Lim, Y.–R., & Oh, D.–K. (2011). Microbial metabolism and biotechnological production of d–allose. *Applied Microbiology and Biotechnology*, *91*(2), 229–235. https://doi.org/10.1007/s00253–011–3370–8

Lin, L., Yan, R., Liu, Y., & Jiang, W. (2010). In–depth investigation of enzymatic hydrolysis of biomass wastes based on three major components: Cellulose, hemicellulose and lignin. *Bioresource Technology*, *101*(21), 8217–8223. https://doi.org/10.1016/j.biortech.2010.05.084

Liu, W.–J., & Yu, H.–Q. (2021). Thermochemical Conversion of Lignocellulosic Biomass into Mass–Producible Fuels: Emerging Technology Progress and Environmental Sustainability Evaluation. *ACS Environmental Au*, *2*(2). https://doi.org/10.1021/acsenvironau.1c00025

Lødeng, R., & Bergem, H. (2018). Stabilisation of pyrolysis oils. *Direct Thermochemical Liquefaction for Energy Applications*, 193–247. https://doi.org/10.1016/b978–0–08–101029–7.00006–0

López, A., de Marco, I., Caballero, B. M., Laresgoiti, M. F., Adrados, A., & Aranzabal, A. (2011). Catalytic pyrolysis of plastic wastes with two different types of catalysts: ZSM–5 zeolite and Red Mud. *Applied Catalysis B: Environmental*, *104*(3–4), 211–219. https://doi.org/10.1016/j.apcatb.2011.03.030

López–Marín, J., Gálvez, A., del Amor, F. M., & Brotons, J. M. (2020). The Financial Valuation Risk in Pepper Production: The Use of Decoupled Net Present Value. *Mathematics*, *9*(1), 13. https://doi.org/10.3390/math9010013

Lowry, O. H., Rosebrough, N. J., Farr, A. L., Randall, R. J. (1951) Protein measurement with the Folin phenol reagent. *Journal of Biological Chemistry*, *193*, 265–275

Lu, Q., Li, W.–Z., & Zhu, X.–F. (2009). Overview of fuel properties of biomass fast pyrolysis oils. *Energy Conversion and Management*, *50*(5), 1376–1383. https://doi.org/10.1016/j.enconman.2009.01.001

Lu, X., Jiang, J., Sun, K., Sun, Y., & Yang, W. (2021). Enhanced antioxidant activity of aqueous phase bio–oil by hydrothermal pretreatment and its structure–activity relationship. *Journal of Analytical and Applied Pyrolysis*, *153*, 104992. https://doi.org/10.1016/j.jaap.2020.104992

Luo, M., Xiao, L., Chen, X., Lin, K., Liu, B., He, Z., Liu, J., & Zheng, S. (2022). Invasive Alien Plants and Invasion Risk Assessment on Pingtan Island. *Sustainability*, *14*(2), 923. https://doi.org/10.3390/su14020923

Ma, Y., Tian, H., Cheng, H., Xuan, Y., Shang, L., & Yang, Y. (2023). The economic and environmental sustainability of converting *Miscanthus* to hydrocarbon biofuel by pyrolysis and catalytic hydrotreatment. *Biomass and Bioenergy*, *181*, 107041–107041. https://doi.org/10.1016/j.biombioe.2023.107041

Macchia, M., & Benvenuti, S. (2003). Weed community dynamics in perennial medicinal crops of organic agricultural systems. *Advances in Horticultural Science*, *17*(4), 207–214. https://doi.org/10.1400/14250

Maheshwari, N., & Sharma, M. C. (2023). Anticancer properties of some selected plant phenolic compounds: Future leads for therapeutic development. *Journal of Herbal Medicine*, *42*, 100801. https://doi.org/10.1016/j.hermed.2023.100801

Malagón–Romero, D., Torres–Velasquez, A. C., Katherine, L., & Pablo, J. (2023). Pyrolysis of Colombian spent coffee grounds (SCGs), characterization of bio–oil, and study of its antioxidant properties. *International Journal of Sustainable Energy*, *42*(1), 811–829. https://doi.org/10.1080/14786451.2023.2235025

Mandal, G., & Joshi, S. P. (2015). Eco–physiology and habitat invasibility of an invasive, tropical shrub (*Lantana camara*) in western Himalayan forests of India. *Forest Science and Technology*, *11*(4), 182–196. https://doi.org/10.1080/21580103.2014.990062

Manirakiza, P., Covaci, A., & Schepens, P. (2001). Comparative Study on Total Lipid Determination using Soxhlet, Roese–Gottlieb, Bligh & Dyer, and Modified Bligh & Dyer Extraction Methods. *Journal of Food Composition and Analysis*, *14*(1), 93–100. https://doi.org/10.1006/jfca.2000.0972

Mansoori, A., Singh, N., Dubey, S. K., Thakur, T. K., Alkan, N., Das, S. N., & Kumar, A. (2020). Phytochemical Characterization and Assessment of Crude Extracts from *Lantana camara* L. for Antioxidant and Antimicrobial Activity. *Frontiers in Agronomy*, *2*. https://doi.org/10.3389/fagro.2020.582268

Maldonado, J., Oliva, A., Guzmán, L., Molinari, A., & Acevedo, W. (2024). Synthesis, Anticancer Activity, and Docking Studies of Novel Hydroquinone–Chalcone–Pyrazoline Hybrid Derivatives. *International Journal of Molecular Sciences*, *25*(13), 7281–7281. https://doi.org/10.3390/ijms25137281

Masudi, A., Muraza, O., Che, W., & Ubaidillah, U. (2022). Improvements in the stability of biodiesel fuels: recent progress and challenges. *Environmental Science and Pollution Research*, *30*(6), 14104–14125. https://doi.org/10.1007/s11356–022–25048–4

Matayeva, A., Basile, F., Cavani, F., Bianchi, D., & Chiaberge, S. (2019). Development of Upgraded Bio–Oil Via Liquefaction and Pyrolysis. *Studies in Surface Science and Catalysis*, *178*, 231–256. https://doi.org/10.1016/b978–0–444–64127–4.00012–4

Mattos, C., Veloso, M. C. C., Romeiro, G. A., & Folly, E. (2019). Biocidal applications trends of bio–oils from pyrolysis: Characterization of several conditions and biomass, a review. *Journal of Analytical and Applied Pyrolysis*, *139*, 1–12. https://doi.org/10.1016/j.jaap.2018.12.029

Maulinda, L., Husin, H., Arahman, N., Rosnelly, C. M., Syukri, M., Nurhazanah, Nasution, F., Ahmadi. (2023). The Influence of Pyrolysis Time and Temperature on the Composition and Properties of Bio–Oil Prepared from Tanjong Leaves (*Mimusops elengi*). Sustainability 15:13851. https://doi.org/10.3390/su151813851

Máximo, P., Ferreira, L. M., Branco, P. S., & Lourenço, A. (2020). Invasive Plants: Turning Enemies into Value. *Molecules*, *25*(15), 3529. https://doi.org/10.3390/molecules25153529

McCormick, N., & Howard, G. (2013). Beating back biofuel crop invasions: Guidelines on managing the invasive risk of biofuel developments. *Renewable Energy*, *49*, 263–266. https://doi.org/10.1016/j.renene.2012.01.018

McKendry, P. (2002). Energy production from biomass (part 1): overview of biomass. *Bioresource Technology*, *83*(1), 37–46. https://doi.org/10.1016/s0960–8524(01)00118–3

Mehariya, S., Iovine, A., Casella, P., Musmarra, D., Figoli, A., Marino, T., Sharma, N., & Molino, A. (2020). Fischer–Tropsch synthesis of syngas to liquid hydrocarbons. In *Lignocellulosic Biomass to Liquid Biofuels*, 217–248. https://doi.org/10.1016/b978–0–12–815936–1.00007–1

Mehra, K. S., Singh, S., Singh, A. K., Kharkwal, H., & Avikal, S. (2021). Performance, energy, emission and cost analysis of Jatropha (*Jatropha Curcas*) oil as a biofuel for compression ignition engine. *Materials Today: Proceedings*, *43*, 348–354. https://doi.org/10.1016/j.matpr.2020.11.675

Meng, J., Moore, A. M., Tilotta, D. C., Kelley, S. S., Adhikari, S., & Park, S. (2015). Thermal and Storage Stability of Bio–Oil from Pyrolysis of Torrefied Wood. *Energy & Fuels*, *29*(8), 5117–5126. https://doi.org/10.1021/acs.energyfuels.5b00929

Mhlongo, E. S., Ruwanza, S., & Dalu, T. (2024). Perceptions, Knowledge, and Invasion Extent of *Lantana camara* on Household Yards in Rural Communities in Limpopo Province, South Africa. *Society & Natural Resources*, 1–22. https://doi.org/10.1080/08941920.2024.2338773

Michailos, S., & Bridgwater, A. (2019). A comparative techno-economic assessment of three bio-oil upgrading routes for aviation biofuel production. *International Journal of Energy Research*, *43*. https://doi.org/10.1002/er.4745

Midhun, V. C., Jayaprasad, G., Anto, A., & Anish, R. (2023). Preparation and characterisation study of water hyacinth briquettes. *Materials Today: Proceedings*. https://doi.org/10.1016/j.matpr.2023.07.157

Míguez, C., Cancela, Á., Álvarez, X., & Sánchez, Á. (2022). The reuse of bio–waste from the invasive species Tradescantia fluminensis as a source of phenolic compounds. *Journal of Cleaner Production*, *336*, 130293. https://doi.org/10.1016/j.jclepro.2021.130293

Milly, P. J., Toledo, R. T., & Chen, J. (2008). Evaluation of Liquid Smoke Treated Ready-to-Eat (RTE) Meat Products for Control of *Listeria innocua* M1. *Journal of Food Science*, *73*(4). https://doi.org/10.1111/j.1750–3841.2008.00714.x

Miniat, C. F., Fraterrigo, J. M., Brantley, S. T., Callaham, M. A., Cordell, S., Dukes, J. S., Giardina, C. P., Jose, S., & Lovett, G. (2021). Impacts of Invasive Species on Forest and Grassland Ecosystem Processes in the United States. *Invasive Species in Forests and Rangelands of the United States*, 41–55. https://doi.org/10.1007/978–3–030–45367–1_3

Ministry of Rural Development. (2024). https://nregaplus.nic.in/netnrega/WriteReaddata/Circulars/2476Wage_Rate_notification_FY_2024–25.pdf. Accessed 12 December 2024

Moens, L., Black, S. K., Myers, M. D., & Czernik, S. (2009). Study of the Neutralization and Stabilization of a Mixed Hardwood Bio–Oil. *Energy & Fuels*, *23*(5), 2695–2699. https://doi.org/10.1021/ef8009266

Mohan, D., Pittman, C. U., & Steele, P. H. (2006). Pyrolysis of Wood/Biomass for Bio–oil: A Critical Review. *Energy & Fuels*, *20*(3), 848–889. https://doi.org/10.1021/ef0502397

Mohan, D., Shi, J., Nicholas, D. D., Pittman, C. U., Steele, P. H., & Cooper, J. E. (2008). Fungicidal values of bio–oils and their lignin–rich fractions obtained from wood/bark fast pyrolysis. *Chemosphere*, *71*(3), 456–465. https://doi.org/10.1016/j.chemosphere.2007.10.049

Montenegro–Landívar, M. F., Tapia–Quirós, P., Vecino, X., Reig, M., Valderrama, C., Granados, M., Cortina, J. L., & Saurina, J. (2021). Polyphenols and their potential role to fight viral diseases: An overview. *Science of the Total Environment*, *801*, 149719. https://doi.org/10.1016/j.scitotenv.2021.149719

Mtshali, B., Kassim, A., Sibanda, S., & Workneh, T. (2025). Characterization of South African Woody and Non–Woody Invasive Alien Plant Species for Sustainable Bio–Oil Production. *Energies*, *18*(8), 1919–1919. https://doi.org/10.3390/en18081919

Muh, E., Tabet, F., & Amara, S. (2019). Biomass conversion to fuels and value–added chemicals: A comprehensive review of the thermochemical processes. *Current Alternative Energy*, *03*. https://doi.org/10.2174/2405463103666191022121648

Murali, R., & Saravanan, R. (2012). Antidiabetic effect of d–limonene, a monoterpene in streptozotocin–induced diabetic rats. *Biomedicine & Preventive Nutrition*, *2*(4), 269–275. https://doi.org/10.1016/j.bionut.2012.08.008

Nanda, S., Mohanty, P., Pant, K. K., Naik, S., Kozinski, J. A., & Dalai, A. K. (2012). Characterization of North American Lignocellulosic Biomass and Biochars in Terms of their Candidacy for Alternate Renewable Fuels. *BioEnergy Research*, *6*(2), 663–677. https://doi.org/10.1007/s12155–012–9281–4

Nandhini, R. S., Nithya, R. N., & K., V. (2021). GC–MS analysis of Phytochemical compounds in different extracts of *Curculigo orchiodes*. *Research Journal of Pharmacy and Technology*, *14*(8), 4355–4360. https://doi.org/10.52711/0974–360x.2021.00756

Negi, B., Khatri, K., Bargali, S. S., & Bargali, K. (2024). Factors determining the invasion pattern of *Ageratina adenophora* Spreng. in Kumaun Himalaya India.

*Environmental and Experimental Botany*, *228*, 106027. https://doi.org/10.1016/j.envexpbot.2024.106027

Nguyen, D. T. C., Le, H. T. N., Nguyen, T. T., Nguyen, T. T. T., Liew, R. K., Bach, L. G., Nguyen, T. D., Vo, D.–V. N., & Tran, T. V. (2021). Engineering conversion of Asteraceae plants into biochars for exploring potential applications: A review. *Science of the Total Environment*, *797*, 149195. https://doi.org/10.1016/j.scitotenv.2021.149195

Nong, H. T. T., Unpaprom, Y., Chaichompoo, C., & Ramaraj, R. (2021). Biomethane potential of invasive aquatic weed water primrose. *Global Journal of Science & Engineering*, 1–5. https://doi.org/10.37516/global.j.sci.eng.2021.0025

Oasmaa, A., & Czernik, S. (1999). Fuel Oil Quality of Biomass Pyrolysis Oils State of the Art for the End Users. *Energy & Fuels*, *13*(4), 914–921. https://doi.org/10.1021/ef980272b

Ogunkanmi, J. O., Kulla, D. M., Omisanya, N. O., Sumaila, M., Obada, D. O., & Dodoo–Arhin, D. (2018). Extraction of bio–oil during pyrolysis of locally sourced palm kernel shells: Effect of process parameters. *Case Studies in Thermal Engineering*, *12*, 711–716. https://doi.org/10.1016/j.csite.2018.09.003

Olcese, R. N., Lardier, G., Bettahar, M., Ghanbaja, J., Fontana, S., Carré, V., Aubriet, F., Petitjean, D., & Dufour, A. (2013). Aromatic Chemicals by Iron-Catalyzed Hydrotreatment of Lignin Pyrolysis Vapor. *ChemSusChem*, *6*(8), 1490–1499. https://doi.org/10.1002/cssc.201300191

Onokwai, A. O., Ajisegiri, E. S. A., Okokpujie, I. P., Ibikunle, R. A., Oki, M., & Dirisu, J. O. (2022). Characterization of lignocellulose biomass based on proximate, ultimate, structural composition, and thermal analysis. *Materials Today: Proceedings*, *65*, 2156–2162. https://doi.org/10.1016/j.matpr.2022.05.313

Oyebanji, J. A., Okekunle, P. O., Lasode, O. A., & Oyedepo, S. O. (2017). Chemical composition of bio–oils produced by fast pyrolysis of two energy biomass. *Biofuels*, *9*(4), 479–487. https://doi.org/10.1080/17597269.2017.1284473

Özçimen, D., & Ersoy–Meriçboyu, A. (2010). Characterization of biochar and bio–oil samples obtained from carbonization of various biomass materials. *Renewable Energy*, *35*(6), 1319–1324. https://doi.org/10.1016/j.renene.2009.11.042

Özyuğuran, A., & Yaman, S. (2017). Prediction of Calorific Value of Biomass from Proximate Analysis. *Energy Procedia*, *107*, 130–136. https://doi.org/10.1016/j.egypro.2016.12.149

Page, B. D. G., Valerie, N. C. K., Wright, R. H. G., Wallner, O., Isaksson, R., Carter, M., Rudd, S. G., Loseva, O., Jemth, A.–S., Almlöf, I., Font–Mateu, J., Llona–Minguez, S., Baranczewski, P., Jeppsson, F., Homan, E., Almqvist, H., Axelsson, H., Regmi, S., Gustavsson, A.–L., & Lundbäck, T. (2018). Targeted NUDT5 inhibitors block hormone signaling in breast cancer cells. *Nature Communications*, *9*(1). https://doi.org/10.1038/s41467–017–02293–7

Pandey, S. P., & Kumar, S. (2020). Valorisation of *Argemone mexicana* seeds to renewable fuels by thermochemical conversion process. *Journal of Environmental Chemical Engineering*, *8*(5), 104271. https://doi.org/10.1016/j.jece.2020.104271

Parikka, M. (2004). Global biomass fuel resources. *Biomass and Bioenergy*, *27*(6), 613–620. https://doi.org/10.1016/j.biombioe.2003.07.005

Parvej, A. M., Rahman, M. A., & Reza, K. Md. A. (2022). The combined effect of solar assisted torrefaction and pyrolysis on the production of valuable chemicals obtained from water hyacinth biomass. *Cleaner Waste Systems*, *3*, 100027–100027. https://doi.org/10.1016/j.clwas.2022.100027

Patra, J., Kim, S., Hwang, H., Choi, J., & Baek, K.–H. (2015). Volatile Compounds and Antioxidant Capacity of the Bio–Oil Obtained by Pyrolysis of Japanese Red Pine (*Pinus Densiflora* Siebold and Zucc.). *Molecules*, *20*(3), 3986–4006. https://doi.org/10.3390/molecules20033986

Pattanayak, S., Hauchhum, L., Loha, C., & Sailo, L. (2019). Selection criteria of appropriate bamboo based biomass for thermochemical conversion process.

*Biomass Conversion and Biorefinery*. https://doi.org/10.1007/s13399–019–00421–5

Pavia, D. L., Lampman, G. M., Kriz, G. S., & Vyvyan, J. A. (2015). *Introduction to Spectroscopy* (5th ed.). Cengage Learning India Private Limited.

Pejchar, L., & Mooney, H. A. (2009). Invasive species, ecosystem services and human well–being. *Trends in Ecology & Evolution*, *24*(9), 497–504. https://doi.org/10.1016/j.tree.2009.03.016

Petersen, A. M., Chireshe, F., Gorgens, J. F., & Van Dyk, J. (2022). Flowsheet analysis of gasification–synthesis–refining for sustainable aviation fuel production from invasive alien plants. *Energy*, *245*, 123210. https://doi.org/10.1016/j.energy.2022.123210

Pérez, A., Ruiz, B., Fuente, E., Calvo, L. F., & Paniagua, S. (2021). Pyrolysis technology for *Cortaderia selloana* invasive species. Prospects in the biomass energy sector. *Renewable Energy*, *169*, 178–190. https://doi.org/10.1016/j.renene.2021.01.015

Pérez–Postigo, I., Vibrans, H., Bendix, J., & Cuevas–Guzmán, R. (2021). Floristic composition and potential invasiveness of alien herbaceous plant in Western Mexico. *Revista de Biologia Tropical*, *69*(3). https://doi.org/10.15517/rbt.v69i3.45855

Peter, A., Žlabur, J. Š., Šurić, J., Voća, S., Purgar, D. D., Pezo, L., & Voća, N. (2021). Invasive Plant Species Biomass—Evaluation of Functional Value. *Molecules*, *26*(13), 3814. https://doi.org/10.3390/molecules26133814

Petroleum Planning and Analysis Cell. (2025). *Snapshots of India's Oil and Gas Data*. Ppac.gov.in. https://ppac.gov.in/download.php?file=rep_studies/1745216454_Snapshot%20of%20Indias%20OIl%20%20Gas%20Data–March2025_A5_Final.pdf. Accessed 29 January 2025

Pham, L. K. H., Kongparakul, S., Reubroycharoen, P., Karnjanakom, S., Naqvi, S. R., Guan, G., & Samart, C. (2022). Biofuel production with integrated pyrolysis and catalytic upgrading system. In *Elsevier eBooks* (pp. 147–177). Elsevier BV. https://doi.org/10.1016/b978–0–323–85586–0.00012–3

Phillips, E.A. (1959). Methods of Vegetation Study. Henry Holt and Co. Inc., New York.

Phukan, M. M., Bora, P., Gogoi, K., & Konwar, B. K. (2019). Biodiesel from *Saccharomyces cerevisiae*: fuel property analysis and comparative economics. *SN Applied Sciences*, *1*(2). https://doi.org/10.1007/s42452–019–0159–3

Pinheiro, P. F., Martins, G. S., Gonçalves, P. M., Vasconcelos, L. C., Dos, A., Scotá, M. B., Silva, I., Pereira, U. A., & Praça–Fontes, M. M. (2024). Synthesis and evaluation of esters obtained from phenols and phenoxyacetic acid with significant phytotoxic and cytogenotoxic activities. *Environmental Science and Pollution Research*, *31*(50), 60023–60040. https://doi.org/10.1007/s11356–024–35222–5

Premjet, S. (2019). Potential of Weed Biomass for Bioethanol Production. In *Fuel Ethanol Production from Sugarcane*. IntechOpen. https://doi.org/10.5772/intechopen.77507

Rahmawati, R., & Rosleine, D. (2023). Spatial distribution of invasive plants in Bandung, West Java, Indonesia. *Biotropia: The Southeast Asian Journal of Tropical Biology*, *30*(2), 171–182. https://doi.org/10.11598/btb.2023.30.2.1780

Rai, P. K. (2016). Impacts of particulate matter pollution on plants: Implications for environmental biomonitoring. *Ecotoxicology and Environmental Safety*, *129*, 120–136. https://doi.org/10.1016/j.ecoenv.2016.03.012

Ralte, L., Khiangte, L., Thangjam, N. M., Kumar, A., & Singh, Y. T. (2022). GC–MS and molecular docking analyses of phytochemicals from the underutilized plant, *Parkia timoriana* revealed candidate anti–cancerous and anti–inflammatory agents. *Scientific Reports*, *12*(1). https://doi.org/10.1038/s41598–022–07320–2

Ramesh, N., & Murugavelh, S. (2022). A cleaner process for conversion of invasive weed (*Prosopis juliflora*) into energy–dense fuel: kinetics, energy, and exergy analysis of pyrolysis process. *Biomass Conversion and Biorefinery*, *12*, 3067–3080. https://doi.org/10.1007/s13399–020–00747–5

Ramesh, N., & Somasundaram, M. (2020). Thermochemical conversion of *Parthenium hysterophorus* biomass for bio–oil synthesis: kinetics and techno–economic analysis. *Biomass Conversion and Biorefinery*, *12*. https://doi.org/10.1007/s13399–020–00790–2

Ranjini, T., Niral, V., Surekha, Panjavarnam, G., & Gayathri, U. (2024). Diversity and dynamics of weed flora in coconut gardens with varied spacings along the west coast of Kerala, India. *International Journal of Research in Agronomy*, *7*(3S), 19–22. https://doi.org/10.33545/2618060x.2024.v7.i3sa.372

Rapoo, M. T., Singh, S., Chong, K., Banks, S., & Blanco, P. H. (2023). Analytical fast pyrolysis of *P. Juliflora*: A thermal and catalytic study. *Journal of Analytical and Applied Pyrolysis*, *176*, 106254–106254. https://doi.org/10.1016/j.jaap.2023.106254

Ren, Z., Xie, L., Okyere, S. K., Wen, J., Ran, Y., Nong, X., & Hu, Y. (2022). Antibacterial Activity of Two Metabolites Isolated from Endophytic Bacteria *Bacillus velezensis* Ea73 in *Ageratina adenophora*. *Frontiers in Microbiology*, *13*. https://doi.org/10.3389/fmicb.2022.860009

Reuss, S. A., Buhler, D. D., & Gunsolus, J. L. (2001). Effects of soil depth and aggregate size on weed seed distribution and viability in a silt loam soil. *Applied Soil Ecology*, *16*(3), 209–217. https://doi.org/10.1016/s0929–1393(00)00115–3

Reza, M. S., Ahmed, A., Caesarendra, W., Abu Bakar, M. S., Shams, S., Saidur, R., Aslfattahi, N., & Azad, A. K. (2019). *Acacia Holosericea*: An Invasive Species for Bio–char, Bio–oil, and Biogas Production. *Bioengineering*, *6*(2), 33. https://doi.org/10.3390/bioengineering6020033

Rodríguez–Arce, E., & Saldías, M. (2021). Antioxidant properties of flavonoid metal complexes and their potential inclusion in the development of novel strategies for the treatment against neurodegenerative diseases. *Biomedicine & Pharmacotherapy, 143*, 112236. https://doi.org/10.1016/j.biopha.2021.112236

Romero, D. M., Junca, J. S. G., Katherine, L., & Pablo, J. (2023). Elucidating the pyrolysis properties of water hyacinth (*Eichhornia crassipes*) biomass and characterisation of its pyrolysis products. *International Journal of Sustainable Energy*, *42*(1), 72–90. https://doi.org/10.1080/14786451.2023.2167997

Romero–Anaya, A. J., Molina, A., Garcia, P., Ruiz–Colorado, A. A., Linares–Solano, A., & Salinas–Martínez de Lecea, C. (2011). Phosphoric acid activation of recalcitrant biomass originated in ethanol production from banana plants. *Biomass and Bioenergy*, *35*(3), 1196–1204. https://doi.org/10.1016/j.biombioe.2010.12.007

Runnebaum, R. C., Nimmanwudipong, T., Block, D. E., & Gates, B. C. (2011). Catalytic conversion of compounds representative of lignin–derived bio–oils: a reaction network for guaiacol, anisole, 4–methylanisole, and cyclohexanone conversion catalysed by Pt/γ–Al2O3. *Catalysis Science & Technology*, *2*(1), 113–118. https://doi.org/10.1039/C1CY00169H

Ruswanto, R., Nofianti, T., Mardianingrum, R., Kesuma, D., & Siswandono, N. (2022). Design, molecular docking, and molecular dynamics of thiourea–iron (III) metal complexes as NUDT5 inhibitors for breast cancer treatment. *Heliyon*, *8*(9), e10694–e10694. https://doi.org/10.1016/j.heliyon.2022.e10694

Ruwanza, S., & Shackleton, C. M. (2016). Effects of the invasive shrub,Lantana camara, on soil properties in the Eastern Cape, South Africa. *Weed Biology and Management*, *16*(2), 67–79. https://doi.org/10.1111/wbm.12094

Sahoo, A., Kumar, S., Kumar, J., & Bhaskar, T. (2020). A detailed assessment of pyrolysis kinetics of invasive lignocellulosic biomasses *(Prosopis juliflora* and *Lantana camara*) by thermogravimetric analysis. *Bioresource Technology*, *319*, 124060–124060. https://doi.org/10.1016/j.biortech.2020.124060

Sahoo, A., Saini, K., Negi, S., Kumar, J., Pant, K. K., & Bhaskar, T. (2022). Inspecting the bioenergy potential of noxious *Vachellia nilotica* weed via pyrolysis: Thermo–kinetic study, neural network modeling and response surface optimization. *Renewable Energy*, *185*, 386–402. https://doi.org/10.1016/j.renene.2021.12.007

Saikia, P., Gupta, U. N., Barman, R. S., Kataki, R., Chutia, R. S., & Baruah, B. P. (2015). Production and Characterization of Bio–Oil Produced from *Ipomoea carnea* Bio–Weed. *BioEnergy Research*, *8*(3), 1212–1223. https://doi.org/10.1007/s12155–014–9561–2

Salaudeen, M. T., Daniya, E., Olaniyi, O. M., Folorunso, T. A., Bala, J. A., Abdullahi, I. M., Nuhu, B. K., Adedigba, A. P., Oluwole, B. I., Bankole, A. O., & Macarthy, O. M. (2022). Phytosociological survey of weeds in irrigated maize fields in a Southern Guinea Savanna of Nigeria. *Frontiers in Agronomy*, *4*. https://doi.org/10.3389/fagro.2022.985067

Saletnik, B., Zagula, G., Bajcar, M., Czernicka, M., & Puchalski, C. (2018). Biochar and Biomass Ash as a Soil Ameliorant: The Effect on Selected Soil Properties and Yield of Giant Miscanthus (*Miscanthus x giganteus*). *Energies*, *11*(10), 2535. https://doi.org/10.3390/en11102535

Salisu, S. S., Aliyu, A., Atta, A. Y., & El–Yakubu, B. J. (2025). Bimetallic HZSM–5 catalysts: A review on the aromatisation of light alkanes (C1–C5) and liquefied petroleum gas (LPG) for benzene, toluene, and xylene (BTX) production. *Next Research.*, *2*(1), 100181–100181. https://doi.org/10.1016/j.nexres.2025.100181

Santamarina, S., Mateo, R. G., Alfaro–Saíz, E., & Acedo, C. (2023). On the importance of invasive species niche dynamics in plant conservation management at large and local scale. *Frontiers in Ecology and Evolution*, *10*. https://doi.org/10.3389/fevo.2022.1049142

Santos, L., Silva, F., Santos, L., Carregosa, I., & Wisniewski Jr., A. (2017). Potential Bio–Oil Production from Invasive Aquatic Plants by Microscale Pyrolysis Studies.

*Journal of the Brazilian Chemical Society*, *29*(1). https://doi.org/10.21577/0103–5053.20170124

Sarker, T. R., German, C. S., Borugadda, V. B., Meda, V., & Dalai, A. K. (2023). Techno–economic analysis of torrefied fuel pellet production from agricultural residue via integrated torrefaction and pelletization process. *Heliyon*, *9*(6), e16359–e16359. https://doi.org/10.1016/j.heliyon.2023.e16359

Savoia, D. (2012). Plant–derived antimicrobial compounds: alternatives to antibiotics. *Future Microbiology*, *7*(8), 979–990. https://doi.org/10.2217/fmb.12.68

Saynik, P. B., & Moholkar, V. S. (2021). Investigations in influence of different pretreatments on A. donax pyrolysis: Trends in product yield, distribution and chemical composition. *Journal of Analytical and Applied Pyrolysis*, *158*, 105276–105276. https://doi.org/10.1016/j.jaap.2021.105276

Scheibe, A. S., Pimenta, I., Janssen, L., Amabile, T., Vicente, Vasques, R., Alexandre, J., Rita, M.A, S., & Augusto, A. (2022). Products from pyrolysis textile sludge as a potential antibacterial and alternative source of fuel oil. *Cleaner Engineering and Technology*, *6*, 100408–100408. https://doi.org/10.1016/j.clet.2022.100408

Seboka, Y. (2009) Charcoal production: opportunities and barriers for improving efficiency and sustainability. *Bio–carbon Opportunities in Eastern & Southern Africa*, 102–126.

Shackleton, R. T., Witt, A. B. R., Piroris, F. M., & van Wilgen, B. W. (2017). Distribution and socio–ecological impacts of the invasive alien cactus *Opuntia stricta* in eastern Africa. *Biological Invasions*, *19*(8), 2427–2441. https://doi.org/10.1007/s10530–017–1453–x

Shaik, R. S., Gurusinghe, S., Weston, L. A., & Downey, P. (2022). A Historical Perspective on Plant Invasion in Australia. *Springer EBooks*, 129–149. https://doi.org/10.1007/978–3–030–89684–3_6

Shavyrkina, N. A., Budaeva, V. V., Skiba, E. A., Gismatulina, Y. A., & Sakovich, G. V. (2023). Review of Current Prospects for Using Miscanthus–Based Polymers. *Polymers*, *15*(14), 3097–3097. https://doi.org/10.3390/polym15143097

Shen, N., Wang, Q., Zhu, J., Qin, Y., Liao, S., Yi, L., Zhu, Q., Jin, Y., Du, L., & Huang, R. (2016). Succinic acid production from duckweed (*Landoltia punctata*) hydrolysate by batch fermentation of Actinobacillus succinogenes GXAS137. *Bioresource Technology*, *211*, 307–312. https://doi.org/10.1016/j.biortech.2016.03.036

Shezi, M., Kiambi, S. L., & Isa, Y. M. (2024). Seasonal Harvesting Impact on Biomass Fuel Properties and Pyrolysis-Derived Bio-Oil Organic Phase Composition. *GCB Bioenergy*, *16*(12). https://doi.org/10.1111/gcbb.70011

Shi, L., Zhao, W., Yang, Z., Subbiah, V., & Suleria, H. A. R. (2022). Extraction and characterization of phenolic compounds and their potential antioxidant activities. *Environmental Science and Pollution Research*, *29*. https://doi.org/10.1007/s11356–022–23337–6

Shon, M. (2003). Antioxidants and free radical scavenging activity of *Phellinus baumii* (Phellinus of Hymenochaetaceae) extracts. *Food Chemistry*, *82*(4), 593–597. https://doi.org/10.1016/s0308–8146(03)00015–3

Sikarwar, V. S., Zhao, M., Fennell, P. S., Shah, N., & Anthony, E. J. (2017). Progress in biofuel production from gasification. *Progress in Energy and Combustion Science*, *61*, 189–248. https://doi.org/10.1016/j.pecs.2017.04.001

Silverstein, R. M., Webster, F. X., Kiemle, D. J., & Bryce, D. L. (2015). *Spectrometric identification of organic compounds*. Wiley.

Simonetti, G., Brasili, E., & Pasqua, G. (2020). Antifungal Activity of Phenolic and Polyphenolic Compounds from Different Matrices of *Vitis vinifera* L. against Human Pathogens. *Molecules*, *25*(16), 3748. https://doi.org/10.3390/molecules25163748

Singh, A., Nanda, S., Sosa, F. G., & Berruti, F. (2020). Pyrolysis of *Miscanthus* and characterization of value-added bio-oil and biochar products. *The Canadian Journal of Chemical Engineering*. https://doi.org/10.1002/cjce.23978

Singh, G., Passari, A. K., Kumar, N. S., Kumar, B., Nayak, S. C., Ram, H., & Singh, B. P. (2024a). UPLC–ESI MS/MS– and GC–MS–Based Altitudinal Variations in the Bioactive Potential of *Mikania micrantha* and *Ageratum houstonianum*. *Applied Biochemistry and Biotechnology*, *197*. https://doi.org/10.1007/s12010–024–05005–2

Singh, S., Meena, P., Bhoi, R., Saharan, V. K., & George, S. (2024b). Optimization of bio–oil extraction from Chlorella biomass via a green approach to obtain algal–based Di–ethyl phthalate. *Environmental Science and Pollution Research*, *31*(46), 57444–57454. https://doi.org/10.1007/s11356–023–30866–1

Slopiecka, K., Bartocci, P., & Fantozzi, F. (2012). Thermogravimetric analysis and kinetic study of poplar wood pyrolysis. *Applied Energy*, *97*, 491–497. https://doi.org/10.1016/j.apenergy.2011.12.056

Smith, A. L., Klenk, N., Wood, S., Hewitt, N., Henriques, I., Yan, N., & Bazely, D. R. (2013). Second generation biofuels and bioinvasions: An evaluation of invasive risks and policy responses in the United States and Canada. *Renewable and Sustainable Energy Reviews*, *27*, 30–42. https://doi.org/10.1016/j.rser.2013.06.013

Sosnoskie, L. M., & Duke, S. O. (2023). Implications of weakening of the United States Geological Survey Pesticide National Synthesis Project for Weed Scientists. *Weed Science*, *71*(6), 517–519. https://doi.org/10.1017/wsc.2023.59

Sousa, E. O., Miranda, C. M. B. A., Nobre, C. B., Boligon, A. A., Athayde, M. L., & Costa, J. G. M. (2015). Phytochemical analysis and antioxidant activities of *Lantana camara* and *Lantana montevidensis* extracts. *Industrial Crops and Products*, *70*, 7–15. https://doi.org/10.1016/j.indcrop.2015.03.010

Studer, G., Rempfer, C., Waterhouse, A. M., Gumienny, R., Haas, J., & Schwede, T. (2019). QMEANDisCo – Distance Constraints Applied on Model Quality Estimation. *Bioinformatics*, *36*(6). https://doi.org/10.1093/bioinformatics/btz828

Sugumaran, V., Prakash, S., Ramu, E., Arora, A., Bansal, V., Kagdiyal, V., & Saxena, D. (2017). Detailed characterization of bio–oil from pyrolysis of non–edible seed–cakes by Fourier Transform Infrared Spectroscopy (FTIR) and gas chromatography mass spectrometry (GC–MS) techniques. *Journal of Chromatography B*, *1058*, 47–56. https://doi.org/10.1016/j.jchromb.2017.05.014

Sultana, R. (2019). Molecular docking based virtual screening of the breast cancer target NUDT5. *Bioinformation*, *15*(11), 784–789. https://doi.org/10.6026/97320630015784

Sun, M.–H., Zhou, J., Hu, Z.–Y., Chen, L.–H., Li, L.–Y., Wang, Y.–D., Xie, Z.–K., Turner, S., Van Tendeloo, G., Hasan, T., & Su, B.–L. (2020). Hierarchical Zeolite Single–Crystal Reactor for Excellent Catalytic Efficiency. *Matter*, *3*(4), 1226–1245. https://doi.org/10.1016/j.matt.2020.07.016

Suraiya, S., Bristy, S. A., Ali, M. S., Biswas, A., Ali, M. R., & Haq, M. (2023). A Green Approach to Valorizing Abundant Aquatic Weeds for Nutrient–Rich Edible Paper Sheets Production in Bangladesh. *Clean Technologies*, *5*(4), 1269–1286. https://doi.org/10.3390/cleantechnol5040064

Suresh, S., Karthikeyan, S., Saravanan, P., Jayamoorthy, K., & Dhanalekshmi, K. I. (2016). Comparison of antibacterial and antifungal activity of 5–amino–2–mercapto benzimidazole and functionalized Ag3O4 nanoparticles. *Karbala International Journal of Modern Science*, *2*(2), 129–137. https://doi.org/10.1016/j.kijoms.2016.03.003

Suriapparao, D. V., Pradeep, N., & Vinu, R. (2015). Bio–Oil Production from *Prosopis juliflora* via Microwave Pyrolysis. *Energy & Fuels*, *29*(4), 2571–2581. https://doi.org/10.1021/acs.energyfuels.5b00357

Suriapparao, D. V., Reddy, B. R., Rao, C. S., Jeeru, L. R., & Kumar, T. H. (2023). *Prosopis juliflora* valorization via microwave–assisted pyrolysis: Optimization of reaction parameters using machine learning analysis. *Journal of Analytical and Applied Pyrolysis*, *169*, 105811. https://doi.org/10.1016/j.jaap.2022.105811

Świętek, M., Lu, Y.–C., Konefał, R., Ferreira, L. P., Cruz, M. M., Ma, Y.–H., & Horák, D. (2019). Scavenging of reactive oxygen species by phenolic compound–modified maghemite nanoparticles. *Beilstein Journal of Nanotechnology*, *10*, 1073–1088. https://doi.org/10.3762/bjnano.10.108

Tefera, N., Assefa, A., & Tamiru, G. (2020). Distribution and abundance of invasive alien weed species in Wolayita Zone, Ethiopia. *Cogent Food & Agriculture*, *6*(1), 1778434. https://doi.org/10.1080/23311932.2020.1778434

Tekwu, E. M., Pieme, A. C., & Beng, V. P. (2012). Investigations of antimicrobial activity of some Cameroonian medicinal plant extracts against bacteria and yeast with gastrointestinal relevance. *Journal of Ethnopharmacology*, *142*(1), 265–273. https://doi.org/10.1016/j.jep.2012.05.005

Tudge, S. J., Purvis, A., & De Palma, A. (2021). The impacts of biofuel crops on local biodiversity: a global synthesis. *Biodiversity and Conservation*, *30*(11), 2863–2883. https://doi.org/10.1007/s10531–021–02232–5

Tungmunnithum, D., Thongboonyou, A., Pholboon, A., & Yangsabai, A. (2018). Flavonoids and Other Phenolic Compounds from Medicinal Plants for Pharmaceutical and Medical Aspects: An Overview. *Medicines*, *5*(3), 93. https://doi.org/10.3390/medicines5030093

Udomsap, P., Yeinn, Y. H., Hui, J. T. H., Yoosuk, B., Yusuf, S. B., & Sukkasi, S. (2011). Towards stabilization of bio–oil by addition of antioxidants and solvents, and emulsification with conventional hydrocarbon fuels. *IEEE Xplore*. https://doi.org/10.1109/ICUEPES.2011.6497720

Udomsri, S., Martin, A. R., & Fransson, T. H. (2010). Economic assessment and energy model scenarios of municipal solid waste incineration and gas turbine hybrid

dual–fueled cycles in Thailand. *Waste Management*, *30*(7), 1414–1422. https://doi.org/10.1016/j.wasman.2010.02.009

Ugartondo, V., Mitjans, M., & Vinardell, M. (2008). Comparative antioxidant and cytotoxic effects of lignins from different sources. *Bioresource Technology*, *99*(14), 6683–6687. https://doi.org/10.1016/j.biortech.2007.11.038

United Nations. (1992). *Convention on Biological Diversity*. https://www.cbd.int/doc/legal/cbd–en.pdf. Accessed 15 February 2025

Utami, J. P., Diana, S., Arifin, R., Taufiqurrahman, I., Nugraha, K. A., Sari, M. W., & Wardana, R. Y. (2022). Antibacterial activity of *Stachytarpheta jamaicensis* (L.) Vahl roots extract on some bacteria proteins: An in silico and in vitro study. *Journal of Pharmacy & Pharmacognosy Research*, *10*(6), 1087–1102. https://doi.org/10.56499/jppres22.1474_10.6.1087

Vaou, N., Stavropoulou, E., Voidarou, C., Tsigalou, C., & Bezirtzoglou, E. (2021). Towards Advances in Medicinal Plant Antimicrobial Activity: A Review Study on Challenges and Future Perspectives. *Microorganisms*, *9*(10), 2041. https://doi.org/10.3390/microorganisms9102041

Venkatachalam, C. D., Sengottian, M., Ravichandran, S. R., Subramaniyan, K., & Thangamuthu, P. K. (2020). Optimization Studies on Subcritical Water Extraction of Fuels and Fine Chemicals from *Prosopis juliflora*: An Invasive Weed Tree. *Periodica Polytechnica. Chemical Engineering (Print)*, *65*(1), 105–115. https://doi.org/10.3311/ppch.15187

Verma, A. K., Nayak, R., Manika, N., Bargali, K., Pandey, V. N., Chaudhary, L. B., & Behera, S. K. (2022). Monitoring the distribution pattern and invasion status of *Ageratina adenophora* across elevational gradients in Sikkim Himalaya, India. *Environmental Monitoring and Assessment*, *195*(1). https://doi.org/10.1007/s10661–022–10549–z

Wahyuni, I., Sulistijorini, Setiabudi, Meijide, A., Nomura, M., Kreft, H., Rembold, K., Tjitrosoedirdjo, S. S., & Tjitrosoedirdjo, S. (2016). Distribution of Invasive Plant

Species in Different Land–Use Systems in Sumatera, Indonesia. *Biotropia*, *23*(2). https://doi.org/10.11598/btb.2016.23.2.534

Waller, L. P., Allen, W. J., Barratt, B. I. P., Condron, L. M., França, F. M., Hunt, J. E., Koele, N., Orwin, K. H., Steel, G. S., Tylianakis, J. M., Wakelin, S. A., & Dickie, I. A. (2020). Biotic interactions drive ecosystem responses to exotic plant invaders. *Science*, *368*(6494), 967–972. https://doi.org/10.1126/science.aba2225

Wang, A., Melton, A. E., Soltis, D. E., & Soltis, P. S. (2021). Potential distributional shifts in North America of allelopathic invasive plant species under climate change models. *Plant Diversity*. https://doi.org/10.1016/j.pld.2021.06.010

Wang, H., Male, J. L., & Wang, Y. (2013). Recent Advances in Hydrotreating of Pyrolysis Bio–Oil and Its Oxygen–Containing Model Compounds. *ACS Catalysis*, *3*(5), 1047–1070. https://doi.org/10.1021/cs400069z

Wang, J., Ding, W., Wang, R., Du, Y., Liu, H., Kong, X., & Li, C. (2015). Identification and Bioactivity of Compounds from the Mangrove Endophytic Fungus Alternaria sp. *Marine Drugs*, *13*(7), 4492–4504. https://doi.org/10.3390/md13074492

Waterhouse, A. M., Studer, G., Robin, X., Bienert, S., Tauriello, G., & Schwede, T. (2024). The structure assessment web server: for proteins, complexes and more. *Nucleic Acids Research*, *52*, gkae270. https://doi.org/10.1093/nar/gkae270

Wauton, I., & Ogbeide, S. E. (2019). Characterization of pyrolytic bio–oil from water hyacinth (*Eichhornia crassipes*) pyrolysis in a fixed bed reactor. *Biofuels*, *12*, 1–6. https://doi.org/10.1080/17597269.2018.1558838

Whitford, P. B. (1949). Distribution of Woodland Plants in Relation to Succession and Clonal Growth. *Ecology*, *30*(2), 199–208. https://doi.org/10.2307/1931186

Williams, C. L., Westover, T. L., Emerson, R. M., Tumuluru, J. S., & Li, C. (2015). Sources of Biomass Feedstock Variability and the Potential Impact on Biofuels Production. *BioEnergy Research*, *9*(1), 1–14. https://doi.org/10.1007/s12155–015–9694–y

Wolpert, M., & Hellwig, P. (2006). Infrared spectra and molar absorption coefficients of the 20 alpha amino acids in aqueous solutions in the spectral range from 1800 to 500 cm−1. *Spectrochimica Acta Part A: Molecular and Biomolecular Spectroscopy*, *64*(4), 987–1001. https://doi.org/10.1016/j.saa.2005.08.025

Wright, M. M., Daugaard, D. E., Satrio, J. A., & Brown, R. C. (2010). Techno–economic analysis of biomass fast pyrolysis to transportation fuels. *Fuel*, *89*, S2–S10. https://doi.org/10.1016/j.fuel.2010.07.029

Wu, C.–L., Li, Z.–X., Shen, S.–H., Zhang, Y.–C., Jiao, F.–C., Li, H.–X., Wu, W.–Z., & Mao, L.–R. (2025). Co–pyrolysis of coal and biomass: microcrystalline structure and co–pyrolysis characteristics. *Energy Sources Part a Recovery Utilization and Environmental Effects*, *47*(1), 14–29. https://doi.org/10.1080/15567036.2025.2507086

Xian, X., Hong–yan, Z., Wang, R., Zhang, H., Chen, B., Huang, H., Liu, W., & Wan, F. (2022). Predicting the potential geographical distribution of *Ageratina adenophora* in China using equilibrium occurrence data and ensemble model. *Frontiers in Ecology and Evolution*, *10*. https://doi.org/10.3389/fevo.2022.973371

Yang, J.–F., Yang, C.–H., Liang, M.–T., Gao, Z.–J., Wu, Y.–W., & Chuang, L.–Y. (2016). Chemical Composition, Antioxidant, and Antibacterial Activity of Wood Vinegar from *Litchi chinensis*. *Molecules*, *21*(9), 1150. https://doi.org/10.3390/molecules21091150

Yang, Q., Jin, B., Zhao, X., Chen, C., Cheng, H., Wang, H., He, D., Zhang, Y., Peng, J., Li, Z., & Han, M. (2022). Composition, Distribution, and Factors Affecting Invasive Plants in Grasslands of Guizhou Province of Southwest China. *Diversity*, *14*(3), 167. https://doi.org/10.3390/d14030167

Yang, X., Li, L., Lv, X., Luo, W., Li, D., Liang, C., Wee, A. K. S., & Long, W. (2021). Closed–Canopy Tropical Forests of Hainan, (China) Are Resilient against Invasive Herbs and Shrubs. *Forests*, *12*(11), 1596. https://doi.org/10.3390/f12111596

Yang, X.–Q., Kushwaha, S. P. S., Saran, S., Xu, J., & Roy, P. S. (2013). Maxent modeling for predicting the potential distribution of medicinal plant, *Justicia adhatoda* L. in Lesser Himalayan foothills. *Ecological Engineering*, *51*, 83–87. https://doi.org/10.1016/j.ecoleng.2012.12.004

Yemm, E. W., Willis, A. J. (1954) The estimation of carbohydrates in plant extracts by anthrone. Biochem J 57:508–514. https://doi.org/10.1042/bj0570508

Yu, L., Yan, J., & Sun, Z. (2017). D–limonene exhibits anti–inflammatory and antioxidant properties in an ulcerative colitis rat model via regulation of iNOS, COX–2, PGE2 and ERK signaling pathways. *Molecular Medicine Reports*, *15*(4), 2339–2346. https://doi.org/10.3892/mmr.2017.6241

Yusuf, H. A. N., Alasow, A. A., & Mennan, H. (2024). Significant weed species, density and frequency in sesame cultivated areas of middle Shabelle Province in Somalia. *Acta Agriculturae Scandinavica, Section B — Soil & Plant Science*, *74*(1). https://doi.org/10.1080/09064710.2024.2392525

Zapata, B., Balmaseda, J., Fregoso–Israel, E., & Torres–García, E. (2009). Thermo–kinetics study of orange peel in air. *Journal of Thermal Analysis and Calorimetry*, *98*(1), 309–315. https://doi.org/10.1007/s10973–009–0146–9

Zhang, Y., Brown, T. R., Hu, G., & Brown, R. C. (2013). Techno–economic analysis of monosaccharide production via fast pyrolysis of lignocellulose. *Bioresource Technology*, *127*, 358–365. https://doi.org/10.1016/j.biortech.2012.09.070

Zhang, D., Pan, R., Chen, R., & Xu, X. (2019). Pyrolysis Characteristics and Reaction Mechanisms of Pine Needles. *Applied Biochemistry and Biotechnology*, *189*(4), 1056–1083. https://doi.org/10.1007/s12010–019–03057–3

Zhang, H.–Y., Goncalves, P., Copeland, E., Qi, S.–S., Dai, Z.–C., Li, G.–L., Wang, C.–Y., Du, D.–L., & Thomas, T. (2020). Invasion by the weed *Conyza canadensis* alters soil nutrient supply and shifts microbiota structure. *Soil Biology and Biochemistry*, *143*, 107739. https://doi.org/10.1016/j.soilbio.2020.107739

Zhang, L., Hu, X., Hu, K., Hu, C., Zhang, Z., Liu, Q., Hu, S., Xiang, J., & Zhang, S. (2018). Progress in the reforming of bio–oil derived carboxylic acids for hydrogen generation. *Journal of Power Sources*, *403*, 137–156. https://doi.org/10.1016/j.jpowsour.2018.09.097

Zhang, S.–S., Tan, Q.–W., & Guan, L.–P. (2021). Antioxidant, anti–inflammatory, antibacterial, and analgesic activities and mechanisms of quinolines, indoles and related derivatives. *Mini–Reviews in Medicinal Chemistry*, *21*. https://doi.org/10.2174/1389557521666210111145011

Zhang, T., Liang, F., Hu, W., Yang, X., Xiang, H., Wang, G., Fei, B., & Liu, Z. (2017a). Economic analysis of a hypothetical bamboo–biochar plant in Zhejiang province, China. *Waste Management & Research*, *35*(12), 1220–1225. https://doi.org/10.1177/0734242x17736945

Zhang, X., Lei, H., Chen, S., & Wu, J. (2016). Catalytic co–pyrolysis of lignocellulosic biomass with polymers: a critical review. *Green Chemistry*, *18*(15), 4145–4169. https://doi.org/10.1039/c6gc00911e

Zhang, Y., Cui, H., Yi, W., Song, F., Zhao, P., Wang, L., & Cui, J. (2017b). Highly effective decarboxylation of the carboxylic acids in fast pyrolysis oil of rice husk towards ketones using $CaCO_3$ as a recyclable agent. *Biomass and Bioenergy*, *102*, 13–22. https://doi.org/10.1016/j.biombioe.2017.04.004

Zhao, H. (2019). Chapter Four – Energy Crisis: "Natural Disaster" and "Man–Made Calamity." *The Economics and Politics of China's Energy Security Transition*, 65–98. https://doi.org/10.1016/b978–0–12–815152–5.00004–x

Zhao, Z., Yuan, L., Li, W., Tian, B., & Zhang, L. (2020). Re–invasion of *Spartina alterniflora* in restored saltmarshes: Seed arrival, retention, germination, and establishment. *Journal of Environmental Management*, *266*, 110631. https://doi.org/10.1016/j.jenvman.2020.110631

Zheng–qiang, L., Jun, N., Xin–yu, Z., Chao–zhi, Z., Rui, A., Xu, Y., Rong, S., & Xiao–yan, Y. (2024). Antioxidant and anti–inflammatory function of *Eupatorium*

*adenophora* Spreng leaves (EASL) on human intestinal Caco–2 cells treated with tert–butyl hydroperoxide. *Scientific Reports*, *14*(1). https://doi.org/10.1038/s41598–024–61012–7

Zhou, X., Moghaddam, T. B., Chen, M., Wu, S., Zhang, Y., Zhang, X., Adhikari, S., & Zhang, X. (2021). Effects of pyrolysis parameters on physicochemical properties of biochar and bio–oil and application in asphalt. *Science of the Total Environment*, *780*, 146448. https://doi.org/10.1016/j.scitotenv.2021.146448

Zhuang, J., Li, M., Pu, Y., Ragauskas, A., & Yoo, C. (2020). Observation of Potential Contaminants in Processed Biomass Using Fourier Transform Infrared Spectroscopy. *Applied Sciences*, *10*(12), 4345. https://doi.org/10.3390/app10124345

Zihare, L., & Blumberga, D. (2017). Invasive Species Application in Bioeconomy. Case Study *Heracleum sosnowskyi* Manden in Latvia. *Energy Procedia*, *113*, 238–243. https://doi.org/10.1016/j.egypro.2017.04.060

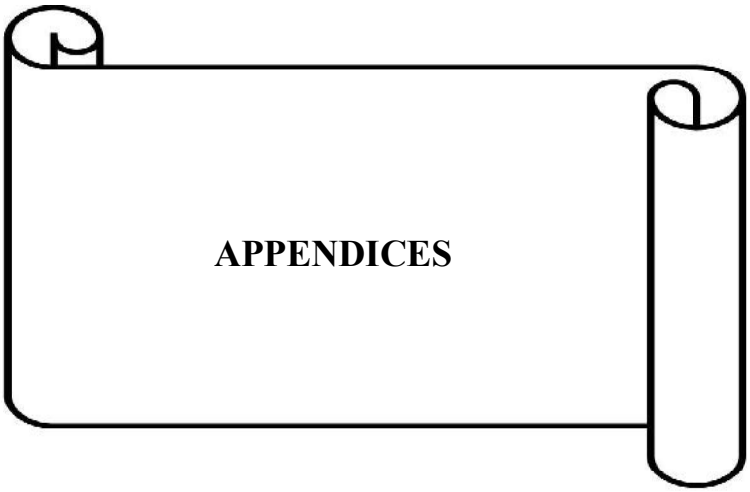

# APPENDICES

# Appendix I

## Graphical Abstract

*Ageratina adenophora*
Family: Asteraceae

*Lantana camara*
Family: Verbenaceae

*Stachytarpheta jamaicensis*
Family: Verbenaceae

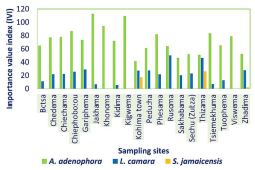


Population and distribution assessment

Biomass characterization

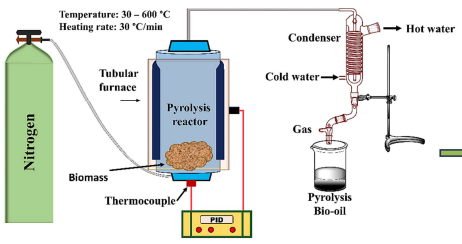


Pyrolysis

Bio-oil characterization

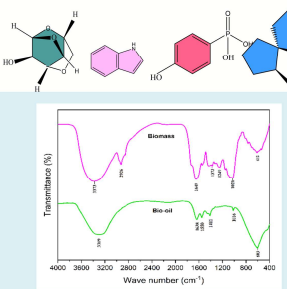


Spectroscopic analyses

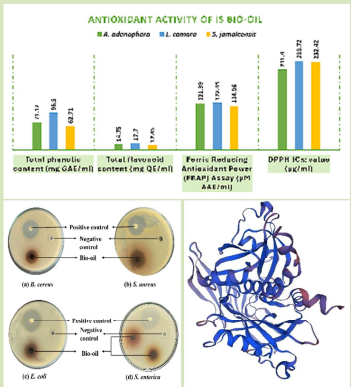


Antioxidant, Antimicrobial and *In silico* investigation

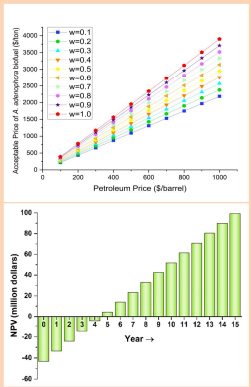


Economic analysis

# Appendix II

## Description of species under investigation

### *Ageratina adenophora*

**Family:** Asteraceae

**English Name:** Eupatory, Crofton weed

**Nativity:** Tropical America

**Distribution in India:** Kerala, Tamil Nadu

**Propagation:** Seeds

**Phenology (Flowering & Fruiting):** August – February

**Description:**

Perennial, glandular hairy, erect herbs to 1 – 2 m tall.

*Leaves:* Opposite, deltoid–ovate, margin serrate, purple below, leaf blade 3–8 cm,

*Inflorescence:* Clustered, in corymbose cymes; phyllaries glandular–puberulent, heads homogamous.

*Flowers:* 10 – 60 per head, cylindric, corolla white, pink tinged.

*Achenes:* 5 angled, 5 ribbed, pappus white, feathery.

**Remarks:** Occasional weed in forest clearings and along road sides at higher elevations in Western Ghats.

## *Lantana camara*

**Family:** Verbenaceae

**English Name:** Wild Sage

**Nativity:** Tropical America (introduced in India as an ornamental shrub during 1809–1810)

**Distribution in India:** Throughout

Propagation: Seeds

**Phenology (Flowering & Fruiting):** Throughout the year

**Description:**

Straggling, armed shrubs, up to 2.5 m tall.

*Leaves:* 2–6 x 1.5–3.5 cm, base cordate, margin crenate serrate, rugose and hispid above, sparsely hispid beneath.

*Flowers:* In various colours pink, white, crimson, orange or rose, in axillary, capitate spikes.

*Drupes:* Ripe black, 3–4 mm in diam., globose.

**Remarks:** Aggressive colonizer. Common weed of forests, plantations, habitation, waste lands and scrub lands.

## *Stachytarpheta jamaicensis*

**Family**: Verbenaceae

**English Name**: Snakeweed, porter weed, rattail.

**Nativity**: Tropical America

**Distribution in India**: Throughout

**Propagation**: Seeds

**Phenology (Flowering & Fruiting):** Throughout the year, but is most abundant during spring, summer and autumn

**Description:**

Small shrub, 1–2.5 m tall, with subcylindrical, glabrous branches.

*Leaves:* Opposite–decussate, ovate to elliptic, 3.6 cm long, 1.5 – 2.5 cm broad, serrate, cuneate, scabrous, shortly petiolate; petiole 1 – 1.5 cm long.

*Spikes:* Elongated, up to 25 cm long, slender, glabrescent or sparsely pubescent.

*Flowers:* Blue with whitish centre, 5 mm across, bracteate with linear–lanceolate acuminate bracts. Calyx–tube 4 – 5 mm long, 4– toothed, glabrous.

*Corolla:* Tube as long or slightly exceeding the calyx; limb 4–5–lobed, with lobes 1.5 – 2 mm long.

*Fruit:* With persistent style, splitting into two, 1–seeded pyrenes.

**Remarks:** Aggressive colonizer. Occasional weed of gardens, roadsides and open moist deciduous forests.

***Plate 1***

Infestation of *A. adenophora* in a secondary forest [Chedema (25.68309 °N; 94.0364 °E)].

Roadside infestation of *L. camara* [Kigwema (25.56883 °N; 94.14516 °E)].

Roadside infestation of *S. jamaicensis* [Thizama (25.73824 °N; 94.10955 °E)].

***Plate 2***

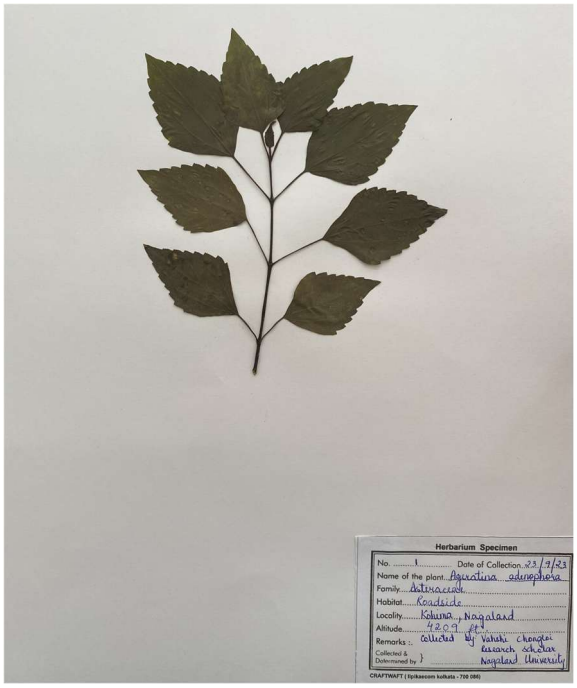


Herbarium of *A. adenophora* preserved for botanical reference (authentication).

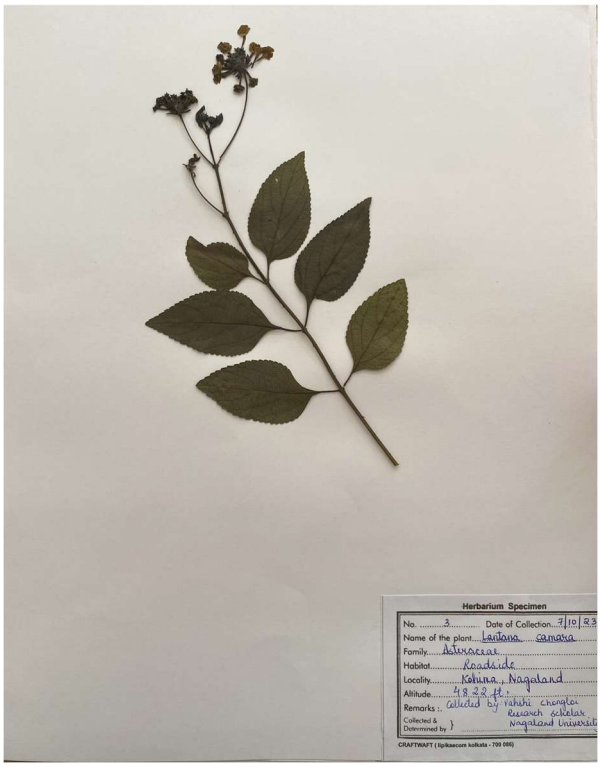


Herbarium of *L. camara* preserved for botanical reference (authentication).

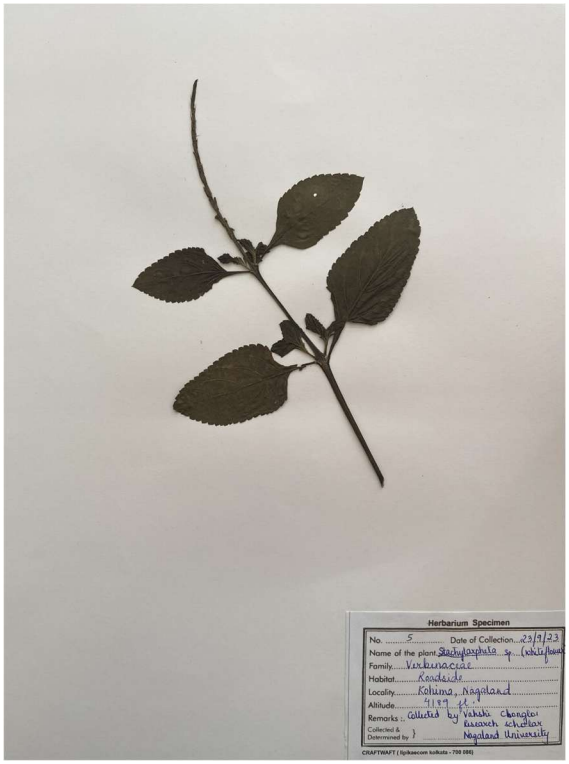


Herbarium of *S. jamaicensis* preserved for botanical reference (authentication).

भारत सरकार/GOVERNMENT OF INDIA
पर्यावरण वन एवंजलवायु परिवर्तन मंत्रालय/MINISTRY OF ENVIRONMENT, FOREST & CLIMATE CHANGE
भारतीय वनस्पति सर्वेक्षण/BOTANICAL SURVEY OF INDIA
प्रभारी वैज्ञानिक का कार्यालय/OFFICE OF THE SCIENTIST IN-CHARGE
पर्वी क्षेत्रीय केंद्र/EASTERN REGIONAL CENTRE

दूरभाष/Telephone: 0364- 2223971, 2223618 ई-मेल/e-mail- bsibsishll@yahoo.co.in Telefax: 0364- 2224119

संख्या/No.: BSI/ERC/ Tech/2023-24/ 1845 दिनांक/Dated: 26/02/2024

सेवा में/To,

Vahshi Chongloi
Ph.D Scholar
Dept. of Forestry
Nagaland University
Nagaland-798627

विषय/Sub.: Identification of plant specimens.

महोदया/Madam,

With reference to your letter regarding the subject cited above, I am to inform you that your plant specimens have been identified and confirmed as below-

| Sl. No. | Name of Specimen | Family | Collection Number |
|---|---|---|---|
| 1. | *Ageratina adenophora* (Spreng.) R.M.King & H.Rob. | Asteraceae | 01 |
| 2. | *Bidens pilosa* L. | Asteraceae | 02 |
| 3. | *Lantana camara* L. | Verbenaceae | 03 |
| 4. | *Ageratum houstonianum* Mill. | Asteraceae | 04 |
| 5. | *Stachytarpheta jamaicensis* (L.) Vahl | Verbenaceae | 05 |

धन्यवाद/Thanking You

भवदीय/Yours sincerely

डॉ. एन. ऑडियो/Dr. N. Odyuo
वैज्ञानिक-ई एवं कार्यालय प्रमुख/ Scientist-E & Ho.O

Identification and authentication of species by the Botanical Survey of India, Eastern Regional Centre, Shillong.

# Appendix III

## Survey questionnaire on IS

Name of respondent:

Age:

Gender:

Education:

Village:

Occupation:

Phone number:

Email address:

A. General Awareness & Availability

1. Are you aware of the presence of *Ageratina adenophora*, *Lantana camara* and *Stachytarpheta jamaicensis* in your village?

   ☐ Yes ☐ No

2. Where are these species commonly found?

☐ Farmland ☐ Forest ☐ Roadside ☐ Near human settlements ☐ Other (specify): _____

3. How often do you see these plants?

☐ Throughout the year ☐ Only during certain months (mention):

B. Local Name & Identification

1. What is the local name of these species?

*A. adenophora*:

*L. camara*:

*S. jamaicensis*:

2. Are they confused with any useful plants?

☐ Yes ☐ No — If yes, which plant? _____

C. Seasonal Pattern & Prevalence

1. During which season(s) do you observe the following invasive species the most?

| | *A. adenophora* | *L. camara* | *S. jamaicensis* |
|---|---|---|---|
| Summer (March – May) | ☐ | ☐ | ☐ |
| Monsoon (June – Sept.) | ☐ | ☐ | ☐ |
| Post monsoon (Oct. – Nov.) | ☐ | ☐ | ☐ |
| Winter (Dec. – Feb.) | ☐ | ☐ | ☐ |

2. What kind of **growth behavior** do you notice in these species during their active season?

☐ Grow very fast and spread quickly

☐ Dominate and suppress other plants

☐ Form dense patches or thickets

☐ Regrow even after cutting

☐ Shed seeds heavily

☐ Dry out but regrow from roots next season

☐ Other observations (specify): _____

D. Spread and Causes

1. How long have you seen these plants in your area?

☐ <5 years ☐ 5–10 years ☐ 10+ years

2. What do you think helps them spread?

☐ Seeds ☐ Wind ☐ Animal movement ☐ No use ☐ Forest fire ☐ Other:

3. Do you witness increase in their population?

☐ Rapidly ☐ Slowly ☐ No change ☐ Don't know

E. Impact on Agriculture and Livelihood

1. Do these species reduce crop yield or affect soil?

☐ Yes ☐ No ☐ Don't know

2. Any damage to livestock or grazing area?

☐ Yes ☐ No ☐ Don't know

3. Do they affect access to forest produce or water?

☐ Yes ☐ No ☐ Don't know

F. Effect on Human and Animal Health

1. Do you or others experience allergies or rashes near these plants?

☐ Yes ☐ No ☐ Don't know

2. Have animals shown sickness after grazing in infested areas?

☐ Yes ☐ No ☐ Not applicable

3. Are you aware of any toxic effects of these plants?

☐ Yes ☐ No — If yes, which plant? _____

G. Local Uses

1. Are these plants used in any of the following?

| | *A. adenophora* | *L. camara* | *S. jamaicensis* |
|---|---|---|---|
| Heating | ☐ | ☐ | ☐ |
| Fencing | ☐ | ☐ | ☐ |
| Medicinal | ☐ | ☐ | ☐ |
| Manure | ☐ | ☐ | ☐ |
| Grazing | ☐ | ☐ | ☐ |

2. Any traditional beliefs/rituals associated:

H. Local Control & Management

1. What do villagers do to remove or control these species?

☐ Uprooting ☐ Burning ☐ Cutting ☐ Chemicals ☐ Nothing

2. Which method is most effective in your view?

_____

3. Have any government or NGO projects helped?

☐ Yes ☐ No ☐ Don't know

I. Changes Observed Over Time

1. Have native plants reduced in number since these invasive plants appeared?

☐ Yes ☐ No ☐ Don't know

2. Has soil fertility or water retention changed?

☐ Yes ☐ No ☐ Don't know

3. Do birds or animals avoid areas with these species?

☐ Yes ☐ No ☐ Don't know

**Additional Local Insights**

- Have you observed any benefits or harms not listed above? ……
……
- What do you think is the best way to manage these species in your village? ……
……

# Appendix IV

## Molecular docking simulation of established drugs and IS ligands against NUDT5 protein

***Plate 1***

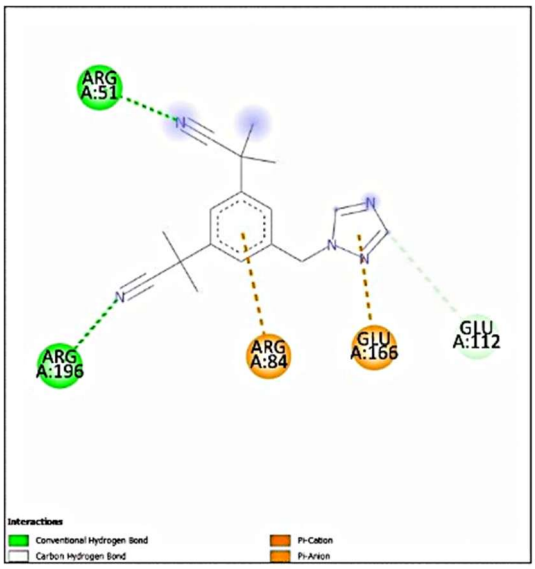


Anastrozole

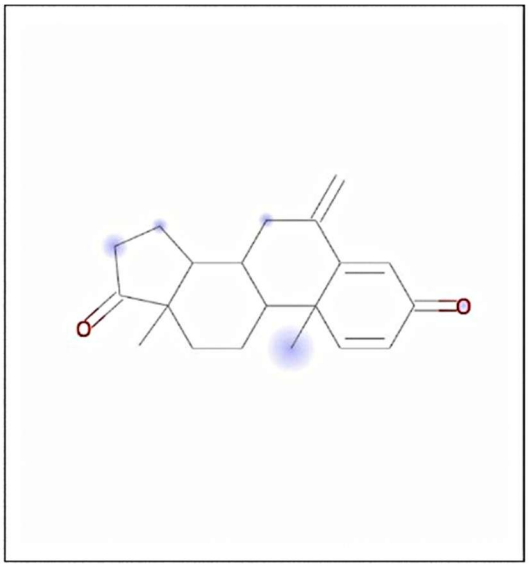

Exemestane

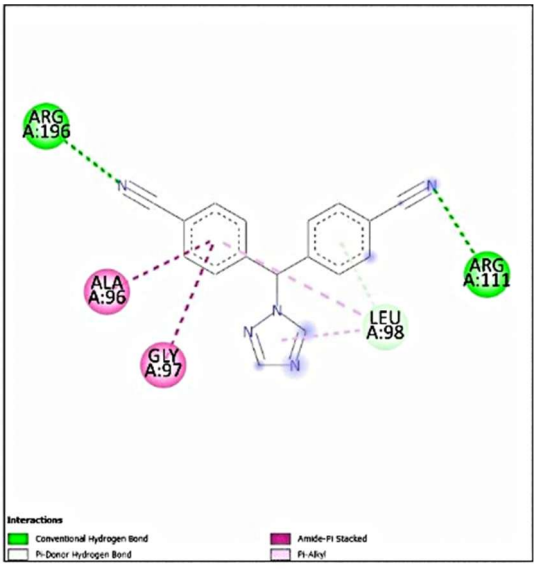


Letrozole

2D representations of the docked ligands with the NUDT5 protein for standards.

***Plate 2***

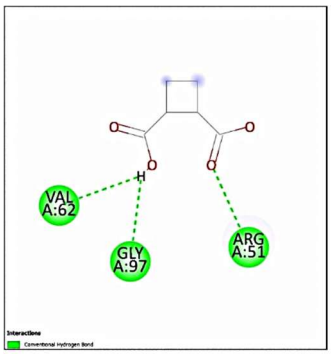


1,2-Cyclobutanedicarboxylic acid, cis-

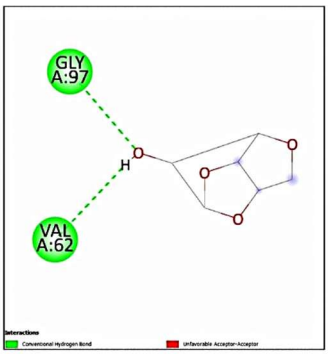


1,4 3,6-Dianhydro-alpha-d-glucopyranose

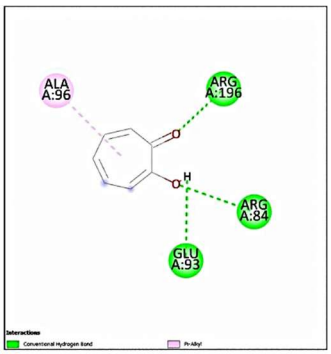


2,4,6-Cycloheptatrien-1-one, 2-hydroxy-

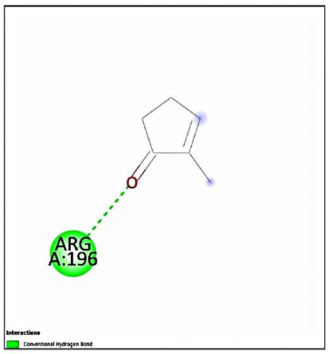


2-Cyclopenten-1-one, 2-methyl-

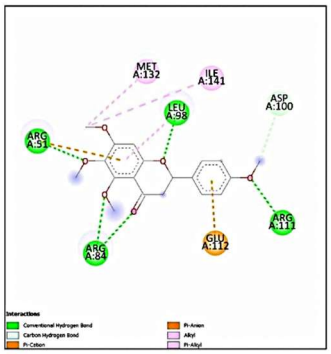


5,6,7,4'-Tetramethoxyflavanone

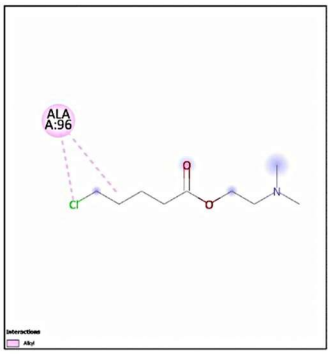


5-Clorovaleric acid, 2-dimethylaminoethyl ester

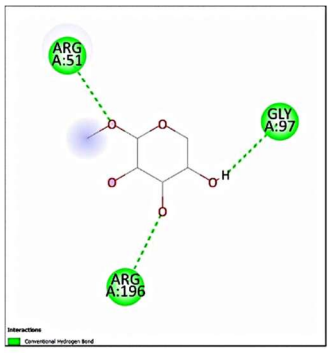


beta-L-Arabinopyranoside, methyl

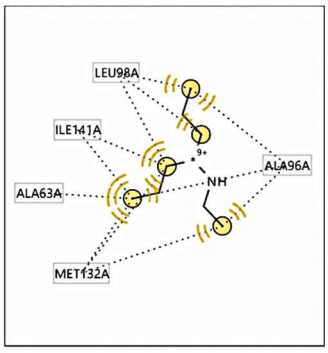


Boraneamine, n-ethyl-1,1-dipropyl-

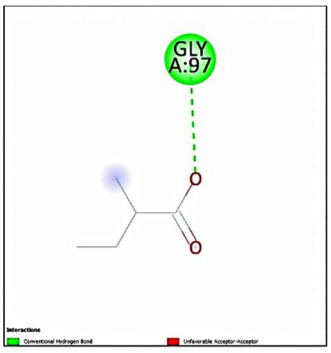


Butanoic acid, 2-methyl-

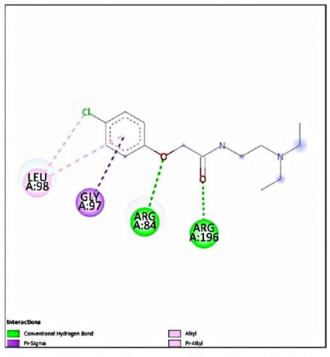


Clofexamide

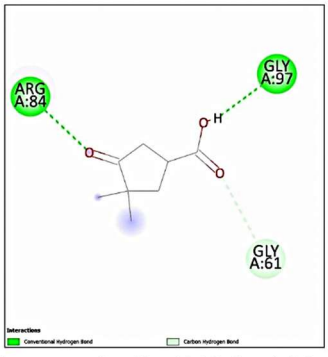


Cyclopentanecarboxylic acid, 3,3-dimethyl-4-oxo-

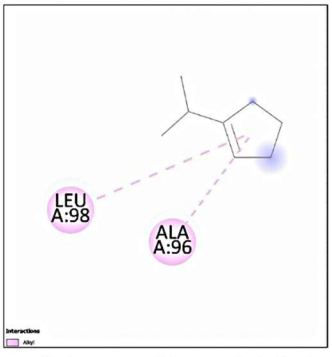


Cyclopentene, 1-(1-methylethyl)-

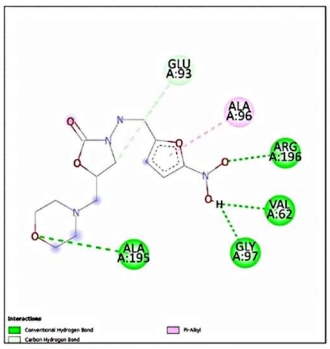


Furaltadone

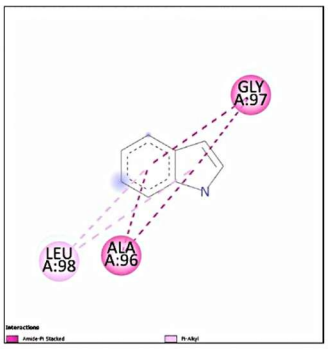


Indole

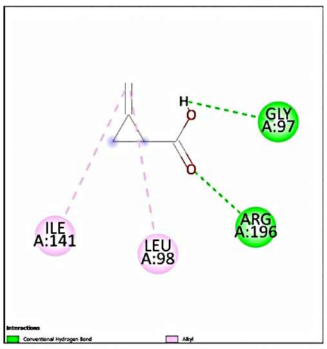


Methylenecyclopropanecarboxylic acid

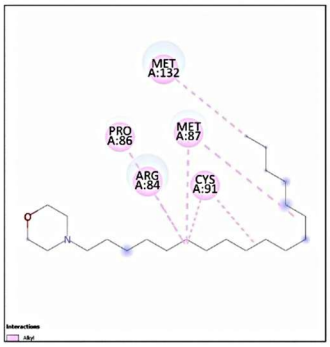


Morpholine, 4-octadecyl-

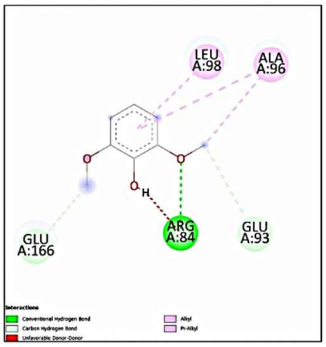


Phenol, 2,6-dimethoxy

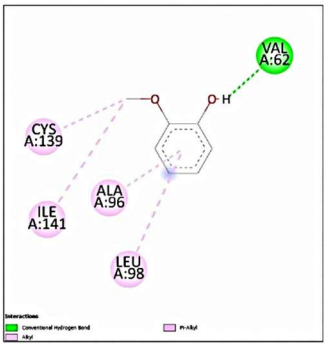


Phenol, 2-methoxy-

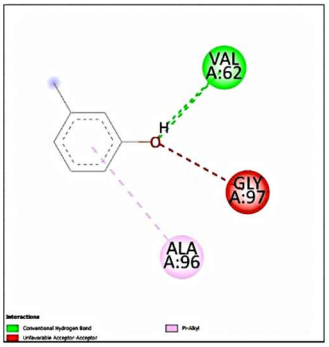


Phenol, 3-methyl-

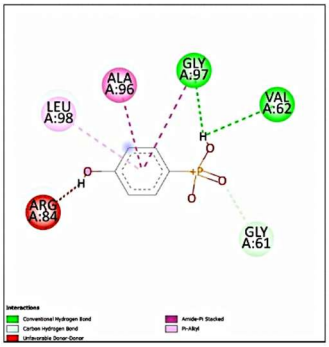


Phosphonic acid, (p-hydroxyphenyl)-

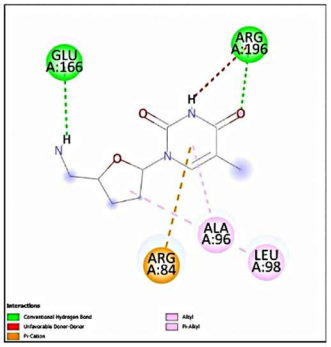


Pyrimidine-2,4(1H,3H)-dione, 1-(5-aminomethyl-2-tetrahydrofuryl)-5-methyl

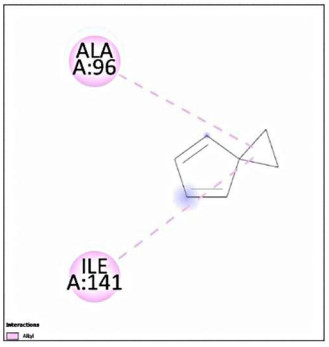


Spiro[2,4]hepta-4,6-diene

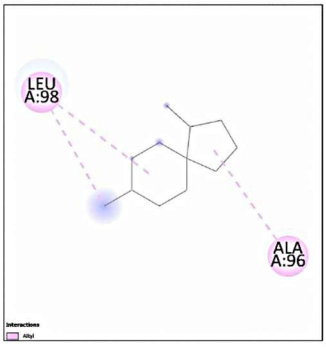


Trans,cis-1,8-dimethylspiro[4.5]decane

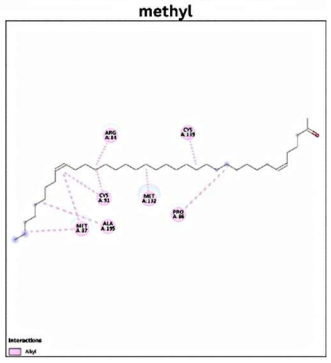

Z,Z-6,28-Heptatriactontadien-2-one

2D representations of the docked ligands with the NUDT5 protein for *A. adenophora.*

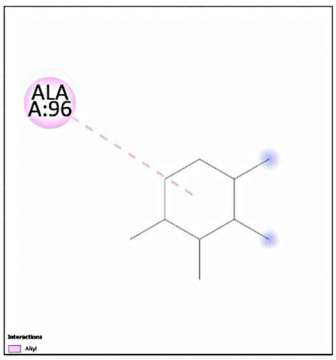


1R,2c,3t,4t-Tetramethyl-cyclohexane

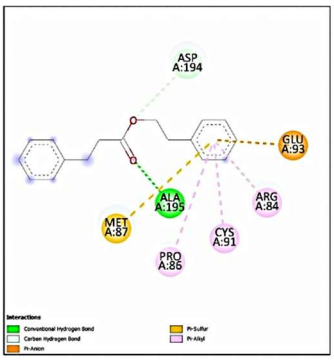


2-Phenethyl-beta-phenylpropionate

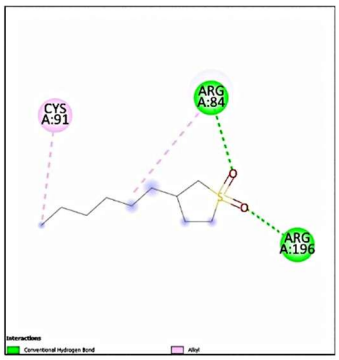


3-n-Hexylthiolane, S,S-dioxide

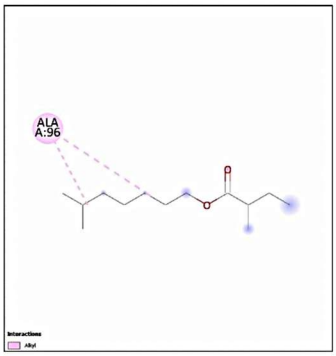


6-Methylheptyl 2-methylbutanoate

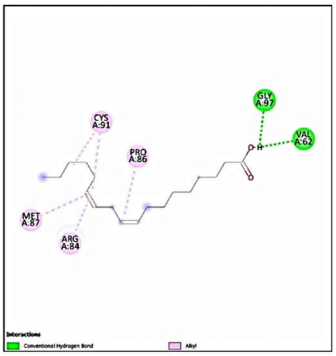


9,12-Octadecadienoic acid (z,z)-

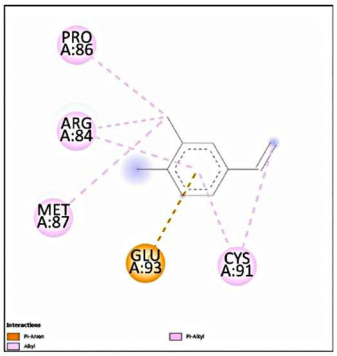


Benzene, 4-ethenyl-1,2-dimethyl-

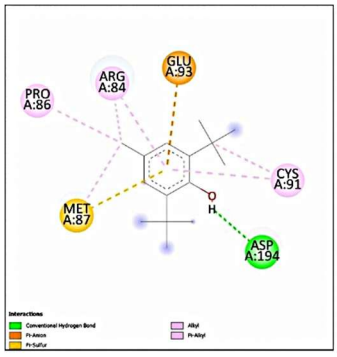


Butylated hydroxytoluene

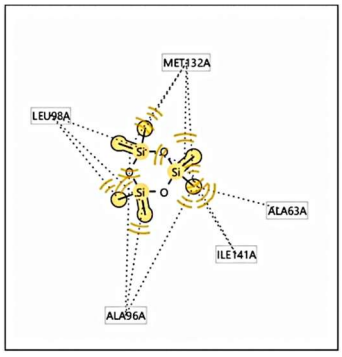


Cyclotrisiloxane, hexamethyl-

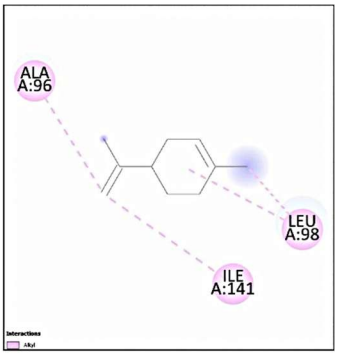


D-limonene

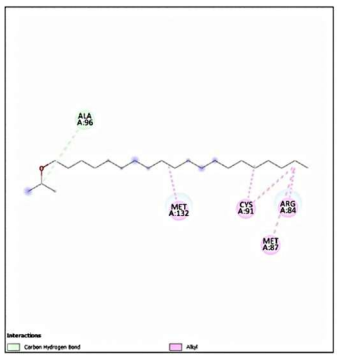


Eicosyl isopropyl ether

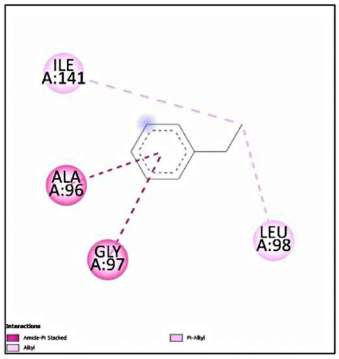


EthylBenzene

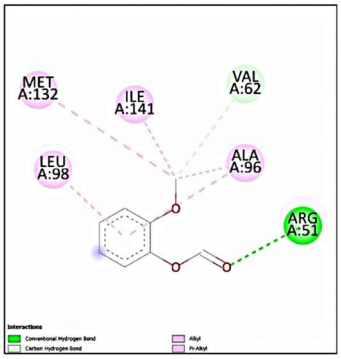


Formic acid, 2-methoxyphenyl ester

***Plate 3***

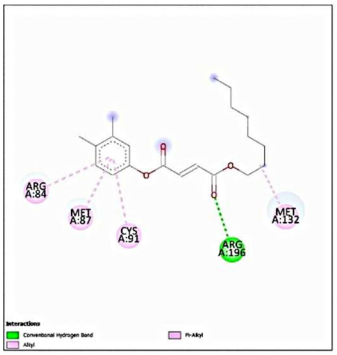


Fumaric acid, 3,4-dimethylphenyl octyl ester

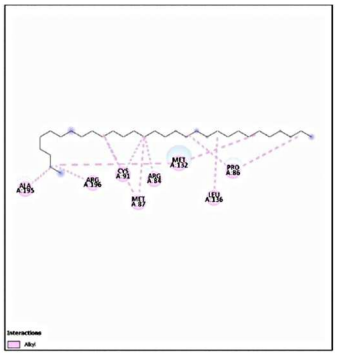

Hentriacontane

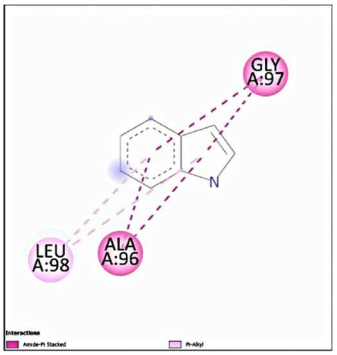


Indole

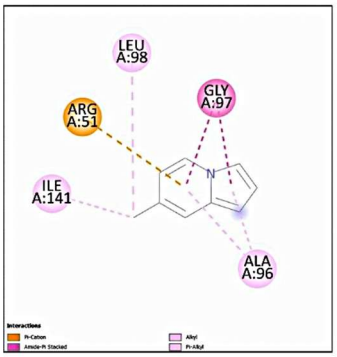


Indolizine, 7-methyl-

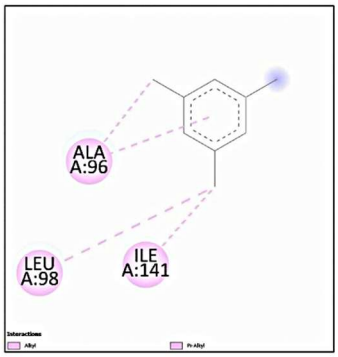


Mesitylene

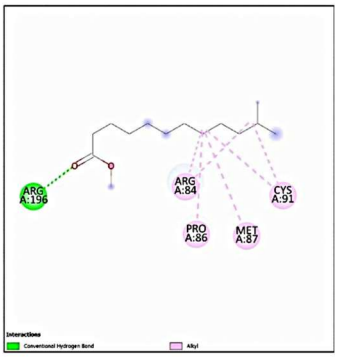


Methyl 11-methyl-dodecanoate

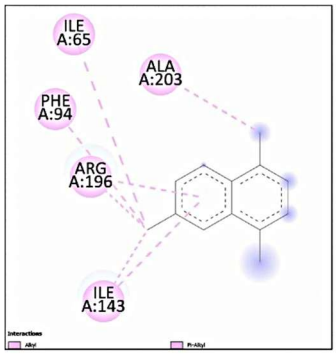


Naphthalene, 1,4,6-trimethyl-

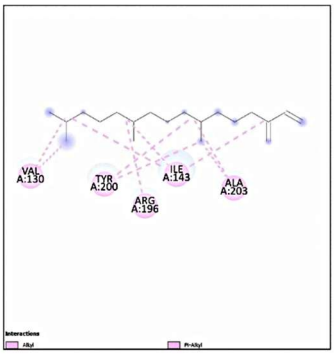


Neophytadiene

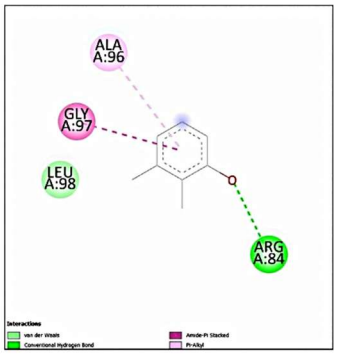


Phenol, 2,3-dimethyl-

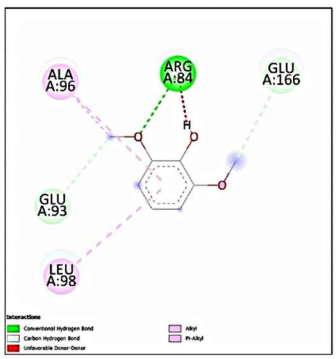


Phenol, 2,6-dimethoxy

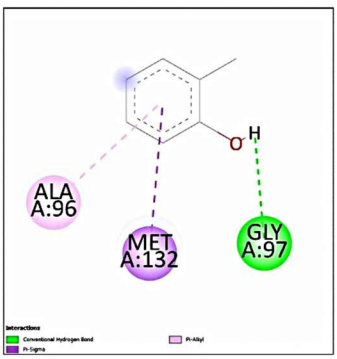


Phenol, 2-methyl-

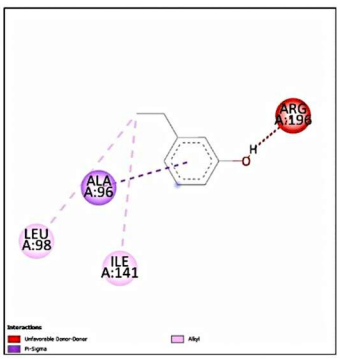


Phenol, 3-ethyl-

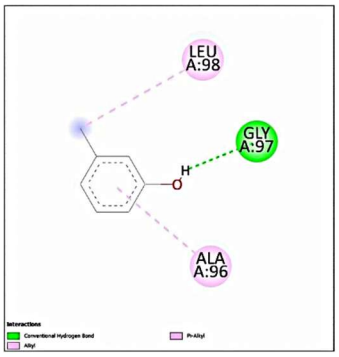


Phenol, 3-methyl-

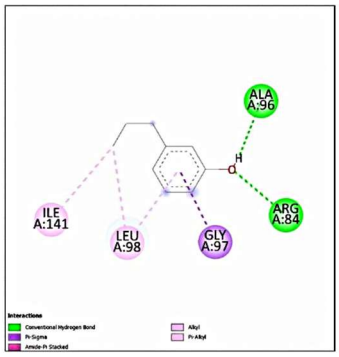


Phenol, 3-propyl-

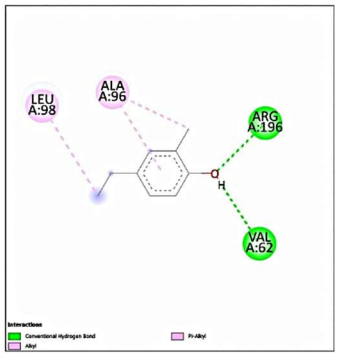


Phenol, 4-ethyl-2-methyl-

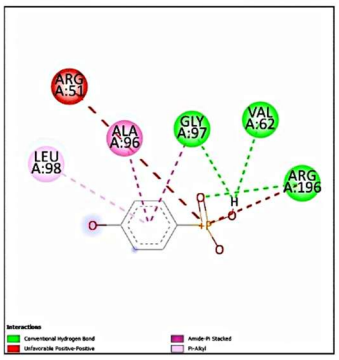


Phosphonic acid, (p-hydroxyphenyl)-

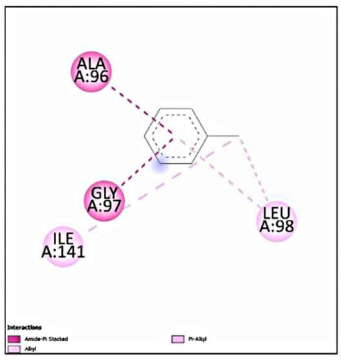


Toluene

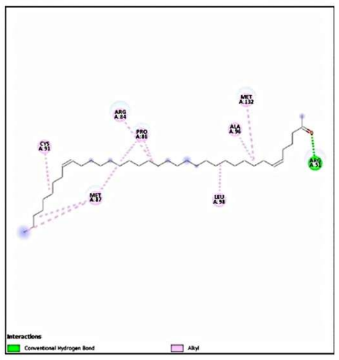

Z,Z-6,28-Heptatriactontadien-2-one

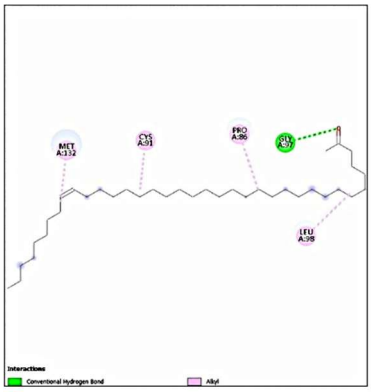

Z-28-Heptatriaconten-2-one

2D representations of the docked ligands with the NUDT5 protein for *L. camara.*

## ***Plate 4***

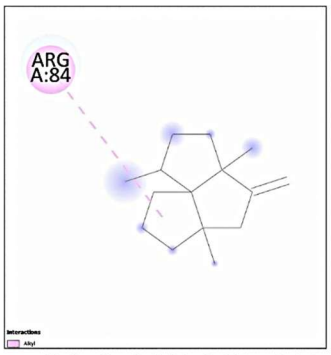


(1r,3as,5as,8ar)-1,3a,5a-Trimethyl-4-methylenedecahydrocyclopenta[c]pentalene

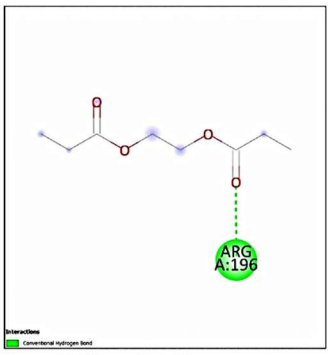


1,2-Ethanediol, dipropanoate

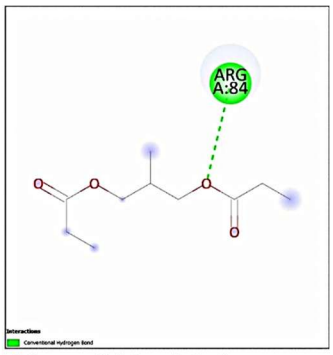


1,3-Propanediol, 2-methyl-, dipropanoate

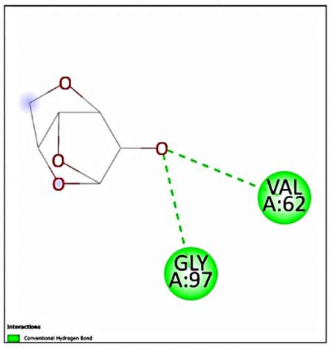


1,4 3,6-Dianhydro-.alpha.-d-glucopyranose

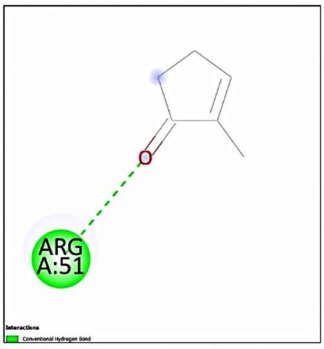


2-Cyclopenten-1-one, 2-methyl-

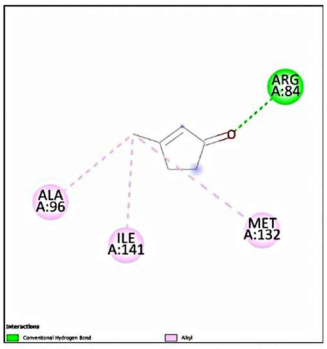


2-Cyclopenten-1-one, 3-methyl-

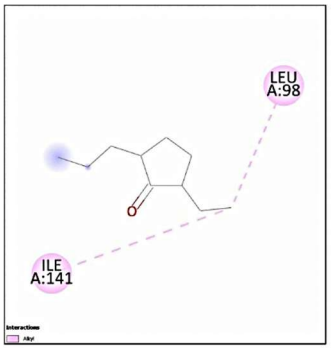


2-Ethyl-5-propylcyclopentanone

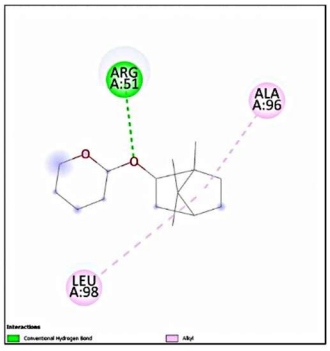


2-Isobornyloxy-tetrahydropyran

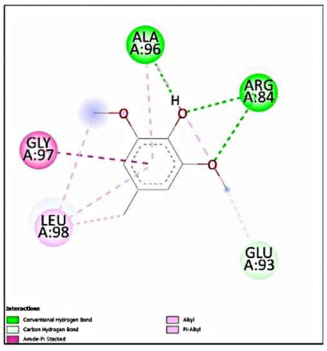


3,5-Dimethoxy-4-hydroxytoluene

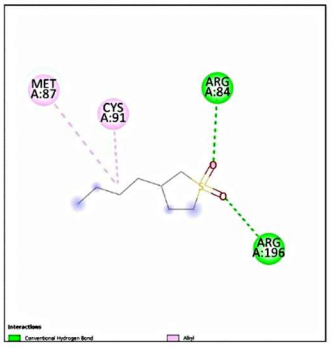


3-n-Butylthiolane, S,S-dioxide

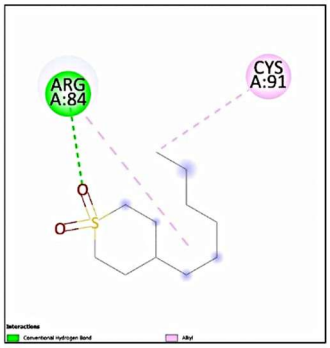


4-n-Hexylthiane, S,S-dioxide

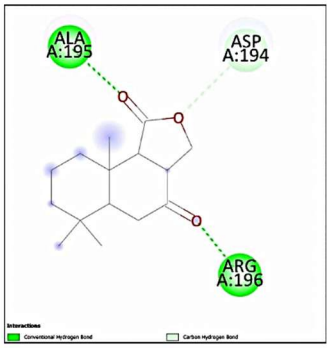


6,6,9a-Trimethyl-decahydronaphtho[1,2-c]furan-1,4-dione

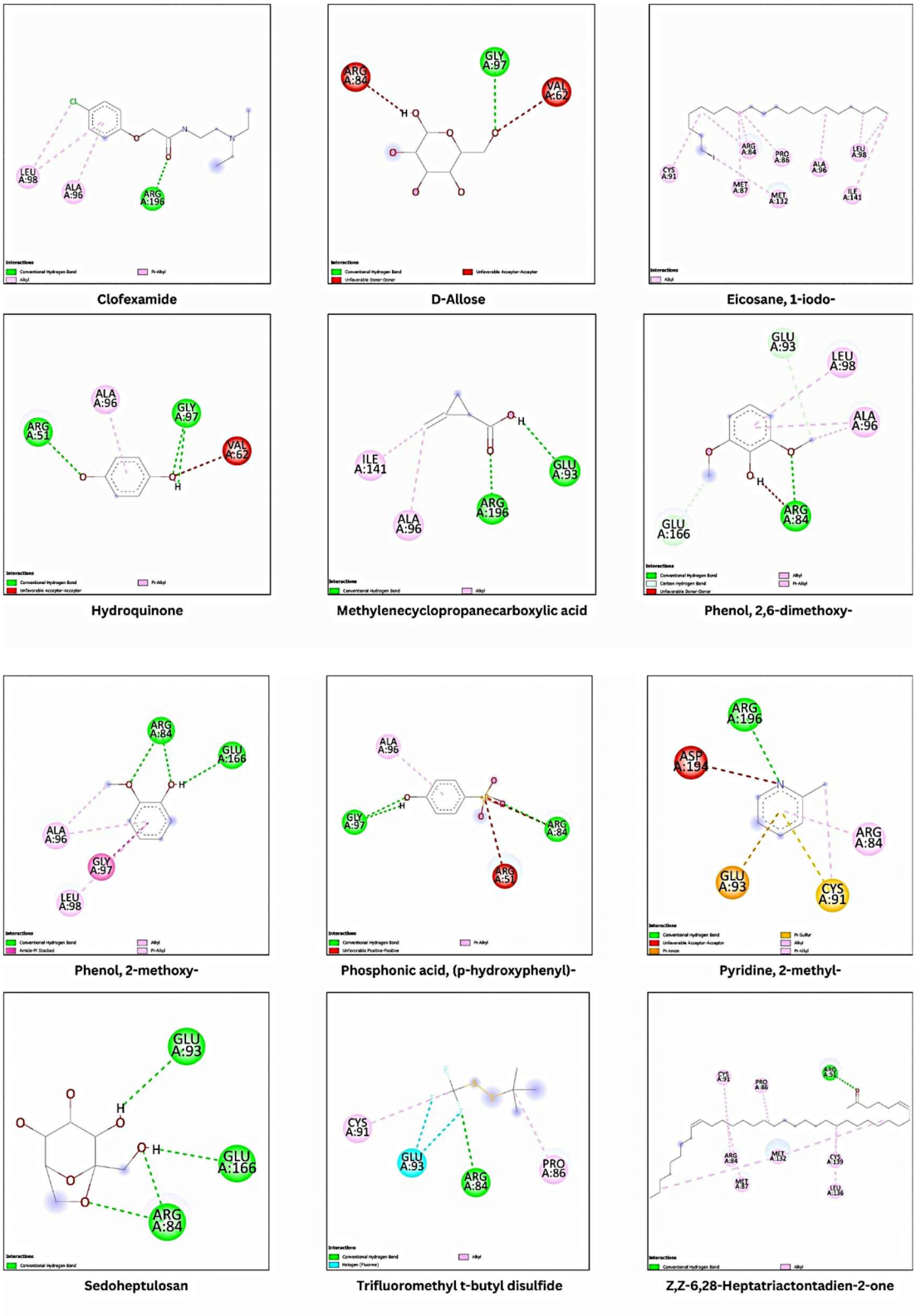


2D representations of the docked ligands with the NUDT5 protein for *S. jamaicensis.*

# Appendix V

# LIST OF PUBLICATIONS, PATENT AND PAPER PRESENTATIONS

## Paper publications

1. **Vahshi Chongloi**, Mayur Mausoom Phukan, Plaban Bora. Miscellaneous Prospects of Invasive *Lantana camara* Biomass – A Standpoint on Bioenergy Generation and Value Addition. Environmental Science and Pollution Research. https://doi.org/10.1007/s11356–024–35042–7 (Spinger Nature)
2. **Vahshi Chongloi**, Partha Pratim Gogoi, Samson Rosly Sangma, Upasana Bora Sinha, Plaban Bora, Mayur Mausoom Phukan. Antioxidant, Antimicrobial and In Silico Investigations on Pyrolytic Bio–oil from Invasive *Stachytarpheta jamaicensis* Biomass. Environmental Science and Pollution Research. https://doi.org/10.1007/s11356–025–36741–5 (Spinger Nature)
3. Samson Rosly Sangma, Mayur Mausoom Phukan, **Vahshi Chongloi**, Dakeshwar Kumar Verma, Plaban Bora, Sony Kumari, Pranay Punj Pankaj. Phytochemical Profiling, Antioxidant and Antimicrobial Investigations on *Viburnum simonsii* Hook. F. & Thoms, An Unexplored Ethnomedicinal Plant of Meghalaya, India. Future Journal of Pharmaceutical Sciences 2023, 9 (114). https://doi.org/10.1186/s43094–023–00567–0 (Spinger Open)
4. Samson Rosly Sangma, Mayur Mausoom Phukan, Dhrubajyoti Gogoi, Pranay Punj Pankaj, **Vahshi Chongloi**. Phytochemistry, Bioactivity and In silico studies on *Goniothalamus simonsii* Hook. F. Thoms: An endangered medicinal plant. Chemistry and Biodiversity 2025. https://doi.org/10.1002/cbdv.202501513 (Wiley)

## Patent

1. Dr. Mayur Mausoom Phukan, Ms. **Vahshi Chongloi**, Dr. Plaban Bora, Dr. Pranay Punj Pankaj. Pyrolyzer For Conversion of Biomass and Agricultural Wastes into Bio–Oil and Biochar. Design No. 417482–001. Date: 20–05–2024 (Indian patent)

## Papers communicated

1. **Vahshi Chongloi**, Mayur Mausoom Phukan, Samson Rosly Sangma, Vimha Ritse, Plaban Bora, Betokali K Zhimomi, Nabajit Hazarika, Pitambar Sedai, Dipul Kalita. Bioprospecting and Distribution Modelling of Invasive Ageratina adenophora for Bioenergy Generation and Value–Enhancement. Journal of Energy Institute. (Elsevier)
2. **Vahshi Chongloi**, Mayur Mausoom Phukan, Plaban Bora, Samson Rosly Sangma. Green energy from green invaders: Repurposing invasive plant species as emerging feedstock. Applied Energy. (Elsevier)
3. **Vahshi Chongloi**, Mayur Mausoom Phukan, Plaban Bora, Sedevikhonuo Noudi, Tangmong, Rupamjyoti Nath. Samson Rosly Sangma. Economic feasibility analysis of a biomass processing plant: A perspective on invasive biomass. Indian Economic Review. (Springer Nature)
4. Samson Rosly Sangma, Mayur Mausoom Phukan, S Sultana, D Sharma, P Chowdhuri, R Kumar, R Saha, **Vahshi Chongloi**. Phytochemical Analysis, Antioxidant, Antimicrobial and Cytotoxicity Properties of Citrus latipes (Swingle) Yu. Tanaka, A Threatened Ethnomedicinal Plant of Northeast, India Journals of Herbs, Spices & Medicinal Plants. (Taylor & Francis)
5. Dipanka Kashyap Borthakur, Plaban Bora, Mayur Mausoom Phukan, **Vahshi Chongloi**. Performance of Waste Expanded Polystyrene as Bitumen Modifier: A Comparative Assessment with Virgin Bitumen. Environmental Science and Pollution Research. (Spinger Nature)

## Paper presntations in conference/seminar/workshop

1. Presented paper titled "*Lantana camara* as a Potential Bioenergy Feedstock" in the ICBB–2022 organized by the Department of Botany, Nagaland University, Lumami 798627, Nagaland, India, held on September 19–21, 2022.
2. Presented paper titled "Investigation of *Bidens pilosa* as Prospective Feedstock for Bio–Fuel Generation" in the Two Days National Seminar on Land Use and Bioresource Management for Sustainable Livelihood, jointly organized by Department of Environmental Science, Mizoram University, Mizoram Science, Technology & Innovation Council (MISTIC) & National Bank for Agriculture & Rural Development (NABARD) on 27–28 March. 2023 (Best oral presentation).
3. Presented paper titled "Thermochemical Characterization of *Ageratina adenophora* to Evaluate its Feedstock Potential for Bio–Energy" at the National Conference on "Emerging challenges in the Frontiers of Chemical Science (ECFCS–2023) jointly organized by Manipur University Chemistry Alumni Association (MU–CAA) & Department of Chemistry, Manipur University on 29–30 March, 2023.
4. Paper presentation on "Biomass Valorization: Exploring Invasive Species as Sustainable Feedstock for Bioenergy Production and Value–Added Products" in Two days National seminar on Anthropology in the 21 century: emerging areas of research in Northeast India and its role in national development held on 19 – 20 March, 2024 organized by Department of Anthropology, Nagaland University.
5. Paper presentation on "Investigation of Invasive Species Biomass as Potential Feedstock for Bioenergy Generation and Value–Enhancement" at the National Conference on Recent Trends in Environmental Pollution and Health NCRTEPH 2024 organized by the Department of Zoology, Nagaland University, Lumami on 28–29 November 2024.
6. Paper presentation on "Exploring the In Silico, Antimicrobial and Antioxidant Potential of Pyrolysis–Derived Bio–Oil from Invasive *Ageratina adenophora*" at the International Conference on Medicinal Plants, Biodiversity

Conservation, Natural Products for Health Care Needs in Traditional System of AYUSH Medicine (MBNHA 2025) held on 7–8 May 2025 organized by Department of Forestry, Nagaland University.

Environmental Science and Pollution Research (2024) 31:59041–59057
https://doi.org/10.1007/s11356-024-35042-7

RESEARCH ARTICLE

# Miscellaneous prospects of invasive *Lantana camara* biomass—a standpoint on bioenergy generation and value addition

Vahshi Chongloi[1] · Mayur Mausoom Phukan[1] · Plaban Bora[2]

Received: 6 May 2024 / Accepted: 16 September 2024 / Published online: 27 September 2024


**Abstract**
Investigation of *Lantana camara* biomass for potential bioenergy generation integrates invasive species (IS) management with the unabated demand for bio-energy. In the present investigation, *L. camara* was used to produce bio-oil by thermochemical conversion (pyrolysis). The resultant product evinced energy yield of 62.58% with 64.95% of elemental carbon (C) content and endorsed the suitability of *L. camara* bio-oil for biofuel applications and value addition. Thermogravimetric (TG-DTG) analysis revealed a short thermal degradation profile, whereas spectroscopic analyses detected a host of organic compounds such as esters, phenols, ketones, aldehydes, aliphatics, and aromatics. The economic analysis of *L. camara* biomass conversion technology carried out in this study proved to be commercially competitive and viable versus petroleum refining. Antimicrobial and antioxidant assays with bio-oil evinced highest zone of inhibition (ZOI) against *Candida albicans* (31.02 mm), and displayed strong antioxidant property (DPPH $IC_{50}$ value 233.72 ± 0.2 µg/ml). The bio-oil exhibited rheological characteristics of shear thinning and pseudoplastic fluid, particularly at low and intermediate shear rates. The present study highlights the multifaceted advantages of utilizing *L. camara* biomass, which include environmental remediation via waste management, bioenergy generation, and the feasibility of generating value-added products.

**Keywords** Bioenergy · Invasive species · Waste management · Bio-oil · Economic analysis · Antioxidant · Antimicrobial

## Introduction

Ecosystems, both natural and agricultural, are significantly impacted by the rapid dispersal of invasive plant species (Liao et al. 2013; Míguez et al. 2022). The rampant expansion of invasive species (IS) in addition to pests and pathogens lead to a humungous annual loss of US$ 248 billion to world agriculture (Fried et al. 2017). IS not only display exceptionally fast growth rates, but successfully compete with native plants for nutrients, water, sunlight, and space. Consequently, IS are one of the leading agents of land degradation, evinced by marked decrease in growth and productivity of extant species (Hanberry 2023). A study by Qiu et al. (2023) reported nutrient enrichment significantly accelerated encroachment by IS, via increased reproductive potential in comparison to the native species. The resultant modification of ecological complexity and soil resources by increased IS colonization accelerated environmental degradation and pollution; this in turn caused significant reduction in native biodiversity (Rai 2021).

Control of invasive species is cited as one of the main obstacles to ecosystem restoration (Dong et al. 2019). National governments and biodiversity conservation planners have prioritized control of IS, to resolve detrimental effects on natural resources, ecosystems, and sustainability of ecosystem management services (Zhang et al. 2022). For efficient management and prevention of invasive alien species, the European Parliament and the Council (EPC) published regulation No. 1143/2014 (European Union 2014). The Weeds of National Significance (WoNS) programme of Australia also focused on the management and control of IS that constituted substantial risks to ecosystems and biodiversity (Shaik et al. 2022). Integrated weed management (IWM) strategies envisage formulating national and international policies, developing conducive habitats, designing tools for

Responsible Editor: Ta Yeong Wu

✉ Mayur Mausoom Phukan
mayur_101@yahoo.com

[1] Department of Forestry, School of Sciences, Nagaland University, Lumami 798627, Nagaland, India

[2] Department of Energy Engineering, Assam Science and Technology University, Guwahati 781013, India

Environmental Science and Pollution Research
https://doi.org/10.1007/s11356-025-36741-5

RESEARCH ARTICLE

# Antioxidant, antimicrobial and in silico investigations on pyrolytic bio-oil from invasive *Stachytarpheta jamaicensis*

Vahshi Chongloi[1] · Partha Pratim Gogoi[2] · Samson Rosly Sangma[1] · Upasana Bora Sinha[2] · Plaban Bora[3] · Mayur Mausoom Phukan[1]

Received: 5 February 2025 / Accepted: 3 July 2025


**Abstract**
Bio-oils, obtained from thermochemical conversion of invasive species (IS) biomass, require in-depth research and analysis to access its bioactive compounds with therapeutic value. Therefore, sustainable biomass valorization, chemical characterization, bioactive assays and in silico drug discovery formed part of the present investigation on the bio-oil derived from the entire shrub of invasive *Stachytarpheta jamaicensis*. The thermochemical conversion of biomass was initiated by pyrolysis ranging from ambient to 700 °C, at a heating rate of 30 °C/min. Thermogravimetric analysis demonstrated a rapid degradation profile of the biomass. Spectroscopic analyses identified a diverse array of organic compounds including aliphatics, aromatics, aldehydes, ketones and phenols that endorsed its valuable chemical feedstock potential. The bio-oil displayed strong antioxidant potential by neutralizing free radicals with a half-maximal inhibitory concentration value of 232.42 ± 1.1 µg/ml, and potent antimicrobial activity with the highest zone of inhibition of 19.48 ± 0.8 mm against *Candida albicans*. This may be attributed to the complex spectrum of bioactive compounds in the bio-oil, highlighting its candidature for pharmaceutical applications. Molecular docking studies further identified key bioactive ligands including 3,5-dimethoxy-4-hydroxytoluene and phenol, 2-methoxy- that mirrored notable binding affinities to well-established breast cancer therapeutics such as anastrozole and letrozole. The integration of appropriate bioresource utilization, bioactive profiling and bio-oil application strongly affirmed the potential for therapeutic breakthroughs and futuristic drug discovery from repurposed invasive species biomass.

**Keywords** Biomass · Bioresource utilization · Thermochemical conversion · Bioactive compounds · Pharmaceuticals · Molecular docking

## Introduction

Well-established invasive species (IS) typically dominate both native and extant species, escalate ecosystem disruption, biodiversity loss and extinction. The IS are hallmarked as primary drivers of decline in global biodiversity by their extreme and detrimental impact on natural habitats (Máximo et al. 2020). Infamous for their ability to modify extant plant communities, the IS hinder ecosystem restoration by altering soil properties, fire regimes, nitrogen cycling and hydrological dynamics; all vital parameters of biodiversity and human well-being (Zhang et al. 2018). The strategies undertaken for effective IS management include prompt detection, swift eradication, impact mitigation and ecosystem restoration. Among the varied strategies adopted, the two most apparent to the public at large are early detection and mitigation; the former is facilitated by community engagement and the latter by removal through mechanical, biological or chemical means (Máximo et al. 2020). Despite unabated effort and expenditure, the varied blueprints to control and eliminate IS have yielded low success. Consequently, to address the impracticability of complete IS eradication, exploration of alternative approaches for its utilization will possibly elicit the best bargain by unlocking their full potential and preserving the ecological balance.

Responsible Editor: Ta Yeong Wu

✉ Mayur Mausoom Phukan
mayur_101@yahoo.com; mayurmausoom@gmail.com

[1] Department of Forestry, School of Sciences, Nagaland University, Lumami 798627, Nagaland, India

[2] Department of Chemistry, School of Sciences, Nagaland University, Lumami 798627, Nagaland, India

[3] Department of Chemical Engineering, Assam Engineering College, Guwahati 781013, India

Published online: 15 July 2025

Sangma *et al.*
*Future Journal of Pharmaceutical Sciences* (2023) 9:114
https://doi.org/10.1186/s43094-023-00567-0

Future Journal of Pharmaceutical Sciences

RESEARCH Open Access

# Phytochemical profiling, antioxidant and antimicrobial investigations on *Viburnum simonsii* Hook. f. & Thoms, an unexplored ethnomedicinal plant of Meghalaya, India

Samson Rosly Sangma[1], Mayur Mausoom Phukan[1*], Vahshi Chongloi[1], Dakeshwar Kumar Verma[2], Plaban Bora[3], Sony Kumari[4] and Pranay Punj Pankaj[5]

**Abstract**

**Background** *Viburnum simonsii* Hook. f. & Thoms is one of the 17 *Viburnum* species reported from India. *Viburnum* species such as *Viburnum opulus* and *Viburnum grandiflorum* have been used since time immemorial to treat various ailments and their therapeutic claims have been scientifically validated. However, the species under investigation despite having a long traditional usage history for the treatment of various illnesses in Meghalaya, India has grossly remained unexplored to date. No scientific report validating its therapeutic claim has been reported thus far. Therefore, the present study was mainly focused on investigating the antioxidant and antimicrobial properties of *V. simonsii* and its phytochemical profile.

**Result** Preliminary phytocompound assessment revealed the presence of alkaloids, phenolics, steroids, glycoside and terpenoids. The fruit extract displayed good antioxidant activity with phenolic and flavonoid content of 250.20 ± 8.12 mgGAE/g and 40.65 ± 1.31 mgQE/g respectively, and $IC_{50}$ value of 131.35 ± 1.71 µg/ml. In antimicrobial assay, inhibitory activity was observed against gram-positive bacteria (*Staphylococcus aureus* and *Bacillus cereus*) with 17.80 ± 0.80 mm and 15.78 ± 2.62 mm zone of inhibition respectively. However, no activity was observed against gram-negative bacteria (*Escherichia coli and Salmonella enterica*) as well as fungus (*Candida albicans*). The absorption bands in the FTIR spectra of the sample corresponded to the presence of primary and secondary alcohols, alkanes, amines, aliphatic ethers, etc. Further, the GC–MS analysis revealed the presence of phytocompounds such as neophytadiene, β-sitosterol, α-amyrin, lupeol, etc., which have bioactivity especially anticancer, antimicrobial, antioxidant and anti-inflammatory activities.

**Conclusions** The findings of the present study demonstrated that *V. simonsii* possessed appreciable antioxidant and antimicrobial activity and may be a potential target for pharmaceutical research.

**Keywords** Ethnomedicine, *Viburnum simonsii*, Meghalaya, Antioxidant, FTIR, GC–MS, Antimicrobial

*Correspondence:
Mayur Mausoom Phukan
mayur_101@yahoo.com
Full list of author information is available at the end of the article

*Chemistry & Biodiversity*

WILEY-VCH

CHEMISTRY & BIODIVERSITY

RESEARCH ARTICLE

# Phytochemical Profiling, Bioactivity Evaluation and In Silico Insights Onto *Goniothalamus simonsii* Hook. f. Thoms.: An Endangered Medicinal Plant

Samson Rosly Sangma[1] | Mayur Mausoom Phukan[1] | Dhrubajyoti Gogoi[2] | Pranay Punj Pankaj[3] | Vahshi Chongloi[1]

[1]Department of Forestry, School of Sciences, Nagaland University, Lumami, Nagaland, India | [2]Programme of Biotechnology, Faculty of Science, Assam Down Town University, Guwahati, Assam, India | [3]Department of Zoology, School of Sciences, Nagaland University, Lumami, Nagaland, India

**Correspondence:** Mayur Mausoom Phukan (mayur_101@yahoo.com)

**Received:** 2 May 2025 | **Revised:** 7 October 2025 | **Accepted:** 10 October 2025

**Keywords:** antioxidant activity | cytotoxicity | GC–MS | *Goniothalamus simonsii* | molecular docking

**ABSTRACT**

*Goniothalamus simonsii* Hook. f. Thoms., an endangered medicinal plant is endemic to the state of Meghalaya, India. Its wide use in traditional medicine in Meghalaya for treating gastrointestinal complications, throat irritation and typhoid fever, is not matched by scientific reports on its pharmacological attributes. The present investigation evaluated the phytochemical constituents by GC–MS analysis; while bioactivities including antioxidant, antimicrobial and cytotoxicity were assessed by DPPH, agar-well diffusion and MTT methods, respectively. The leaf extract showed elevated content of phenolics (154.76 ± 7.98 mg GAE/g) and flavonoids (55.91 ± 3.05 mg QE/g). GC–MS analysis identified compounds included *cis*-vaccenic acid, kavain, 3-methoxy-2-(quinoxalin-6-yliminomethyl), spathulenol, aziridine, stigmasterol, *n*-hexadecanoic acid, cholest-4-en-3-one, coniferyl alcohol and so forth. Leaf extract displayed $IC_{50}$ value of 437.38 ± 13.11 μg/mL in the DPPH assay. The extracts displayed antimicrobial activity (13.21–22.63 mm) against a broad spectrum of bacteria, with minimum inhibitory concentration (MIC) values ranging > 1000–58.59 μg/mL. The antiproliferative effect was observed against colon cancer cell line (HT-29) with $IC_{50}$ value of 9.8 ± 7.84 μg/mL. Docking results demonstrated that stigmasterol exhibited the highest binding affinity for target protein CDK2, with docking score of −8.9 kcal/mol. These findings serve as a catalyst for additional research on *G. simonsii* as a prospective bioresource for bioactive compounds in future phytotherapeutics.

## 1 | Introduction

Ever since the days of antiquity mankind has relied heavily on plants for the treatment of numerous ailments. In modern times, despite the accessibility and efficacy of synthetic medications for various diseases, certain parts of the populace continue to favour traditional remedies for their low risk of detrimental side effects [1]. The adverse effects associated with modern pharmaceuticals have revived public interest in herbal remedies, which form the cornerstone of traditional medicine. Moreover, in response to the global demands for primary healthcare, the World Health Organisation (WHO) has lent support to the integration of traditional medicine, engendered by accessibility, cost-effectiveness and widespread cultural acceptance, to treat or alleviate various ailments and enhance overall well-being [2]. The influence of ethnomedicinal plants on the advancement of the human healthcare system is profound. It is estimated that around 70% of the pharmaceutical medications currently prescribed originate from compounds derived from plants [3]. Approximately, 7000 medicinal compounds derived from plants have emerged as vital drugs in Western medicine. In light of recent advancements in modern medicine, majority of the

INTELLECTUAL PROPERTY INDIA
PATENTS | DESIGNS | TRADE MARKS
GEOGRAPHICAL INDICATIONS

सत्यमेव जयते

ORIGINAL
क्रम सं/ Serial No. : 174742

**पेटेंट कार्यालय, भारत सरकार** **The Patent Office, Government Of India**

**डिजाइन के पंजीकरण का प्रमाण पत्र | Certificate of Registration of Design**

| | | |
|---|---|---|
| डिजाइन सं. / Design No. | : | 417482-001 |
| तारीख / Date | : | 20/05/2024 |
| पारस्परिकता तारीख / Reciprocity Date* | : | |
| देश / Country | : | |

प्रमाणित किया जाता है कि संलग्न प्रति में वर्णित डिजाइन जो *PYROLYZER FOR CONVERSION OF BIOMASS AND AGRICULTURAL WASTES INTO BIO-OIL AND BIOCHAR* से संबंधित है, का पंजीकरण, श्रेणी 15-99 में 1.Dr. Mayur Mausoom Phukan 2. Miss Vahshi Chongloi 3.Dr. Plaban Bora 4.Dr. Pranay Punj Pankaj के नाम में उपर्युक्त संख्या और तारीख में कर लिया गया है।

Certified that the design of which a copy is annexed hereto has been registered as of the number and date given above in class 15-99 in respect of the application of such design to *PYROLYZER FOR CONVERSION OF BIOMASS AND AGRICULTURAL WASTES INTO BIO-OIL AND BIOCHAR* in the name of 1.Dr. Mayur Mausoom Phukan 2. Miss Vahshi Chongloi 3.Dr. Plaban Bora 4.Dr. Pranay Punj Pankaj.

डिजाइन अधिनियम, 2000 तथा डिजाइन नियम, 2001 के अध्यधीन प्रावधानों के अनुसरण में।
In pursuance of and subject to the provisions of the Designs Act, 2000 and the Designs Rules, 2001.

जारी करने की तिथि :
Date of Issue : 09/07/2024

महानियंत्रक पेटेंट, डिजाइन और व्यापार चिह्न
Controller General of Patents, Designs and Trade Marks

*पारस्परिकता तारीख (यदि कोई हो) जिसकी अनुमति दी गई है तथा देश का नाम। डिजाइन का स्वत्वाधिकार पंजीकरण की तारीख से दस वर्षों के लिए होगा जिसका विस्तार, अधिनियम एवं नियम के निबंधनों के अधीन, पाँच वर्षों की अतिरिक्त अवधि के लिए किया जा सकेगा। इस प्रमाण पत्र का उपयोग विधिक कार्यवाहियों अथवा विदेश में पंजीकरण प्राप्त करने के लिए नहीं हो सकता है।

The reciprocity date (if any) which has been allowed and the name of the country. Copyright in the design will subsist for ten years from the date of Registration, and may under the terms of the Act and Rules, be extended for a further period of five years. This Certificate is not for use in legal proceedings or for obtaining registration abroad.